

**Veratryl Alcohol: Mechanism of Oxidation
by Lignin Peroxidase and Role in Lignin Degradation**

Dawei Sheng

M.S., Peking University, 1990

B.S., Peking University, 1987

A dissertation submitted to the faculty of the
Oregon Graduate Institute of Science and Technology
in partial fulfillment of the
requirements for the degree of
Doctor of Philosophy
in
Biochemistry and Molecular Biology

February 1998

The dissertation "Veratryl Alcohol: Mechanism of Oxidation by Lignin Peroxidase and Role in Lignin Degradation" by Dawei Sheng has been examined and approved by the following examination committee:

Michael H. Gold, Advisor
Institute Professor

David R. Boone
Professor

Thomas M. Loehr
Professor

V. Renganathan
Associate Professor

ACKNOWLEDGMENTS

I wish to express thanks and gratitude to Professor Michael H. Gold for his guidance and support throughout the course of my research; to Professors Thomas H. Loehr, V. Renganathan, and David R. Boone for sitting on my committee and reading my thesis; to Dr. Margaret Alic and Heather Youngs for their help in writing manuscripts and their friendship; and to Dr. Dinesh K. Joshi, Dr. Lakshmi Akileswaran, and Ms. Mary Mayfield-Gambill for their technical help during the initial stages of the work and for their friendship.

My sincere appreciation to all my colleagues in Professor Gold's lab for providing a helping and congenial atmosphere where this work was achieved.

TABLE OF CONTENTS

ACKNOWLEDGMENTS	iii
TABLE OF CONTENTS	iv
LIST OF TABLES	ix
LIST OF FIGURES	xi
ABSTRACT	xiii
CHAPTER 1 INTRODUCTION	1
1.1 Biodegradation of Lignin	1
1.1.1 Lignin: Structure and classification	1
1.1.2 Lignin-degrading microorganisms	2
1.1.3 Biodegradation of lignin by white-rot fungi	5
1.2 Enzymes Involved in Lignin Biodegradation by White-rot Basidiomycete Fungi	6
1.2.1 Laccase	7
1.2.2 Lignin peroxidase and manganese peroxidase	10
1.2.3 Hydrogen peroxide-generating enzymes	12
1.3 Organic Compounds Secreted by White-rot Fungi	13
1.4 Heme Peroxidases	16
1.4.1 Classification of heme peroxidases	16
1.4.2 Peroxidase catalytic cycle	18
1.4.3 Amino acids involved in the heme peroxidase catalytic cycle	21
1.5 Lignin Peroxidase: Structure and Functions	24
1.5.1 General properties of lignin peroxidase	24
1.5.2 Crystal structure of lignin peroxidase	29
1.5.3 Substrates for lignin peroxidase	33

1.5.4	Kinetic and thermodynamic properties of lignin peroxidase catalyzed reactions	38
1.5.5	The role of VA in LiP catalyzed reactions	45

CHAPTER 2 NITRATION OF VERATRYL ALCOHOL BY LIGNIN

	PEROXIDASE AND TETRANITROMETHANE	48
2.1	Introduction	48
2.2	Materials and Methods	50
	2.2.1 Enzyme preparation	50
	2.2.2 Chemicals	50
	2.2.3 Enzyme reactions	52
	2.2.4 Product analysis	53
2.3	Results	54
	2.3.1 Nitration of VA (I)	54
	2.3.2 Oxidation of 1,4-dimethoxybenzene (II)	57
	2.3.3 Oxidation of tyrosine (III)	59
	2.3.4 Reactions with $\cdot\text{NO}_2$	59
2.4	Discussion	61
	2.4.1 Oxidation of VA (I)	62
	2.4.2 Oxidation of 1,4-dimethoxybenzene (II)	65
	2.4.3 Oxidation of tyrosine (III)	66
	2.4.4 Conclusions	68

CHAPTER 3 OXIDATION OF FERROCYTOCHROME C BY LIGNIN

	PEROXIDASE	69
3.1	Introduction	69
3.2	Materials and Methods	70
	3.2.1 Protein preparation	70
	3.2.2 Chemicals	71
	3.2.3 Determination of oxidation rates	71
	3.2.4 Protection of lignin peroxidase from inactivation by H_2O_2	72
	3.2.5 Inactivation of lignin peroxidase during the reaction	72

3.2.6	Effect of ferricytochrome <i>c</i> on the lignin peroxidase oxidation of veratryl alcohol	72
3.3.	Results	73
3.3.1	Ferrocycytochrome <i>c</i> oxidation by LiP	73
3.3.2	Effect of pH and veratryl alcohol	73
3.3.3	Steady-state kinetics	77
3.3.4	Effect of ionic strength	81
3.3.5	Inhibition of veratryl alcohol oxidation by ferricytochrome <i>c</i>	81
3.4	Discussion	81
3.4.1	Effect of pH and veratryl alcohol	85
3.4.2	Peroxidase ping-pong mechanism	89
3.4.3	Effect of ionic strength	90
3.4.5	Cytochrome <i>c</i> binding site	91

CHAPTER 4 IRREVERSIBLE OXIDATION OF FERRICYTOCHROME C

	BY LIGNIN PEROXIDASE	94
4.1	Introduction	94
4.2	Experimental Procedures	95
4.2.1	Protein preparation	95
4.2.2	Chemicals	96
4.2.3	Spectrophotometric measurements	96
4.2.4	Atomic absorption spectrometry	97
4.2.5	LiP inactivation by H ₂ O ₂	97
4.2.6	HPLC analysis of veratraldehyde formation	97
4.2.7	SDS-PAGE	97
4.2.8	Isolation and amino acid analysis of Cc ³⁺ reaction products	97
4.3	Results	98
4.3.1	Cc ³⁺ oxidation by LiP	98
4.3.2	HPLC analysis of VA oxidation	103
4.3.3	Dimerization of Cc ³⁺	103
4.4	Discussion	106
4.4.1	LiP-catalyzed bleaching of Cc ³⁺	109

4.4.2	Effects of VA on the LiP-catalyzed oxidation of Cc^{3+}	111
4.4.3	Polymerization of Cc^{3+} and formation of dityrosine	117
4.4.4	Conclusions	118

**CHAPTER 5 OXIDATIVE POLYMERIZATION OF RIBONUCLEASE A BY
LIGNIN PEROXIDASE FROM *PHANEROCHAETE*
CHRYSOSPORIUM: ROLE OF VERATRYL ALCOHOL IN
POLYMER OXIDATION 119**

5.1	Introduction	119
5.2	Experimental Procedures	120
5.2.1	Protein preparation	120
5.2.2	Chemicals	121
5.2.3	Fluorescence spectrophotometry	121
5.2.4	UV-visible spectrophotometry	121
5.2.5	HPLC analysis of VA oxidation	122
5.2.6	LiP inactivation studies	122
5.2.7	Identification of dityrosine	122
5.2.8	SDS-PAGE and amino acid analysis	122
5.2.9	Transient-state kinetic studies	123
5.3	Results	124
5.3.1	LiP oxidation of RNase and tyrosine	124
5.3.2	SDS-PAGE and amino acid analysis of oxidized RNase	124
5.3.3	RNase oxidation and veratraldehyde formation	127
5.3.4	Effects of RNase and VA on the H_2O_2 -induced inactivation of LiP	132
5.3.5	Transient-state kinetic studies	132
5.4	Discussion	135
5.4.1	LiP-catalyzed polymerization of RNase	139
5.4.2	RNase oxidation and veratraldehyde formation	140
5.4.3	LiP inactivation	142
5.4.4	Transient-state kinetics	143
5.4.5	VA as a radical mediator	144

CHAPTER 6 HALOPEROXIDASE ACTIVITY OF MANGANESE PEROXIDASE	
FROM <i>PHANEROCHAETE CHRYSOSPORIUM</i>	146
6.1 Introduction	146
6.2 Experimental Procedures	148
6.2.1 Enzyme preparation	148
6.2.2 Chemicals	148
6.2.3 Enzyme assays	148
6.2.4 Transient-state kinetics	149
6.2.5 Inactivation of MnP	149
6.2.6 Halide binding	150
6.2.7 Bromination of organic substrates	150
6.3 Results	151
6.3.1 Haloperoxidase activity	151
6.3.2 Steady-state kinetics studies	151
6.3.3 Reduction of peroxidase compound I by halides	155
6.3.4 Identification of bromination products	155
6.3.5 Halide binding	158
6.3.6 Enzyme inactivation	158
6.4 Discussion	162
6.4.1 Bromination of organic substrates	164
6.4.2 Enzyme inactivation	165
6.4.3 Halide binding to MnP	165
CHAPTER 7 FINAL COMMENTS AND FUTURE DIRECTIONS	167
7.1 VA Binding Site of LiP	168
7.2 Other Aromatic Compounds as Redox Mediators of VA	169
7.3 Studies of Lignin Oxidation by LiP	170
LITERATURE CITED	171
BIOGRAPHICAL SKETCH	201

LIST OF TABLES

1.1	The Production of Extracellular Oxidative Enzymes by White-Rot Fungi Basidiomycetes	8
1.2	The Production of Aromatic Alcohol/Aldehyde by White-Rot Fungi	15
1.3	Molecular Masses (M) and the Isoelectric Points of Lignin Peroxidases from Selected White-Rot Fungi	26
1.4	Electronic Absorption Spectral Maxima of Lignin Peroxidase and Other Heme Proteins	27
1.5	Spectral Characteristics of Oxidized Intermediates of Lignin Peroxidase . .	28
1.6	Transient-State Kinetic Parameters of LiP: Compounds I and II Reduction by Aromatic Compounds	39
1.7	Kinetic parameters of the Reactions of LiP Compounds I and II with H ₂ O ₂ and Peracetic Acid	42
2.1	Mass Spectra of Products or Their Derivatives Formed by LiP in the Presence of H ₂ O ₂ and TNM	51
2.2	Oxidation of VA (I) by LiP in the Presence of TNM	56
2.3	Oxidation of 1,3-Dimethoxybenzene (II) by LiP in the Presence of TNM .	58
2.4	Oxidation of Tyrosine (III) by LiP in the Presence of TNM	60
3.1	Veratryl Alcohol and Ferrocyclochrome <i>c</i> Oxidation by LiP	76
3.2	Kinetic Parameters of LiP and CCP Reactions	82
4.1	Fe Content and Soret Absorbance of Cc ³⁺	102
4.2	Veratraldehyde Formation in Reactions Containing Cc ³⁺ or Cc ²⁺	105
4.3	Amino Acid Analysis of Native Cc ³⁺ and Cc ³⁺ Oxidation Products	107
4.4	Steady-State Kinetic Parameters for the LiP Oxidation of Cc ²⁺ , Cc ³⁺ , and VA	112
5.1	Amino Acid Analyses of Native and Oxidized RNase Proteins	128

5.2	Veratraldehyde Formation in the Presence and Absence of RNase	131
5.3	Transient-State Kinetic Values for the Reductions of LiP Compounds I and II by VA and RNase	137
6.1	Steady-state Kinetic Parameters of Mn ^{II} and I ⁻ Oxidations by Wild-Type MnP, MnP D179N, and MnP E25Q-179N	154

LIST OF FIGURES

1.1	Schematic structural formula for lignin	3
1.2	Protoporphyrin IX	17
1.3	α -Carbon diagram of lignin peroxidase	30
1.4	Stereoview of the active site environment of lignin peroxidase	31
1.5	Stereoview of hypothetical complex between veratryl alcohol and lignin peroxidase	34
1.6	The mechanism of veratryl alcohol oxidation by lignin peroxidase	36
1.7	Interrelationship between the oxidized intermediates of lignin peroxidase . .	44
2.1	LiP oxidations in the presence of TNM	55
2.2	Proposed mechanism for the LiP oxidation of VA (I) in the presence of TNM	64
2.3	Proposed mechanism for the dimerization and nitration of tyrosine (III) . .	67
3.1	Oxidation of ferrocyclochrome <i>c</i> by LiP	74
3.2	pH profile for LiP oxidation of ferrocyclochrome <i>c</i> in the presence or absence of veratryl alcohol	75
3.3	Effect of veratryl alcohol and ferrocyclochrome <i>c</i> on lignin peroxidase stability and activity	78
3.4	Inactivation of LiP by H ₂ O ₂ during the oxidation of ferrocyclochrome <i>c</i> . . .	79
3.5	Effect of H ₂ O ₂ concentration on the stimulation of cytochrome <i>c</i> oxidation by VA	80
3.6	Effect of ionic strength on the initial velocity of ferrocyclochrome <i>c</i> oxidation by LiP	83
3.7	Inhibitory effect of ferricytochrome <i>c</i> on veratryl alcohol oxidation by LiP	84
4.1	Cc ³⁺ oxidation by LiP	99

4.2	Effect of VA and enzyme concentration on the oxidation of Cc^{3+}	100
4.3	pH dependence of the oxidation of Cc^{3+} and VA	101
4.4	Effect of H_2O_2 concentration on the stimulation of Cc^{3+} oxidation by VA	104
4.5	Effects of VA and Cc^{3+} on LiP inactivation by H_2O_2	115
4.6	SDS-PAGE of Cc^{3+} oxidation products	116
5.1	Fluorescence spectra of RNase and tyrosine oxidation by LiP	125
5.2	SDS-PAGE of RNase oxidation products	126
5.3	Effect of VA on the oxidation of RNase	129
5.4	Effect of RNase concentration on the lag time for VA oxidation by LiP	130
5.5	Effects of RNase and VA on LiP inactivation	133
5.6	Effects of RNase and VA on the LiP visible spectra	134
5.7	Order plots of the reductions of LiPI (A) and LiPII (B) by RNase	136
5.8	Proposed mechanism for the dimerization of tyrosine by peroxidases	141
6.1	MnP-catalyzed formation of triiodide and tribromide complexes	152
6.2	pH dependence of MnP-catalyzed iodide and bromide oxidations	153
6.3	Transient-state kinetics for the reduction of MnP compound I by bromide (A) and iodide (B)	156
6.4	Products obtained from the bromination of various substrates by MnP	157
6.5	Bromide binding to MnP	159
6.6	Bleaching of the heme prosthetic group of MnP	160
6.7	MnP inactivation assay (Selwyn test)	161

ABSTRACT

Veratryl Alcohol: Mechanism of Oxidation by Lignin Peroxidase and Role in Lignin Degradation

Dawei Sheng

Supervising Professor: Michael H. Gold

The mechanism of veratryl (3,4-dimethoxybenzyl) alcohol (VA) (I) oxidation and the role of VA (I) in polymeric substrate oxidation by lignin peroxidase (LiP) were investigated by chemical and kinetic studies.

LiP, in the presence of H_2O_2 and tetranitromethane (TNM), oxidizes VA (I) to veratraldehyde (II), 4,5-dimethoxy-2-nitrobenzyl alcohol (III), and 3,4-dimethoxy-nitrobenzene (IV). The formation of the nitro aromatics is explained by a mechanism involving the one-electron oxidation of VA by LiP to produce the corresponding cation radical, which loses a proton to generate the benzylic radical. The latter reduces TNM to generate the trinitromethane anion and the nitrogen dioxide radical ($\cdot\text{NO}_2$). $\cdot\text{NO}_2$ couples with the VA cation radical to yield III and IV. These results provide evidence for the formation of the VA cation radical and the first chemical evidence for the formation of the VA benzylic radical in LiP-catalyzed reactions.

Protein substrates, including ferrocyanochrome c (Cc^{2+}), ferricytochrome c (Cc^{3+}) and ribonuclease A (RNase), were used as polymeric lignin model compounds to investigate the role of VA in the LiP-catalyzed oxidation of polymeric lignin. Although LiP can oxidize Cc^{2+} to Cc^{3+} directly, VA stimulates this reaction at low pH and high concentrations of H_2O_2 . LiP irreversibly oxidizes Cc^{3+} in the presence of H_2O_2 and this reaction is dependent on VA at all pHs. Atomic absorption and UV/vis spectroscopy indicate that the oxidation of Cc^{3+} is accompanied by a loss of

heme iron and the possible oxidation of the porphyrin ring. SDS-PAGE analysis of Cc^{3+} oxidation products demonstrates the formation of a covalently linked dimer of this substrate. Amino acid analysis indicates that Tyr residues in the Cc^{3+} protein are oxidized to Tyr radicals and these radicals subsequently undergo intermolecular radical coupling, resulting in dimerization of some of the substrate.

RNase also was used as a substrate for LiP. Fluorescence spectroscopy, SDS-PAGE, and amino acid analyses indicate that LiP catalyzes RNase dimerization via Tyr radical coupling. UV/vis spectroscopy indicates that in the presence of 100 μ M H_2O_2 , relatively low concentrations of RNase and VA, together but not individually, prevent LiP inactivation by H_2O_2 . Steady-state kinetic studies show that VA stimulates RNase oxidation; however, RNase inhibits VA oxidation by LiP. Stopped-flow and rapid scan methods demonstrate that the reduction of LiP compound I to the native enzyme by RNase occurs via two single-electron steps. At pH 3.0, the reductions of LiP compound I and II by RNase obey second-order kinetics, with rate constants of $4.7 \times 10^4 \text{ M}^{-1}\text{s}^{-1}$ and $1.1 \times 10^4 \text{ M}^{-1}\text{s}^{-1}$, respectively. These rates were significantly enhanced in the presence of VA. All of these results support a mechanism in which VA serves as an enzyme-bound redox cofactor for LiP.

CHAPTER 1

INTRODUCTION

1.1 Biodegradation of Lignin

Lignin is the most abundant aromatic polymer on earth. It is found in all higher plants and comprises 15–36% of the total lignocellulosic material in wood (Lin & Dence, 1992). Lignin provides increased rigidity to the plant cell wall, minimizes water permeation across the cell walls of vascular tissues and protects plants from pathogenic organisms (Sarkanen & Ludwig, 1971). Since lignin physically protects most of the world's cellulose and hemicellulose from enzymic hydrolysis, the breakdown and potential utilization of lignin are of enormous significance.

The study of lignin biodegradation was initiated following the elucidation of lignin structure in the 1960s and after assays were developed for lignin biodegradation using lignin model compounds and ¹⁴C-labeled lignins in the 1980s (Crawford, 1981). Research on lignin biodegradation has accelerated greatly during the past 15 years following the discovery of lignin-degrading peroxidases. Our understanding of the catalytic and enzymatic properties of lignin-modifying peroxidases and their biochemistry, molecular biology and potential applications in pulping, bleaching and converting lignins to useful products, followed from their discovery.

This section is a brief overview of lignin structure, the microorganisms involved in lignin degradation, and a review of studies on lignin biodegradation by white-rot basidiomycetes.

1.1.1 Lignin: Structure and classification

The components of wood vary depending on the species, but the major structural constituents are cellulose (50–60%), hemicellulose (5–15%) and lignin

(15–35%) (Lin & Dence, 1992). Lignin is found in all vascular plants, including ferns (Crawford, 1981). Lignin is found within secondary cell walls and is closely associated with cell wall polysaccharides. Lignin is synthesized from three substituted cinnamyl alcohol precursors (Fig. 1.1)—4-hydroxycinnamyl (coumaryl) alcohol, 4-hydroxy-3-methoxycinnamyl (coniferyl) alcohol, and 3,5-dimethoxy-4-hydroxycinnamyl (sinapyl) alcohol. Free radical condensation of these alcohols, initiated by plant cell wall peroxidases (Harkin & Obst, 1973), results in the formation of a heterogeneous, amorphous, optically inactive, random and highly branched polymer. Figure 1.1 shows a schematic formula for an angiosperm lignin. Over 10 interphenylpropane linkage types occur. The major linkage type is the β -O-4 linkage, seen between units 1,2; 4,5; 6,7; 7,8; 9,10; etc. The condensation reaction also results in the formation of cross-linkages between lignin and hemicellulose. Aromatic or cinnamic acids esterified through side-chain hydroxyl groups are also found in the lignins of grasses and certain woods (Monties, 1994).

1.1.2 Lignin-degrading microorganisms

Most wood-degrading microorganisms degrade wood polysaccharides by means of hydrolases, such as cellulases and xylanases. Many organisms are able to modify lignin, but, due to its complex and heterogeneous structure, only a few groups of fungi can completely degrade lignin to CO₂ and H₂O (Kirk & Farrell, 1987).

1.1.2.1 Lignin-degrading bacteria

Bacteria can degrade low-molecular-weight lignin-related compounds (Buswell & Odier, 1987b; McCarthy, 1987; Vicuna, 1988; Zimmermann, 1990). These bacteria include actinomycetes (*Streptomyces* sp.) and some Gram-negative eubacteria (*Pseudomonas* and *Xanthomonas* spp.). Polymeric lignin degradation by bacteria is insignificant compared to that by wood-decaying fungi. Most of the enzymes involved in the bacterial degradation of lignin substructures are intracellular, explaining the restricted effect on polymeric lignin. Peroxidases possibly involved in lignin degradation have been discovered in several streptomyces (Ramachandra et al., 1988; Adhi et al., 1989; Mliki & Zimmermann, 1992), and a peroxidase secreted

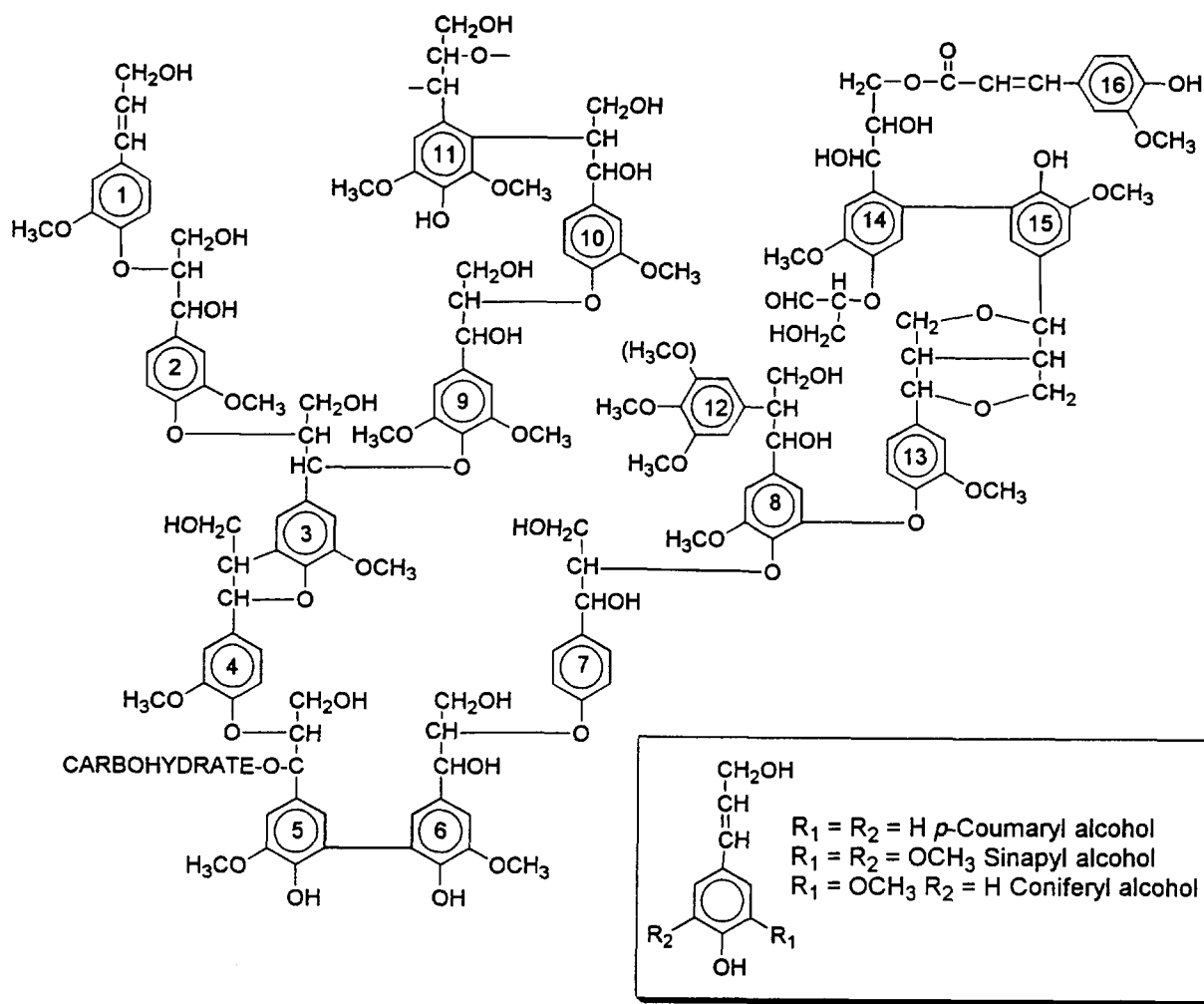


Figure 1.1 Schematic structural formula for lignin, adapted from Adler (1977). The three precursor alcohols of lignin are shown at the lower right.

by *Streptomyces viridosporus* has been characterized (Ramachandra et al., 1988; Z. M. Wang et al., 1990).

1.1.2.2 Lignin-degrading fungi

Wood-rotting fungi are the major microorganisms responsible for wood degradation. They are capable of extensively decomposing all the major structural components of wood (Kirk & Farrell, 1987), including cellulose, hemicellulose, and lignin. Wood-rotting fungi have been classified into three categories: white-rot, brown-rot, and soft-rot fungi, according to the color, the composition, and the histological characteristics of the decayed wood (Kirk & Cowling, 1984; Blanchette, 1991).

The name "white-rot" comes from the observation that these organisms degrade cell wall lignin leaving behind the colorless cellulose. More than one thousand species of white-rot fungi have been found, and almost all belong to Basidiomycetes (Gilbertson, 1980). Among ligninolytic microorganisms, white-rot basidiomycetes are the most efficient of all known lignin degraders.

Brown-rot fungi are taxonomically very similar to white-rot fungi and also belong to Basidiomycetes. Brown-rot fungi are usually defined as wood-rotting fungi that decompose and remove carbohydrates (cellulose and hemicellulose), but leave a residue of modified lignin. The brown-rotted lignin is typically dark brown, has a decreased methoxy content (Kirk & Adler, 1970; Kirk, 1975) and is almost equal in weight to the lignin in sound wood (Eriksson, 1990; Blanchette, 1991). Significant amounts of phenolic hydroxyl groups are introduced into brown-rotted lignin (Kirk, 1975; Crawford, 1981; Jin et al., 1990). The dark brown color is due to the formation of additional quinones and conjugated carbonyl groups in the decayed lignin (Kirk, 1975).

Soft-rot fungi attack moist wood, producing a characteristic softening of the surface of the wood tissue (Blanchette, 1991). Most of these fungi are Ascomycetes and Deuteromycetes. It has been shown that soft-rot fungi are poor at degrading dehydrogenated polymerizates (DHPs), however, they are able to mineralize lignin-related phenolic compounds (Ander et al., 1984, 1988). Although soft-rot fungi may play an important role in degrading lignin in nature, cultivation of these organisms in

the laboratory is difficult. Little is known about the enzymes they produce which are involved in lignin degradation.

1.1.3 Biodegradation of lignin by white-rot fungi

White-rot basidiomycetes are primarily responsible for initiating the decomposition of lignin in wood (Crawford, 1981; Buswell & Odier, 1987b; Kirk & Farrell, 1987; Gold et al., 1989). Thus, much effort has been devoted toward understanding the lignin biodegradation system in white-rot basidiomycetes. Elemental and functional group analyses of white-rotted lignins provided evidence that the degradation of lignin by white-rot fungi is an oxidative process. White-rotted lignin contains less carbon and hydrogen, and more oxygen than sound lignin. It also shows a decrease in methoxy groups and an increase in carbonyl and carboxyl groups (Kirk & Chang, 1974, 1975). Structural analysis of lignin fragments released from decayed lignin shows that vanillin, vanillic acid, syringaldehyde, syringic acid, dimethoxybenzoquinone, methoxybenzoquinone, methoxyhydroquinone, and coniferyl alcohol are released as major fragments (Kirk & Chang, 1974, 1975). The product analysis suggests that lignin degradation may occur through C-C bond cleavage at C_α - C_β linkages in propyl side chains and at alkyl-phenyl (C_α - C_1) linkages, as well as through C-O bond cleavage at β -ether linkages in aryl ether structures (Fig. 1.1).

The white-rot lignin-degrading fungus, *Phanerochaete chrysosporium*, has become a model for the most current studies. This fungus was chosen because (a) it efficiently degrades both lignin and cellulose, (b) it is thermotolerant (an optimal growth temperature of 38°C), (c) it produces asexual spores prolifically—an advantage for genetic manipulation, and (d) it forms sexual fruiting structures in culture (Burdvall & Eslyn, 1974; Gold & Cheng, 1978). By determining the $^{14}\text{CO}_2$ released from ^{14}C -DHPs under different conditions, it has been established that the ligninolytic activity of *P. chrysosporium* is induced by nutrient carbon, sulfur, or nitrogen starvation, which triggers the onset of secondary metabolism (Jeffries et al., 1981). The addition of ammonium or glutamate to nitrogen-limited cultures raises the concentration of intracellular glutamate (Fenn & Kirk, 1981), sharply decreases the

concentration of cAMP (MacDonald et al., 1984), restores primary growth, and halts the lignin degradation (Fenn & Kirk, 1981).

1.2 Enzymes Involved in Lignin Biodegradation by White-rot Basidiomycete Fungi

The structural features of lignin require that the enzymes involved in its biodegradation should be extracellular, nonspecific, and oxidative. The relationship between ligninolytic activity and Bavendamm's assay has been known for almost 70 years. Bavendamm showed that most white-rot fungi, which are capable of degrading lignin, produce a colored zone around the mycelium on agar plates containing tannin and that this colorization is caused by phenol oxidase secreted by the fungi (Bavendamm, 1928). Kirk and Kelman confirmed that the ligninolytic activities of wood-rotting fungi correlate well with positive Bavendamm's assays (Kirk & Kelman, 1965). Therefore, it is reasonable to consider that phenol oxidases are integral to lignin degradation.

Traditionally, three types of enzymes have been considered as phenol oxidases (Ander & Eriksson, 1976): tyrosinase, laccase, and peroxidase. Tyrosinase uses oxygen to oxidize monophenols, producing *o*-diphenols or *o*-quinones, and can also oxidize catechol to *o*-quinones. This enzyme, however, has a relatively narrow substrate specificity and is intracellular. As a result, it is probably not a key enzyme in lignin oxidation. Laccase catalyzes the oxidation of a large variety of phenolic compounds by abstracting one electron and one proton from phenolic hydroxyl groups to generate phenoxy radicals. The free radicals undergo disproportionation or polymerization via radical coupling. Laccase also has the capacity to oxidize nonphenolic compounds under certain conditions, e.g., if the reaction mixture is supplemented with 2,2'-azino bis(3-ethylbenzothiazoline)-6-sulfonic acid (ABTS) (Bourbonnais & Paice, 1990). Laccase uses oxygen as an electron acceptor which is ultimately reduced to water. Extracellular laccases are typically produced by white-rot fungi (Eriksson, 1990); however, the physiological function of laccase is not clear. Peroxidases catalyze reactions similar to laccase, but use hydrogen peroxide rather

than oxygen as the electron acceptor. Two families of heme peroxidases, lignin peroxidase (LiP) and manganese peroxidase (MnP), have been purified from *P. chrysosporium* as well as other white-rot fungi (see Section 1.5). The accumulated evidence suggests that these two families of peroxidases, and peroxide-generating enzymes, are the major extracellular components of the lignin degradation system of this organism. Extracellular lignin-degrading enzymes produced by wood-rotting fungi are summarized in Table 1.1.

1.2.1 Laccase

Nearly all white-rot fungi produce extracellular laccase (benzenediol:oxygen oxidoreductase, E.C. 1.10.3.2). Laccase catalyzes the one-electron oxidation of phenolic compounds, reducing O₂ by four electrons to H₂O. Fungal laccases are copper-containing, glycosylated enzymes with 11–25% carbohydrate.

Laccases from the ascomycete *Neurospora crassa* (Lerch et al., 1978) and the basidiomycete *Trametes versicolor* (Fahraeus & Reinhammar, 1967; Reinhammar, 1984) have been studied biochemically and biophysically. Gene sequences of laccase have been reported from the ascomycetes *Neurospora crassa* (Germann & Lerch, 1986) and *Aspergillus nidulans* (Aramayo & Timberlake, 1990) and the basidiomycetes *Trametes (Coriolus) hirsutus* (Kojima et al., 1990), *Phlebia radiata* (Saloheimo et al., 1991), and *Agaricus bisporus* (Perry et al., 1993a,b). The gene sequences suggest a close similarity between laccase and ascorbate oxidase, a copper-containing protein from higher plants (Messerschmidt & Huber, 1990).

The catalytic cycle of fungal laccase may be similar to that of ascorbate oxidase. Laccase from *T. versicolor* contains four coppers of three structural types: one type I, one type II, and two type IIIs. During the catalytic cycle, type I copper is first reduced by one electron derived from phenolic substrates, and the electron is transferred to the trinuclear copper cluster. Four copper ions eventually are reduced to Cu(I), and the O₂ is reduced to H₂O by the type II copper. Laccases from different fungi show high diversity in terms of molecular mass (60–100 kDa) and substrate specificity (Wood, 1980; Reinhammar, 1984; Karhunen et al., 1990). Since a three-

Table 1.1

The Production of Extracellular Oxidative Enzymes
by White-Rot Fungi Basidiomycetes^a

Fungus	LiP ^b	MnP	Lac	GLOX	AAO
<i>Armillaria mellea</i>	-	+	+		
<i>Armillaria ostoyae</i>	-	+	+		
<i>Bjerkandera adusta</i>	+	+	+/-	+	+
<i>Bjerkandera sp. BOS55</i>	+	+	+/-	+	+
<i>Cerporiopsis subvermispora</i>	-	+	+	-	
<i>Corioloopsis occidentalis</i>	+	+			
<i>Daedaleopsis confragosa</i>	-	+	+	-	-
<i>Dichomitus squalens</i>	-	+	+		-
<i>Ganoderma australis</i>		+			
<i>Inonotus (Phellinus) weirii</i>	-	-			
<i>Junghuhnia separabilima</i>	+		+		
<i>Lentinula edodes</i>	+/-	+	+		
<i>Merulius (Phlebia) tremellosus</i>	+/-	+	+		
<i>Panus tigrinus</i>	-	+	+		
<i>Phanerochaete chrysosporium</i>	+	+	-	+	-
<i>Phanerochaete flavido alba</i>	+	+			
<i>Phanerochaete magnolia</i>	+	+			
<i>Phlebia brevispora</i>	+	+	+	+	
<i>Phlebia ochraceofulva</i>	+	-	+		
<i>Phlebia radiata</i>	+	+	+	+	
<i>Phlebia subserialis</i>	-	+			
<i>Phellinus igniarius</i>	-	-	+		
<i>Phellinus pini</i>	+	+			
<i>Phleurotus ostreatus</i>	-	+	+		+
<i>Phleurotus sajor-caju</i>	-	+	+		+
<i>Pycnoporus cinnabarinus</i>	-	-	+		
<i>Stereum hirsutum</i>	-	+	+		
<i>Trametes gibbosa</i>	+	+	+		
<i>Trametes hirsuta</i>	+	+	+		
<i>Trametes versicolor</i>	+	+	+	+	+
<i>Trametes villosa</i>	-	+	+	+	-

^a de Jong et al., 1994; Hatakka, 1994. ^bLiP, lignin peroxidase; MnP, manganese peroxidase; Lac, laccase; GLOX, glyoxal oxidase; AAO, aryl alcohol oxidase.

dimensional crystal structure of laccase is not available, the topology and coordination of the active site of laccase are not precisely known. Therefore, more work needs to be done to determine the structure and catalytic mechanisms accurately.

The role of laccase in lignin degradation is not clear. Work with various phenolic lignin model dimers and purified laccase shows that certain degradation reactions occur, especially in syringyl models (Kirk et al., 1968b; Leonowicz et al., 1984; Morohoshi & Haraguchi, 1987; Wariishi et al., 1987; Kawai et al., 1988; Higuchi 1989a). Condensation reactions are dominant in guaiacyl models (Kirk et al., 1968a). When isolated lignin is treated with laccase, polymerization through radical coupling is observed as a major consequence of one-electron oxidations. A small amount of depolymerization occurs, and a trace amount of 2,6-dimethoxy-1,4-benzoquinone is identified. So it is believed that the major function of laccase is modification rather than degradation of lignin. Lignin has less than 20% free phenolic hydroxyl groups in its phenylpropanoid unit (Sarkanen & Ludwig, 1971). Therefore, lignin might be a poor substrate for laccase. However, laccase from *T. versicolor* is able to oxidize non-phenolic lignin model compounds in the presence of "radical mediators," such as ABTS (Bourbonnais & Paice, 1990; Muheim et al., 1992) and syringaldehyde (Kawai et al., 1989). In addition, *Pycnoporus cinnabarinus* produces 3-hydroxyanthranilate that can also act as a mediator for laccase in the oxidation of nonphenolic substrates (Eggert et al., 1996). The laccase-ABTS system also is able to delignify hardwood Kraft pulp (Bourbonnais & Paice, 1990).

Other roles for laccase in lignin degradation have been proposed. One possible function of laccase may be detoxification of low-molecular-mass phenols released during lignin degradation (Bollag et al., 1988). In addition, laccase may produce specific chemical transformations required for degradation by other enzymes. Finally, in the presence of appropriate oxidizable phenolic accessory substances or primary substrates, laccase can also produce Mn^{III} from Mn^{II} (Archibald & Roy, 1992). Mn^{III} can further oxidize lignin (see Section 1.2.2). These reports suggest a complicated role for laccase in lignin biodegradation, details of which remain to be elucidated.

1.2.2 Lignin peroxidase and manganese peroxidase

In 1983, Gold's and Kirk's groups independently announced the discovery of an extracellular enzyme involved in lignin biodegradation in the white-rot fungus *P. chrysosporium* (Glenn et al., 1983; Tien & Kirk, 1983; Gold et al., 1984). The enzyme subsequently was named lignin peroxidase (LiP, ligninase, EC 1.11.1.7). Later, a second enzyme involved in lignin degradation, manganese peroxidase (MnP, EC 1.11.1.13), was discovered and purified in Gold's laboratory (Kuwahara et al., 1984; Glenn & Gold, 1985). Both enzymes exist as a series of isozymes, which are encoded by multiple related genes (Kirk & Farrell, 1987; Leisola et al., 1987; Stewart et al., 1992; Gold & Alic, 1993; Cullen, 1997). LiP is found in certain white-rot fungi; however, MnP is found in almost all white-rot fungi known to degrade lignin (Périeré & Gold, 1991; Orth et al., 1993; Hatakka, 1994; Périeré et al., 1996).

1.2.2.1 Lignin peroxidase

LiP oxidizes non-phenolic lignin substrates by abstracting one electron to generate aryl cation radicals which are decomposed nonenzymatically (Harvey et al., 1986; Kirk & Farrell, 1987; Gold et al., 1989; Eriksson, 1990). Reactions of LiP with a variety of lignin model compounds and synthetic lignins have been studied extensively. Catalytic mechanisms have been elucidated and the capacity for C_α-C_β bond cleavage, ring opening, and other reactions has been demonstrated (Kirk & Farrell, 1987; Gold et al., 1989; Eriksson 1990). Polymeric compounds such as synthetic lignins (Hammel et al., 1993) and proteins (Wariishi et al., 1994) have also been used as lignin model compounds to elucidate the mechanisms of polymer oxidations catalyzed by LiP.

1.2.2.2 Manganese peroxidase

MnP is produced by white-rot fungi under ligninolytic conditions. The enzyme was first discovered in cultures of *P. chrysosporium* (Kuwahara et al., 1984; Glenn & Gold, 1985).

MnP is a glycoprotein and contains one iron protoporphyrin IX prosthetic group per molecule of enzyme (Glenn & Gold, 1985). The enzymes exist as several related isozymes and are encoded by a family of genes in *P. chrysosporium* (Gold & Alic, 1993). MnP is only expressed under ligninolytic conditions (limited nitrogen).

Immunoblot analysis and Northern (RNA) blot analysis show that the expression of manganese peroxidase in nitrogen-limited cultures of the lignin-degrading fungus *P. chrysosporium* is regulated at the level of gene transcription by Mn^{II} and various other chemicals, including H_2O_2 , ethanol, sodium arsenite, and 2,4-dichlorophenol, as well as by heat shock (Bonnarme & Jeffries, 1990; Brown et al., 1990, 1991; Li et al., 1995).

Both the spectral characteristics and the catalytic cycle of MnP are very similar to those of LiP and horseradish peroxidase (HRP) (Renganathan et al., 1986; Wariishi et al., 1988, 1989, 1992; Banci et al., 1992). However, Mn^{II} is required for reducing MnP compound II efficiently to the native enzyme and completing the catalytic cycle (Wariishi et al., 1988, 1989, 1992). Mn^{III} produced by the oxidation of Mn^{II} must form a chelator complex before it can oxidize phenolic substrates (Wariishi et al., 1992). Organic acids are good chelators (Glenn et al., 1986) and basidiomycetes produce oxalic acid (Wariishi et al., 1992; Kuan & Tien, 1993b), malonic acid (Wariishi et al., 1992; Kuan & Tien, 1993b), pyruvic acid (Archibald, 1992), and malic acid (Sasaki & Takao, 1967). Mn^{III} /oxalate and Mn^{III} /malonate form very stable complexes and can function as diffusible redox mediators. The MnP/ Mn^{II} /malonate system oxidizes several phenolic substrates including lignin model compounds and xenobiotics (Tuor et al., 1992; Valli et al., 1992). Furthermore, the Mn^{III} -chelator complex is a freely diffusible oxidant, and consequently can oxidize lignin within the woody matrix. *In vitro* studies show that both oxalic and malonic acids stimulate MnP activity. However, maximum MnP activity requires 1 mM oxalic acid and 50 mM malonic acid, respectively, at pH 4.5. 1–2 mM oxalic acid is produced in shaking cultures of *P. chrysosporium* under low-nitrogen conditions, in contrast, less than 20 μ M malonic acid is produced under the same conditions. These observations suggest that oxalic acid may function as the Mn^{II} / Mn^{III} chelator under physiological conditions. In addition, purified MnP can depolymerize synthetic lignin (DHP) (Wariishi et al., 1991b) and also degrades high-molecular-mass chlorolignin (Lackner et al., 1991). MnP is the predominant enzyme involved in kraft pulp bleaching (Paice et al., 1993) and decolorization of bleach plant effluents (Michel et al., 1991).

The binding site of Mn^{II} in MnP has been studied by molecular dynamics simulation (Banci et al., 1992, 1993), crystal structure (Sundaramoorthy et al., 1994), and site-directed mutagenesis (Kusters-van Someren et al., 1995; Kishi et al., 1996). These studies show that the Mn^{II} ion is hexacoordinated to the carboxylate oxygens of Glu35, Glu39, and Asp179, a heme propionate oxygen, and two waters. One of the water ligands is H-bonded to the second heme propionate. Mutations of Mn^{II} binding site ligands greatly affect the catalytic properties of MnP (Kusters-van Someren et al., 1995; Kishi et al., 1996). The turnover numbers (k_{cat}) for Mn^(II) oxidation by MnP(D179N) and MnP(E35Q-D179N) decrease 300- and 1000-fold with respect to that of the wild-type enzyme. The apparent dissociation constant (K_m) values for mutant MnP (E35Q) and MnP (E35Q-D179N) are 60 and 110 times higher than that of wild-type MnP. These results indicate that the proposed Mn binding site is also the productive site. In addition, the K_m and k_{cat} values for phenol, ferrocyanate, and iodide ion are similar for wild-type MnP and the binding variants (Kusters-van Someren et al., 1995); Kishi et al., 1996; Sheng & Gold, 1997a), suggesting that these substrates are not oxidized at the proposed Mn binding site.

1.2.3 Hydrogen peroxide-generating enzymes

A variety of intracellular and extracellular H₂O₂-generating enzymes from white-rot fungi have been purified. These enzymes use oxygen as an electron acceptor to oxidize a variety of substrates, such as carbohydrates, alcohols, and other organic compounds.

Intracellular oxidases, including glucose-1-oxidase (β -D-glucose:oxygen 2-oxidoreductase, EC 1.1.3.4) (Kelley & Reddy, 1986), pyranose-2-oxidase (pyranose:oxygen 2-oxidoreductase, EC 1.1.3.10) (Eriksson et al., 1986), and methanol oxidase (alcohol oxidase, EC 1.1.3.13) (Nishida & Eriksson, 1987), have been examined. It is still not clear whether H₂O₂ generated by intracellular oxidases is used by extracellular peroxidases. In addition, intracellular catalases from several white-rot fungi have been reported, so H₂O₂ may be disproportionated by catalase before it reaches the extracellular environment.

Extracellular oxidases are believed to be directly involved in lignin biodegradation, because H_2O_2 produced by these enzymes can serve as a co-substrate for peroxidases. Extracellular aryl-alcohol oxidase was first found in cultures of *T. versicolor* (Farmer et al., 1960). Generally, extracellular aryl-alcohol oxidases contain FAD as a cofactor (Muheim et al., 1990). Aryl-alcohol oxidases are also found in other white-rot fungi, such as *Pleurotus ostreatus* (Sannia et al., 1991), *Pleurotus sajor-caju* (Bourbonnais & Paice, 1988), and *Bjerkandera adusta* (Muheim et al., 1990). Another extracellular enzyme, glyoxal oxidase, has been purified from the ligninolytic cultures of *P. chrysosporium* (Kersten & Kirk, 1987). This enzyme oxidizes glyoxal, methylglyoxal, and several other α -hydroxy carbonyl and dicarbonyl compounds, coupled to the reduction of O_2 to H_2O_2 . Both glyoxal and methylglyoxal have been identified in the extracellular culture medium of *P. chrysosporium* under ligninolytic conditions (Kersten & Kirk, 1987). Spectroscopic and biochemical studies demonstrate that this enzyme has a free-radical-coupled copper complex in the catalytic site which is similar to that found in galactose oxidase (Whittaker et al., 1996), although no significant homology between these two enzymes is observed. (Kersten & Cullen, 1993; Kersten et al., 1995). Glyoxal oxidase was purified in an inactive form and was activated by LiP, which is produced under the same conditions, in the presence of aromatic alcohols, phenols, and lignins. This result suggests that this enzyme maybe involved in lignin degradation and in the regulation of lignin degradation (Kurek & Kersten, 1995). Finally, it has been reported that H_2O_2 can be generated as an intermediate in glyoxylate oxidation by MnP under aerobic conditions (Kuan & Tien, 1993a).

1.3 Organic Compounds Secreted by White-rot Fungi

Aryl alcohols (de Jong et al., 1994) and other organic compounds such as oxalic acid, malonic acid, and glyoxal (Kersten & Kirk, 1987; Wariishi et al., 1992; Kuan & Tien, 1993b; Kishi et al., 1994) are detected in the cultures of several white-rot fungi under ligninolytic conditions. The common feature of these compounds is that they do not contain nitrogen. It is not surprising that wood is the unique

substrate for these fungi. It offers a nitrogen limiting environment with a high carbon/nitrogen ratio. Under such nitrogen-limiting condition, these fungi always suffer nutritional imbalance or nitrogen starvation during the growth. To maintain a good carbon/nitrogen balance, they must dispose of the excess carbon in the form of nitrogen free metabolites such as aryl alcohol, other organic compounds, and polysaccharides. In addition to this physiological requirement, studies also show that aryl alcohols and non-aromatic compounds may play important roles in lignin degradation.

Aryl alcohols are found in the cultures of both white- and brown-rot fungi (de Jong et al., 1994). Several fungi producing *de novo* veratryl (3,4-dimethoxybenzyl)alcohol (VA), as well as other benzyl alcohols and aldehydes, are listed in Table 1.2. VA concentrations can reach as high as 2 mM in the ligninolytic culture medium of *P. chrysosporium* (Leisola et al., 1986). Pulse-labeling and isotope-trapping experiments show that the VA is derived from phenylalanine with cinnamate, benzoate, and/or benzaldehyde as intermediates (Jensen et al., 1994).

Oxalic acid, glyoxal, and methylglyoxal are also detected in certain white- and/or brown-rot fungal cultures (Kersten & Kirk, 1987; Wariishi et al., 1992; Kuan & Tien, 1993b; Kishi et al., 1994; Shimada et al., 1994). Oxalate metabolism is linked to both the tricarboxylic acid (TCA) and glyoxylic cycles, and its formation is catalyzed by oxaloacetase and glyoxylate oxidase, respectively. In white-rot fungi, oxalate is converted to CO₂ and formic acid by a decarboxylase (Shimada et al., 1994). LiP and MnP also can convert oxalate to CO₂. Oxalate concentration can be as high as 2 mM in cultures of *P. chrysosporium* under ligninolytic conditions (Kishi et al., 1994). This concentration of oxalate stimulates maximum MnP activity in *in vitro* assays, suggesting that the physiological role of oxalate is probably to chelate Mn^{III}. Glyoxal and methylglyoxal also are secreted in ligninolytic cultures of *P. chrysosporium* (Kersten & Kirk, 1987). In addition, the production of glyoxal oxidase and peroxidases (LiP, MnP) and the production of glyoxal and methylglyoxal temporally overlap in ligninolytic cultures of *P. chrysosporium*, suggesting that glyoxal and methylglyoxal may function as major oxidase substrates (Kersten & Kirk, 1987).

Table 1.2

The Production of Aromatic Alcohol/Aldehyde by White-Rot Fungi^a

Fungus	VA ^b	AA	BA	CA	DA
<i>Armillaria ostoyae</i>	o		o,•		
<i>Armillaria mellea</i>	o,•	•	o,•		
<i>Bjerkandera adusta</i>	o,•	o,•	o,•	o,•	o,•
<i>Bjerkandera sp. BOS55</i>	o,•	o,•		o,•	o,•
<i>Coriolopsis occidentalis</i>	o				
<i>Dichomitus squalens</i>	•	•	o		
<i>Hypholoma fasciculare</i>					o,•
<i>Ischnoderma benzoinum</i>	•	o,•	•		
<i>Lentinula edodes</i>	o				
<i>Oudemansiella mucida</i>					o,•
<i>Phanerochaete chrysosporium</i>	o,•				
<i>Phlebia radiata</i>	o		o,•		
<i>Pleurotus ostreatus</i>		•			
<i>Pycnoporus cinnabarinus</i>	o				
<i>Ramaria sp.158</i>				•	•
<i>Trametes gibbosa</i>	o,•				
<i>Trametes hirsuta</i>	•				
<i>Trametes versicolor</i>	o			•	
<i>Trichaptum pergamenum</i>	o,•		•		

^a de Jong et al., 1994.^b The production of veratryl (VA), anisyl (AA), benzyl (BA), 3-chloro-anisyl (CA), and 3,5-dichloroanisyl alcohols (DA) (o) and aldehydes (•).

1.4 Heme Peroxidases

1.4.1 Classification of heme peroxidases

Peroxidases are found in most organisms from bacteria to animals. The primary function of peroxidases is to oxidize molecules at the expense of H_2O_2 . The substrates for peroxidases range from low-molecular-mass compounds, such as phenols, halogen ions, and thiocyanate ion, to compounds with molecular masses > 10 kD, such as ferrocyanochrome *c* and lignin. Structurally, most peroxidases contain ferric protoporphyrin IX (Fig. 1.2) as a prosthetic group.

Plant peroxidases are thought to participate in a variety of biological pathways, including synthesis of the cell wall, lignin, and suberin, metabolism of hormones such as indole-3-acetic acid, stress responses, and fatty acid metabolism (Grisebach, 1981; Higuchi, 1989b). Among the plant peroxidases, horseradish peroxidase (HRP) has been extensively studied. Other well characterized plant peroxidases include turnip peroxidase (Mazza, 1968), Japanese radish peroxidase (Dunford & Stillman, 1976), peanut peroxidase (Buffard et al., 1990; Schuller et al., 1996), and ascorbate peroxidase (Patterson & Poulos 1995; Patterson et al., 1995; Marquez et al., 1996)

Bacteria and other microorganisms also produce peroxidases. One of the best characterized peroxidases, cytochrome *c* peroxidase (CcP), is purified from the intermembrane space of the mitochondria of baker's and brewer's yeast (Williams & Stewart, 1976; Maccacchini et al., 1979; Maccacchini, 1981). CcP catalyzes the oxidation of ferrocyanochrome *c in vitro*. The role of CcP *in vivo* is not clear although there is evidence suggesting that CcP may support oxidative phosphorylation in the absence of cytochrome oxidase (Erecínska et al., 1973). Nevertheless, protein engineering and structural studies on CcP have been used as a model in the elucidation of peroxidase reaction mechanisms and electron transfer pathways, as well as the interaction between the enzyme and its polymeric substrate, ferrocyanochrome *c* (Goodin et al., 1986; Ferrer et al., 1991; Pelletier & Kraut, 1992).

The fungal chloroperoxidase from *Caldarimyces fumago* (Morris & Hager, 1966) and the marine algal bromoperoxidase from *Penicillus capitatus* (Manthey &

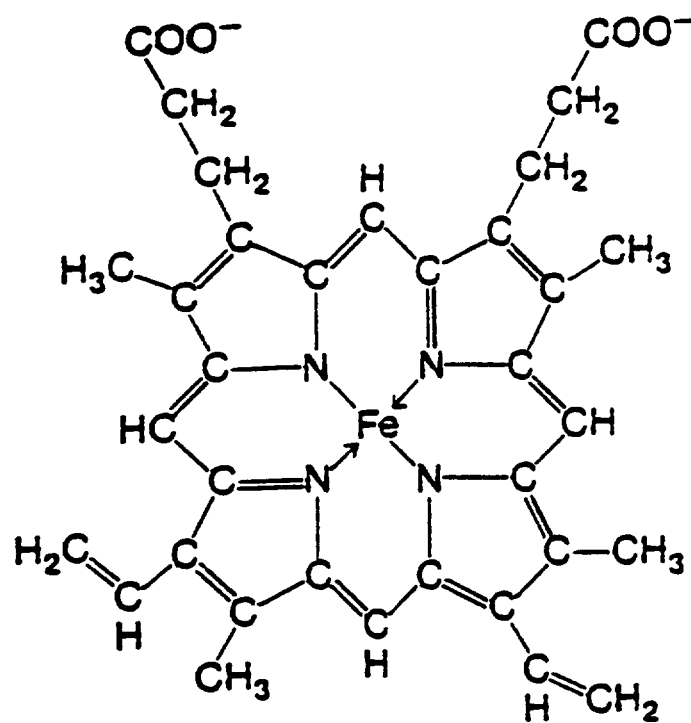


Figure 1.2 Protoporphyrin IX.

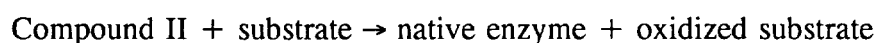
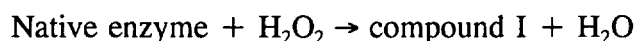
Hager, 1981) have also been characterized. The chloroperoxidase is able to catalyze the oxidation of chloride ion, as well as a wide variety of compounds.

Bromoperoxidases use bromide ion (but not chloride) to brominate organic compounds and may be involved in antimicrobial systems. Other fungal peroxidases, including *Coprinus cinereus* peroxidase (CIP), *Arthromyces ramosus* peroxidase (ARP) have been isolated. Although CIP shows 40–45% amino acid sequence identity to LiPs and MnPs from *P. chrysosporium*, CIP is unable to degrade lignin. CIP resembles HRP in terms of its enzymatic specificity (Kunishima et al., 1994; Petersen et al., 1994).

LiP and MnP from *P. chrysosporium* share general structural features with other plant, yeast, and fungal peroxidases. Among these peroxidases, HRP and CcP have been the most extensively characterized. Therefore, HRP and CcP have served as models for the characterization of LiP and MnP. Mammalian peroxidases play important roles in antibacterial systems and in hormone synthesis, but these enzymes are beyond the scope of this discussion.

1.4.2 Peroxidase catalytic cycle

The reaction center of plant and fungal peroxidases is a ferric protoporphyrin IX, in which the iron is chelated by the four pyrrole nitrogen atoms of the macrocycle and axially coordinated by an imidazole nitrogen atom of His from the protein (Fig. 1.2). The oxidation state of iron in the resting state is +3 as determined by Mössbauer, electron paramagnetic resonance (EPR), and resonance Raman spectroscopic studies (Dunford & Stillman, 1976). These peroxidases have common features in their reaction mechanisms. In general, the peroxidase reaction can be formulated as follows:



The steady-state kinetic mechanism is described as a modified bi-bi ping-pong mechanism (Dunford, 1982). In the first step, upon the addition of H_2O_2 , the native enzyme undergoes a two-electron oxidation to form peroxidase compound I.

Compound I is reduced by one electron to compound II. Finally, native enzyme is

regenerated by the one electron reduction of Compound II. In addition, the reaction between peroxidase compound II and H_2O_2 results in the formation of peroxidase compound III, which is an inactive form of the enzyme (Adediran & Lambeir, 1989; Marquez & Dunford, 1990; Wariishi & Gold, 1990).

Chemical studies demonstrate that peroxidase compound I contains two oxidizing equivalents over the native enzyme. Thus, the iron of peroxidase compound I has a formal oxidation state of +5. The one electron reduction of compound I yields compound II. Thus compound II is one oxidizing equivalent over the native enzyme and has a formal oxidation state of +4 for its iron. All known heme peroxidases have a common compound II electronic structure in which the single oxidizing equivalent is stored as the ferryl (Fe(IV)=O) species as determined by Mössbauer (Schulz et al., 1984), NMR (La Mar et al., 1983), X-ray absorption (Chance et al., 1984), electron nuclear double resonance (ENDOR) (Roberts et al., 1981a), and resonance Raman (Sitter et al., 1985; Hashimoto et al., 1986a,b,c) spectroscopic studies.

The same ferryl species is observed in compound I by spectroscopic studies (Chance et al., 1984; Schulz et al., 1984; Penner-Hahn et al., 1986) and crystal structural studies (Edwards et al., 1987). Thus, peroxidase compound I must store the additional oxidizing equivalent somewhere other than the iron center. Two possible locations are (a) the electron-rich porphyrin ring or (b) an amino acid residue which is close to the iron center and easily oxidized. Dolphin et al. first proposed that the second oxidizing equivalent in the plant peroxidase HRP is stored on the heme porphyrin (Dolphin et al., 1971). Therefore the HRP compound I structure is described as $\text{Fe(IV), P}^\ddagger$. This concept of a π -cation radical in HRP compound I was confirmed by NMR (La Mar et al., 1981), ^{14}N ENDOR (Roberts et al., 1981a,b), and resonance Raman (Felton et al., 1976) studies.

In contrast, electro spectroscopic studies show that CcP compound I resembles HRP compound II, since both intermediates have three unpaired electrons. EPR studies demonstrated that there is a free-radical-like signal at 77 K (Yonetani, 1976) in CcP compound I, suggesting that the second oxidizing equivalent is separated from the iron center and exists as an amino acid radical. Efforts at locating the radical site

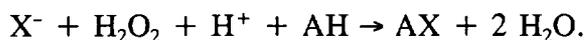
in CcP compound I by ENDOR (Huyett et al., 1995), EPR (Hori & Yonetani, 1985), and site-directed mutagenesis (Fishel et al., 1987; Goodin et al., 1987; Mauro et al., 1988) show that the amino acid residue storing the second oxidizing equivalent is Trp191 on the proximal side of the heme. The formation of the protein radical in the CcP compound I is unique among peroxidases and is essential for electron transfer between CcP and cytochrome *c* (Mauro et al., 1988). Other known plant and fungal peroxidase compounds I contain a porphyrin π -cation radical.

The two-electron reduction of peroxidase compound I to the native enzyme by a reducing substrate normally occurs by two single-electron steps via compound II. In addition, the reaction of peroxidase compound II with various reducing substrates is the rate-limiting step in the peroxidase catalytic cycle (Critchlow & Dunford 1972a,b; Dunford & Cotton, 1975; Hewson & Dunford, 1976; Wariishi et al., 1991a). These phenomena can be explained if the redox potential of compound I is higher than that of compound II. However, the redox potentials determined for compound I and II of a few peroxidases, E1 (compound I/compound II) and E2 (compound II/native enzyme), are similar (Hayashi & Yamazaki 1979; Farhangrazi et al., 1994). Therefore, the redox potential may not explain the higher reactivity of compounds I compared to compound II. Marcus theory has successfully explained the electron transfer in several systems (Marcus & Sutin, 1985). According to Marcus, the activation energy of the electron transfer reaction, ΔG^* , is determined by the driving force of the reaction, ΔG° , and the reorganization energy, λ , according to the equation: $\Delta G^* = (\Delta G^\circ - \lambda)^2 / 4\lambda$. The rate of the reaction is proportional to $\exp(-\Delta G^*/\lambda)$. The reorganization energy represents the energy required to reorganize protein (ligand)-metal bond distances and geometries prior to electron transfer. Reorganization energy may contribute to the different reactivities of compounds I and II. The reduction of compound II involves the release of H₂O and a change in the coordination (hexacoordinate to pentacoordinate) and spin state (low spin to high spin) of the iron center, whereas essentially no change of heme geometry is involved in the reduction of compound I to compound II. In addition, the electron transfer process is affected by the medium through which the electron passes and by the distance between redox centers. The ferryl oxygen atom and the heme center in HRP

compound I are inaccessible to reducing substrates as determined by primary suicide inhibition studies with substituted hydrazines (Ator & Ortiz de Montellano, 1987; Ator et al., 1987; Salowe et al., 1987; Ortiz de Montellano et al., 1988). The higher reactivity of compound I may result from exposure of the porphyrin π -cation radical at a peripheral site, thus reducing the distance to the reducing substrate (Ator & Ortiz de Montellano, 1987; Ator et al., 1987; Salowe et al., 1987; Ortiz de Montellano et al., 1988).

Finally, one atypical reaction mechanism is involved in the peroxidase catalytic cycle. First, certain heme-containing peroxidases, such as chloroperoxidase from *C. fumago*, HRP (Neidleman & Geigert, 1986), and LiP and MnP from *P.*

chrysosporium (Renganathan et al., 1987; Farhangrazi et al., 1992), are known to use H_2O_2 to oxidize halide ions (X^-) to a reactive halogenating species as follows:



Since no definitive evidence for the formation of a short-lived Fe(III)- OX^- intermediate is available, it is generally considered that the halogenation reaction involves compound I of the haloperoxidase without the formation of compound II (Thomas et al., 1970a,b; Sheng & Gold, 1997a). OX^- and its protonated form, hypohalous acid (HOX), are very reactive halogenation agents. Subsequent reactions of these species with substrates produce halogenated products. Halogenation substitutions, catalyzed by peroxidases, usually take place at a carbon atom of the substrate having an activated C-H bond (Neidleman & Geigert, 1986). The presences of a double bond, a phenyl group, and certain heteroatoms are known to activate hydrogen atoms on adjacent carbons, and the halogenation of lignin-related model compounds by LiP and MnP have been reported (Renganathan et al., 1987; Farhangrazi et al., 1992; Sheng & Gold, 1997).

1.4.3 Amino acids involved in the heme peroxidase catalytic cycle

Our understanding of amino acid residues involved in the heme peroxidase catalytic cycle is largely owing to crystal structures and protein engineering studies. These studies elucidated the roles of amino acid residues in O-O bond cleavage, the stabilization of the Fe(IV)=O intermediate, and the control of the heme iron redox

potential. In addition, evidence for amino acid residues which are involved in substrate binding and electron transfer is accumulating.

1.4.3.1 Residues on the distal side of the heme

Distal side amino acids are involved in the peroxide activation and stabilization of peroxidase compound I. The ferric iron in the heme of native peroxidase is hexacoordinate with a displaceable water molecule so that the sixth coordination site of iron is available. Heterolytic cleavage of the H_2O_2 through acid-base catalysis in the heme distal pocket is described by the "push-pull" mechanism (Dawson, 1988). Electron donation by the proximal ligand promotes O–O bond cleavage ("push"). The "pull" derives from the distal side group where the distal His serves as an acid-base catalyst while the distal Arg helps to polarize the peroxide O–O bond. In CcP, the rate of compound I formation decreased five orders of magnitude in the His52Leu mutant (Erman et al., 1993). Similar results were obtained with the His42Ala and His42Val variants of HRP (Newmyer & Ortiz de Montellano, 1995), supporting the premise that the distal His plays an essential role as an acid-base catalyst in the formation of compound I. However, replacement of the proximal His with either Glu or Gln in CcP results in an enzyme that forms compound I at about the same rate as the wild-type enzyme, suggesting that the distal acid-base catalysis, rather than the nature of proximal ligand, is key to the fast rate of compound I formation in peroxidase (Choudhury et al., 1994). The distal Arg is believed to be important for peroxide binding and stabilization of the transient enzyme-substrate complex prior to the cleavage of the RO–OH bond. In CcP, the observed rates of the O–O bond scission step in Arg48Leu and Arg48Lys mutants range between 1000 and 1950 s^{-1} , an estimated two orders of magnitude slower than for the wild-type enzyme (Vitello et al., 1990). Moreover, the crystal structure of CcP shows that the distal Arg is able to rotate, allowing optimal hydrogen bonding interaction with the ferryl oxygen atom in compounds I and II, suggesting that the distal Arg plays a role in stabilizing the peroxidase intermediates (Finzel et al., 1984; Edwards et al., 1987). Interestingly, changing the distal Arg to Lys does not affect the rate of CcP compound I formation significantly, whereas the same mutation in HRP shows a 500-fold decrease in the rate of compound I formation (Vitello et al., 1993; Smulevich et al., 1994). This

indicates that the orientation of the distal Arg in HRP may be different from that in CcP. Besides the amino acid residues directly involved in the O–O cleavage, two side chains and one carbonyl backbone on the distal side are highly conserved (Welinder et al., 1995). These are His, Asn, and Glu. An H-bond between His and Asn has been proposed to ensure that N_ε of the distal His is available for accepting a proton from peroxide.

1.4.3.2. Residues on the proximal side of the heme

The microenvironment at the proximal side of the heme contributes to stabilizing the Fe(IV)=O intermediate, controlling the redox potential and the rate of the O–O bond cleavage reaction. The proximal His in heme peroxidases is H-bonded to an Asp, which imparts more imidazolate character to the His, thus lowering the redox potential of the iron center of the heme and stabilizing the oxyferryl iron in compounds I and II. CcP mutant studies in which the proximal Asp has been converted to Asn (Goodin & McRee, 1993) or the proximal His to Gln (Choudhury et al., 1992, 1994) show a correlation between redox potential and the ability of the ligand to carry a negative charge. Thus, the redox potential of the Fe³⁺/Fe²⁺ couple increases as the negative charge on the proximal ligand decreases. Besides H-bonding to the proximal His, it has been proposed that the proximal His stabilizes the Trp191 radical (Fitzgerald et al., 1995). The crystal structures of the proximal variants show that Glu and Gln are ligated to the heme iron and interact with Asp235 (Choudhury et al., 1992, 1994). The His175Gln mutant remains active, and the His175Glu mutant is seven times more active than the wild-type enzyme. This indicates that the negative charge on the Glu residue provides additional electrostatic stabilization to the heme iron center, thereby increasing the thermodynamic driving force for electron transfer (Goodin et al., 1991; Choudhury et al., 1994). However, compounds I of these mutants are less stable than that of the wild-type CcP (Choudhury et al., 1992, 1994). In wild-type CcP, the indole ring of Trp191 and the imidazole ring of His175 form a parallel π stacking which stabilizes the free radical in CcP (Goodin & McRee, 1993). Changing the His to a non-aromatic residue disrupts this π – π interaction (Choudhury et al., 1994). Therefore, besides enhancing the peroxidase activity, the proximal ligand also may stabilize intermediates in CcP.

1.5 Lignin Peroxidase: Structure and Functions

Progress in the biochemistry, molecular biology, and applications of lignin peroxidase from *P. chrysosporium* has been made during the past 15 years. A number of reviews on the subject have been published (Buswell & Odier, 1987a; Kirk & Farrell, 1987; Gold et al., 1989; Gold & Alic, 1993; Reddy, 1993; Hatakka, 1994; Reddy & D'Souza, 1994; Cullen 1997). Although LiP shares common structural and catalytic features with other plant and fungal peroxidases, it is able to oxidize non-phenolic compounds with the redox potentials beyond the reach of other plant and fungal peroxidases. In addition, in the presence of VA, a secondary metabolite of *P. chrysosporium*, LiP can oxidize polymeric lignin model compounds (Wariishi et al., 1994), aromatic pollutants, and synthetic lignins (Hammel et al., 1993). For this reason, elucidation of the role of VA in the LiP catalyzed reaction has been an active research field. This section describes previous studies on LiP, particularly, the crystal structure of LiP and catalytic properties, and the possible roles of VA in the reaction.

1.5.1 General properties of lignin peroxidase

LiP is expressed by *P. chrysosporium* as a family of isoenzymes with molecular weights ranging from 38 to 43 kD and pI values ranging from 3.3 to 4.7 (Gold & Alic, 1993). The isoenzymes typically contain 10–15 % carbohydrate. The number and abundance of LiP isozymes purified from *P. chrysosporium* varies from 2 to 15 depending on the culture conditions, purification procedures, and strains employed (Higuchi, 1990; Schoemaker, 1990; Tuisel et al., 1990; Blanchette, 1991; Gold & Alic, 1993). The heme proteins separated from the extracellular culture of *P. chrysosporium* BKM-F-1767 (ATCC 24725) grown in defined low-nitrogen medium containing dimethyl succinate buffer, have been designated as H1, H2, ..., H10 (H: heme protein). H1, H2, H6, H7, H8, and H10 show LiP activity as measured by VA oxidation (Gold et al., 1984; Tien & Kirk, 1984) and H3, H4, H5, and H9 show MnP activity, as assayed by Mn^{II} oxidation in the presence of H₂O₂ (Glenn & Gold, 1985).

In white-rot fungi, extracellular LiP production is regulated by nutrient conditions and by buffers in culture. LiP from *P. chrysosporium* is produced during secondary metabolism, which is triggered by nitrogen and carbon depletion. The transition from primary to secondary metabolism in *P. chrysosporium* is positively correlated with an increase in intracellular cAMP concentration (Pall, 1981). This relationship is only observed in cells grown under ligninolytic (low-N) conditions. The production of LiP and MnP may be linked to the rise in intracellular cAMP concentration (Boominathan & Reddy, 1992). Buffers selected for the culture of *P. chrysosporium* also affect the relative abundance of LiP isozymes. Studies of *P. chrysosporium* strain BKM-F-1767 (ATCC 24725) show that in static cultures with low-N medium, LiP H8 is the dominant isozyme when 2,3-dimethylsuccinate is used as the buffer; whereas H2 and H6 are the major isozymes in acetate-buffered cultures. Moreover, LiP H2 and H6 are produced in smaller amounts in shaking culture as compared with stationary cultures (Reddy & D'Souza, 1994). The factors controlling LiP production in various buffers and under various growth conditions (stationary and shaking) remain unknown.

Several white-rot fungi other than *P. chrysosporium* also produce LiP isozymes (Table 1.3). All of these LiP isozymes have molecular weights of 43–47 Kd and pI values of 3.1–3.7. Six LiP isozymes from *Trametes versicolor* were characterized by amino-terminal sequencing, amino acid analysis, carbohydrate analysis, and peptide mapping (Johansson & Nyman, 1993; Johansson et al., 1993). Based on a comparison of the first 35 amino acids in the N-terminals of the LiPs, the degree of similarity among the five LiPs was about 80%.

The native enzyme and the oxidized intermediates, compound I and compound II as well as the ligated form of LiP share the common electronic spectra with the well studied plant peroxidase, HRP. However, LiP is more easily oxidized to a LiPIII-like species (LiPIII*), at H₂O₂ concentrations that are considerably less than that required by other peroxidases (Marquez et al., 1988). As shown in Tables 1.4 and 1.5, electronic absorption maxima for LiP, its oxidized forms, and various ligated forms of the enzyme are similar to those of other heme proteins. UV/VIS spectroscopy, as well as EPR, NMR resonance, and Raman spectroscopy, indicate

Table 1.3

Molecular Masses (M) and the Isoelectric Points
of Lignin Peroxidases from Selected White-Rot Fungi^a

Fungus	Isoenzyme	M (kDa)	pI
<i>Phanerochaete chrysosporium</i> BKM-F-1767 (ATCC-24725)	H1	38	4.7
	H2	38	4.4
	H6	40,42	3.7
	H7	42	ND
	H8	42	3.5
	H10	43	3.3
<i>Phlebia radiata</i> 79 (ATCC 64658)	LiP1	42	4.1
	LiP2	45	3.9
	LiP3	44	3.2
<i>Phlebia radiata</i> L 12-41	PrS-L1	39	4.2
	PrS-L2	39-40	3.1
<i>Coriolus versicolor</i>	LiP1	43-45	3.4
	LiP2		3.2
	LiP3		
<i>Junghuhnia separabilima</i>	LiPH2	47	3.5
	LiPH3	44	3.5
	LiPH4	43	3.4
<i>Phlebia ochraceofulva</i>	LiP1	40	ND
	LiP2	44	ND
	LiP3	38	ND
	LiP4	43	ND
	LiP5	44,46	ND

^a Hatakka, 1994.

Table 1.4

Electronic Absorption Spectral Maxima of Lignin Peroxidase and Other Heme Proteins^a

System	nm			
Ferric, high spin				
Native LiP, pH 4.5	407	500		632
AquometMb, pH 7.0	409	505		635
Catalase	405	500	535	630
HRP, pH 6.0	403	500		641
Cytochrome P-450-cam	391	500		646
Ferric, low spin				
Cytochrome b5	360	425	541	578
CN ⁻ -LiP	360	423	540	
CN ⁻ -metMb	359	423	540	
CN ⁻ -HRP		422		580
CN ⁻ -P-450		439		
N ₃ ⁻ -LiP		418	540	575
N ₃ ⁻ -metMb		420	540	570
N ₃ ⁻ -HRP		416	534	565
N ₃ ⁻ -P-450		427		
Ferrous				
LiP		435	556	
deoxy-Mb		434	556	
HRP		437	556	
P-450		411	540	
Ferrous CO				
LiP		420	535	568
Mb	343	423	542	574
HRP		423	541	575
P-450	368	446	551	

^a (Gold et al., 1984; Andersson et al., 1987).

Table 1.5
Spectral Characteristics of Oxidized Intermediates
of Lingin Peroxidase^a

Enzyme intermediates	Absorption Maxima ^a			
Native LiP	407.6 (133)	500 (8.1)		632 (2.7)
LiPI	408 (55)		550	608 (sh) ^c 650 (4.5)
LiPII	420 (108)	525 (7.5)	556 (7.5)	
LiPIII	414 (106)	543 (8.8)	578 (7.6)	
LiPIII*	419 (90)	543 (9.0)	578 (7.9)	

^a Gold et al., 1984; Renganathan & Gold, 1986; Wariishi & Gold, 1990.

^b Values in parentheses are extinction coefficients expressed in $\text{mM}^{-1}\text{cm}^{-1}$.

^c Shoulder.

that the native form of LiP exists as a ferric, high-spin, pentacoordinated heme protein with the protein ligated to the heme iron through the proximal His. Comparison of *lip* cDNAs also suggests that a proximal and distal His and a distal Arg are conserved in the active site of LiP. The crystal structure of LiP confirmed that the heme environment of LiP is similar to that of other plant and fungal peroxidases (Poulos et al., 1993).

1.5.2 Crystal structure of lignin peroxidase

1.5.2.1 General features of LiP crystal structure

The overall topography of LiP from *P. chrysosporium* is very similar to that of CcP, the first crystal structure solved in the heme peroxidase family (Finzel et al., 1984; Poulos et al., 1993) (Fig. 1.3). LiP contains 49 more amino acid residues than CcP located at the C-terminus. Structurally, LiP can be divided into N- and C-domains with the heme embedded in a crevice. As observed in CcP, helices B and F bracket the distal and proximal faces of the heme. In contrast to the similarities in the overall structure, LiP has four disulfide bonds whereas CcP has none. Like other plant and fungal peroxidases, LiP also contains two gram-atoms of calcium per mole of enzyme. On the proximal side the Ca ligand, Ser177, is at the C-terminal end of proximal helix and immediately follows the heme ligand His 176. On the distal side the Ca ligand, Asp48, immediately follows the distal His 47 at the C-terminal of the distal helix. Calcium is very important for HRP activity (Haschke & Friedhoff, 1978). In LiP, calcium ion may be involved in maintaining the integrity of the active site (Poulos et al., 1993) and in providing thermal stability (Nie & Aust, 1997). LiP crystal structure studies (Poulos et al., 1993) also confirm that there is one N-linked carbohydrate located at Asn257. A second O-linked carbohydrate is tentatively proposed for Ser334 (Fig. 1.3).

1.5.2.2 Active site of LiP and relevance to the catalytic cycle

Fig. 1.4 shows a stereoview of the active site environment of LiP. Arg43, Phe46, and His52 form the peroxide binding pocket (Poulos et al., 1993). Details of the hydrogen-bond network between the distal His47 and other regions, as observed in CcP, are conserved in LiP. The N_δ atom of His47 donates an H-bond to the side

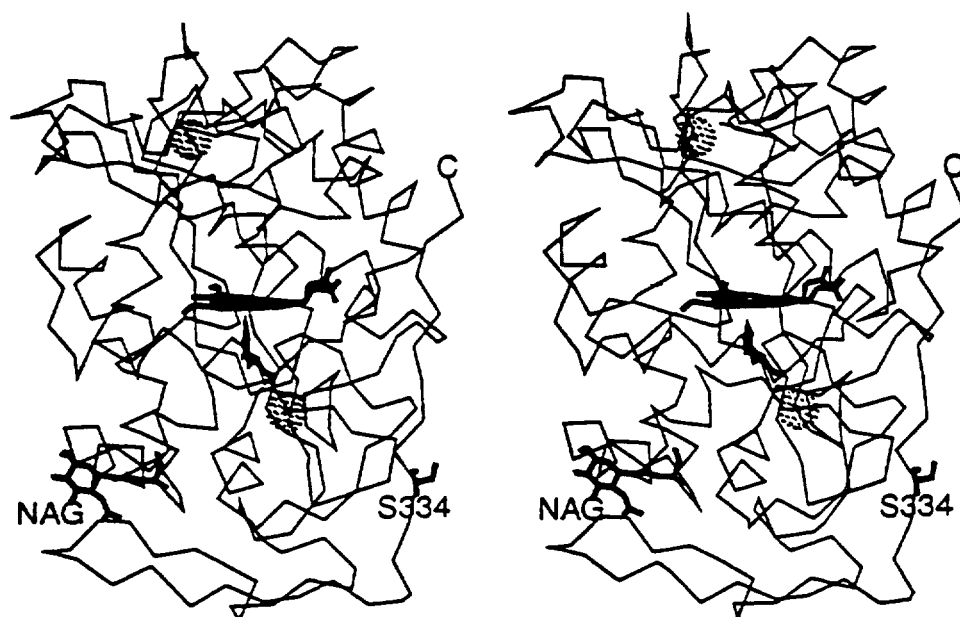


Figure 1.3 α -Carbon diagram of lignin peroxidase (Poulos et al., 1993).

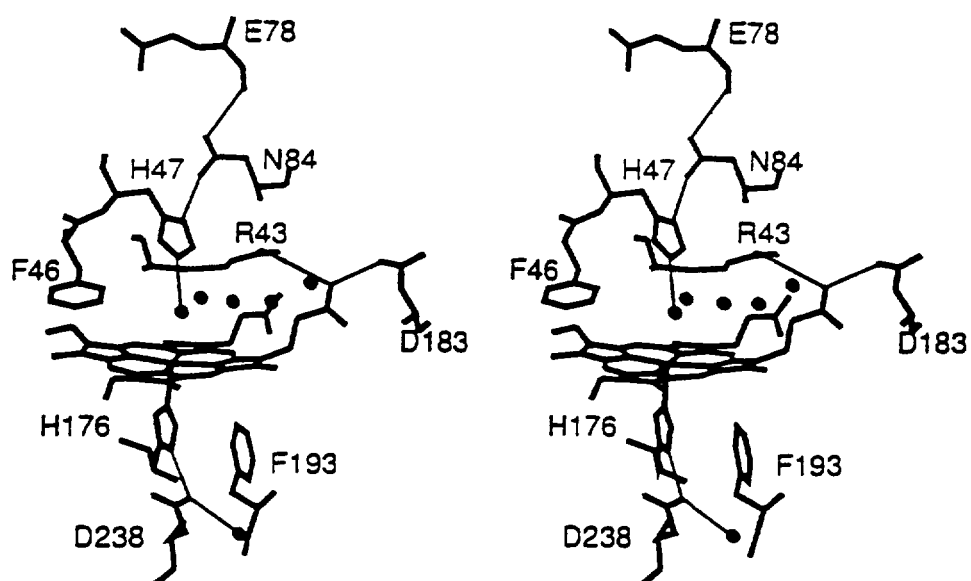


Figure 1.4 Stereoview of the active site environment of lignin peroxidase (Poulos et al., 1993).

chain oxygen of Asn84 and the side chain nitrogen of Asn82 donates an H-bond to the peptide carbonyl oxygen atom of Glu78. In addition, the peptide carbonyl oxygen of Ile85 H-bonds with the side chain of Arg 43. The distal His is approximately the same distance from the iron in both LiP (5.3 Å) and CcP (5.5 Å). The similarity of the architecture on the distal sides of LiP and CcP suggests that the mechanism of compound I formation proposed for CcP operates in LiP as well (Poulos & Kraut, 1980; Finzel et al., 1984). In this mechanism, the incoming peroxide donates a proton to the distal His, which is unprotonated, owing to the H-bond pattern between this His and Asn82, which ensures that the N ϵ is available to accept a proton. The distal Arg serves two functions. First, it aids in stabilizing the developing negative charge of the peroxide OH⁻ leaving group. Secondly, once the O–O bond is cleaved, the distal Arg rotates to H-bond to the ferryl oxygen atom of compound I, thereby stabilizing it (Edwards et al., 1987).

At the proximal side of LiP, His176 coordinates with the heme iron atom. The buried Asp235 carboxylate group accepts an H-bond from His176. This H-bond imparts anionic character to the proximal His, and thereby helps to lower the redox potential of the heme iron and stabilize compound I. An obvious difference between LiP and CcP is that Phe46 (distal site) and Phe 193 (proximal site) in LiP are Trp residues in CcP. Functionally, these differences may explain how these two peroxidases differ in storing the oxidizing equivalents of compound I. In both peroxidases, compound I stores one oxidizing equivalent as the Fe (IV)–O group, but CcP is unique in that the second equivalent is stored as an amino acid free radical (Yonetani, 1976). The available evidence strongly favors Trp191 as the radical site (Mauro et al., 1988; Sivaraja et al., 1989; J. M. Wang et al., 1990). The equivalent residue in LiP is Phe193. LiP is oxidized to a porphyrin π -cation radical, as is proposed for most plant and fungal peroxidases (Dolphin et al., 1971; Renganathan et al., 1986), since the redox potential for the oxidation of Phe is higher than that for Trp.

1.5.2.3 Substrate binding

It is still not clear whether LiP oxidizes lignin directly or via a small molecular mediator. The heme of LiP is buried and unavailable for interaction with

polymeric substrates (Poulos et al., 1993); however, LiP can oxidize nonphenolic aromatic compounds. In particular, the oxidation of VA by LiP has been well-studied. VA appears to be a favored substrate for LiP and it is secreted as a secondary metabolite, coinciding with LiP production in *P. chrysosporium*. In addition, it plays very important roles in the LiP oxidation of recalcitrant substrates (see Section 1.5.5). Therefore, elucidation of the binding of this small aromatic compound to LiP would be useful. Unfortunately, the crystal structure of the VA–LiP complex is unavailable, owing either to the weak binding of VA or to the conditions used for crystal growth. However the binding of VA to LiP has been examined by computational modeling (Poulos et al., 1993). Modeling shows that VA binds to a pocket 6–7 Å from the heme (Fig. 1.5). There are very few unfavorable contacts in the docked complex, and only the side chain of Ile85 has to move slightly to accommodate the substrate. The primary contacts between VA and LiP are with Ile85, Val184, Gln222, Phe148, and His82. The benzylic OH of VA appears to form an H-bond with His82. More studies are needed to localize the VA binding site unambiguously.

1.5.3 Substrates for lignin peroxidase

LiP catalyzes the oxidation of a large variety of compounds. These include inorganic ions (Br^- , I^-) (Renganathan et al., 1987; Farhangrazi et al., 1992), substituted benzenes (Kersten et al., 1990; Valli et al., 1990; Joshi & Gold, 1996), phenols (Koduri & Tien, 1995), lignin model dimers (Miki et al., 1986), pollutants (Hammel et al., 1986; Joshi & Gold, 1994), dyes (Paszczynski et al., 1992; Spadaro et al., 1992; Spadaro & Renganathan, 1994; Chivukula et al., 1995), polymeric lignin model compounds (Wariishi et al., 1994), (see Chapters 3, 4, and 5), and synthetic lignins (Hammel et al., 1993). The molecular weights of these compounds range from hundreds of daltons (inorganic ions, substituted benzene) up to more than 10,000 daltons for biopolymers such as ferrocyanochrome *c*. The mechanisms involved in these oxidation reactions have been extensively investigated.

During halide ion oxidation to OX^- , it is believed that LiP compound I is reduced to the native enzyme directly instead of forming compound II. The highly

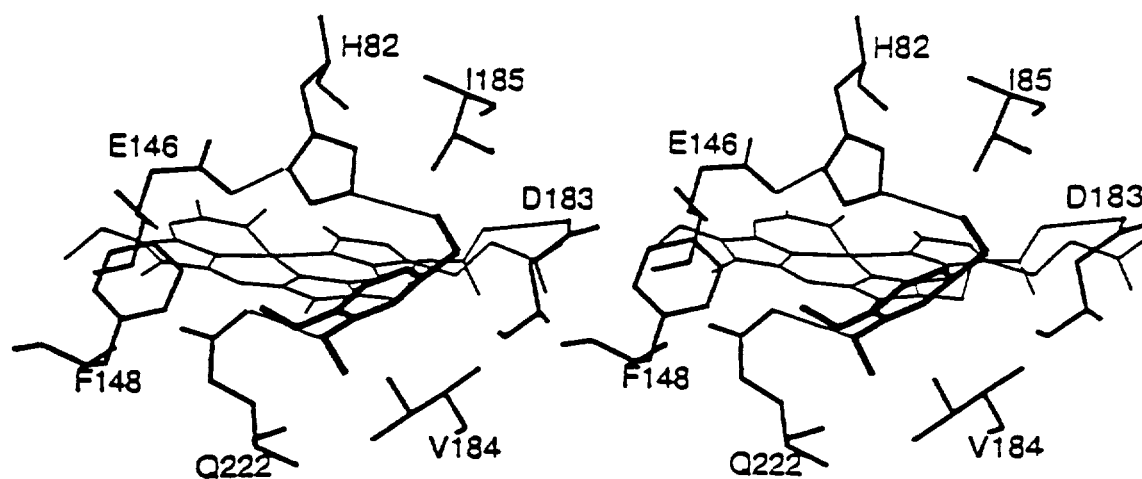


Figure 1.5 Stereoview of hypothetical complex between veratryl alcohol and lignin peroxidase (Poulos et al., 1993).

reactive OX^- species can react either with excess X^- to produce X_2 and H_2O or with organic substrates to generate halogenated products. LiP can act as a bromoperoxidase but not as a chloroperoxidase, suggesting that the redox potential of LiP compound I is lower than that of the redox couple of Cl^-/ClO^- (Renganathan et al., 1987). LiP catalyzes the bromination of aromatic rings, 1,3-diketones, and α,β olefins conjugated to aromatic rings. Even though it has been reported that white-rot fungi are an important natural source of halomethanes (Harper, 1985), the involvement of LiP or MnP in these *in vivo* halogenation reactions is not clear. The possible physiological significance of these reactions will require the identification of halogenated compounds produced by *P. chrysosporium*

The LiP oxidation of VA has been well-studied. LiP oxidizes VA to veratraldehyde as the dominant product with other minor products such as quinones and lactones. The following mechanism is believed to be involved in the LiP catalyzed oxidation of VA (Schmidt et al., 1989; Joshi & Gold, 1996) (Fig. 1.6). The oxidized LiP intermediates, compounds I and compound II, remove one electron from the aromatic ring to form a VA cation radical. The latter loses a proton immediately after it is formed to produce the VA benzylic radical. The VA benzylic radical can be further oxidized by LiP compounds I or II to form veratraldehyde or can react with oxygen in a non-enzymatic reaction to generate the aldehyde. Water also can attack the VA cation radical, followed by subsequent demethoxylation to produce quinones. Alternatively, the adduct of the VA cation radical and H_2O and the HOO radical can undergo intramolecular rearrangements to produce lactones. The reaction mechanism of lignin model dimer oxidation by LiP has also been investigated. The β -O-4 lignin dimer, which accounts for more than 50% of the linkages in lignin, is oxidized by LiP to form a cation radical (Miki et al., 1986; Umezawa & Higuchi, 1989). The latter reacts with H_2O or O_2 , leading to the formation of monomeric products. Synthetic lignins (DHPs) have been used to demonstrate the ability of LiP to oxidize polymeric compounds. Hammel et al. (1993) used ^{14}C - and ^{13}C -labeled DHPs to show that LiP catalyzes the cleavage reaction to yield low-molecular-weight products. In addition to the cleavage reaction, LiP also catalyzes polymerization of DHPs, probably because purified LiP, unlike the

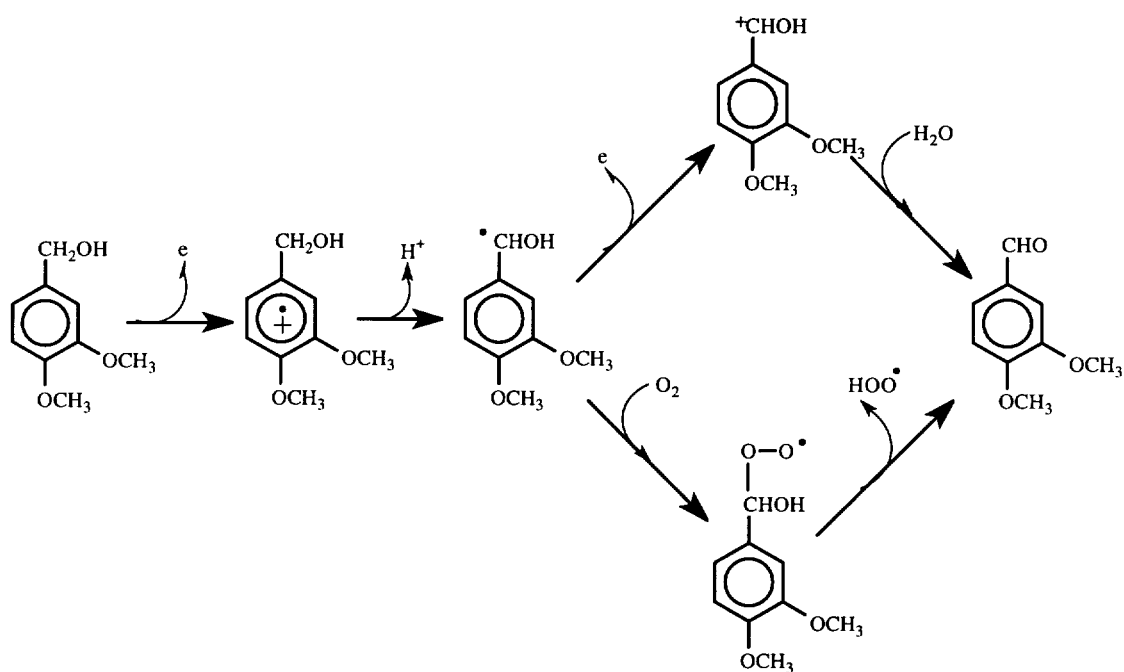


Figure 1.6 The mechanism of veratryl alcohol oxidation by lignin peroxidase, adapted from Schmidt et al. (1989).

intact fungus, cannot remove lignin fragments that are susceptible to repolymerization. When exhaustively methylated DHPs are used as substrates, the polymerization reaction is almost totally inhibited, suggesting that oxidation of the free phenolic groups in synthetic lignin is responsible for the polymerization reaction. Under the same conditions, ^{13}C NMR experiments (Hammel et al., 1993) demonstrate that LiP cleaves the synthetic lignin at the C_α position to yield the substituted benzylic aldehydes, which is in agreement with the mechanism proposed from the lignin dimer model compound studies (Miki et al., 1986). Proteins also have been used as lignin model compounds, and the roles of VA in the reaction have been studied. Wariishi et al. (1994) used ferrocyanochrome *c* as a lignin model compound and showed that LiP catalyzes the one electron oxidation of this substrate. VA appears to protect the enzyme from inactivation by H_2O_2 , particularly at low pH and high concentrations of H_2O_2 (Wariishi et al., 1994). However, VA may also act as an enzyme-bound mediator (see below). The oxidation of proteins by peroxidase systems has been investigated *in vitro*. It has been reported, that, in the presence of peroxidase and H_2O_2 (Amado et al., 1984), both free tyrosine and tyrosine residues in protein can be oxidized to tyrosine radicals. The latter can couple to form a dimer of tyrosine, called dityrosine, as shown below.

The tyrosine radicals in protein can couple by means of intramolecular and/or intermolecular mechanisms. When the tyrosine radicals couple intermolecularly, dimeric as well as highly polymeric protein aggregates are formed. Dityrosine is found in hydrolysates of some native structural proteins (Amado et al., 1984), and the dityrosine cross-links are responsible for their insoluble and elastic properties. Elastin from the aorta of chick embryos, collagen of rat and cow skin, bovine ligamentum nuchae proteins, uterus proteins of cats, and skin proteins of arthropods have all been shown to contain small amounts of dityrosine. Apart from these connective tissue proteins, dityrosine has been identified in tussah silk, wool keratin, adhesive proteins of sea mussels, proteins of cataract lens, and bovine dental enamel matrix. The formation of dityrosine is a marker for certain biological processes, such as egg fertilization (Kay et al., 1982; Kay & Shapiro 1987; Battaglia & Shapiro, 1988) and aging processes (Huggins et al., 1993; Wells-Knecht et al., 1993). LiP catalyzes

dityrosine formation from free tyrosine and from tyrosine in selected proteins. The details of these reactions are discussed in Chapters 3 and 4.

1.5.4 Kinetic and thermodynamic properties of lignin peroxidase catalyzed reactions

Detailed kinetic properties of LiP-catalyzed reactions are generally obtained from transient-state (pre-steady-state) kinetic studies. Like other plant and fungal peroxidases, LiP has a strong absorption in the Soret region ($\epsilon_{407} = 133 \text{ mM}^{-1}\text{cm}^{-1}$), facilitating kinetic measurements.

As with peroxidases, the initial catalytic step is the reaction of native LiP with H_2O_2 . The formation of LiP compound I obeys second-order kinetics with a rate constant of $(6.5 \pm 0.2) \times 10^5 \text{ M}^{-1} \text{ s}^{-1}$ over the pH range 3.0–7.4 (Marquez et al., 1988). Unlike other peroxidases, the rate constant of LiP compound I formation is independent of pH in the range of 3.0 to 8.0. Formation of compound I in HRP and other peroxidases is pH-dependent. The distal ionization groups of peroxidases have low pK_a values, with a $\text{pK}_a < 3.0$ for HRP (Araiso et al., 1980) and chloroperoxidase (Lambeir & Dunford, 1983; Sun et al., 1994), and a $\text{pK}_a < 4.5$ for CcP (Balny et al., 1987). Presumably, these ionizable groups play a role in the heterolytic cleavage of H_2O_2 . The unique lack of pH dependence in LiP compound I formation suggests that such an ionization may not occur in LiP.

LiP compound I shows characteristic features of a π -cation electronic structure. Diode array spectroscopy demonstrates that the reduction of LiP compound I to native enzyme by organic substrates proceeds through two single-electron steps via the formation of compound II. Generally, second-order reactions are observed in the reduction of LiPI with various aromatic substrates, as shown in the following equation (see also Fig. 1.7).



LiP-substrate complex formation is too fast to measure and the reaction is irreversible. The second-order rate constants for LiPI reduction by various substrates are listed in Table 1.6. Unlike LiP compound I formation, the reduction reactions of LiP compound I by various substrates are pH dependent. Transient-state kinetic

Table 1.6

Transient-State Kinetic Parameters of LiP:
Compounds I and II Reduction by Aromatic Compounds

Substrates	LiPI		LiPII
	Second order rate constant ($M^{-1}s^{-1}$)	First order rate constants (S^{-1})	Apparent dissociation constants (M)
VA ^a	2.6×10^6	7	2.1×10^{-4}
Anisyl alcohol ^b	2.3×10^3	Poor substrate for LiPII	
3,4,5-trimethoxy benzene ^b	2.4×10^4	17	8.4×10^{-4}
1,2,4,5-tetra-methoxybenzene ^c	1.1×10^7	24	1.6×10^{-5}

^a Wariishi et al. (1991), pH 3.0

^b Koduri & Tien, (1994), pH 3.5

^c Koduri et al. (1996), pH 3.0

studies demonstrate the existence of an ionizable group with a pK_a of 3.0 when VA is used as the reducing substrate (Wariishi et al., 1991a). This result agrees with results from steady-state kinetic studies (Tien et al., 1986; Renganathan et al., 1987). Such a low pH optimum also suggests that the protonation of a carboxylate group may be involved. Crystal structures of LiP indicate two possibilities for such a low pH optimum. First, one heme propionate H-bonds with residue Asp183, forming a carboxylate-carboxylate H-bond. At high pH, this H-bond may be disrupted, leading to some subtle change in the heme pocket that is critical for the binding and/or electron transfer. The second possibility occurs at the proposed VA binding pocket. His82 and Glu146 form an ion pair/H-bonding interaction. Modeling of VA binding suggests a possible H-bond interaction between the VA and His82. Disruption of this interaction could affect substrate binding directly. Finally, the third possibility is not connected with the disruption of substrate-protein interaction. In HRP, the redox potential of compound I increases as the pH decreases (Hayashi & Yamazaki, 1979) thus making the compound I a better oxidizing agent at low pH. If the assumption holds true for LiP, then low pH is required to attain the redox levels necessary to oxidize those high redox potential nonphenolic substrates.

LiP compound II has a formal oxidation state of +4, with one oxidizing equivalent stored as an $Fe^{IV}=O$ species. The reduction reaction of LiPII with most reducing substrates obeys first-order kinetics, which involves a rapid binding equilibrium between LiPII and substrate followed by electron transfer:

The apparent dissociation constant (K_d) (M) and first-order rate constant (k_{cat}) (s^{-1}) are determined from the equation: $k_{obs} = k [S]/(K_d + [S])$ by best-fitting, where k_{obs} is the observed reaction rate at a single concentration of substrate ($[S]$). The rate constants for the reduction of LiPII by several substrates are summarized in Table 1.6.

By converting the first-order rate constant for the LiPII reduction reaction to a second-order rate constant (k/K_d), it is clear that the rate of LiP compound II reduction is about 10 times slower than LiPI reduction by the same substrate. This indicates that the reduction of LiPII is the rate-limiting step in the catalytic cycle. Initially, it was thought that the difference in the reduction rates for LiPI and LiPII

was due to the difference in the redox potentials of LiPI and LiPII, due to the general belief that peroxidase compound I was a better oxidant than compound II. However, the very limited redox potential data for HRP indicates that the redox potentials of HRP compounds I and II are essentially identical (Hayashi & Yamazaki, 1979; Farhangrazi et al., 1994), thus the difference between the rates of LiPI and LiPII reduction is probably not due to a difference in their redox potentials. Another possibility is that the reduction of LiPII as well as compounds II of other peroxidases, involves a change in the geometry of the heme iron center, whereby the heme iron changes its coordination number and spin state. This may result in a higher reorganization energy and a decrease in the electron transfer rate.

LiP is inactivated at a much lower concentration of H_2O_2 , as compared with HRP. Moreover, H_2O_2 is produced by *P. chrysosporium* under ligninolytic conditions, thus, the inactivation reaction may have an effect on lignin biodegradation. Using fast-scanning techniques, Wariishi et al. showed that LiP compound II reacts with H_2O_2 to form two spectroscopically distinguishable species, LiPIII and LiPIII* (Wariishi & Gold, 1990; Wariishi et al., 1990). The reaction is believed to occur as follows.

Both LiPIII and LiPIII* are enzymatically inactive and the iron is $Fe^{III}-O_2^-$. (Dunford & Stillman, 1976; Wariishi & Gold, 1990; Wariishi et al., 1990). LiPIII has a maximal absorption at 414 nm. A 5-nm red shift is observed for LiPIII* (Wariishi & Gold, 1990; Wariishi et al., 1990). The addition of excess H_2O_2 to LiPIII results in the reversible formation of LiPIII*, suggesting that the latter is a non-covalent complex of LiPIII and H_2O_2 (Wariishi & Gold, 1990; Wariishi et al., 1990). The kinetic parameters for the reaction of LiPII and LiPIII with H_2O_2 and peracetic acid are summarized in Table 1.7.

The second-order rate constant for the reaction of LiPII with H_2O_2 is estimated to be $1 \times 10^4 M^{-1}s^{-1}$ (k/K_d) (Wariishi & Gold, 1990; Wariishi et al., 1990), which is about 6% of the rate for the reaction of LiPII with VA. Therefore, even in the presence of a moderate amount of a reducing substrate such as VA, some conversion of LiPII to LiPIII* would be expected. The rate constant for the reaction of LiPII with H_2O_2 decreases as the pH increases, with a pK_a value of 4.0. This explains why

Table 1.7
Kinetic Parameters of the Reactions of LiP Compounds I and II with H₂O₂ and Peracetic Acid^a

Oxidized enzyme	Substrate	LiPIII formation		LiPIII* formation	
		First-order rate constant s ⁻¹	Apparent dissociation constant M	Forward second-order rate constant M ⁻¹ s ⁻¹	Reverse first-order rate constant s ⁻¹
LiPII	H ₂ O ₂	7.9 ± 0.5	(5.8 ± 0.6) × 10 ⁻⁴		
	AcOOH	4.6 ± 0.6	(1.1 ± 0.6) × 10 ⁻⁴		
LiPIII	H ₂ O ₂			(3.7 ± 0.2) × 10 ²	(6.6 ± 0.6) × 10 ⁻²
	AcOOH			(2.9 ± 0.2) × 10 ²	(6.4 ± 0.6) × 10 ⁻²

^a Wariishi et al., 1990.

LiP is more sensitive to H_2O_2 at lower pH (Wariishi et al., 1990).

The reaction between LiPIII^* and VA has also been investigated. As mentioned earlier, LiPIII^* is an Fe(III)-O_2^- species. The addition of VA to LiPIII^* results in the conversion of LiPIII^* to the native enzyme accompanied by the release of stoichiometric amounts of superoxide (Wariishi & Gold, 1990; Wariishi et al., 1990). A similar reaction between LiPIII and VA does not occur, confirming that LiPIII and LiPIII^* are different species. The reaction of LiPIII^* with VA follows second-order kinetics with a rate constant of $1.7 \times 10^1 \text{ M}^{-1}\text{s}^{-1}$ at pH 3.0 (Wariishi & Gold, 1990; Wariishi et al., 1990). Based on this observation, it has been proposed that one role of VA is to rescue LiP by returning LiPIII^* to the native enzyme (Wariishi & Gold, 1990; Wariishi et al., 1990). The overall pathway for the LiP-catalyzed reaction is shown in Fig. 1.7.

Compared with the kinetic studies of the LiP-catalyzed reaction, the thermodynamic features of this reaction have not been well characterized, largely due to the absence of data regarding the redox potentials of the LiPI/LiPII and LiPII/native couples. Our current understanding of the thermodynamic features of the LiP reaction is derived from the empirical estimations. Schoemaker et al. estimated that the redox potential of oxidized LiP is well below 1.35 V vs Normal Hydrogen Electrode (NHE) at pH 3.0 because it acts as a bromoperoxidase, but not as a chloroperoxidase (Renganathan et al., 1987; Farhangrazi et al., 1992; Schoemaker et al., 1994). The redox potentials for peroxidase-oxidized intermediates are available only for HRP (Hayashi & Yamazaki, 1979) and the *Arthromyces ramosus* peroxidase (Farhangrazi et al., 1994). At neutral pH, the HRPI/HRPII couple has a redox potential of 0.92 V versus NHE, and the redox potential of the HRPII/HRP couple is 0.94 V versus NHE. At low pH, HRP will oxidize non-phenolic compounds with redox potentials up to 1.36 V vs NHE (Kersten et al., 1990), which is much higher than the redox potentials of HRP compound I and compound II. This indicates that it is not necessary for oxidized HRP to have a higher redox potential than its substrate. LiPI also oxidizes aromatic compounds with redox potentials of 1.6 V vs NHE (Kersten et al., 1990). Although the redox potential of the ferro/ferric couple of LiP is 0.14 V higher than that of HRP (Millis et al., 1989), this does not necessarily mean

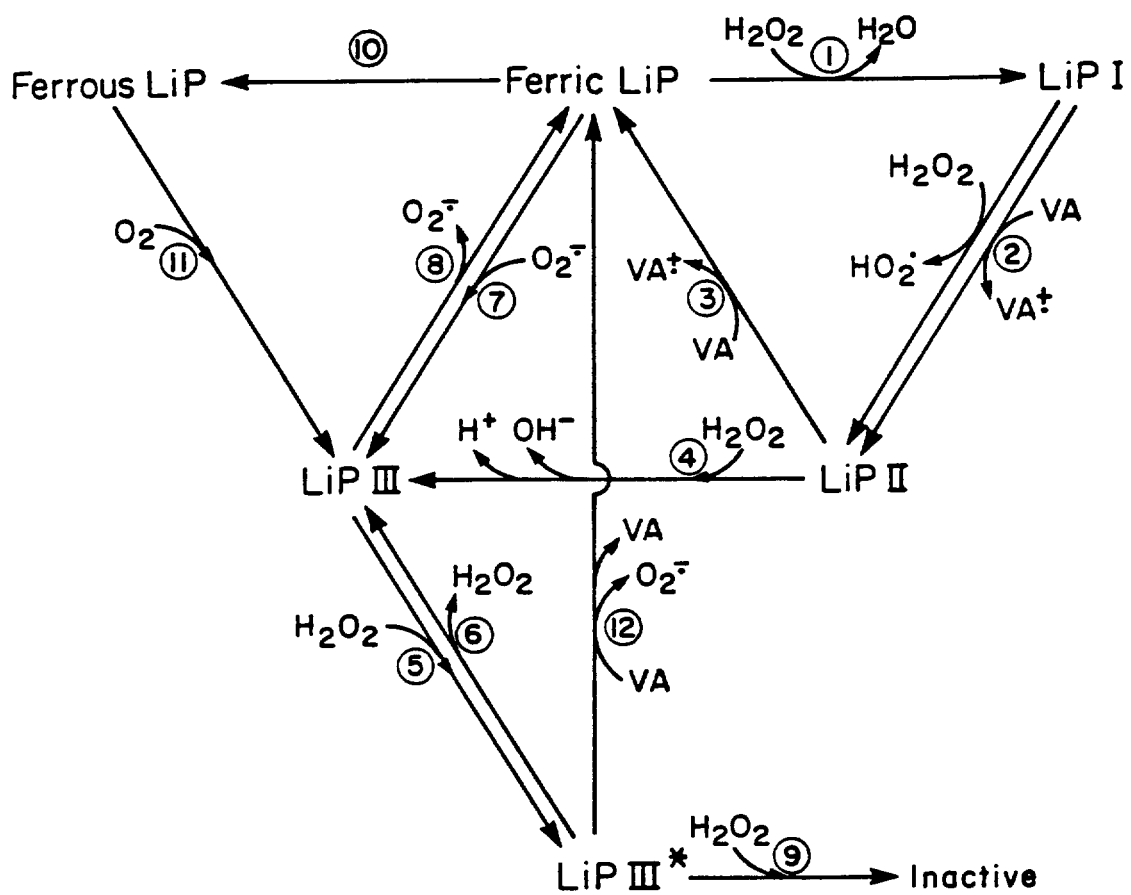


Figure 1.7 Interrelationship between the oxidized intermediates of lignin peroxidase (Wariishi et al., 1990).

that the redox potentials of oxidized LiP species are considerably higher than those of HRP. Assuming this is true, it has been estimated that the redox potentials of LiP oxidized intermediates are probably only slightly higher than those of HRP (Schoemaker et al., 1994). The redox potential of VA is 1.45 V vs NHE at pH 3.0 in aqueous buffer (Fawer et al., 1991); therefore, the reductions of LiPI and LiPII are endergonic ($\Delta G > 0$) and the reductions of LiPI and LiPII should be reversible. However, this is contrary to the results of transient-state kinetic studies. To explain this contradiction, it has been proposed that the VA benzylic radical derived from VA oxidation by LiP (Fig. 1.6) has an estimated redox potential of 0.55 V vs NHE (Schoemaker et al., 1994), which is far below those of the LiP oxidized intermediates. This VA benzylic radical is immediately oxidized to veratraldehyde in a highly exergonic reaction; i.e., the driving force in the reaction is the difference in redox potentials between oxidized LiP (LiPI and LiPII) and the benzylic radical. This proposal is supported by stoichiometry studies which demonstrate that the ratio between H_2O_2 consumption and veratraldehyde formation is close to 1:1 (Tien et al., 1986), suggesting that the reaction between the benzylic radical and molecular oxygen is not significant. More studies on the thermodynamic features of the LiP reaction, particularly the roles of VA in the reaction, are needed.

1.5.5 The role of VA in LiP catalyzed reactions

VA, a secondary metabolite of *P. chrysosporium*, stimulates the LiP-catalyzed oxidation of a variety of compounds. Anisyl alcohol and 4-methoxymandelic acid, which are recalcitrant substrates, can be easily oxidized by LiP in the presence of VA (Harvey et al., 1986; Valli et al., 1990; Chung & Aust, 1995; Tien & Ma, 1997). In addition, crystal structure studies show that the heme in LiP is buried and unavailable for direct interaction with polymeric substrates. However, in the presence of VA, LiP appears to be able to oxidize polymeric substrates, such as synthetic lignin (Hammel et al., 1993), ferrocyanide (Wariishi et al., 1994), and pancreatic ribonuclease A (see Chapter 5). Therefore, some form of long-range electron transfer must be involved. Several mechanisms have been proposed to explain the role of VA in the LiP reaction.

Harvey first proposed that VA could act as a diffusible mediator in LiP-catalyzed reactions (Harvey et al., 1986). The VA cation radical, derived from a one electron oxidation by LiP, was proposed to diffuse away from the enzyme active site and oxidize terminal substrates such as anisyl alcohol or a polymeric substrate. A central question regarding this mechanism is whether the VA cation radical is stable enough to diffuse away from the enzyme before it loses a proton to produce a VA benzylic radical. Chemical studies on similar compounds indicate that this type of cation radical is very unstable, because both the methoxy and alcohol groups make the benzylic proton very acidic. Recently, VA cation radicals produced by pulse radiolysis were studied by UV-VIS spectroscopy (Candeias & Harvey, 1995; Harvey & Candeias, 1995). The results suggested that the VA cation radical was stable enough to diffuse away from the enzyme active site and, therefore, could function as a diffusible mediator in the oxidation of polymeric substrates. However, this conclusion was strongly contradicted by fast flow EPR studies in which the free VA cation generated enzymatically was not stable ($t_{1/2} \sim 0.6$ ms). In contrast, the enzyme-bound VA cation radical was stable ($t_{1/2} \sim 400$ ms) (Khindaria et al., 1995, 1996). Our chemical evidence from studies of methoxybenzene oxidation by LiP also suggest that the half life of the VA cation radical is too short to allow significant diffusion (Joshi & Gold, 1996).

A second role proposed for VA in LiP-catalyzed reactions is to protect the enzyme from inactivation by H_2O_2 . Wariishi et al. (Wariishi & Gold, 1990; Wariishi et al., 1990) showed that LiPIII*, an inactive form of the enzyme generated by the reaction of LiPII with excess H_2O_2 , can be converted back to the native enzyme in the presence of VA. Alternatively, VA could compete with H_2O_2 for LiPII, thereby preventing the formation of LiPIII and LiPIII* (Valli et al., 1990; Kuan et al., 1993).

A third possible role for VA in the LiP reaction is a cofactor that is part of an electron transfer relay between the active site and polymeric substrates that are inaccessible to the LiP heme. Computational modeling of the VA binding site in LiP suggests that VA is located between the heme and the enzyme surface (Poulos et al., 1993). In addition, fast-flow EPR studies indicate that the enzyme-bound VA cation is much more stable than free the VA cation radical (Khindaria et al., 1996). These

observations suggest that VA may function as an electron transfer cofactor in the LiP reaction.

In this thesis, the mechanism of VA oxidation by LiP and the role of VA in the LiP-catalyzed polymeric compounds oxidation are studied. In Chapter 2, we demonstrate the formation of VA cation radical and benzylic radical. In Chapters 3, 4, and 5, we use protein substrates as lignin model compounds and the role of VA in these reactions is studied. In Chapter 3, the reaction of ferrocyanochrome *c* oxidation by LiP is characterized. VA stimulates this reaction at low pH and high H₂O₂ concentrations. In Chapter 4, we show that the ferricytochrome, the product of ferrocyanochrome *c* oxidation, can be further oxidized by LiP. This oxidation reaction is accompanied with the loss of iron in ferricytochrome *c* protein and the dimerization of this protein. In Chapter 5, by using a non-heme protein, bovine pancreatic ribonuclease A, we studied both steady-state and transient-state kinetics of RNase A oxidation by LiP. Our results suggest that VA functions as an enzyme-bound cofactor in the LiP-catalyzed polymeric compounds oxidation. Finally, in Chapter 6, the haloperoxidase activity of Mn peroxidase was studied.

CHAPTER 2
NITRATION OF VERATRYL ALCOHOL
BY LIGNIN PEROXIDASE AND TETRANITROMETHANE*

2.1 Introduction

Lignin is a heterogeneous, random, phenylpropanoid polymer that constitutes 20–30% of woody plant cell walls (Sarkanen & Ludwig, 1971). White-rot basidiomycete fungi are primarily responsible for initiating the depolymerization of lignin and therefore play a key role in the earth's carbon cycle (Buswell & Odier, 1987; Kirk & Farrell, 1987; Gold et al., 1989). The best-studied lignin-degrading fungus, *Phanerochaete chrysosporium*, secretes two heme peroxidases, manganese peroxidase and lignin peroxidase (LiP)**, which, along with an H₂O₂-generating system, appear to be the major extracellular components of its lignin degradative system (Buswell & Odier, 1987; Kersten & Kirk, 1987; Kirk & Farrell, 1987; Gold et al., 1989; Higuchi, 1990).

Nucleotide sequences of a number of LiP cDNA and genomic clones (Tien & Tu, 1987; Ritch & Gold, 1992; Gold & Alic, 1993; Cullen, 1997), as well as crystal structures of LiP (Edwards et al., 1993; Piontek et al., 1993; Poulos et al., 1993), demonstrate that important catalytic residues, including the proximal and distal His, the distal Arg, and an H-bonded Asp, are all conserved within the heme pocket.

* Reprinted with permission from: Sheng, D., Joshi, D. K., and Gold, M. H. (1998) Nitration of Veratryl Alcohol by Lignin Peroxidase and Tetranitromethane. *Arch. Biochem. Biophys.*, in press. Copyright 1998 Academic Press.

** Abbreviations used: DMSO, dimethyl sulfoxide; GC-MS, gas chromatography-mass spectrometry; HPLC, high performance liquid chromatography; KO₂, potassium superoxide; LiP, lignin peroxidase; •NO₂, nitrogen dioxide radical; SOD, superoxide dismutase; TNM, tetranitromethane; VA, veratryl (3,4-dimethoxybenzyl) alcohol.

Although LiP shares spectral and kinetic features with other plant and fungal peroxidases, the enzyme has several unique characteristics. These include a redox potential that apparently is higher than those of most other peroxidases (Buswell & Odier, 1987; Kirk & Farrell, 1987; Gold et al., 1989; Schoemaker, 1990), a very low pH optimum (Tien et al., 1986; Renganathan et al., 1987), and an unusually high reactivity between LiP compound II and H_2O_2 (Wariishi & Gold, 1990; Wariishi et al., 1990). The high redox potentials of the oxidized intermediates of LiP enable this enzyme to oxidize nonphenolic compounds via the formation of an aryl cation radical (Kersten et al., 1985; Renganathan et al., 1986; Kirk & Farrell, 1987; Gold et al., 1989; Higuchi, 1990; Joshi & Gold, 1996).

Veratryl (3,4-dimethoxybenzyl) alcohol (VA), a secondary metabolite of *P. chrysosporium*, stimulates the LiP oxidation of synthetic lignin (Hammel et al., 1993), proteins (Wariishi et al., 1994; Sheng & Gold, 1998), and a variety of other recalcitrant substrates (Haemmerli et al., 1986; Harvey et al., 1986). The mechanism(s) by which VA stimulates LiP oxidations remains under discussion. VA has been shown to protect LiP from H_2O_2 -derived inactivation (Wariishi & Gold, 1990; Wariishi et al., 1990), as well as to enable the enzyme to complete its catalytic cycle by reducing LiPII back to its native form (Valli et al., 1990; Koduri & Tien, 1994). Furthermore, since the heme in LiP is buried and therefore unavailable for direct interaction with polymeric substrates (Edwards et al., 1993; Piontek et al., 1993; Poulos et al., 1993), some form of long-range electron transfer must be involved in the oxidation of polymeric substrates. It has been suggested that the cation radical, produced via the LiP oxidation of VA, can diffuse away from the enzyme surface and oxidize terminal polymeric substrates (Harvey et al., 1986). However, recent chemical studies (Joshi & Gold, 1996), as well as fast-flow electron spin resonance (ESR) studies of the VA cation radical produced by LiP (Khindaria et al., 1995, 1996), suggest that the radical is too short-lived to act as a diffusible mediator. At any rate, the detailed pathway for the oxidation of VA by LiP is of considerable interest. In the present study, we report additional chemical evidence for the formation of the VA cation radical and novel evidence for its deprotonation to form the corresponding benzylic radical.

2.2 Materials and Methods

2.2.1 Enzyme Preparation

LiP isozyme 2 (H8) was purified from the extracellular medium of acetate-buffered cultures of *P. chrysosporium* strain OGC101, as described previously (Gold et al., 1984; Wariishi et al., 1990). The purified LiP was electrophoretically homogeneous and had an R_z ($A_{408/280}$) value of 5.0. LiP concentration was determined at 408 nm using an extinction coefficient of $133 \text{ mM}^{-1} \text{ cm}^{-1}$ (Gold et al., 1984). Superoxide dismutase (SOD) and glucose oxidase were obtained from Sigma.

2.2.2 Chemicals

VA (I), 1,4-dimethoxybenzene (II), and benzyl alcohol were obtained from Aldrich and purified by silica gel column chromatography (ethyl acetate:hexane = 1:1, v/v) before use. H_2O_2 , tyrosine (III), and 3-nitrotyrosine (XIII) were obtained from Sigma. The concentration of H_2O_2 in the stock solution was determined as described previously (Cotton & Dunford, 1973). Deuterated water (99.9%) was obtained from Cambridge Isotope Laboratory. All other chemicals were reagent grade.

2.2.2.1 Deuterium-labeled compounds

(Benzyl- $^2\text{H}_2$)-VA and (formyl- ^2H)-veratraldehyde were prepared as previously described (Joshi & Gold, 1996). Reactions in deuterated water (95%) were carried out as described for reactions in H_2O .

2.2.2.2 4,5-Dimethoxy-2-nitrobenzyl acetate

3,4-Dimethoxybenzyl acetate was prepared via the acetylation of VA as follows: a mixture of VA (1.6 g), acetic anhydride (2.0 g) and pyridine (0.8 g) was heated at 80°C for 10 min and washed with dilute HCl to remove the pyridine. 3,4-Dimethoxybenzyl acetate (0.5 g) was dissolved in 7 ml of acetic acid at 0°C , and nitric acid (0.5 g) was added slowly with stirring. Following the reaction, crushed ice was added, followed by ethyl acetate extraction. The organic phase was evaporated, and the 4,5-dimethoxy-2-nitrobenzyl acetate was recrystallized using benzene and hexane. The mass spectral data for the product are shown in Table 2.1.

Table 2.1

Mass Spectra of Products or Their Derivatives
Formed by LiP in the Presence of H₂O₂ and TNM

Compounds	Mass spectrum m/z (relative intensity)
veratraldehyde (IV)	166 (100), 165 (44), 151 (14), 137 (3), 122 (3), 95 (27), 79 (13)
(<i>formyl</i> - ² H)-veratraldehyde (IV')	167 (100), 165 (40), 152 (14), 137 (4), 122 (5), 96 (25)
4,5-dimethoxy-2-nitrobenzyl alcohol acetate (from V)	255 (31), 196 (15), 167 (65), 151 (22), 136 (100), 108 (17), 92 (45)
(<i>benzyl</i> - ² H ₂)-4,5-dimethoxy-2-nitrobenzyl alcohol acetate (from V')	257 (30), 198 (15), 169 (70), 152 (22), 137 (100), 109 (20)
3,4-dimethoxy-nitrobenzene (VI)	183 (100), 168 (6.6), 153 (9.9), 137 (12), 92 (12)
methylene-2,4-dinitrophenylhydrazine (from VII)	210 (100), 164 (12), 122 (23), 91 (26)
2,5-dimethoxy-nitrobenzene (XI)	183 (100), 122 (28), 107 (47), 92 (12)

NMR (CDCl₃): δ 2.19 (3H,s,-COCH₃), 3.96 (6H,s,C₄-OCH₃,C₅-OCH₃), 5.50 (2H,s,ArCH₂CO-), 7.05 (1H,s,ArH) and 7.74 (1H,s,ArH).

2.2.2.3 3,4-Dimethoxynitrobenzene (VI)

Dimethyl sulfate (1 g) was added to a solution containing 4-nitrocatechol (0.5 g) and NaOH (0.27 g) in 7 ml of water. The mixture was stirred at room temperature for 12 h after which the crude products were extracted with ethyl acetate and the organic phase was washed with water. The product was purified by silica gel column chromatography using ethyl acetate and hexane (1:1, v:v). The mass spectral data for VI are shown in Table 2.1.

2.2.2.4 2,5-Dimethoxynitrobenzene (XI)

Nitric acid was added slowly to a solution of 1,4-dimethoxybenzene (II) in 5 ml of acetic acid at 0°C. The reaction mixture was extracted with ethyl acetate, and the crude product was purified by silica gel column chromatography using dichloromethane as the eluant. The mass spectral data for XI are shown in Table 2.1.

2.2.3 Enzyme reactions

Reaction mixtures consisted of LiP (0.025 μ M or 0.1 μ M, as indicated) and aromatic substrate (500 μ M), with or without tetranitromethane (TNM) (100 μ M), in 20 mM sodium succinate, pH 4.5. Reactions were initiated by the addition of H₂O₂ (100 μ M) or glucose (1 mM) and glucose oxidase (0.005 U/ml). The reactions were also conducted under the same conditions in the presence of both VA (0.5 mM) and benzyl alcohol (2 mM). Reactions were carried out at room temperature under air or argon.

Control reactions were performed with boiled enzyme or with the omission of LiP or H₂O₂. SOD (2 U/ml) was added to the reactions with VA and H₂O₂, as indicated, to eliminate any superoxide generated during the reaction. In addition, to determine if superoxide was involved in the tyrosine nitration reaction, two control reactions were carried out. First, a reaction was conducted with LiP, tyrosine, glucose oxidase, and glucose as described above but under argon. Secondly, a control reaction was conducted with LiP, H₂O₂, tyrosine, and KO₂. As indicated, dimethyl sulfoxide (DMSO) (15%, v/v) was used as an \cdot NO₂ spin trap (Pace &

Kalyanraman, 1993). Enzyme activity in the presence of DMSO was determined by measuring the formation of veratraldehyde (IV), as previously described (Gold et al., 1984; Tien et al., 1986).

2.2.3.1 Reactions with nitrogen dioxide

$\cdot\text{NO}_2$ was generated chemically by the slow addition of concentrated nitric acid to copper foil. The $\cdot\text{NO}_2$ was displaced from the reaction tubing, using nitrogen as the carrier gas, and passed through hot copper tubing (100–150°C) to prevent $\cdot\text{NO}_2$ dimerization (Pedler et al., 1957). The $\cdot\text{NO}_2$ was bubbled through the reaction mixture containing LiP (0.1 μM), VA (500 μM), and H_2O_2 (100 μM) in 20 mM sodium succinate buffer, pH 4.5. Control experiments lacked LiP or H_2O_2 . The pH remained unchanged during the course of the reaction.

2.2.4 Product analysis

Reaction products were identified by comparing their retention times on high-performance liquid chromatography (HPLC) or gas chromatography (GC) and by comparing their mass spectral fragmentation patterns with chemically prepared standards. Product yields were quantitated by HPLC, using calibration curves obtained with commercial or chemically prepared standards.

The reaction products also were analyzed directly by HPLC, using a reverse phase C-18 column (LiChrospher 100 RP-18, 5 μm , 125 \times 4 mm), with a flow rate of 1 ml/min. The products generated during the oxidation of VA (I) were analyzed using a linear gradient of acetonitrile in 0.05% H_3PO_4 (0–50% acetonitrile in 22 min). Since the retention times of veratraldehyde (IV) and 4,5-dimethoxy-2-nitrobenzyl alcohol (V) were similar, veratraldehyde (IV) was quantitated with the detector set at 280 nm, a wavelength at which the absorbance of V was negligible. The latter was quantitated at 360 nm, a wavelength at which veratraldehyde (IV) did not absorb. The products derived from the oxidation of 1,4-dimethoxybenzene (II) were analyzed using a linear gradient of acetonitrile in 0.05% H_3PO_4 (25–45% in 15 min). The reaction products of tyrosine (III) oxidation were analyzed using a linear gradient of acetonitrile in 0.05% H_3PO_4 (0–11% in 15 min).

For GC-MS analysis, the products were extracted with ethyl acetate at pH 1.0 and the organic phase was dried over sodium sulfate. The solvent was evaporated under nitrogen, and the crude extracts were derivatized using acetic anhydride and pyridine (2:1, v:v). To identify formaldehyde, an excess of 2,4-dinitrophenylhydrazine in glacial acetic acid was used to stop the reaction, and the mixture was incubated at 80°C for 5 min. Products were extracted with ethyl acetate, dried over sodium sulfate, evaporated under nitrogen, and analyzed by GC-MS. GC-MS was performed at 70 eV on a VG Analytic 7070E mass spectrometer with an HP 5790A gas chromatograph and a 30-m fused silica column (DB-5, J&W Scientific). The oven temperature was programmed from 70 to 320°C at a rate of 10°C/min.

¹H NMR was performed on a Varian Unity 400 NMR spectrometer with chemical shifts expressed as parts per million downfield from an internal standard of tetramethylsilane.

2.3 Results

2.3.1 Nitration of VA (I)

The oxidation of VA (I) by LiP in the presence of H₂O₂ and TNM yielded veratraldehyde (IV), 4,5-dimethoxy-2-nitrobenzyl alcohol (V), 3,4-dimethoxy-nitrobenzene (VI), formaldehyde (VII), and trinitromethane (VIII) (Fig. 2.1A) as the major products. Products IV, V, VI and VIII, or their derivatives, were identified by comparing their retention times on HPLC and/or GC, and their mass spectra, for aromatics, with those of authentic standards (Table 2.1). The HPLC retention times (min) of these products were 14.2 (IV), 14.0 (V), 18.7 (VI), and 7.8 (VIII). Trinitromethane was identified by comparing its HPLC retention time with that of the product of the reaction between TNM and potassium superoxide (KO₂). When KO₂ was allowed to react with TNM, a large amount of trinitromethane (VIII) was generated, confirming that superoxide anion can reduce TNM (McCord & Fridovich, 1969). In the absence of TNM, veratraldehyde (IV) was the only product observed (Table 2.2). When the reaction was carried out in the presence of 2 mM benzyl

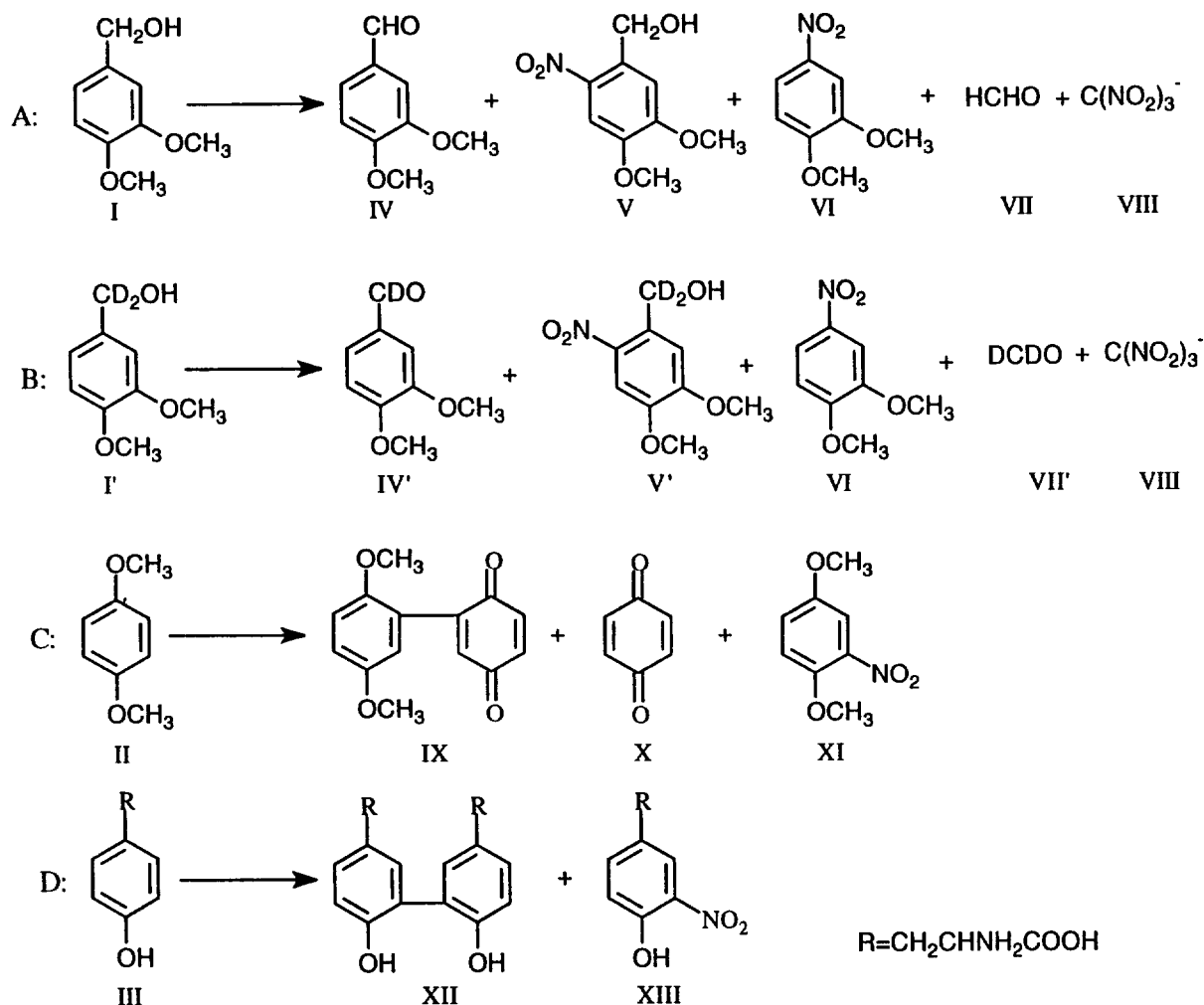


Figure 2.1 LiP oxidations in the presence TNM. Reactions contained LiP (0.025 μ M with H₂O₂, 0.1 μ M with glucose oxidase), H₂O₂ (100 μ M), or glucose (1 mM), and glucose oxidase (0.005 U/ml), TNM (100 μ M), and substrate (500 μ M) in 20 mM sodium succinate, pH 4.5. Substrates were veratryl alcohol (I) (A); (*benzyl*-²H₂)-veratryl alcohol (B); 1,4-dimethoxybenzene (II) (C), and tyrosine (III) (D). Reactions were performed and products analyzed as described in the text. 3-Nitrotyrosine (XIII) was observed only when glucose/glucose oxidase was used as the H₂O₂ source.

Table 2.2Oxidation of VA (I) by LiP in the Presence of TNM^a

Reactions ^b	Product formed (nmoles)		
	IV ^c	V	VI
H ₂ O ₂ (100 μM) TNM (0)	103	0	0
H ₂ O ₂ (100 μM) TNM (100 μM)	97	19	8.5
H ₂ O ₂ (100 μM) TNM (100 μM) SOD (2 U/ml)	99	22	7.0
H ₂ O ₂ (100 μM) TNM (100 μM) anaerobic	95	17	9.0
glucose/glucose oxidase TNM (0)	99	0	0
glucose/glucose oxidase TNM (100 μM)	85	29	13

^a Reaction mixtures (1 ml) consisted of LiP (0.02 μM with H₂O₂; 0.1 μM with glucose oxidase), VA (500 μM), H₂O₂ (100 μM) or glucose (1 mM), glucose oxidase (0.005 U/ml), with or without TNM (100 μM), with or without SOD (2 U/ml), in 20 mM sodium succinate, pH 4.5. Reactions were carried out under aerobic or anaerobic conditions for 30 min as described in the text.

^b Products were quantitated by HPLC, as described in the text.

^c IV = veratraldehyde; V = 4,5-dimethoxy-2-nitrobenzyl alcohol; VI = 3,4-dimethoxy nitrobenzene.

alcohol, no nitration of benzyl alcohol was observed, and the product profile of the VA nitration reaction did not change.

Table 2.2 shows the yields of products IV, V, and VI (Fig. 2.1) that were generated by the LiP oxidation of VA (I) in the presence of TNM. When glucose/glucose oxidase was used to generate H₂O₂, the yield of veratraldehyde (IV) was unchanged, but the yields of the nitrated products (V and VI) increased somewhat, suggesting that some superoxide was produced in the glucose oxidase reaction. However, neither anaerobic conditions nor the presence of SOD affected the product yields when the reaction was conducted in H₂O₂ (Table 2.2). The addition of DMSO (15%, v/v) to the reaction conducted in H₂O₂ (Pace & Kalyanraman, 1993) as a spin trap for $\cdot\text{NO}_2$ inhibited the formation of the nitrated products; however, the yield of veratraldehyde (IV) formed in the absence of TNM was unaffected by DMSO (data not shown), ruling out the possibility of enzyme inactivation under these conditions.

When the LiP oxidation of VA (I) in the presence of TNM was carried out in deuterated water, no incorporation of deuterium was observed in the reaction products. However, when (*benzyl-²H)VA (I') was used as the substrate, (*formyl-²H)veratraldehyde (IV')* and (*benzyl-²H)4,5-dimethoxy-2-nitrobenzyl alcohol (V')* were formed, as well as 3,4-dimethoxynitrobenzene (VI) (Fig. 2.1B). The deuterated products had essentially the same retention times as the non-deuterated products on HPLC and GC. MS analysis demonstrated that both benzylic deuterium atoms were retained in V' (Table 2.1), indicating that there was no benzylic hydrogen exchange between the substrate and the solvent.*

2.3.2 Oxidation of 1,4-dimethoxybenzene (II)

The oxidation of II by LiP, in the presence of H₂O₂ and TNM, yielded 2-(2,5-dimethoxyphenyl)-1,4-benzoquinone (IX), 1,4-benzoquinone (X), and 2,5-dimethoxynitrobenzene (XI) as the major products (Fig. 2.1C, Table 2.3), as well as minor products reported previously (data not shown) (Joshi & Gold, 1996). The products, or their derivatives, were identified by comparing their retention times on HPLC or GC and their mass spectra with those of authentic compounds (Table 2.1). The yield

Table 2.3
 Oxidation of 1,4-Dimethoxybenzene (II)
 by LiP in the Presence of TNM^{a,b}

Reactions	Product formed (nmoles)		
	IX ^c	X	XI
H ₂ O ₂ (100 μM) TNM (0)	29	9	0
H ₂ O ₂ (100 μM) TNM (100 μM)	24	7	8
H ₂ O ₂ (100 μM) TNM (100 μM) SOD (2 U/ml)	26	7	8
H ₂ O ₂ (100 μM) TNM (100 μM) anaerobic	26	9	9
glucose/glucose oxidase TNM (0)	27	11	0
glucose/glucose oxidase TNM (100 μM)	22	7	30

^a Reaction mixtures (1 ml) consisted of LiP (0.025 μM with H₂O₂, 0.1 μM with glucose oxidase), 1,4-dimethoxybenzene (500 μM), H₂O₂ (100 μM) or glucose (1 mM), glucose oxidase (0.005 U/ml), with or without TNM (100 μM), with or without SOD (2 U/ml), in 20 mM sodium succinate, pH 4.5. Reactions were carried out under aerobic or anaerobic conditions for 30 min as described in the text.

^b Products were quantitated by HPLC, as described in the text.

^c IX = 2-(2,5-dimethoxyphenyl)-1,4-benzoquinone; X = 1,4-benzoquinone; XI = 2,5-dimethoxy nitrobenzene.

of XI increased dramatically when glucose/glucose oxidase was used to generate H_2O_2 , but the yields of IX and X were not affected significantly (Table 2.3). In reactions conducted in the presence of H_2O_2 , neither anaerobic conditions nor the addition of SOD to the reaction affected product yields (Table 2.3). When DMSO was included in the reaction, the nitrated compound XI was not formed, but the yields of IX and X were not affected (data not shown).

2.3.3 Oxidation of tyrosine (III)

The LiP-catalyzed oxidation of tyrosine (III), in the presence of H_2O_2 and TNM, yielded dityrosine (XII) as the major product (Fig. 2.1D), as well as additional polymerized forms of tyrosine (data not shown). Under these conditions, no nitration of tyrosine was observed. However, when glucose/glucose oxidase was used to generate H_2O_2 , 3-nitrotyrosine (XIII) was formed, in addition to the dimer (XII) (Fig. 2.1D, Table 2.4). The products were identified by comparing their retention times on HPLC with those of authentic compounds. As shown in Table 2.4, when the reaction was conducted with glucose and glucose oxidase but under argon, only 15% of the nitrated product was detected, as compared to the reaction conducted under air, suggesting the involvement of superoxide. Furthermore, when the LiP reaction was conducted in the presence of H_2O_2 and KO_2 , 3-nitrotyrosine (XIII) was formed, strongly suggesting that superoxide is able to reduce TNM in the reaction. However, no 3-nitrotyrosine was detected if LiP was omitted from this latter reaction (Table 2.4).

2.3.4 Reactions with $\cdot NO_2$

In order to demonstrate that $\cdot NO_2$ was involved in the formation of the nitroaromatic products, chemically generated $\cdot NO_2$ was bubbled into the reaction mixture containing LiP, VA (I), and H_2O_2 , without TNM. Both nitrated products, V and VI, resulting from the nitration of VA (I) (Fig. 2.1A), were identified by their HPLC retention times and their mass spectra (Table 2.1), as described above. When the reaction mixture lacked LiP or H_2O_2 , nitrated products were not detected.

Table 2.4Oxidation of Tyrosine (III) by LiP in the Presence of TNM^a

Reactions	3-Nitrotyrosine formed ^b (XIII) (nmoles)
H ₂ O ₂ (100 μM) TNM (100 μM) LiP	0
H ₂ O ₂ (100 μM) TNM (100 μM) LiP KO ₂ (100 μM)	10
H ₂ O ₂ (100 μM) TNM (100 μM) KO ₂ (100 μM) without LiP	0
glucose/glucose oxidase TNM (100 μM) LiP under air	34
glucose/glucose oxidase TNM (100 μM) LiP under argon	5.0

^a Reaction mixtures (1 ml) consisted of LiP (0.025 μM with H₂O₂, 0.1 μM with glucose/glucose oxidase), tyrosine (500 μM), H₂O₂ (100 μM) or glucose (1 mM), glucose oxidase (0.005 U/ml), with or without TNM (100 μM), in 20 mM sodium succinate, pH 4.5. KO₂ (100 μM) was added where indicated. Reactions were carried out under aerobic or anaerobic conditions for 30 min as described in the text.

^b 3-Nitrotyrosine was quantitated by HPLC, as described in the text.

2.4 Discussion

LiP catalyzes the oxidation of nonphenolic aromatic substrates, including lignin model compounds, via the formation of aryl cation radical intermediates (Kersten et al., 1985; Buswell & Odier, 1987; Kirk & Farrell, 1987; Schoemaker, 1990; Joshi & Gold, 1996). VA, a secondary metabolite of *P. chrysosporium*, is a preferred substrate for LiP (Buswell & Odier, 1987; Kirk & Farrell, 1987; Gold et al., 1989; Higuchi, 1990). VA also stimulates the LiP-catalyzed depolymerization of synthetic lignin (Hammel et al., 1993) and the oxidation of cytochrome *c* and a variety of recalcitrant aromatic substrates (Haemmerli et al., 1986; Harvey et al., 1986; Valli et al., 1990; Wariishi et al., 1994; Sheng & Gold, 1998). Several mechanisms have been proposed to explain this stimulation of LiP-catalyzed reactions by VA. VA apparently protects and rescues the enzyme from H₂O₂-induced inactivation (Valli et al., 1990; Wariishi & Gold, 1990; Wariishi et al., 1990). Furthermore, in the presence of a poor reducing substrate, VA reduces LiP compound II, thereby ensuring the completion of the LiP catalytic cycle and preventing H₂O₂ from converting compound II to compound III, an inactive form of the enzyme (Valli et al., 1990; Koduri & Tien, 1994). It has also been argued that VA acts as a radical mediator, whereby the VA cation radical produced via the one-electron oxidation of VA oxidizes substrates with a lower redox potential. These substrates include 2-keto-4-thiomethylbutyric acid (Kuwahara et al., 1984), chlorpromazine (Goodwin et al., 1995), and guaiacol (Harvey & Palmer, 1990; Koduri & Tien, 1995). However, unlike lignin, the above substrates are small molecules which might interact directly with an enzyme-bound VA cation radical. In contrast, X-ray crystallographic studies demonstrate that the LiP heme is buried and thus unavailable for direct interaction with polymeric lignin (Edwards et al., 1993; Piontek et al., 1993; Poulos et al., 1993). Therefore, VA might play a role in electron transfer between the heme and the polymeric substrate. Indeed, studies on the depolymerization of lignin by LiP (Hammel et al., 1993) and on the LiP-catalyzed oxidation of ferrocytochrome *c* (Wariishi et al., 1994) and ferricytochrome *c* (Sheng & Gold, 1998) suggest that VA may be involved in long-range electron transfer.

There are two possible mechanisms by which the VA cation radical could act as a charge transfer mediator: the VA cation radical could diffuse away from the active site and oxidize polymeric lignin at a distance from the enzyme, or VA could bind in the active site and act as an electron transfer bridge between the heme and the exposed surface of the enzyme, i.e., VA could function as an enzyme cofactor. Recently, a VA cation radical produced by pulse radiolysis was studied using UV-visible spectroscopy (Candeias & Harvey, 1995). The results of these studies suggest that the VA cation radical is stable enough to act as a diffusible mediator. However, fast-flow ESR studies indicate that the free cation radical is very unstable ($t_{1/2} \sim 0.6$ ms), whereas the enzyme-bound VA cation radical is very stable ($t_{1/2} \sim 370$ ms) (Khindaria et al., 1995, 1996). Finally, our chemical evidence (Joshi & Gold, 1996) suggests that the VA cation radical is too short-lived to act as a diffusible mediator. The results presented here provide additional evidence for the formation of a VA cation radical and the first evidence for the formation of a benzylic radical intermediate from the cation radical.

2.4.1 Oxidation of VA (I)

The oxidation of VA (I) by LiP yields veratraldehyde (IV) as the major product (Fig. 2.1A, Table 2.2). The VA cation radical, formed by a LiP-catalyzed one-electron oxidation, rapidly loses a proton to form a hydroxy-substituted benzylic radical (Schmidt et al., 1989). Under anaerobic conditions, this benzylic radical is further oxidized by LiP and subsequently reacts with water to form veratraldehyde (Schmidt et al., 1989; Joshi & Gold, 1996). Under aerobic conditions, the benzylic radical also could react with oxygen to form a peroxy radical which yields veratraldehyde.

TNM is a well-characterized oxidant, which readily accepts electrons from phenols and other organic compounds (Riordan & Vallee, 1971; Prutz et al., 1985; Ebersson & Radner, 1991; Ebersson et al., 1992) and which reacts with inorganic compounds such as superoxide to form $\cdot\text{NO}_2$ and the trinitromethane anion. It has been proposed that the benzylic radical derived from the VA cation radical is a good reductant, with an estimated redox potential of 0.55 V versus normal hydrogen

electrode (Schoemaker et al., 1994). Therefore, we used TNM to detect the benzylic radical formed during the LiP oxidation of VA. Such a benzylic radical should react with TNM to generate $\cdot\text{NO}_2$, and the latter would react with the VA cation radical to form nitroaromatic compounds.

As shown in Fig. 2.1A and Table 2.2, the LiP oxidation of VA (I), in the presence of TNM, results in the formation of 4,5-dimethoxy-2-nitrobenzyl alcohol (V) and 3,4-dimethoxynitrobenzene (VI), as well as veratraldehyde (IV), formaldehyde (VII), and trinitromethane (VIII). The same nitrated products, V and VI, are obtained when chemically generated $\cdot\text{NO}_2$ replaces TNM in the reaction. Furthermore, the addition of DMSO to the reaction, as a spin trap for $\cdot\text{NO}_2$ (Pace & Kalyanraman, 1993), inhibits the formation of the nitrated products. These results indicate that $\cdot\text{NO}_2$ is involved in the nitration reactions.

The nature of the products formed in this reaction suggests the mechanism shown in Fig. 2.2. The initial oxidation of VA by LiP yields the cation radical, which rapidly loses a proton to form the corresponding benzylic radical. This benzylic radical reduces TNM to form the trinitromethane anion and the $\cdot\text{NO}_2$. The anion accepts a proton from the medium to form trinitromethane. The attack of the $\cdot\text{NO}_2$ at C-6 of the VA cation radical, followed by loss of a proton, generates 4,5-dimethoxy-2-nitrobenzyl alcohol (V). Alternatively, the attack of $\cdot\text{NO}_2$ at C-1 of the VA cation radical, and subsequent loss of formaldehyde (VII), yields 3,4-dimethoxynitrobenzene (VI).

Theoretically, V could be formed by an alternative mechanism, whereby the $\cdot\text{NO}_2$ reacts with the benzylic radical at C-6 and undergoes aromatization to generate the benzylic carbanion, which would accept a proton from the medium. Our results rule out this mechanism, since no deuterium is incorporated into the product when the reaction is carried out in deuterated water (data not shown). Furthermore, when LiP oxidizes (*benzyl*- $^2\text{H}_2$)VA in the presence of TNM, both of the substrate deuterium atoms are retained in the V' (Fig. 2.1B). These results support the proposed mechanism.

The reaction of TNM with superoxide could generate $\cdot\text{NO}_2$. Under aerobic conditions, superoxide could be produced in a reaction between the benzylic radical

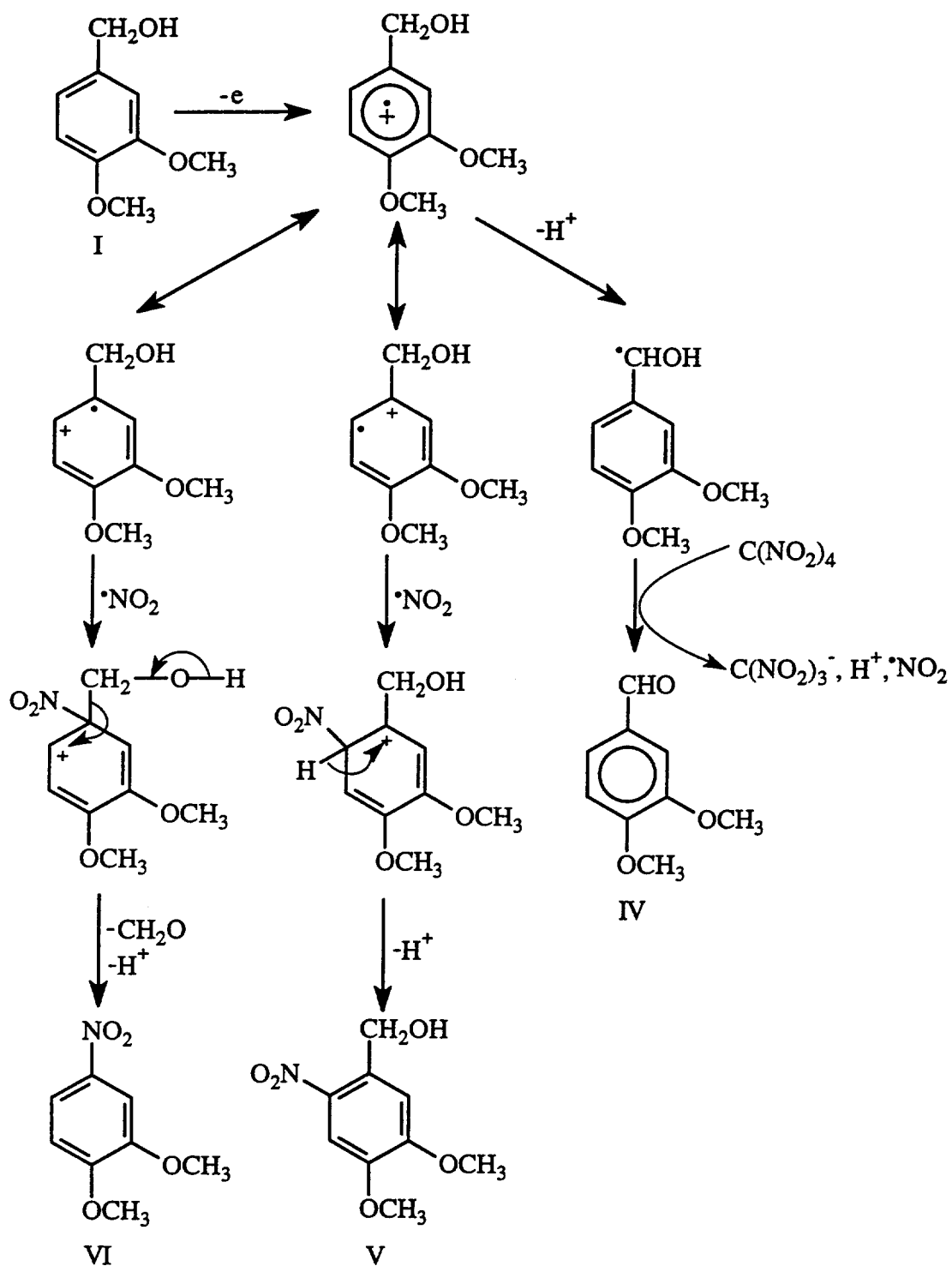


Figure 2.2 Proposed mechanism for the LiP oxidation of VA (I) in the presence of TNM.

and molecular oxygen (Schmidt et al., 1989). However, neither the addition of SOD nor the removal of oxygen affects the formation of the nitroaromatic products during VA oxidation in the presence of H_2O_2 (Table 2.2). This strongly suggests that $\cdot NO_2$ is formed from the reaction of the benzylic radical with TNM. The increased yields of the nitroaromatic products when glucose/glucose oxidase is used to generate H_2O_2 probably is due to an increase in the formation of $\cdot NO_2$, resulting from the reaction of TNM with the small amount of superoxide generated by glucose oxidase.

Incubation of VA, LiP, and H_2O_2 in the presence of chemically generated $\cdot NO_2$ also results in the formation of the nitrated products IV and V, suggesting that $\cdot NO_2$ is directly involved in the nitration of VA. In addition, the presence of benzyl alcohol does not affect the product profile for VA nitration by LiP, indicating that NO_2^+ , a general nitration agent, is not formed. If the highly reactive species NO_2^+ were formed, it would nitrate both benzyl alcohol and VA. The absence of benzyl alcohol nitration also suggests that $\cdot NO_2$ is reacting with the VA cation radical, rather than with neutral VA.

Compared to the yield of veratraldehyde, relatively low yields of nitrated products are obtained from the LiP-catalyzed oxidation of VA in the presence of H_2O_2 and TNM. The benzylic radical probably is required to reduce LiP compound II to the native enzyme, as well as to reduce TNM to form $\cdot NO_2$ (Fig. 2.2). The reduction of LiP compound II by the VA benzylic radical is believed to be the driving force in the LiP catalytic cycle (Schoemaker et al., 1994). The low yield of nitrated products, as well as previous results indicating that the VA cation radical is too short-lived to diffuse away from the LiP active site (Khindaria et al., 1995, 1996; Joshi & Gold, 1996), suggest that these reactions occur very close to the active site of LiP.

2.4.2 Oxidation of 1,4-dimethoxybenzene (II)

Recently we proposed a detailed mechanism for the oxidation of 1,4-dimethoxybenzene (II) by LiP (Joshi & Gold, 1996). In this mechanism, the initial oxidation of II generates the corresponding cation radical, which reacts either with water or with another dimethoxybenzene. Subsequent reactions generate a variety of semiquinone or substituted cyclodieryl radicals (Joshi & Gold, 1996). Since these

latter radicals are less stable than the benzylic radical generated from the VA cation radical, in the presence of TNM we would expect a lower yield of nitrated product from 1,4-dimethoxybenzene (II) than from VA (I). The oxidation of II by LiP in the presence of TNM generates 2-(2,5-dimethoxyphenyl)-1,4-benzoquinone (IX), 1,4-benzoquinone (X), and 2,5-dimethoxynitrobenzene (XI) (Fig. 2.1B), as well as previously reported minor products (Joshi & Gold, 1996) (data not shown). The formation of XI can be explained by a mechanism similar to that proposed above for the formation of V from VA (Fig. 2.2). The attack of $\cdot\text{NO}_2$ at C-2 of the LiP-generated 1,4-dimethoxybenzene cation radical, is followed by aromatization and loss of a proton, yielding XI. The yields of 2,5-dimethoxynitrobenzene (XI) increase significantly when glucose/glucose oxidase is used as a source for H_2O_2 (Table 2.3). This can be explained by the increased formation of $\cdot\text{NO}_2$ resulting from the reaction between TNM and superoxide in the presence of glucose/glucose oxidase, as compared with the relatively low levels of $\cdot\text{NO}_2$ generated from reactions between TNM and the unstable radicals resulting from the LiP oxidation of II.

2.4.3 Oxidation of tyrosine (III)

The major product of the LiP-catalyzed oxidation of tyrosine is the tyrosine dimer, dityrosine, but significant amounts of nitrotyrosine also are formed when H_2O_2 is replaced with glucose and glucose oxidase (Fig. 2.1C). The nonenzymatic nitration of tyrosine by TNM in basic solution has been observed previously (Riordan & Vallee, 1972). As shown in Fig. 2.3, at pHs greater than 8, the tyrosine phenoxy anion can transfer an electron to TNM, forming the tyrosine radical, $\cdot\text{NO}_2$, and the trinitromethane anion. Radical coupling of tyrosine radicals leads to the formation of dityrosine. The attack of $\cdot\text{NO}_2$ at C-3 of the tyrosine radical results in the formation of 3-nitrotyrosine, without the involvement of a cation radical (Fig. 2.3) (Riordan & Vallee, 1972). The pKa of the tyrosine phenoxy group is about 10. Thus, under acidic conditions (pH 4.5), the phenoxy anion does not exist and no direct nitration of tyrosine by TNM would occur. The LiP-catalyzed oxidation of tyrosine (III) in the presence of H_2O_2 and TNM results in the formation of the tyrosine phenoxy radical, and radical coupling leads to the formation of dityrosine (XII) (Fig. 2.1C). Neither

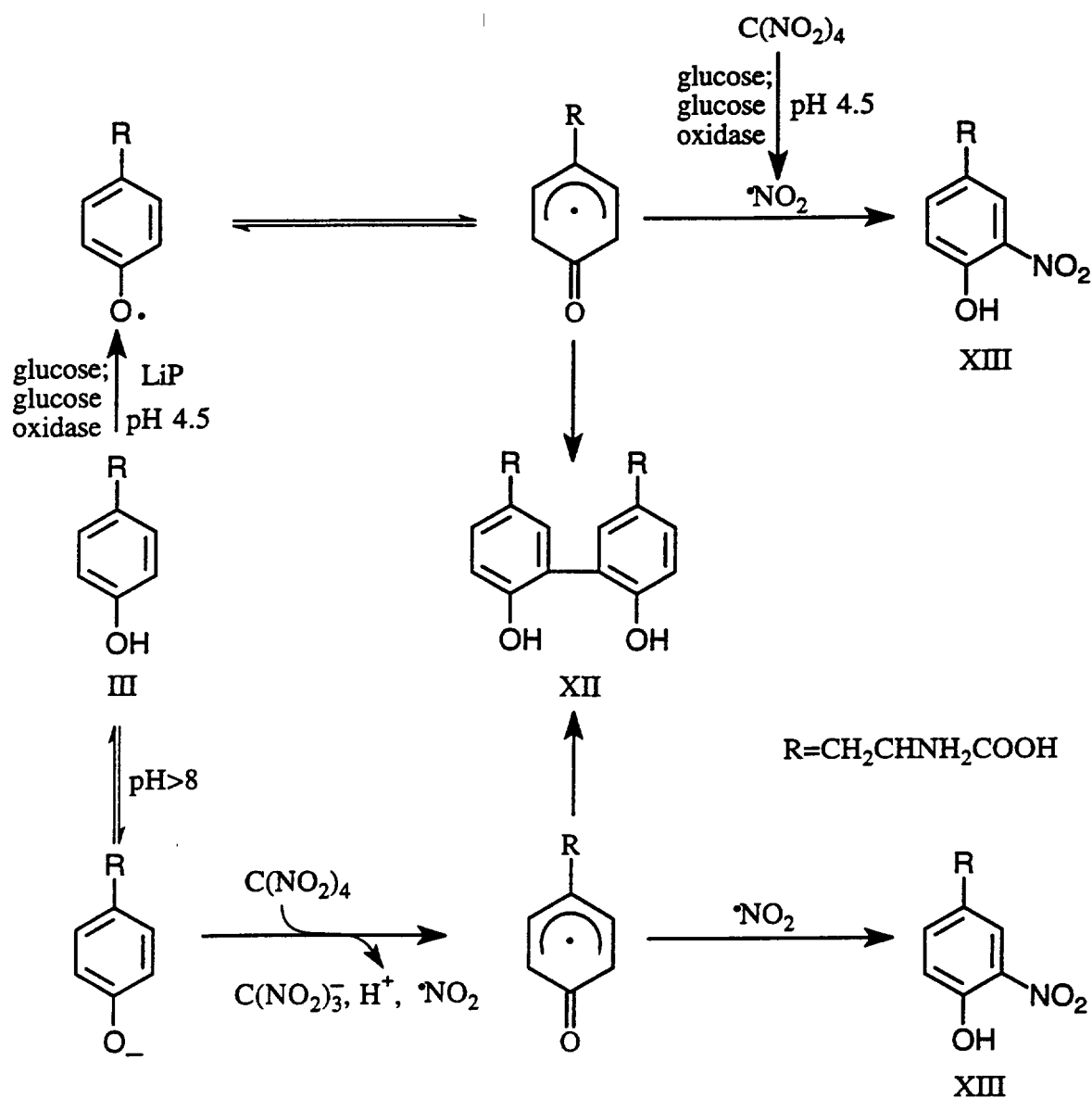


Figure 2.3 Proposed mechanisms for the dimerization and nitration of tyrosine (III). The mechanism for the reaction of tyrosine with TNM at basic pH is modified from Riordan and Vallee (42). The mechanism for the oxidation of tyrosine by LiP, in the presence of TNM, glucose, and glucose oxidase, at acidic pH, is based on the results in Fig. 1D and Table IV.

3-nitrotyrosine (XIII) (Table 2.4) nor trinitromethane (data not shown) is detected, since the reaction does not form an efficient reducing intermediate, equivalent to the phenoxy anion or the VA benzylic radical, needed to produce $\cdot\text{NO}_2$. In contrast, a significant amount of 3-nitrotyrosine (Table 2.4), as well as dityrosine and the trinitromethane anion (data not shown), are formed when glucose/glucose oxidase is used to generate H_2O_2 in the presence of TNM (Fig. 2.1C). This can be explained by the production of $\cdot\text{NO}_2$ from the reaction between superoxide generated by glucose/glucose oxidase and TNM. Nitrotyrosine also is formed when the reaction is conducted in the presence of H_2O_2 and KO_2 , indicating that TNM is reduced by superoxide. Furthermore, much less nitrotyrosine is formed if the reaction with glucose oxidase and glucose is conducted under argon, suggesting that TNM is not serving as an effective direct electron acceptor for glucose oxidase in this reaction. As shown in Fig. 2.3, LiP oxidizes tyrosine to the tyrosine radical, which couples with another tyrosine radical to form dityrosine, or couples with $\cdot\text{NO}_2$ to form 3-nitrotyrosine.

2.4.4 Conclusions

The LiP-catalyzed oxidation of VA (I), in the presence of TNM, leads to the formation of 4,5-dimethoxy-2-nitrobenzyl alcohol (V) and 3,4-dimethoxynitrobenzene (VI), as well as veratraldehyde (IV). These data suggest that LiP oxidizes VA to the cation radical, which undergoes rapid deprotonation to produce the corresponding benzylic radical. The benzylic radical reduces TNM, forming veratraldehyde and $\cdot\text{NO}_2$. The $\cdot\text{NO}_2$ subsequently reacts with the VA cation radical to form the nitrated products. The yields of nitrated products obtained from the LiP-catalyzed oxidations of 1,4-dimethoxybenzene (II) and tyrosine (III), in the presence of TNM, support the proposed mechanism for the LiP oxidation of VA. These results provide further evidence for the formation of a VA cation radical. This also constitutes the first chemical evidence for the formation of a benzylic radical in the LiP oxidation of VA. The low yields of nitrated products obtained in the reaction with VA suggest that the reactions may be occurring very close to the LiP active site. Unlike polymeric lignin, TNM may have access to the VA benzylic radical while the latter is bound to the enzyme.

CHAPTER 3

OXIDATION OF FERROCYTOCHROME *c* BY LIGNIN PEROXIDASE*

3.1 Introduction

Lignin is a heterogeneous, random, phenylpropanoid polymer that constitutes 20-30% of woody plant cell walls (Sarkanen & Ludwig, 1971). White rot basidiomycetous fungi are primarily responsible for initiating the depolymerization of lignin, which is a key step in the earth's carbon cycle (Gold et al., 1989; Kirk & Farrell, 1987; Buswell & Odier, 1987). The best-studied lignin-degrading fungus, *Phanerochaete chrysosporium*, secretes two extracellular heme peroxidases, manganese peroxidase and lignin peroxidase (LiP)** which, along with an H₂O₂-generating system, are apparently major extracellular components of its lignin degradative system (Gold et al., 1989; Kirk & Farrell, 1987; Buswell & Odier, 1987; Hammel et al., 1993; Wariishi et al., 1991b; Higuchi, 1991; Schoemaker, 1990). Nucleotide sequences of several LiP cDNAs and genes (Tien & Tu, 1987; Gold & Alic, 1992; Ritch et al., 1991) as well as the recently published LiP X-ray crystal structures (Edwards et al., 1993; Poulos et al., 1993; Piontek et al., 1993) demonstrate that important catalytic residues including the proximal and distal His, the distal Arg and an H-bonded Asp are all conserved within the heme pocket.

LiP also shares mechanistic features with other plant and fungal peroxidases. Characterization of the formation and reactions of the oxidized intermediates LiPI,

* Reprinted with permission from: Wariishi, H., Sheng, D., and Gold, M. H. (1994) Oxidation of Ferrocycytochrome *c* by Lignin Peroxidase. *Biochemistry* 33, 5545-5552. Copyright 1994 American Chemical Society.

** Abbreviations used are: CCP, cytochrome *c* peroxidase; HRP, horseradish peroxidase; LiP, lignin peroxidase; LiPI, LiPII, and LiPIII, LiP compounds I, II, and III; VA, 3,4-dimethoxybenzyl (veratryl) alcohol; VA⁺, VA cation radical.

LiPII and LiPIII indicates that the oxidized states and catalytic cycle of LiP are similar to those of horseradish peroxidase (Gold et al., 1989; Renganathan & Gold, 1986; Marquez et al., 1988; Dunford & Stillman, 1976; Tien et al., 1986). Yet LiP has several unique features, including an apparently higher redox potential (Gold et al., 1989; Kirk & Farrell, 1987; Schoemaker, 1990), a very low pH optimum of ~ 3.0 (Tien et al., 1986; Renganathan et al., 1987; Wariishi et al., 1991a), and an unusually high reactivity of compound II with H_2O_2 (Wariishi & Gold, 1991; Wariishi et al., 1990). LiP slowly depolymerizes synthetic polymeric lignin in the presence of VA (Hammel et al., 1993) and effectively oxidizes nonphenolic lignin models and aromatic pollutants with redox potentials beyond the reach of other peroxidases (Gold et al., 1989; Kirk & Farrell, 1987; Buswell & Odier, 1987; Schoemaker, 1990; Valli et al., 1992b). Since, as in CCP, the heme group in LiP is buried (Edwards et al., 1993; Poulos et al., 1993; Piontek et al., 1993), it is not available to interact directly with polymeric substrates. In this report, we utilize ferrocyanochrome *c* as a model polymeric substrate for LiP, and discuss the implications of our findings for lignin oxidation by the enzyme.

3.2 Materials and Methods

3.2.1 Protein preparation

LiP isozyme 2 (H8) was purified from cultures of *P. chrysosporium* strain OGC101 as previously described (Wariishi & Gold, 1990; Gold et al., 1984). The purified enzyme was electrophoretically homogeneous and had an RZ value (A_{408}/A_{280}) of ~ 5.0 . Enzyme concentrations were determined at 408 nm using an extinction coefficient of $133 \text{ mM}^{-1} \text{ cm}^{-1}$ (Gold et al., 1984). Horse heart ferricytochrome *c* was obtained from Sigma. Stock solutions of ferrocyanochrome *c* were prepared by dissolving ferricytochrome *c* in water, then adding excess potassium dithionite as described (Kang & Erman, 1982). Excess dithionite was removed by gel filtration on a Sephadex G-10 column equilibrated with argon-saturated water. After gel filtration, the ferrocyanochrome *c* solution ($>97\%$ in the reduced state) was stored under argon. The stock solution concentration was determined spectroscopically after each series of

experiments and data were used for kinetic analysis only with solutions which were > 95% ferrocyanochrome *c*. Concentrations of ferri- and ferrocyanochrome *c* were determined using an ϵ_{410} of $106 \text{ mM}^{-1} \text{ cm}^{-1}$ and an ϵ_{550} of $27.7 \text{ mM}^{-1} \text{ cm}^{-1}$, respectively (Margoliash & Frohwirt, 1959). HRP (type VI) was purchased from Sigma and yeast CCP was kindly supplied by Dr. A. G. Mauk (University of British Columbia, Canada). Concentrations of HRP and CCP were determined using an ϵ_{402} of $102 \text{ mM}^{-1} \text{ cm}^{-1}$ (Dunford & Stillman, 1976) and an ϵ_{408} of $98 \text{ mM}^{-1} \text{ cm}^{-1}$ (Vitello et al., 1990b), respectively.

3.2.2 Chemicals

H_2O_2 (30% solution) was obtained from Sigma and the stock solution concentration was determined as described (Cotton & Dunford, 1973). VA was purchased from Aldrich. All other chemicals were reagent grade. All solutions were prepared using deionized water from a Milli Q 50 system (Millipore).

3.2.3 Determination of oxidation rates

Ferrocyanochrome *c* oxidation was monitored at room temperature at 550 nm using a Shimadzu UV-260 spectrophotometer with a 1-cm light path. The initial oxidation rate was calculated using a $\Delta\epsilon_{550}$ of $19.5 \text{ mM}^{-1} \text{ cm}^{-1}$ between ferri- and ferricyanochrome *c* (Kang & Erman, 1982). The initial velocities were corrected for the uncatalyzed H_2O_2 oxidation of ferrocyanochrome *c*. The oxidation of VA to veratrylaldehyde was monitored at 310 nm ($\epsilon_{310} = 9.3 \text{ mM}^{-1} \text{ cm}^{-1}$) (Gold et al., 1989; Kirk & Farrell, 1987; Buswell & Odier, 1987).

$1/v$ versus $1/[\text{ferrocyanochrome } c]$ was plotted at several fixed concentrations of H_2O_2 . Reaction mixtures contained LiP ($1 \mu\text{g/ml}$), ferrocyanochrome *c* ($8\text{-}100 \mu\text{M}$), and H_2O_2 ($20\text{-}100 \mu\text{M}$). The reaction was initiated by the addition of H_2O_2 . Buffers used were 10 mM K-succinate for the LiP and HRP reactions, and 10 mM K-phosphate for the CCP reaction at the indicated pHs. The ionic strength of the reaction mixture was adjusted with KNO_3 . Owing to the low ionic strength, the pH was remeasured after the reactions were completed. The pH change over the course

of the reaction was less than 0.03 in all cases. Reactions were carried out under both air and argon.

3.2.4 Protection of lignin peroxidase from inactivation by H₂O₂

The ability of ferrocyanochrome *c* and VA to protect LiP from H₂O₂ was investigated. Reaction mixtures consisted of LiP (50 µg/ml, ~ 1.2 µM), H₂O₂ (120 µM) in 10 mM Na-succinate, pH 3.0. Reactions were run at 25°C in the presence of ferrocyanochrome *c* (250 µM), VA (250 µM) or no additives. Periodically during the reaction a 20-µl aliquot was removed and LiP activity was measured in an assay mixture consisting of enzyme, 5 mM VA and 0.1 mM H₂O₂ in 20 mM Na-succinate, pH 3.0. The VA oxidation rate was corrected for the inhibition caused by ferricytochrome *c* in the aliquot.

3.2.5 Inactivation of lignin peroxidase during the reaction

LiP inactivation during the course of the reaction was monitored via a previously reported procedure (Selwyn, 1965). In these Selwyn tests the rate of ferricytochrome *c* produced at pH 3.0 was plotted against (LiP concentration × time) at three LiP concentrations. LiP concentrations of 1, 2 and 4 µg/ml were used for reactions conducted in the absence of VA. LiP concentrations of 0.1, 0.2 and 0.4 µg/ml were used for reactions conducted in the presence of VA. To compensate for the differences in enzyme concentration, the recorder chart speed was varied accordingly.

3.2.6 Effect of ferricytochrome *c* on the lignin peroxidase oxidation of veratryl alcohol

Reaction mixtures contained LiP (1 µg/ml), VA (50-500 µM), and H₂O₂ (100 µM) in the presence of ferricytochrome *c* (0-10 µM). The generation of superoxide during aerobic VA oxidation by LiP has been reported (Schmidt et al., 1989), and ferricytochrome *c* is readily reduced by superoxide to form ferrocyanochrome *c*. To avoid interference from the possible reduction of ferricytochrome *c* by superoxide, the

isosbestic point between ferri- and ferrocytochrome *c* (337 nm) was used to monitor VA oxidation, using an ϵ_{337} of $2.06 \text{ mM}^{-1} \text{ cm}^{-1}$. The reaction was initiated by the addition of H_2O_2 and carried out under aerobic conditions.

3.3 Results

3.3.1 Ferrocytochrome *c* oxidation by LiP

The visible spectral change observed when ferrocytochrome *c* was treated with LiP/ H_2O_2 is shown in Fig. 3.1A. During the course of the reaction, the 550-nm and 520-nm bands indicative of ferrocytochrome *c* decreased and a new peak appeared at 528 nm. This conversion has several isosbestic points (Fig. 3.1A) which are identical to those observed during the CCP oxidation of ferrocytochrome *c* and during autooxidation (data not shown), strongly suggesting that LiP oxidizes ferrocytochrome *c* to ferricytochrome *c* via a single-electron step. The LiP-catalyzed oxidation of cytochrome *c* is much faster than autooxidation or oxidation with H_2O_2 alone (Fig. 3.1B). As shown in Fig. 3.1B, HRP has minimal activity with ferrocytochrome *c*.

3.3.2 Effect of pH and veratryl alcohol

The effect of pH on the LiP-catalyzed oxidation of ferrocytochrome *c* in the presence and the absence of VA is shown in Fig. 3.2. In the presence of VA, ferrocytochrome *c* oxidation increased continuously as the pH was lowered to 3.0. This is similar to the pH dependence for VA oxidation by LiP (Tien et al., 1986; Renganathan et al., 1987). In the absence of VA, the activity increased with decreasing pH to a maximum at pH 4.0, beyond which the activity decreased considerably. The addition of VA had little effect above pH 4.5, but it enhanced the rate significantly below pH 3.5.

To explore the role of VA in this reaction, two assay methods were used to measure the initial velocities. In the first assay (method A), the reducing substrate and LiP were preincubated in the buffer solution for 20 s, after which H_2O_2 was added to initiate the reaction. In the second assay (method B), H_2O_2 and LiP were

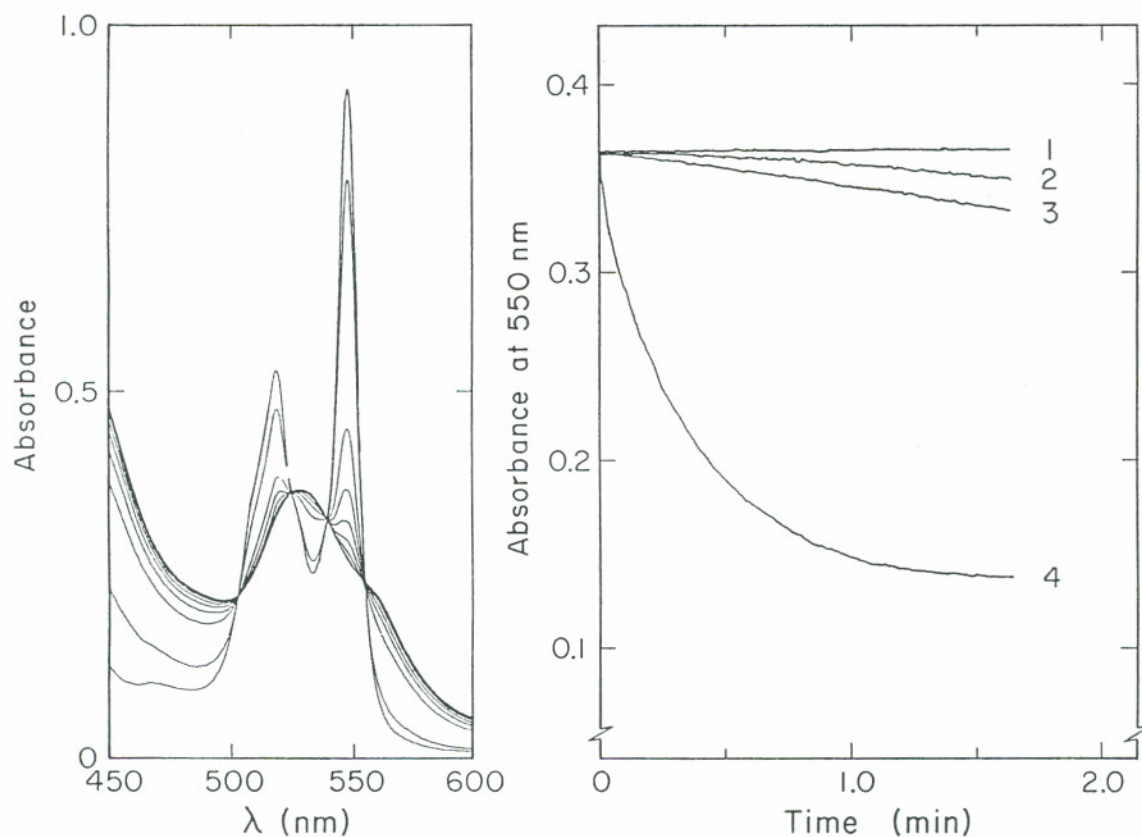


Figure 3.1 Oxidation of ferrocyanochrome *c* by LiP. A: Spectra were recorded at 2 min intervals. Reaction mixtures consisted of LiP (0.5 $\mu\text{g/ml}$), ferrocyanochrome *c* (30 μM), H_2O_2 (100 μM) in potassium succinate, pH 6.2 (μ ; 0.01). B: Ferrocyanochrome *c* oxidations were monitored at 550 nm under aerobic conditions. Trace 1 (spontaneous autoxidation): ferrocyanochrome *c* (13 μM) in potassium succinate, pH 4.5 (μ ; 0.01). Trace 2: Same as 1 with addition of 100 μM H_2O_2 . Trace 3: Same as 2 with addition of HRP (1 $\mu\text{g/ml}$). Trace 4: Same as 2 with addition of LiP (1 $\mu\text{g/ml}$).

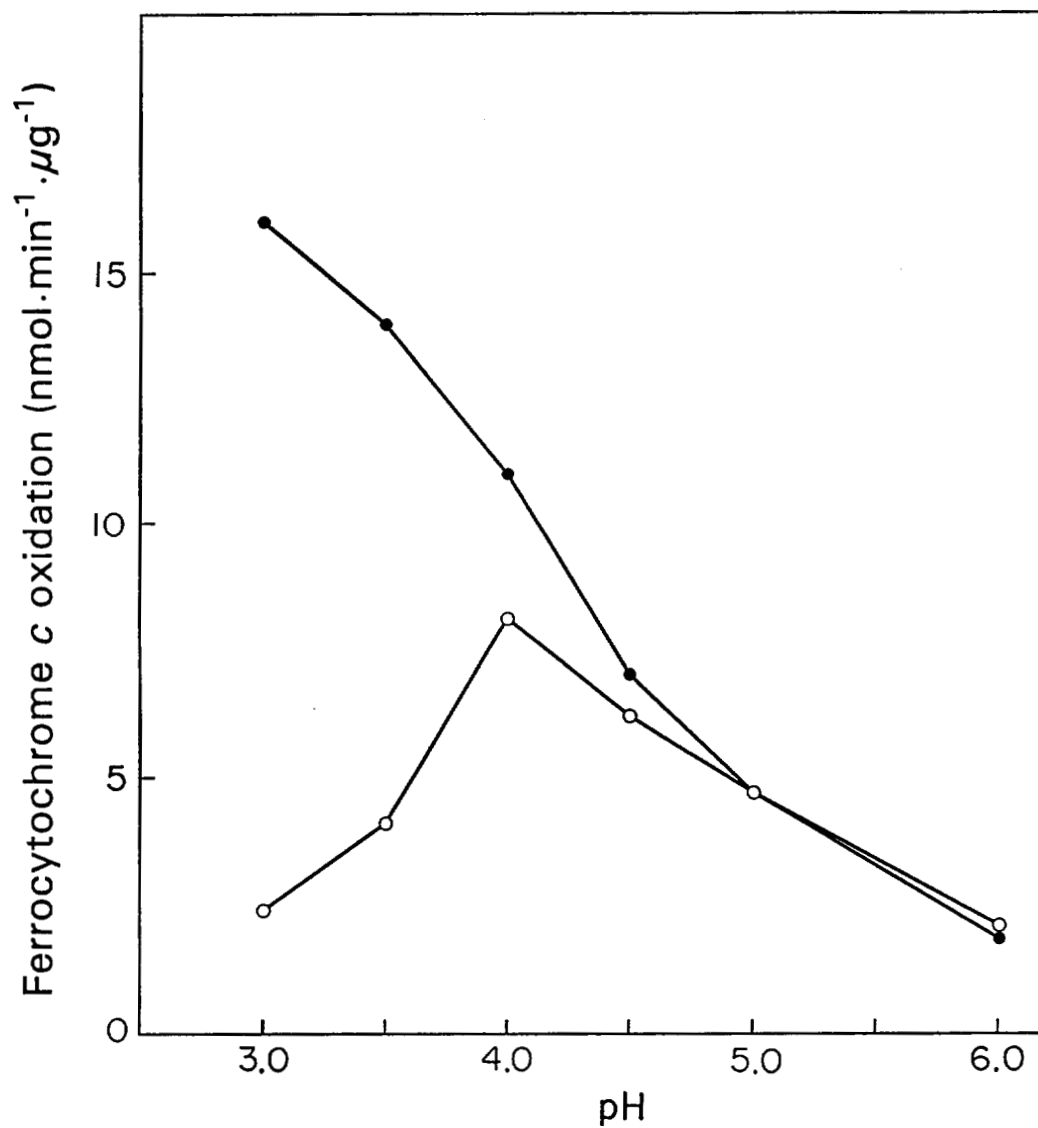


Figure 3.2 pH profile for LiP oxidation of ferrocyanochrome *c* in the presence or absence of veratryl alcohol. Reaction mixtures consisted of LiP (1 $\mu\text{g}/\text{ml}$), ferrocyanochrome *c* (20 μM), and H_2O_2 (100 μM) in potassium succinate (μ ; 0.01) without VA (○) and with VA (0.5 mM) (●).

Table 3.1
Veratryl Alcohol and Ferrocyanochrome *c* Oxidation by LiP

pH	Assay method ^a	nmol · min ⁻¹ · μg ⁻¹			
		VA oxidation (%) ^b		Ferrocyanochrome <i>c</i> oxidation (%) ^b	
3.04	A	21.34		2.90	
	B	18.90	(89)	1.56	(54)
3.97	A	11.03		8.32	
	B	10.81	(98)	6.41	(73)
5.04	A	2.87		4.83	
	B	2.84	(99)	4.62	(96)
6.12	A	1.61		2.80	
	B	1.58	(98)	2.73	(98)

^a Method A: 20-s preincubation of the reducing substrate and LiP in buffer, prior to addition of H₂O₂ to initiate the reaction. Method B: 20-s preincubation of LiP and H₂O₂ in buffer, prior to addition of reducing substrate to initiate the reaction. Reaction mixtures consisted of LiP (1 μg/ml), H₂O₂ (0.1 mM), and VA (0.5 mM) or ferrocyanochrome *c* (20 μM) in potassium succinate (μ; 0.01).

^b Percentage of the rate for method B over that for method A.

preincubated for 20 s in the buffer, after which the reducing substrate was added to initiate the reaction. Table 3.1 shows the initial rates at several pHs with either VA or ferrocyanochrome *c* as substrate.

The direct effect of cytochrome *c* or VA on H_2O_2 inactivation of LiP also was investigated (Fig. 3.3). When LiP was incubated with $120 \mu\text{M}$ H_2O_2 at pH 3.0, almost all activity was lost within 2 min. at 25°C . However, in the presence of $250 \mu\text{M}$ VA, essentially all LiP activity was retained. Under the same conditions in the presence of ferrocyanochrome *c*, 70% of the LiP activity was lost within the first 2 min.

The effect of LiP inactivation on the rate of cytochrome *c* oxidation at pH 3.0 is shown in Fig. 3.4. In these experiments, the rate of ferricytochrome *c* formed was plotted against (LiP concentration \times time) at three different LiP concentrations (Selwyn, 1965). At pH 3.0, in the presence of $65 \mu\text{M}$ H_2O_2 and in the absence of VA, the Selwyn test demonstrated that the enzyme was inactivated during the course of the reaction (Fig. 3.4A). When the reaction was conducted under the same conditions in the presence of $500 \mu\text{M}$ VA, the Selwyn test indicated that the enzyme was not inactivated significantly (Fig. 3.4B). Finally, at pH 3.0 with $6.5 \mu\text{M}$ H_2O_2 , the enzyme was not inactivated significantly even in the absence of VA (Fig. 3.4C).

The results in Fig. 3.5 show the stimulatory effect of VA on the oxidation of ferrocyanochrome *c* at various H_2O_2 concentrations. At pH 3.0, in the presence of $100 \mu\text{M}$ H_2O_2 , VA stimulated the reaction approximately 7-fold with maximal effect at $\sim 250 \mu\text{M}$ VA. In contrast, at pH 3.0 in the presence of 3 or $6 \mu\text{M}$ H_2O_2 , the effect of VA was minimal. These results show that the VA stimulatory effect increased with increasing concentrations of H_2O_2 in the reaction mixture.

3.3.3 Steady-state kinetics

The family of plots, $1/v$ versus $1/[\text{ferrocyanochrome } c]$ at various fixed concentrations of H_2O_2 , yielded a set of parallel lines, indicating a ping-pong mechanism for the LiP oxidation of ferrocyanochrome *c*. Reactions were carried out at pH 4.0 under aerobic conditions. The secondary plot of primary y-intercepts versus $1/[\text{H}_2\text{O}_2]$ showed a linear relationship but passed through the origin within

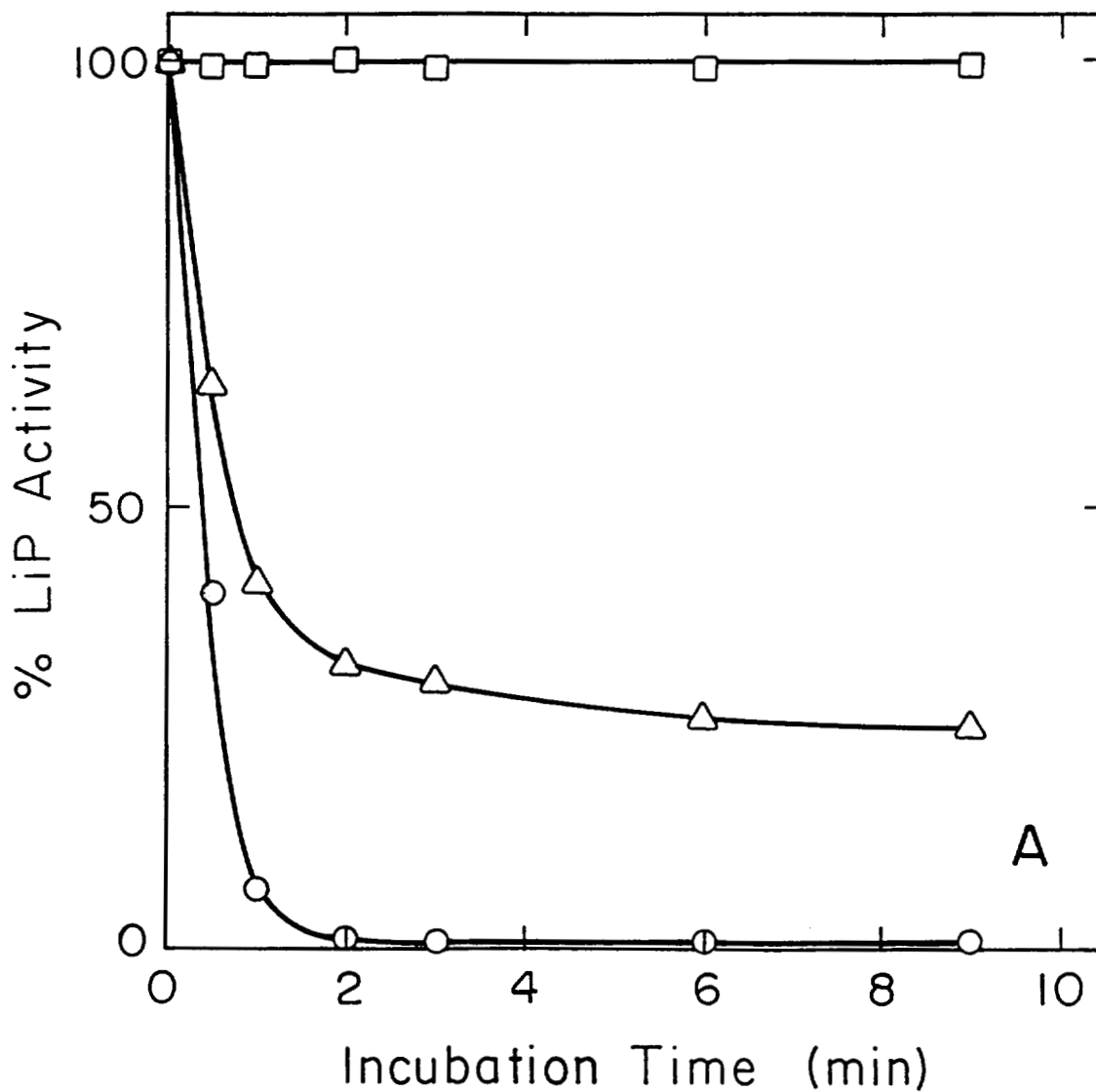


Figure 3.3 Effect of veratryl alcohol and ferrocyanochrome *c* on lignin peroxidase stability and activity. A. LiP (50 $\mu\text{g/ml}$) was incubated with H_2O_2 (120 μM) in 10 mM K-succinate, pH 3.0 in the absence (○) or in the presence of either VA (250 μM) (□), or ferrocyanochrome *c* (250 μM) (△). Periodically, aliquots (20 μl) were removed and assayed for LiP activity as described in the text.

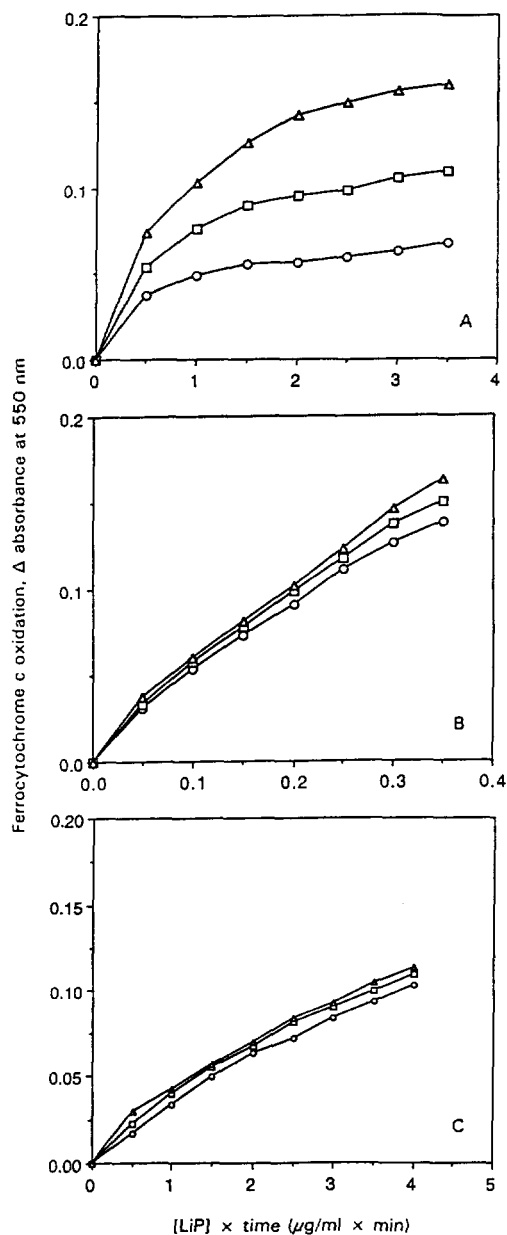


Figure 3.4 Inactivation of LiP by H_2O_2 during the oxidation of ferrocyanochrome *c*. The amount of ferricytochrome *c* produced is plotted against (enzyme concentration \times time) as described (Selwyn, 1965). All reaction mixtures contained $20 \mu\text{M}$ ferrocyanochrome *c* in 10 mM K-succinate, $\text{pH } 3.0$. A. Reactions contained $65 \mu\text{M}$ H_2O_2 , and either 1.0 (\circ), 2.0 (\square) or 4.0 (\triangle) μg of LiP but no VA. B. Reactions contained $65 \mu\text{M}$ H_2O_2 , $500 \mu\text{M}$ VA and either 0.1 (\circ), 0.2 (\square), or 0.4 (\triangle) LiP. C. Reactions contained $6.5 \mu\text{M}$ H_2O_2 and either 1.0 (\circ), 2.0 (\square) or 4.0 (\triangle) LiP but no VA. The recorder chart speed was run at 1 cm/min , 2 cm/min , or 4 cm/min to compensate for the three enzyme concentrations used.

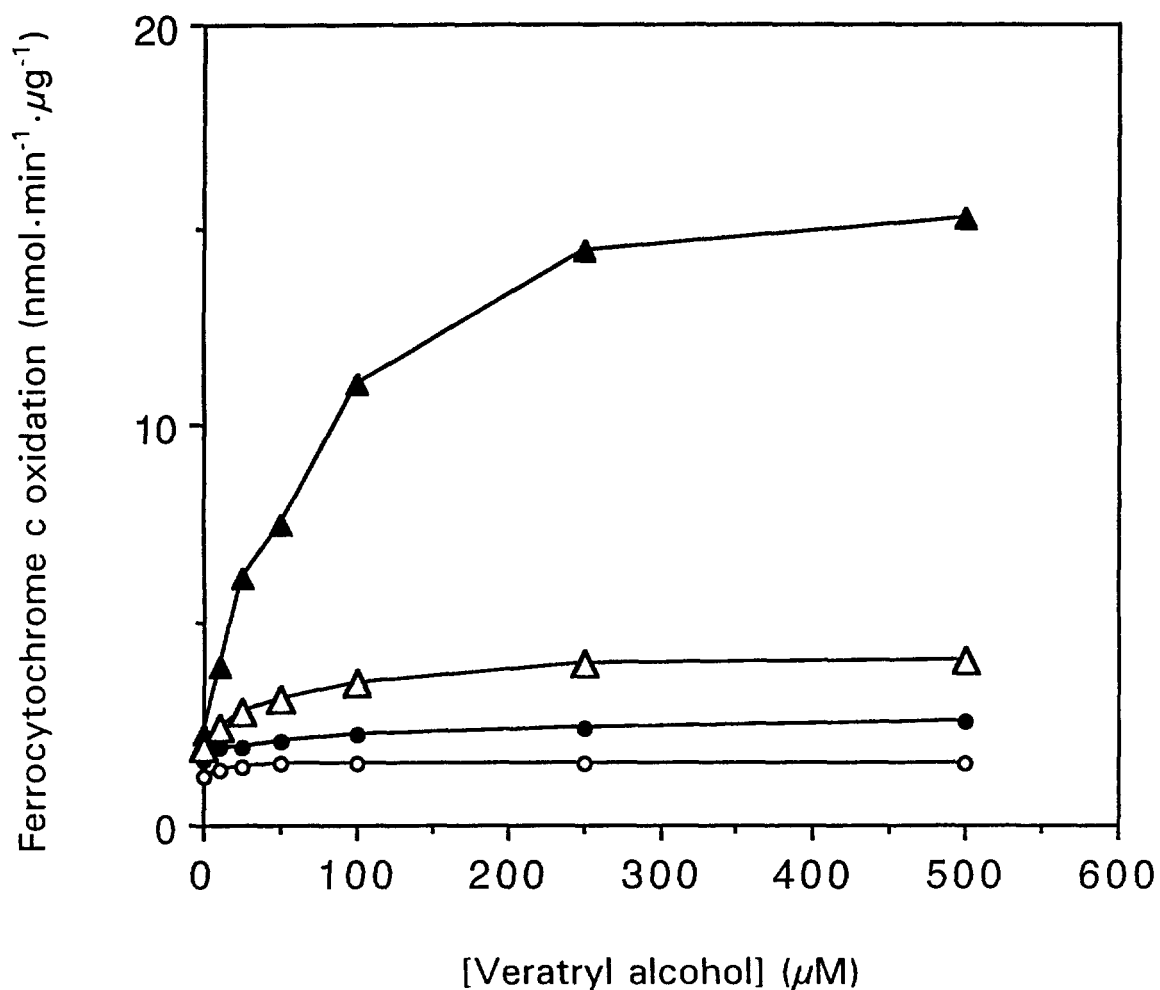


Figure 3.5 Effect of H₂O₂ concentration on the stimulation of cytochrome *c* oxidation by VA. Reaction mixtures contained LiP (1 μg/ml), VA (0.0-0.5 mM), and ferrocyanochrome *c* (20 μM) in 10 mM K-succinate, pH 3.0. Reactions were initiated by addition of H₂O₂ to a final concentration of 3 (○), 6 (●), 9 (△) or 100 (▲) μM and ferrocyanochrome *c* oxidation was monitored as described in the text.

experimental error, suggesting that the reaction obeys peroxidase ping-pong kinetics rather than classical ordered bi-bi ping-pong kinetics (data not shown). For this reason, the K_m for H_2O_2 could not be determined. However, at a fixed $[H_2O_2]$, the apparent K_m and k_{cat} for ferrocyclochrome *c* could be determined. CCP reactions were carried out at pH 7.3 in potassium phosphate buffer. Table 3.2 summarizes these kinetic parameters at an $[H_2O_2]$ of 100 μM . CCP did not oxidize VA under the conditions used.

3.3.4 Effect of ionic strength

A plot of the logarithm of the initial velocity versus the square root of the ionic strength exhibited a linear relationship at pH 4.0 (Fig. 3.6). As the ionic strength increased, the rate of ferrocyclochrome *c* oxidation by LiP decreased.

3.3.5 Inhibition of veratryl alcohol oxidation by ferricyclochrome *c*

The family of plots, $1/v$ versus $1/[VA]$ at various fixed concentrations of ferricyclochrome *c*, intercepted on the x-axis (Fig. 3.7). A linear relationship of the secondary plot, y-intercept versus $[ferricyclochrome\ c]$, demonstrated noncompetitive inhibition (Fig. 3.7, inset). The K_i for ferricyclochrome *c* was determined to be 2.5 μM .

3.4 Discussion

Although considerable work has been reported on the mechanism of LiP, the precise role of this enzyme in polymeric lignin degradation remains unclear. The role that VA plays in the lignin degradative system also is still under discussion. VA stimulates the LiP-catalyzed depolymerization of synthetic lignin (Hammel et al., 1993) and the LiP-catalyzed oxidation of a variety of poor reducing substrates (Valli et al., 1992b; Harvey et al., 1986; Renganathan et al., 1985; Haemmerli et al., 1986). *P. chrysosporium* produces VA under ligninolytic conditions; VA is a good reducing substrate for LiP (Gold et al., 1989; Kirk & Farrell, 1987; Buswell & Odier, 1987). A variety of mechanisms have been postulated to account for the

Table 3.2
Kinetic Parameters of LiP and CCP Reactions^a

Enzyme	Substrate	$K_{m(\text{app})}$ (μM)	$k_{\text{cat}(\text{app})}$ (s^{-1})
LiP	ferrocyanochrome <i>c</i>	68.2	257
	veratryl alcohol	113	19
CCP	ferrocyanochrome <i>c</i>	18.3	175

^a Values were determined at a H_2O_2 concentration of $100 \mu\text{M}$. The LiP reaction with VA was carried out in potassium succinate, pH 3.04 (μ ; 0.01). The LiP reaction with ferrocyanochrome *c* was carried out at pH 4.0. CCP reactions were carried out in potassium phosphate, pH 7.3 (μ ; 0.01). Reaction mixtures consisted of enzymes (LiP, $1 \mu\text{g}/\text{ml}$; CCP, $0.5 \mu\text{g}/\text{ml}$), reducing substrates (ferrocyanochrome *c*, $10\text{-}100 \mu\text{M}$; VA, $50\text{-}500 \mu\text{M}$) and H_2O_2 .

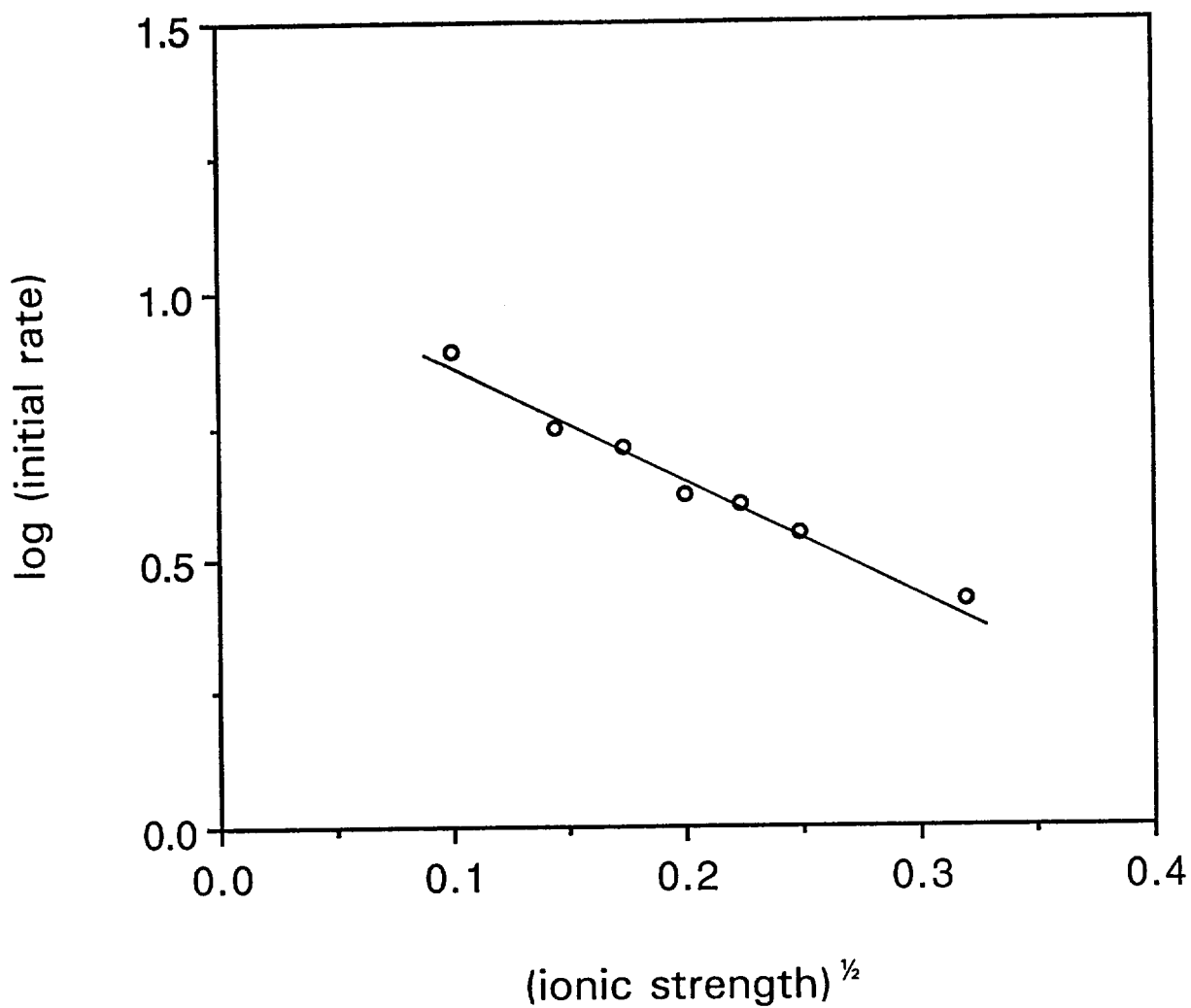


Figure 3.6 Effect of ionic strength on the initial velocity of ferrocyanide oxidation by LiP. The logarithm of initial velocities were plotted against the square root of the ionic strength at pH 4.0. Reaction mixtures consisted of LiP (1 $\mu\text{g/ml}$), ferrocyanide *c* (17 μM), and H_2O_2 (100 μM).

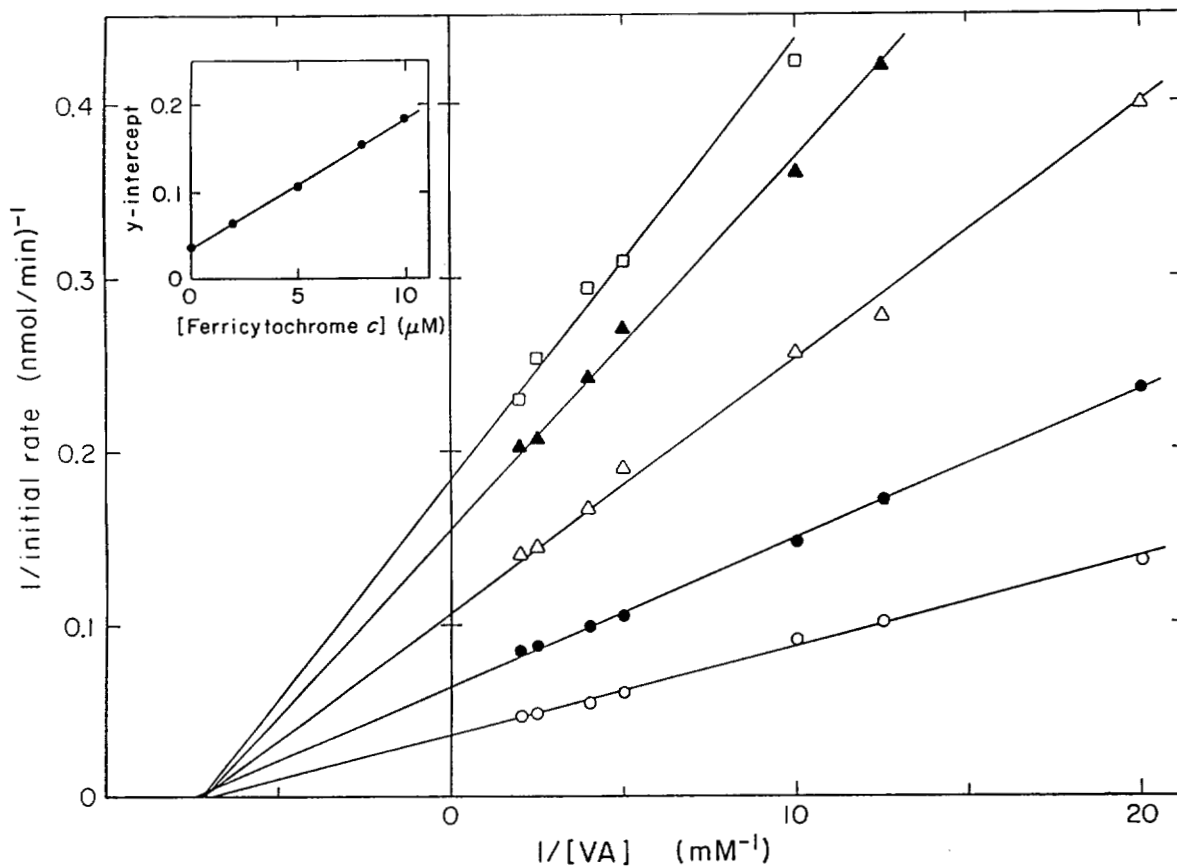


Figure 3.7 Inhibitory effect of ferricytochrome *c* on veratryl alcohol oxidation by LiP. Reaction mixtures contained LiP (1 $\mu\text{g/ml}$), VA (0.05-0.5 mM), H_2O_2 (100 μM), and fixed [ferricytochrome *c*] of 0 (\circ), 1.97 (\bullet), 4.95 (Δ), 7.92 (\blacktriangle), and 9.89 (\square) μM in potassium succinate, pH 3.04. Inset: Replot of the y-intercept versus [ferricytochrome *c*] (μM).

stimulation of LiP reactions by VA. One role of VA appears to be protection of the enzyme from H₂O₂-derived irreversible inactivation (Wariishi & Gold, 1989; 1990), although the exact protection mechanism(s) has not been clarified. A second proposed role for VA is that of a diffusible radical mediator, wherein the VA⁺ produced via the one-electron oxidation of VA diffuses and, in turn, oxidizes the terminal substrate (lignin) some distance from the surface of the enzyme (Harvey et al., 1986; 1987; Akamatsu et al., 1990; Popp et al., 1990). However, both the long-range mediation by a diffusible VA⁺ and the formation of a catalytic LiPII-VA⁺ complex (Harvey et al., 1987) have been challenged (Wariishi et al., 1991a, 1992a; Valli et al., 1990; Cui & Dolphin, 1990). Recent crystal structures of LiP demonstrate that the heme group is buried in the protein (Edwards et al., 1993; Poulos et al., 1993; Piontek et al., 1993) and that a narrow access channel may be available to H₂O₂ and small aromatic compounds such as VA. Indeed, a protein-binding site for VA has been postulated via computer modeling (Poulos et al., 1993). This raises the question of whether LiP can directly attack polymeric lignin or whether VA plays some role in electron transfer between the buried heme and the polymeric substrate. To investigate the interaction between the enzyme and a polymeric substrate, we utilized ferrocyanochrome *c* as a model polymer. Ferrocyanochrome *c* was selected as a polymeric substrate since (i) its heme iron is low spin and hexacoordinated (Ferguson-Miller et al., 1979), assuring that it does not react with H₂O₂ to form higher redox states such as compounds I and II of peroxidases; (ii) ferro-/ferricyanochrome *c* is a well-characterized one-electron couple, limiting complexities in the reactions; (iii) the molecular weight of horse heart cytochrome *c* (~12,300 kDa) is considerably larger than the average molecular weight of chemically synthesized lignin (3000-5000 kDa); and finally, (iv) the heme in cytochrome *c* is buried (Pelletier & Kraut, 1992; Ferguson-Miller et al., 1979).

3.4.1 Effect of pH and veratryl alcohol

Below pH 3.5, ferrocyanochrome *c* oxidation by LiP is enhanced significantly by VA. The lower the pH, the greater the effect of VA. In contrast, above pH 4.5 the effect of VA on the reaction is negligible (Fig. 3.2). To examine the role of VA

in the reaction, several experiments were conducted. Initially, two assay methods were used to measure the initial velocities for LiP oxidation of ferrocyanochrome *c* and VA (Table 3.1).

Preincubation of LiP with H₂O₂ at pH 3 for 20 s before initiating the reaction results in ~50% loss of the ferrocyanochrome *c* oxidation activity. In contrast, only ~10% loss of LiP activity is observed with VA as the substrate (Table 3.1). This may be explained by our previous finding that LiPII has an unusually high reactivity with H₂O₂, generating LiPIII (Wariishi & Gold, 1990; Wariishi et al., 1990). The latter reacts further with H₂O₂, causing irreversible heme bleaching via the intermediate formation of LiPIII*. We have shown previously that VA both reduces LiPII efficiently and reacts with the intermediate LiPIII* to regenerate native LiP (Wariishi & Gold, 1990; Wariishi et al., 1990). The 10% activity loss with respect to VA oxidation probably is caused by the irreversible inactivation of the enzyme during the 20 s incubation period. In contrast, ferrocyanochrome *c* does not react with the intermediate LiPIII* to regenerate native LiP (see below), and at pH 3, ferrocyanochrome is a relatively poor substrate as compared to VA. Thus, in the presence of both ferrocyanochrome *c* and H₂O₂ but in the absence of VA, the enzyme does not complete its catalytic cycle. Instead, it is rapidly converted to LiPIII*, followed by slow irreversible enzyme inactivation. Since LiPIII* is not catalytically active, 50% loss of activity is seen for ferrocyanochrome *c* oxidation; most likely 40% of the loss is caused by LiPIII* formation and 10% by enzyme inactivation.

We have reported that the reaction of LiPII with H₂O₂ is pH dependent with a pK_a of 4.2, and that the reaction rate dramatically decreases above pH 4 (Wariishi et al., 1990). Thus, the rate for irreversible inactivation also decreases above pH 4 (Wariishi et al., 1990). This previous finding may explain why above pH 4 no loss is observed for VA oxidation activity by preincubation of LiP with H₂O₂ (Table 3.1). As the pH increases, the loss of ferrocyanochrome *c* oxidation activity also decreases, correlating well with our previous findings on the pH dependence of LiP inactivation (Wariishi & Gold, 1990).

The electron transfer reaction increases as the pH decreases. The protonated forms of LiPI and LiPII are most active for one-electron transfer from VA (Wariishi

et al., 1991a). However, the enzyme inactivation rate also rapidly increases as pH decreases, possibly explaining why LiP oxidation of ferrocyanochrome *c* has an apparent pH optimum at 4.0 in the absence of VA.

The ability of VA and ferrocyanochrome *c* to protect LiP directly from H₂O₂-derived inactivation also was examined (Fig. 3.3). Both VA and ferrocyanochrome *c* protect the enzyme but the extent of protection is much greater with VA. We have reported that VA protects the enzyme via two mechanisms: (i) by stimulating the reduction of LiPII to the native enzyme thus, preventing the reaction of LiPII with H₂O₂; and (ii) by converting LiPIII* back to the native enzyme (Wariishi & Gold, 1990). Ferrocyanochrome *c* is a good reducing substrate for LiP above pH 4.0 (Fig. 3.2). The reactivity of LiPIII* with cytochrome *c* was examined at pH 3.0. Owing to the strong absorptivity of ferrocyanochrome *c*, the spectral shifts due to LiPIII* conversion are difficult to observe. However, a shoulder at 578 nm attributable to LiPIII* remains for several minutes after addition of ferrocyanochrome *c*. This shoulder is observed in LiPIII* spectra but is not observed with native LiP or with ferro- or ferricytochrome *c*. Furthermore, this shoulder disappears upon addition of VA to LiPIII* (Wariishi & Gold, 1990).

These results suggest that at pH 3.0 and in the presence of 100 μ M H₂O₂, ferrocyanochrome *c* reduction of LiPII is unable to compete with the rapid conversion of LiPII to LiPIII*. In addition, ferrocyanochrome *c* is unable to convert LiPIII* to the native enzyme. Thus, at pH 3.0 in the presence of 100 μ M H₂O₂ and in the absence of VA, LiP would be inactivated during the oxidation of ferrocyanochrome *c*. This inactivation also accounts, at least in part, for the slow rate of ferrocyanochrome *c* oxidation observed at pH 3.0. Under the same conditions but in the presence of VA, LiP should not be inactivated.

To examine the possible inactivation of LiP during the course of ferrocyanochrome *c* oxidation, we conducted a simple test. Selwyn (1965) showed that when the product formed during the reaction is plotted against (enzyme concentration \times time), enzyme inactivation during the course of the reaction will become apparent. The results shown in Fig. 3.4A demonstrate that LiP is inactivated during the course

of the reaction at pH 3.0 in the presence of 65 μM H_2O_2 . Fig. 3.4B shows that VA protects against this inactivation. Finally, Fig. 3.4C shows that significant inactivation does not occur when the reaction is conducted in the presence of only 6.5 μM H_2O_2 . The exact mechanism of this protection has not been elucidated. However, it is likely to involve the comparative facile reduction of LiPII in the presence of VA and conversion of LiPIII* to the native enzyme. At pH 3.0, LiPII is readily converted to LiPIII in the presence of H_2O_2 . Apparently, the oxidation of VA by LiPII effectively competes with the conversion of LiPII to LiPIII. At pH 3.0 and in the presence of 100 μM H_2O_2 , the rate of ferrocyanide oxidation apparently does not compete with the rate of LiPII conversion to LiPIII. At pH 3.0, the presence of VA significantly stimulates ferrocyanide oxidation, at least in part by protecting LiP from inactivation, but the mechanism(s) for this remains unclear. At least three possibilities are feasible: (i) VA may act as an enzyme-binding activator such that the binding of VA stimulates the direct transfer of an electron from the alternate substrate (ferrocyanide) to the heme in LiP; (ii) by reacting rapidly with LiPII, VA stimulates completion of the peroxidatic cycle and prevents the formation of LiPIII* (Wariishi & Gold, 1990; Paszczyński & Crawford, 1991); alternatively, (iii) VA bound in the heme pocket may mediate the electron transfer directly. In this case, VA would act as a cofactor cycling between the fully reduced and the radical cation oxidation states. The radical cation would accept an electron from ferrocyanide and in turn be reoxidized by LiPI and LiPII. This alternative does not require VA to diffuse into the aqueous medium as proposed by Harvey et al. (1986) with subsequent rapid loss of a proton. As shown in Fig. 3.4, when the reaction is conducted at pH 3.0 in the presence of 6.5 μM H_2O_2 , LiP is not inactivated, suggesting that VA stimulates the oxidation of ferrocyanide only at relatively high concentrations of H_2O_2 . The results shown in Fig. 3.5 confirm that VA stimulates the oxidation of ferrocyanide in the presence of high concentrations of H_2O_2 ; but in the presence of low concentrations of H_2O_2 (3-6 μM), there is minimal stimulation by VA. Furthermore, there is minimal stimulation by VA above pH 4.0, even in the presence of high concentrations of H_2O_2 . These

observations suggest that the VA stimulation of cytochrome *c* oxidation is due to its capacity to foster efficient enzyme turnover at pH 3.0 and 100 μM H_2O_2 , conditions which are optimal for activity. In the absence of VA, the enzyme is rapidly inactivated under these conditions.

3.4.2 Peroxidase ping-pong mechanism

A linear relationship is obtained for the plot of $1/v$ against $1/[\text{ferrocyanochrome } c]$, suggesting that only one ferrocyanochrome *c* equivalent is involved in each reduction step of the catalytic cycle. The series of plots of $1/v$ against $1/[\text{ferrocyanochrome } c]$ at various fixed $[\text{H}_2\text{O}_2]$ yield parallel lines. The secondary plot of primary y-intercepts ($1/V_{\text{max}}$) against $1/[\text{H}_2\text{O}_2]$ passes through the origin. In classical ordered bi-bi ping-pong kinetics, K_m and V_{max} are assigned from the secondary plot. This difference between classical ping-pong and peroxidase ping-pong mechanisms is well documented, resulting from the irreversible reactions of the peroxidase catalytic cycle (Dunford, 1991). Both the irreversible formation of LiPI by H_2O_2 and irreversible reductions of LiPI and LiPII by VA have been reported (Marquez et al., 1988; Wariishi et al., 1991a,b). The LiP oxidation of ferrocyanochrome *c* obeys peroxidase ping-pong kinetics rather than classical ordered bi-bi ping-pong kinetics. This strongly suggests that the reductions of LiPI and LiPII by ferrocyanochrome *c* also are irreversible. Peroxidase ping-pong kinetics also have been observed for Mn^{II} oxidation by manganese peroxidase (Wariishi et al., 1992).

To compare the rates of ferrocyanochrome *c* oxidation by LiP and CCP, steady-state kinetic parameters were determined. The kinetics of CCP reactions depend upon the ferrocyanochrome *c* concentration (Kang & Erman, 1982; Margoliash et al., 1976; Kang et al., 1977). With the concentrations used in this study, the kinetics display no such complexity. For CCP, a double reciprocal plot of the initial velocity versus ferrocyanochrome *c* concentration shows a linear relationship at 100 μM H_2O_2 (data not shown). At pH 7.3 and 100 μM H_2O_2 , a $K_{m(\text{app})}$ for ferrocyanochrome *c* of 18.2 μM and a $k_{\text{cat}(\text{app})}$ of 175 s^{-1} are obtained for CCP (Table 3.2). A $K_{m(\text{app})}$ of 15.2 μM and a $k_{\text{cat}(\text{app})}$ of 209 s^{-1} at 170 μM $[\text{H}_2\text{O}_2]$ were recently reported for CCP (DePillis et al.,

1991). In contrast, Yonetani and Ray (1965) reported a $k_{\text{cat(app)}}$ of 1800 s^{-1} at $176 \mu\text{M}$ $[\text{H}_2\text{O}_2]$ at pH 6.0 with a different CCP preparation. At pH 4.0 and an H_2O_2 concentration of $100 \mu\text{M}$, LiP shows a $K_{\text{m(app)}}$ of $68 \mu\text{M}$ and a $k_{\text{cat(app)}}$ of 25.7 s^{-1} for ferrocyanochrome *c*. Although CCP/ H_2O_2 is a better catalyst of ferrocyanochrome *c* oxidation than LiP/ H_2O_2 , ferrocyanochrome *c* oxidation by LiP is significant. Indeed, LiP has a $K_{\text{m(app)}}$ of $113 \mu\text{M}$ and a $k_{\text{cat(app)}}$ of 19 s^{-1} for VA at $100 \mu\text{M}$ H_2O_2 (Table 3.1). The faster rate for ferrocyanochrome *c* oxidation may be explained in part by the lower redox potential of ferrocyanochrome *c* (0.26 V) vs. $\sim 1.5 \text{ V}$ for VA. However, VA oxidation to veratraldehyde requires 2 one-electron steps, which also accounts for the lower turnover number. The $K_{\text{m(app)}}$ for these two substrates suggest that the polymeric substrate may bind more strongly to the enzyme. We carried out additional experiments to characterize the binding of ferrocyanochrome *c* to LiP.

3.4.3 Effect of ionic strength

Ferrocyanochrome *c* oxidation by CCP is inhibited at high ionic strength (Kim et al., 1990). Detailed kinetic studies have shown that ionic strength has a strong effect on the binding interaction of ferrocyanochrome *c* with CCP compounds I and II, but not on compound I formation or the rate of electron transfer (Kim et al., 1990; Loo & Erman, 1975). The equilibrium dissociation constant for ferricytochrome *c* and native CCP is also dependent upon ionic strength (Erman & Vitello, 1980). These studies demonstrated a 1:1 binding between CCP and cytochrome *c* and suggest that an electrostatic interaction between CCP and cytochrome *c* is the rate-determining step (Kim et al., 1990; Loo & Erman, 1975; Erman & Vitello, 1980).

The initial velocity of ferrocyanochrome *c* oxidation by LiP/ H_2O_2 also decreases with increasing ionic strength. A plot of the logarithm of the initial rate versus the Debye-Hückel ionic strength function at pH 4.0 (Fig. 3.6) indicates that the rate-determining step(s) of this reaction depend upon ionic strength. These results suggest that electrostatic binding of LiP and cytochrome *c* is the rate-determining step. However, a direct interaction between the LiP heme and the polymeric substrate is ruled out by recent X-ray crystallographic studies of LiP (Edwards et al., 1993;

Poulos et al., 1993; Piontek et al., 1993) which show that the heme is buried and not available to interact directly with the substrate. This is supported by our previous results showing that the heme edge is not available for modification with aryl hydrazine (DePillis et al., 1990). All of these results suggest that protein surface electrostatic interaction between LiP and cytochrome *c* is required for the reaction. Involvement of an electrostatic surface interaction is consistent with the binding of these two proteins which would be oppositely charged in the pH range of 4.5-6.0. LiP isozymes have pIs of 3.2-3.9 (Leisola et al., 1987), and cytochrome *c* has a pI of 10.7 (Ferguson-Miller et al., 1979). Like LiP, CCP also is an acidic protein (Yonetani, 1967).

3.4.4 Cytochrome *c* binding site

Recent crystallographic and modeling studies suggest that LiP may have a VA binding site in an access channel near the buried heme (Poulos et al., 1993). If electrostatic surface interactions are involved in the binding of LiP to cytochrome *c*, then the sites for the two substrates would be distinct and VA oxidation by LiP should be inhibited by cytochrome *c* in a noncompetitive manner. In this study ferricytochrome *c* was utilized as an inhibitor. Although it is not a substrate for LiP the surface amino acids and charge which control the electrostatic binding are identical for ferri- and ferrocytochrome *c*.

The family of plots, $1/v$ versus $1/[VA]$ at various fixed concentrations of ferricytochrome *c* demonstrate a noncompetitive inhibition pattern (Fig. 3.7), suggesting that VA is oxidized at a site separate from the cytochrome *c* binding site. From the secondary plot of y -intercept versus [ferricytochrome *c*], the K_i for ferricytochrome *c* was determined to be $2.5 \mu\text{M}$ (Fig. 3.7, inset), demonstrating that it is an effective noncompetitive inhibitor of VA oxidation by LiP. Others have suggested that noncompetitive inhibition of VA oxidation by a terminal LiP substrate implies that VA is acting as a radical mediator in the reaction (Akamatsu et al., 1990; Popp et al., 1990). However, in this experiment, we have used ferricytochrome *c* which is not a substrate for LiP; therefore, the noncompetitive inhibition kinetics

strongly suggest the existence of different binding sites rather than a radical mediation mechanism, at least in this case. These kinetics are consistent with the assumption that cytochrome *c* is oxidized through surface interaction with LiP and that VA may be oxidized in a binding pocket relatively closer to the heme edge.

Ferrocycytochrome *c* also is oxidized by LiP/H₂O₂ in the absence of VA above pH 4.0. This electron transfer reaction most likely occurs via surface interaction of the two proteins. In this case, an electron relay system through amino acid residues is possibly involved as proposed for the CCP reaction (Pelletier & Kraut, 1992). X-ray crystallographic studies on CCP-cytochrome *c* complexes have suggested that the interaction between these proteins is highly specific (Pelletier & Kraut, 1992) and LiP may have a similar surface docking site for cytochrome *c*. Recently, it was been demonstrated that CCP oxidizes monomeric phenols at the buried heme edge whereas it interacts with ferrocycytochrome *c* on the surface of the protein (DePillis et al., 1991). A similar model could be proposed for LiP. However, the direct access of small aromatic substrates (such as VA) with the heme edge has not yet been demonstrated conclusively. Indeed, (i) aryl hydrazine modifies the heme edge of CCP but not of LiP (DePillis et al., 1990; 1991), and (ii) LiP has a narrower heme access channel than CCP (Poulos et al., 1993).

This is the first report of ferrocycytochrome *c* oxidation by LiP. Although ferrocycytochrome *c* has a lower redox potential than the phenolic groups and aromatic rings in lignin, this system may serve as a useful model for probing the mechanism of electron transfer between the buried heme of the enzyme and polymeric substrates. In particular, study of ferrocycytochrome *c* oxidation by LiP should aid our attempts to elucidate the stimulating role of VA in some LiP-catalyzed reactions. Manganese peroxidase also is capable of oxidizing ferrocycytochrome *c*, but this reaction is strictly dependent upon the presence of Mn^{II} (unpublished). Manganese peroxidase does not oxidize cytochrome *c* directly; rather the substrate is oxidized by Mn^{III} chelator complexes generated by the enzyme (Glenn et al., 1986). Thus, LiP oxidizes cytochrome *c* through a direct interaction, and this reaction is stimulated by VA at low pH and high [H₂O₂]. In contrast, manganese peroxidase oxidizes cytochrome *c*

through the redox mediation of a diffusible Mn^{III} complex. These observations may reflect the mechanisms used by these two peroxidases in the oxidation of polymeric lignin.

Further spectral, kinetic, and structural studies aimed at probing the role of VA in this reaction are planned.

CHAPTER 4
IRREVERSIBLE OXIDATION OF FERRICYTOCHROME *c*
BY LIGNIN PEROXIDASE*

4.1 Introduction

White-rot basidiomycetous fungi are primarily responsible for initiating the depolymerization of lignin in wood, which is a key step in the earth's carbon cycle (Buswell & Odier, 1987; Kirk & Farrell, 1987; Gold et al., 1989). The best-studied lignin-degrading fungus, *Phanerochaete chrysosporium*, secretes two extracellular heme peroxidases, manganese peroxidase and lignin peroxidase (LiP),** which, along with an H₂O₂-generating system, are apparently the major extracellular components of its lignin degradative system (Buswell & Odier, 1987; Kersten & Kirk, 1987; Kirk & Farrell, 1987; Gold et al., 1989; Higuchi, 1990; Schoemaker, 1990; Hammel et al., 1993). Nucleotide sequences of a number of LiP cDNA and genomic clones (Tien & Tu, 1987; Smith et al., 1988; Ritch et al., 1991; Gold & Alic, 1993), as well as several LiP crystal structures (Edwards et al., 1993; Piontek et al., 1993; Poulos et al., 1993), demonstrate that important peroxidase catalytic residues, including the proximal and distal His, the distal Arg, and an H-bonded Asp, are all conserved within the heme pocket of LiP. Furthermore, neither Lip nor MnP contain Try residues (Tien & Tu, 1987; Smith et al., 1988; Ritch et al., 1991; Gold & Alic, 1993). The crystal structure also indicates that the heme of LiP is buried and therefore unavailable for direct interaction with polymeric substrates such as lignin.

* Reprinted with permission from: Sheng, D. and Gold, M. H. (1998) Irreversible Oxidation of Ferricytochrome *c* by Lignin Peroxidase. *Biochemistry* 37, 2029-2036. Copyright 1998 American Chemical Society.

** Abbreviations: Cc²⁺, ferrocycytochrome *c*; Cc³⁺, ferricytochrome *c*; HPLC, high performance liquid chromatography; HRP, horseradish peroxidase; LiP, lignin peroxidase.

The mechanism of long-range electron transfer between the heme of LiP and polymeric substrates has not been fully elucidated.

Veratryl (3,4-dimethoxybenzyl) alcohol (VA), a secondary metabolite secreted by *P. chrysosporium*, stimulates the rates of LiP-catalyzed oxidations of synthetic lignin and other polymers (Hammel et al., 1993; Wariishi et al., 1994) and a variety of non-phenolic lignin model compounds and aromatic pollutants (Hammel et al., 1986; Valli et al., 1992a,b; Joshi & Gold, 1994) whose redox potentials are beyond the reach of other plant and fungal peroxidases. However, the mechanism of VA stimulation of LiP reactions is still unresolved. To explore the possible role of VA in long-range electron transfer reactions by LiP, we are examining the LiP oxidation of model polymeric substrates. Previously, we used ferrocyclochrome *c* (Cc^{2+}) as a model polymeric substrate and demonstrated that LiP oxidizes Cc^{2+} to ferricyclochrome *c* (Cc^{3+}). We also observed that Cc^{3+} is a non-competitive inhibitor of VA oxidation by LiP (Wariishi et al., 1994). This inhibition led us to examine the possible oxidation of Cc^{3+} by LiP. Herein, we demonstrate that, in the presence of VA, LiP catalyzes irreversible oxidative damage to Cc^{3+} , and VA appears to act as a redox mediator in the reaction. SDS-PAGE and amino acid analyses indicate that Cc^{3+} oxidation is accompanied in part by dimerization of the substrate, presumably mediated by the intermolecular coupling of Tyr residues in the protein.

4.2 Experimental Procedures

4.2.1 Protein preparation

LiP isoenzyme 2 (H8) was purified from cultures of *P. chrysosporium* strain OGC101 as previously described (Gold et al., 1984; Wariishi & Gold, 1990). The purified enzyme was electrophoretically homogeneous and had an R_z value (A_{408}/A_{280}) of 5.0. The enzyme concentration was determined at 408 nm using an extinction coefficient of $133 \text{ mM}^{-1} \text{ cm}^{-1}$ (Gold et al., 1984). Horse heart Cc^{3+} , horseradish peroxidase (HRP), and glucose oxidase were obtained from Sigma. Cytochrome *c* peroxidase (CcP) was generously provided by Grant Mauk (University of British Columbia, Vancouver, Canada). Cc^{2+} was prepared by adding excess sodium

dithionite to Cc^{3+} in water as described (Kang & Erman, 1982; Wariishi et al., 1994). Excess sodium dithionite was removed by gel filtration on a Sephadex G-10 column with argon-saturated 10 mM potassium sulfate as the eluant. The concentrations of Cc^{3+} and Cc^{2+} were determined using extinction coefficients of $106 \text{ mM}^{-1} \text{ cm}^{-1}$ at 410 nm and $27 \text{ mM}^{-1} \text{ cm}^{-1}$ at 550 nm, respectively (Margoliash & Frowirt, 1959).

4.2.2 Chemicals

H_2O_2 (30% solution) was obtained from Sigma and the concentrations of stock solutions were determined as described (Cotton & Dunford, 1973). VA was obtained from Aldrich and purified by silica gel column chromatography (ethyl acetate:hexane, 1:1, v:v) before use. All other chemicals were reagent grade. All solutions were prepared using deionized water from a Milli-Q 50 system (Millipore).

4.2.3 Spectrophotometric measurements

The oxidations of Cc^{3+} and VA were measured at room temperature with a Shimadzu UV-260 spectrophotometer in cells with a 1-cm light path. Reaction mixtures for Cc^{3+} oxidation contained Cc^{3+} ($10 \mu\text{M}$), LiP [$1 \mu\text{g/ml}$ ($0.024 \mu\text{M}$) or as indicated], with or without VA ($500 \mu\text{M}$), in 20 mM sodium succinate, pH 3.0 or as indicated in the legends to the figures. The ionic strength was adjusted with potassium sulfate. The reactions were initiated by the addition of H_2O_2 ($100 \mu\text{M}$). The rate of Cc^{3+} oxidation was determined by following the decrease in absorbance at 408 nm, the Soret maximum. Cc^{2+} oxidations were carried out as described previously (Wariishi et al., 1994). LiP oxidations of VA to veratraldehyde were performed as described previously and followed at 310 nm (extinction coefficient, $9.3 \text{ mM}^{-1} \text{ cm}^{-1}$) (Kirk & Farrell, 1987; Gold et al., 1989). CcP and HRP reactions with Cc^{3+} were carried out at both pH 3.0 (sodium succinate, 20 mM) and pH 7.0 (sodium phosphate, 20 mM) containing Cc^{3+} ($10 \mu\text{M}$), H_2O_2 ($100 \mu\text{M}$), and enzymes ($10 \mu\text{g/ml}$).

4.2.4 Atomic absorption spectrometry

A Perkin-Elmer 630 atomic absorbance spectrometer was used to determine the protein-bound iron at 249 nm, using ferrous chloride as a standard. Reaction mixtures (7 ml), as described above, were incubated at room temperature for 15 min. Aliquots (1 ml) were removed to measure the decrease in the Soret band; the remaining 6 ml were concentrated and washed with water by ultrafiltration (Amicon-10) and analyzed by atomic absorption spectrometry for protein-bound iron.

4.2.5 LiP inactivation by H₂O₂

Reaction mixtures consisted of LiP (100 µg/ml, ~2.4 µM) and H₂O₂ (100 µM) in 20 mM sodium succinate, pH 3.0. Reactions were carried out at 25°C, with or without VA and/or Cc³⁺, as indicated. Aliquots (20 µl) were removed at intervals, and LiP activity was assayed using VA (5 mM) and H₂O₂ (100 µM) in 20 mM sodium succinate, pH 3.0, as previously described (Kirk & Farrell, 1987; Gold & Alic, 1993).

4.2.6 HPLC analysis of veratraldehyde formation

High-performance liquid chromatography (HPLC) was carried out with an HP Lichrospher 100 RP-18 column. Veratraldehyde formation was analyzed at 280 nm using a linear gradient of acetonitrile in 0.05% phosphoric acid (0–50% over 22 min). The veratraldehyde was quantitated using a calibration curve obtained with a standard.

4.2.7 SDS-PAGE

Reaction mixtures (1 ml), as described above, were incubated at room temperature for 15 min. The reaction mixtures were concentrated to 100 µl by ultrafiltration (Amicon-10) and aliquots (20 µl) were analyzed by SDS-PAGE (Mini-PROTEIN, BioRad) (Laemmli, 1970).

4.2.8 Isolation and amino acid analysis of Cc³⁺ reaction products

Reaction mixtures, as described above, were concentrated by ultrafiltration to a final volume of 500 µl, heated in loading buffer without 2-mercaptoethanol, and

subjected to SDS-PAGE. The SDS-PAGE pattern for native Cc^{3+} is essentially identical whether heated in the presence or absence of 2-mercaptoethanol (data not shown). The monomer and dimer bands were cut from the gel, and the proteins were eluted in Tris-glycine buffer, pH 8.0, and dialyzed exhaustively against deionized water. Amino acid analysis was performed at the Beckman Institute, Stanford University, Stanford, CA.

4.3 Results

4.3.1 Cc^{3+} oxidation by LiP

Fig. 4.1 shows the oxidation of Cc^{3+} by LiP in the presence of H_2O_2 (100 μM) and VA (500 μM). Bleaching of the Cc^{3+} Soret band was observed, but there were no major shifts in the peaks. The absorbance at 695 nm, indicative of the iron-sulfur bond in Cc^{3+} (Ivanetich et al., 1976), also did not shift (data not shown). In the absence of VA, Cc^{3+} was oxidized at a very slow rate either in the presence of H_2O_2 alone or in the presence of LiP plus H_2O_2 (Fig. 4.2). In contrast, in the presence of 100 μM VA, the rate of Cc^{3+} oxidation by LiP was approximately 12-fold faster (Fig. 4.2A). Under similar conditions, neither CcP nor HRP was able to oxidize Cc^{3+} either at pH 3.0 or 7.0 (data not shown). In the presence of VA, the initial rate of Cc^{3+} oxidation by LiP increased with increasing LiP concentrations between 0.5 and 6.0 $\mu g/ml$ (Fig. 4.2B). Within the pH range of 2.5 to 6.0, the initial rate of Cc^{3+} oxidation in the presence of LiP and VA decreased with increasing pH. Likewise, the initial rate of LiP-catalyzed VA oxidation to veratraldehyde decreased with increasing pH (Fig. 4.3), confirming our earlier work (Renganathan et al., 1987).

The results of atomic absorption spectrometric analysis indicated that approximately 50% of the iron was released from Cc^{3+} following a 15-min incubation with LiP, H_2O_2 (100 μM), and VA (500 μM). Similarly, there was a decrease of approximately 60% in the intensity of the Cc^{3+} Soret band. If the reaction was carried out in either the absence of VA or the absence of LiP, neither a significant loss in the iron content nor a decrease in the Soret band of Cc^{3+} was observed (Table 4.1; Fig. 4.2).

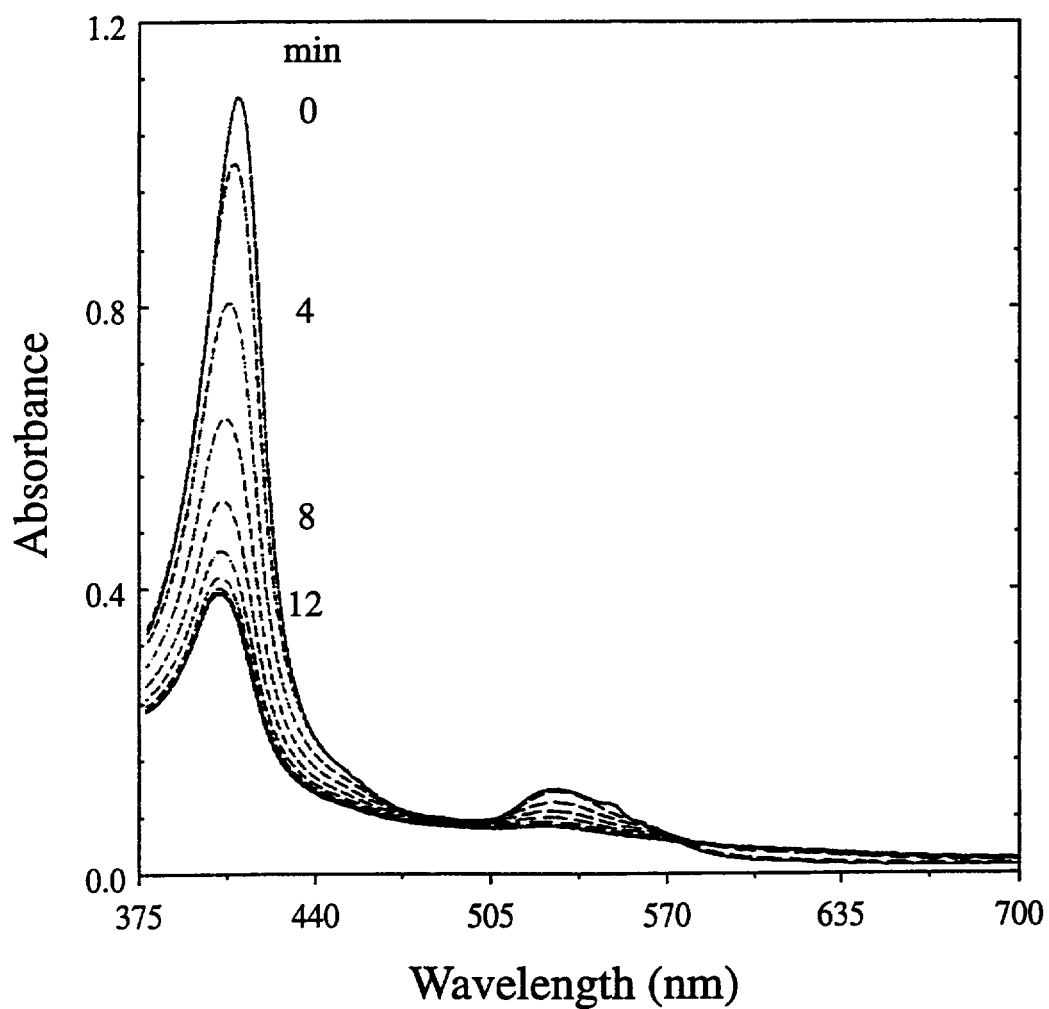


Fig. 4.1 Cc^{3+} oxidation by LiP. Electronic absorption spectra were recorded at 2-min intervals. Reaction mixture consisted of Cc^{3+} ($10 \mu\text{M}$), LiP ($1 \mu\text{g/ml}$), and VA ($500 \mu\text{M}$) in 20 mM sodium succinate, pH 3.0. The reaction was initiated by the addition of H_2O_2 ($100 \mu\text{M}$).

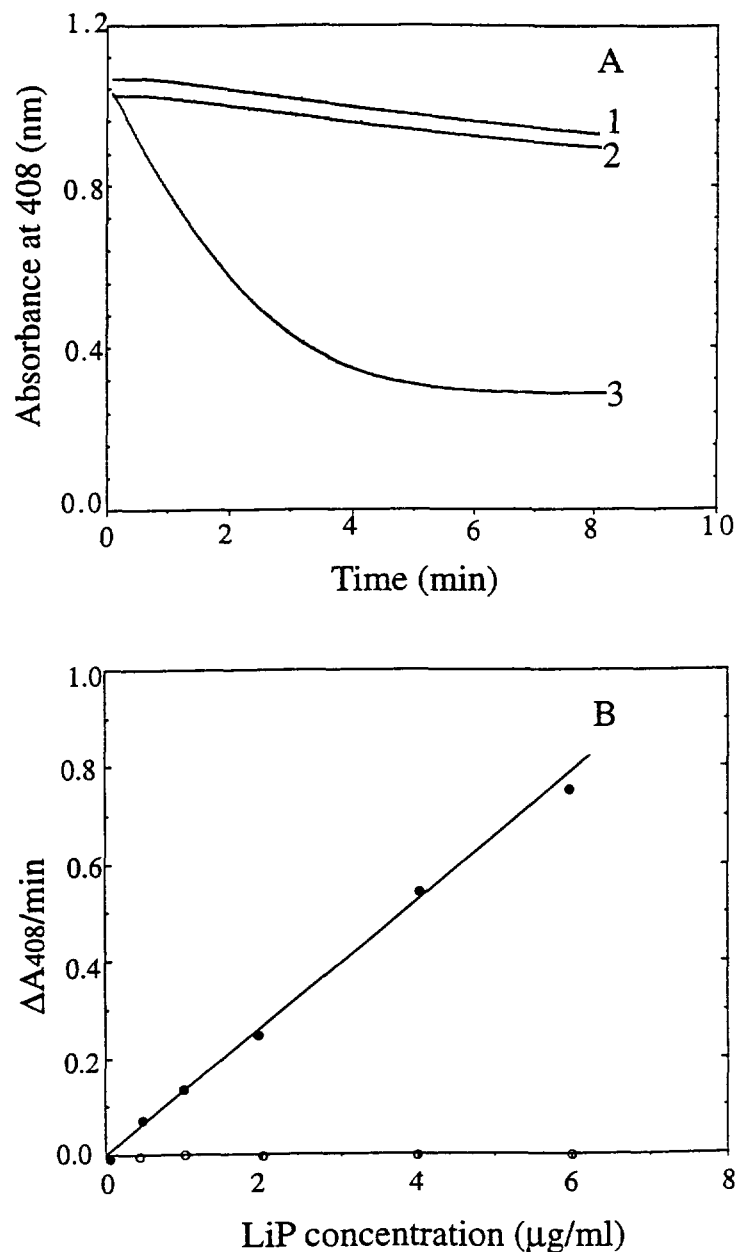


Fig. 4.2 Effect of VA and enzyme concentration on the oxidation of Cc^{3+} . Reactions were monitored by following the decrease in absorbance at 408 nm. (A) All reactions contained Cc^{3+} ($10 \mu\text{M}$) in 20 mM sodium succinate, pH 3.0. Trace 1, H_2O_2 ($100 \mu\text{M}$); trace 2, H_2O_2 ($100 \mu\text{M}$) and LiP ($1 \mu\text{g}/\text{ml}$); trace 3, H_2O_2 ($100 \mu\text{M}$), LiP ($1 \mu\text{g}/\text{ml}$), and VA ($500 \mu\text{M}$). (B) The initial rates of Cc^{3+} oxidation at various LiP concentrations. Reactions contained Cc^{3+} ($10 \mu\text{M}$), LiP (as indicated), and H_2O_2 ($100 \mu\text{M}$) in 20 mM sodium succinate, pH 3.0, with (●) or without (○) VA ($500 \mu\text{M}$).

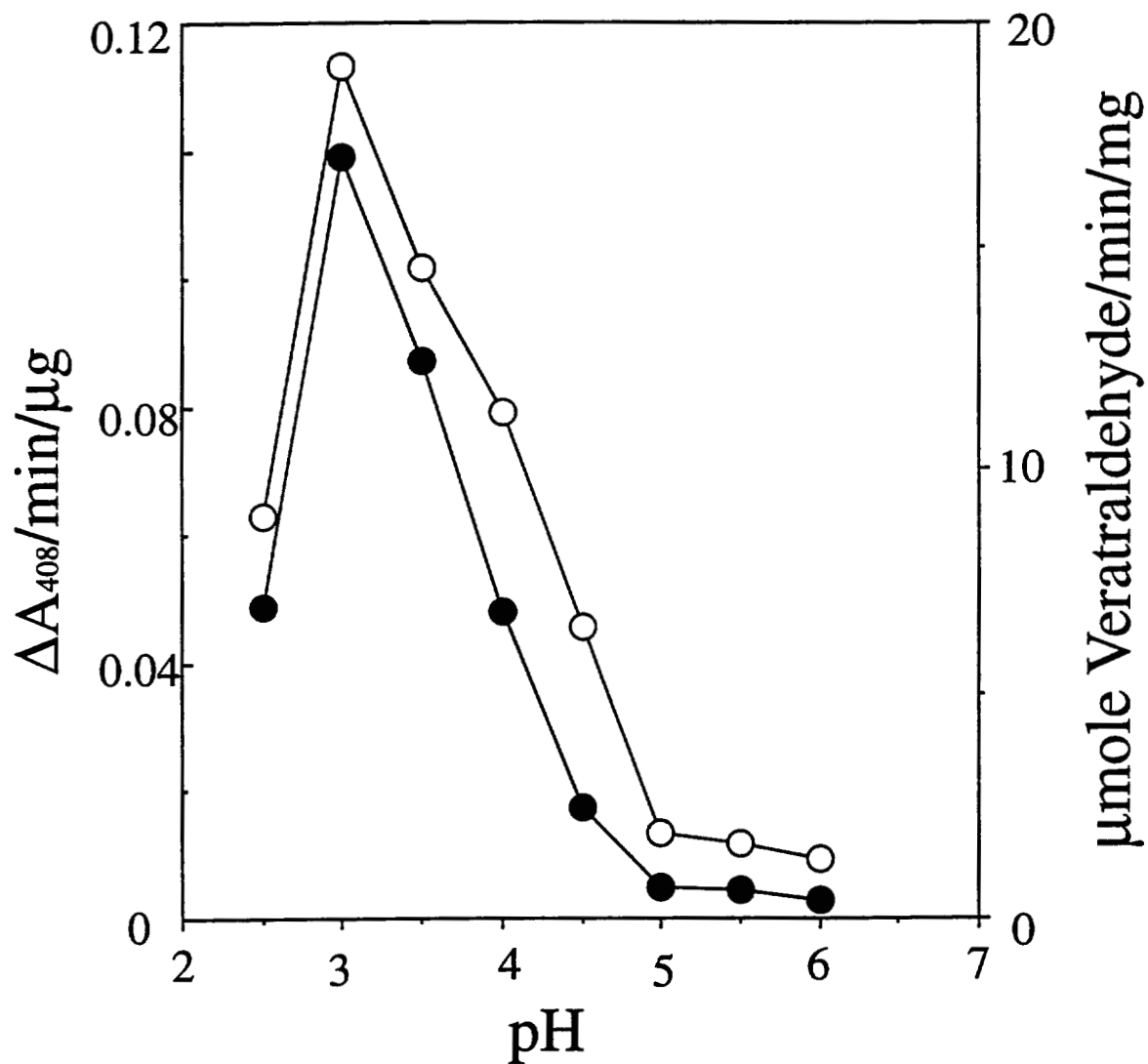


Fig. 4.3 pH dependence of the oxidation of Cc^{3+} and VA. Cc^{3+} oxidation reactions (●) contained Cc^{3+} ($10 \mu M$), H_2O_2 ($100 \mu M$), VA ($500 \mu M$), and LiP ($1 \mu g/ml$) in 20 mM sodium succinate at the indicated pH. VA oxidation reactions (○) contained VA ($500 \mu M$), H_2O_2 ($100 \mu M$), and LiP ($1 \mu g/ml$) in 20 mM sodium succinate at the indicated pH.

Table 4.1
Fe Content and Soret Absorbance of Cc^{3+}

Reaction components ^a	Cc^{3+}	Cc^{3+} , H_2O_2	Cc^{3+} , LiP, H_2O_2	Cc^{3+} , LiP, H_2O_2 , VA
Soret absorbance	100 ^b	96	100	40
Fe content	100 ^c	97	104	56

^a Reactions were as described in the text.

^b Iron concentrations were normalized to 100 for the control with Cc^{3+} alone.

^c Soret absorbance (in parentheses) was normalized to 100 for the control with Cc^{3+} alone.

The oxidation of Cc^{3+} was strictly dependent on the presence of VA at H_2O_2 concentrations of $7.5 \mu M$ or higher (Fig. 4.4). Furthermore, at higher concentrations of H_2O_2 , more VA was required to attain maximal oxidation of Cc^{3+} . For example, in the presence of $100 \mu M H_2O_2$ and $10 \mu M Cc^{3+}$, approximately $500 \mu M$ VA was required to obtain maximal activity. However, even VA concentrations as high as $1 mM$ did not inhibit the oxidation of $10 \mu M Cc^{3+}$ (Fig. 4.4).

The effects of Cc^{3+} and VA on the H_2O_2 -induced inactivation of LiP also were investigated directly (Fig. 4.6). When LiP ($2.4 \mu M$) was incubated with $100 \mu M H_2O_2$ at pH 3.0 and $25^\circ C$, almost all LiP activity was lost within 30 min. Although $20 \mu M$ VA did not prevent this inactivation, essentially all of the LiP activity was retained at $500 \mu M$ VA. Likewise, in the presence of $20 \mu M Cc^{3+}$ alone, 70% of the LiP activity was lost within 30 min. However, in the presence of $100 \mu M H_2O_2$, $20 \mu M Cc^{3+}$, and $20 \mu M$ VA, maximal LiP activity was retained after 30 min. In the presence of $20 \mu M Cc^{3+}$, as little as $5 \mu M$ VA protected LiP from inactivation by H_2O_2 to a significant extent (Fig. 4.6).

4.3.2 HPLC analysis of VA oxidation

The LiP oxidation of VA to veratraldehyde in the presence and absence of Cc^{3+} and Cc^{2+} was measured by HPLC. When the ratio of VA to Cc^{3+} in the reaction was high (500:10 nmole), only 7 nmole of veratraldehyde was formed after 15 min, as compared with 110 nmole formed in the absence of Cc^{3+} . In addition, only trace amounts of veratraldehyde (< 0.1 nmole) were formed at a lower ratio of VA to Cc^{3+} (50:10 nmole) (Table 4.2). No veratraldehyde formation was detected from 500 nmole VA during the complete oxidation of 20 nmole of Cc^{2+} (Table 4.2).

4.3.3 Dimerization of Cc^{3+}

SDS-PAGE experiments indicated that, in the presence of VA, LiP oxidatively polymerized some of the Cc^{3+} molecules. As shown in Fig. 4.6, SDS-PAGE analysis of the reaction products obtained from the LiP oxidation of Cc^{3+} , in the presence but not in the absence of VA, revealed a 26.6-kD protein, corresponding in size to the dimer form of Cc^{3+} . In addition to the Cc^{3+} oxidized monomer, trace amounts of

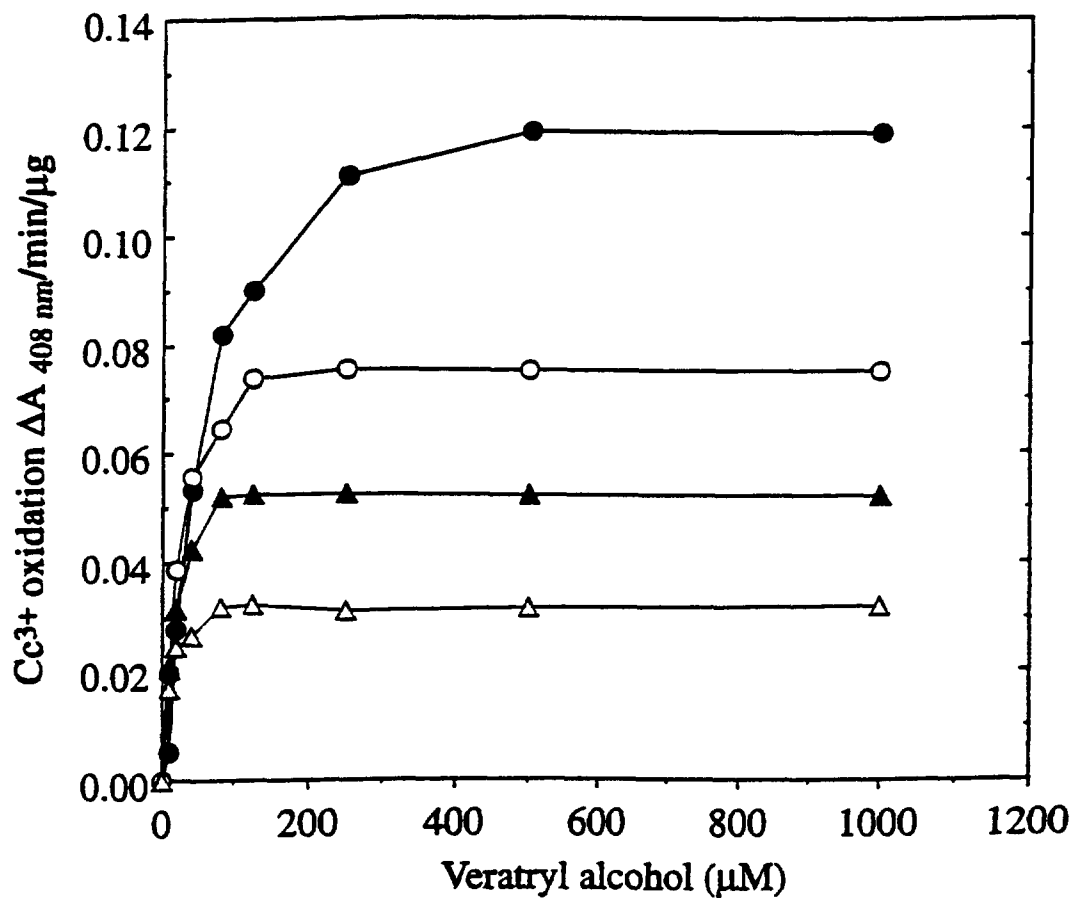


Fig. 4.4 Effect of H₂O₂ concentration on the stimulation of Cc³⁺ oxidation by VA. Reaction mixtures contained LiP (1 μg/ml), VA (as indicated), and Cc³⁺ (10 μM) in 20 mM sodium succinate, pH 3.0. Reactions were initiated by the addition of H₂O₂ to a final concentration of 7.5 (Δ), 15 (▲), 30 (○) and 100 (●) μM, and Cc³⁺ oxidation was monitored by following the decrease in absorbance at 408 nm, as described in the text.

Table 4.2
Veratraldehyde Formation in Reactions Containing Cc^{3+} or Cc^{2+} ^a

Time (min)	VA: 500 nmole		VA: 50 nmole		VA: 500 nmole	
	Cc^{3+} (10 nmole)		Cc^{3+} (10 nmole)		Cc^{2+} (20 nmole)	
	+	-	+	-	+	-
1	2	20	<0.1	5	0	20
4	5	50	<0.1	13	0	50
10	6	90	<0.1	23	0	90
15	7	110	<0.1	30	0	110

^a Reactions contained LiP (1 μ g/ml), H_2O_2 (100 μ M), and VA (50 or 500 nmole, as indicated), with or without Cc^{3+} (10 nmole) or Cc^{2+} (20 nmole), in 20 mM sodium succinate, pH 3.0. Veratraldehyde formation was measured by HPLC at the indicated times as described in the text.

products corresponding in molecular weight to a Cc^{3+} trimer and tetramer also were observed (Fig. 4.6, lane 4). To examine further the dimerization of Cc^{3+} , amino acid analysis was carried out on native Cc^{3+} , on native Cc^{3+} eluted from SDS-PAGE, and on the monomeric and dimeric reaction products of the LiP oxidation of Cc^{3+} eluted from SDS-PAGE (Table 4.3). Comparison of the amino acid content of the reaction products from the LiP oxidation of Cc^{3+} , with those of the native Cc^{3+} proteins and with the theoretical amino acid composition of Cc^{3+} (Bushnell et al., 1990), indicated that the Met and Tyr content decreased in the monomeric and dimeric oxidized products, but that the amino acid compositions of both products were otherwise similar to native Cc^{3+} . In the oxidized monomeric product, the Met content was reduced by 25%, and in the dimeric product the Met content was reduced by 65% with respect to native Cc^{3+} . Methionine sulfoxide was found in the oxidized monomer, and methionine sulfoxide and methionine sulfone were detected in the oxidized dimer by amino acid analysis (data not shown). The Tyr content decreased by 50% in the oxidized monomeric product and by 83% in the oxidized dimeric product. There also was a slight decrease in the Tyr content of native Cc^{3+} recovered from SDS-PAGE, probably due to auto-oxidation during electrophoretic separation (Table 4.3).

4.4 Discussion

LiP is a well-characterized heme peroxidase that is secreted by *P. chrysosporium* under ligninolytic conditions (Buswell & Odier, 1987; Kersten & Kirk, 1987; Kirk & Farrell, 1987; Gold et al., 1989; Higuchi, 1990; Schoemaker, 1990; Gold & Alic, 1993; Hammel et al., 1993). Considerable work has been reported on the structure and mechanism of LiP (Harvey et al., 1986; Valli et al., 1990; Wariishi & Gold, 1990; Wariishi et al., 1990; Gold & Alic, 1993; Koduri & Tien, 1994; Harvey et al., 1995; Koduri et al., 1996; Sutherland et al., 1996; Tien & Ma, 1997). In particular, the crystal structure reveals that the heme of LiP is buried (Edwards et al., 1993; Piontek et al., 1993; Poulos et al., 1993) and, therefore, unavailable for direct interaction with polymeric substrates such as lignin. It has been suggested that

Table 4.3
Amino Acid Analysis of Native Cc³⁺ and Cc³⁺ Oxidation Products

Amino acid	Theoretical ^a	Native Cc ³⁺ ^b	Native Cc ³⁺ ^c	Monomeric product ^d	Dimeric product ^e
Asx	8	7.9	8.2	8.1	8.1
Thr	10	9.3	9.4	9.8	9.1
Glx	12	12.5	12.4	12.5	11.7
Pro	4	4.2	4.1	4.1	4.1
Gly	12	11.6	12.2	12.4	12.6
Ala	6	5.8	6.1	6.0	6.0
Cys	2	nd ^f	nd	nd	nd
Val	3	2.8	3.1	3.1	3.1
<u>Met</u>	2	1.9	1.8	1.5	0.7
Ile	6	6.0	6.4	6.2	6.1
Leu	6	5.5	5.9	5.8	5.3
<u>Tyr</u>	4	3.9	3.5	2.0	0.7
Phe	4	4.0	4.1	4.0	3.7
His	3	3.8	5	4.7	5.6
Lys	19	16	15.9	15.8	15.0
Trp	1	nd	nd	nd	nd
Arg	2	2.0	2.2	2.2	2.2

^a Theoretical amino acid composition.

^b Native Cc³⁺.

^c Native Cc³⁺ eluted from SDS-PAGE.

^d Oxidized Cc³⁺ monomer eluted from SDS-PAGE.

^e Oxidized Cc³⁺ dimer eluted from SDS-PAGE. The amino acid yields were divided by two to correlate with values for the monomer.

^f nd = not determined.

the mechanism of LiP may involve long-distance electron transfer between the heme and substrate at the protein surface (Wariishi et al., 1994). It also has been proposed that LiP oxidizes polymeric substrates via a diffusible oxidized intermediate, the VA cation radical (Harvey et al., 1986, 1987; Akamatsu et al., 1990).

P. chrysosporium produces VA under ligninolytic conditions. VA is a substrate for LiP and also stimulates the LiP-catalyzed depolymerization of synthetic lignin (Hammel et al., 1993) and the oxidation of a variety of recalcitrant aromatic substrates (Renganathan et al., 1985; Haemmerli et al., 1986; Harvey et al., 1986; Valli et al., 1992a; Joshi & Gold, 1993, 1994); however, the precise role(s) of VA in the mechanism of LiP remain to be clarified. It has been reported that VA protects LiP from irreversible inactivation by excess H₂O₂, both by reducing LiP compound II, thereby preventing the formation of compound III, and by directly converting LiP compound III* back to the native enzyme (Valli et al., 1990; Wariishi & Gold, 1990; Wariishi et al., 1990). It also has been reported that VA is obligatory for reducing LiP compound II, thus preventing LiP compound II from reacting with H₂O₂ to form LiP compound III (Valli et al., 1990; Paszcynski & Crawford, 1991; Koduri & Tien, 1994). In addition, it has been proposed that VA functions as a diffusible mediator, wherein the cation radical produced via the one-electron oxidation of VA diffuses away from the active site of LiP and oxidizes the terminal substrate at a distance from the enzyme surface (Harvey et al., 1986, 1987; Akamatsu et al., 1990); however, no direct proof for this diffusible mediator hypothesis has been reported. In contrast, recent chemical and spectroscopic evidence argues against the diffusible mediator hypothesis, indicating that the VA cation radical is too short-lived to diffuse away from the enzyme active site and oxidize the terminal substrate (Joshi & Gold, 1996; Khindaria et al., 1995, 1996). For example, the LiP oxidation of dimethoxytoluene leads to dimer formation via the coupling of a cation radical with a neutral species. In contrast, the LiP oxidation of VA does not lead to dimer formation, strongly suggesting that the VA cation radical loses a benzylic proton extremely rapidly (Joshi & Gold, 1996). In addition, fast-flow electron spin resonance studies indicate that the free VA cation radical is very unstable ($t_{1/2} \sim 0.6$ ms), whereas the enzyme-bound VA cation radical is much more stable ($t_{1/2} \sim 370$ ms) (Khindaria et al., 1995, 1996).

Another possibility exists for the mechanism of VA activation of LiP. VA could act as an enzyme-bound redox cofactor, essentially as was reported recently for Trp191 of CcP (Hahm et al., 1994; Liu et al., 1994; Miller et al., 1994a,b).

We have been studying the involvement of VA in the LiP oxidation of model polymeric substrates. Previously, we demonstrated that LiP oxidizes Cc^{2+} to Cc^{3+} in the presence and absence of VA (Wariishi et al., 1994). However, the redox potential of the Cc^{2+}/Cc^{3+} couple (250 mV) is low compared to that required for lignin oxidation. Therefore, in this study we have examined the involvement of VA in the LiP-catalyzed oxidation of Cc^{3+} .

4.4.1 LiP-catalyzed bleaching of Cc^{3+}

The results shown in Figs. 4.1 and 4.2A demonstrate that LiP oxidation of Cc^{3+} , in the presence of H_2O_2 and VA, is accompanied by a decrease in the Soret band at 408 nm. Atomic absorption spectrometric analysis (Table 4.1) demonstrates that this decrease in the Soret, representing the bleaching of the heme in Cc^{3+} , is accompanied by a loss of iron from the protein.

Several factors could be contributing to the loss of the iron from the heme. First, all of the bands in the Cc^{3+} absorption spectrum decrease without observable wavelength shifting. This suggests that the porphyrin itself is being oxidatively cleaved. If the iron was lost from an intact porphyrin, some shift in the spectrum might be expected. Second, the iron in Cc^{3+} is low spin and hexacoordinated with the sulfur of Met80 as the sixth ligand; thus the iron does not readily react with H_2O_2 to form higher redox states as occurs in the peroxidase catalytic cycle (Dunford & Stillman, 1976). In addition, the heme in Cc^{3+} is covalently attached to the protein by thioether bridges to two cysteine residues (Bushnell et al., 1990). Our amino acid analysis of the oxidized monomer and dimer of Cc^{3+} detects oxidized Met and Tyr residues with no other significant changes in the amino acid composition (Table 4.3). Methionine sulfoxide is found in the oxidized monomer, and both methionine sulfoxide and methionine sulfone are found in the oxidized dimeric product. However, the formation of methionine sulfoxide may not be directly responsible for the bleaching, since Cc^{3+} with Met80 sulfoxide as the sixth ligand exhibits an increase

in the extinction coefficient of the Soret band, as compared with native Cc^{3+} (Ivanetich et al., 1976). Furthermore, the presence of Met80 sulfoxide should be associated with a decrease in the absorbance at 695 nm, since the 695-nm absorbance is believed to be indicative of Met coordination to the heme (Ivanetich et al., 1976). In contrast, the Soret intensity of LiP-oxidized Cc^{3+} decreases (Fig. 4.1), and the 695-nm absorption remains unchanged (data not shown). In addition to porphyrin oxidation, the formation of Met sulfone could partially explain the heme bleaching, since the fully oxidized form of Met80 would not be a ligand for the iron. Third, oxidation of Tyr also might result in heme bleaching. The formation of Tyr radicals from either free Tyr or Tyr residues in certain proteins is known (Amado et al., 1984). In addition, Catalano et al. (1989) have demonstrated that in myoglobin a H_2O_2 -generated Tyr103 radical couples with the meso carbon of the heme prosthetic group. The distance between Tyr103 and the heme meso carbon in myoglobin is about 6 Å. The distance between the only buried Tyr (Tyr67) and the heme meso carbon in Cc is between 4.5 and 6 Å, depending on the orientation (Bushnell et al., 1990); thus, a similar reaction between a Tyr radical and the heme might occur in Cc^{3+} . The formation of a Tyr-heme adduct may distort the heme environment and result in the release of iron and bleaching of the heme. Additional work is required to elucidate the exact chemical mechanism of heme bleaching in this reaction.

The nonenzymatic reaction between Cc^{3+} and H_2O_2 (Fig. 4.2A) has been reported previously (Florence, 1985). It is believed to involve the direct reaction between the heme iron of Cc^{3+} and H_2O_2 , forming a bound hydroxy radical. The latter and H_2O_2 react with the porphyrin to generate carbon monoxide and liberate oxygen, leading to the opening of the porphyrin ring and loss of the Soret absorbance (Florence, 1985). However, to obtain a nonenzymatic reaction rate, as measured by the decrease in the Soret, that is equivalent to the reaction rate obtained in the presence of LiP and VA (Fig. 4.2) would require 15 mM H_2O_2 (Florence, 1985), whereas the LiP reactions contain only 100 μ M H_2O_2 . Furthermore, in the presence of VA, the initial rate of Cc^{3+} oxidation increases with increasing LiP concentration (Fig. 4.2B). Finally, oxygen evolution is not observed following the LiP-catalyzed

oxidation of Cc^{3+} (data not shown), indicating that the oxidation of Cc^{3+} observed here is due to LiP and not to a nonenzymatic reaction between Cc^{3+} and H_2O_2 .

4.4.2 Effects of VA on the LiP-catalyzed oxidation of Cc^{3+}

In previous studies we demonstrated that VA stimulates the LiP-catalyzed oxidation of Cc^{2+} only at low pH and relatively high concentrations of H_2O_2 , indicating that, in these experiments, VA is stimulating the reaction by rescuing LiP from inactivation by H_2O_2 at low pH (Wariishi & Gold, 1990; Wariishi et al., 1990, 1991a, 1994). However, the LiP-catalyzed oxidation of Cc^{3+} is strictly dependent on the presence of VA in the pH range of 2.5–6.0 at a H_2O_2 concentration of 100 μM (Fig. 4.2). The redox potential required for Cc^{2+} oxidation (250 mV) is far lower than that required for tyrosine oxidation, which partially explains why VA is required for Cc^{3+} oxidation but not for Cc^{2+} oxidation. The results in Fig. 4.4 demonstrate that, even at H_2O_2 concentrations as low as 7.5 μM , the rate of Cc^{3+} oxidation is strictly dependent on the presence of VA. Furthermore, at higher H_2O_2 concentrations, increasing amounts of VA are required for maximal Cc^{3+} oxidation. This suggests that the H_2O_2 is being consumed during the reaction and that more VA is required to consume higher concentrations of H_2O_2 . Finally, the results in Fig. 4.4 demonstrate that concentrations of VA as high as 1 mM do not inhibit the rate of Cc^{3+} oxidation, suggesting that VA does not compete with Cc^{3+} for a binding site on LiP, nor is VA specifically reducing LiP compound II. Rather, the oxidation of VA is required as an intermediate step in the oxidation of Cc^{3+} .

As with CcP oxidation of Cc^{2+} (Kang & Erman, 1982), the initial rate of LiP oxidation of Cc^{2+} decreases with increasing ionic strength (Wariishi et al., 1994), implying that an electrostatic interaction between LiP and Cc may be a rate-limiting step in the reaction. At any rate, it implies some interaction between the acidic LiP protein and the basic Cc protein (Koppenol & Margoliash, 1982; Wariishi et al., 1994).

The steady-state kinetic parameters shown in Table 4.4 indicate that the rates of oxidation of Cc^{2+} and VA are similar even though a direct interaction between the heme of LiP and the polymeric Cc^{2+} is not possible. In contrast, computational

Table 4.4
 Steady-State Kinetic Parameters
 for the LiP Oxidation of Cc^{2+} , Cc^{3+} , and VA^a

Substrates	$K_{m \text{ app}}$ (μM)	k_{cat} (s^{-1})	$k_{\text{cat}}/K_{m \text{ app}}$ ($\text{M}^{-1} \text{s}^{-1}$)	Reference
Cc^{2+}	68	25	3.7×10^5	15
Cc^{2+} , VA	1.4	40	2.8×10^7	this work
Cc^{3+} , VA	0.4	1	2.5×10^6	this work
VA	113	19	1.6×10^5	15

^a Reaction conditions were as described in the text and in Wariishi et al. (1994).

modeling indicates that VA binds close to the heme (Poulos et al., 1993). This suggests that the fast oxidation rate with Cc^{2+} is likely due to the lower redox potential of the Cc^{2+}/Cc^{3+} couple (250 mV) as compared with that of VA (1.45 V) (Fawer et al., 1991). However, the highest rates of Cc^{2+} oxidation occur in the presence of VA. In particular, the $K_{m\text{ app}}$ for Cc^{2+} oxidation decreases by ~ 50 -fold in the presence of VA. In addition, we calculate that the second-order rate constant for Cc^{2+} oxidation in the presence of VA is $\sim 2.8 \times 10^7 \text{ M}^{-1} \text{ s}^{-1}$. This is 170-fold higher than the rate for VA oxidation. This large difference in the overall rate as calculated from steady-state kinetic data suggests that the rate of electron transfer between the VA cation radical and Cc^{2+} may be faster than the rate for deprotonation of the VA cation radical. The μM values for the $K_{m\text{ app}}$ for the oxidation of Cc^{3+} in the presence of VA and for the K_i for Cc^{3+} inhibition of VA oxidation suggest an interaction or weak binding between the enzyme and this polymeric substrate. In particular, the low K_i value would not be expected if the VA cation radical was acting as a diffusible redox mediator. In that case, significant amounts of veratraldehyde would be expected, even in the presence of Cc^{3+} .

The stoichiometry of Cc^{2+} oxidation as compared to H_2O_2 consumption is exactly 2:1 in the presence VA (data not shown). Consistent with these results, HPLC analysis shows that there is negligible VA oxidation while Cc^{2+} is being oxidized (Table 4.2). These observations indicate that VA is not an obligatory substrate for the reduction of LiP compound II during Cc^{2+} oxidation, as proposed for the oxidation of anisyl alcohol (Koduri & Tien, 1994). If VA was a required reductant, 0.5 equiv of veratraldehyde should be formed for each equiv of Cc^{2+} oxidized. Owing to the complexity of products formed in the LiP-catalyzed oxidation of Cc^{3+} (Fig. 4.7), it is difficult to determine the stoichiometry between Cc^{3+} oxidation and H_2O_2 consumption. However, VA is absolutely required for the oxidation of Cc^{3+} in the presence of 100 μM H_2O_2 . In this case, a negligible amount of veratraldehyde is formed when LiP oxidizes Cc^{3+} in the presence of a five-fold excess of VA. Although small amounts of veratraldehyde are formed when LiP oxidizes Cc^{3+} in the presence of a 50-fold excess of VA, these amounts are not nearly stoichiometric. Taken together, these results indicate that VA is not acting as a

required reductant for compound II in these reactions. Indeed, the results suggest strongly that the VA cation radical oxidizes Cc^{3+} while still in its enzyme-binding site. In the time it takes to diffuse away, it would lose a proton to form the benzylic radical.

The results in Fig. 4.5, which directly measure the effects of Cc^{3+} and VA on H_2O_2 -induced LiP inactivation, support this latter alternative. In the presence of 100 μM H_2O_2 , 500 μM VA is required to stabilize LiP and 20 μM VA exhibits no protective effect. However, with 20 μM Cc^{3+} and 20 μM VA together, full LiP activity is retained. The simplest explanation for this result is that VA is oxidized to a cation radical which rapidly oxidizes Cc^{3+} , enabling the enzyme to complete its catalytic cycle. Since there are several oxidizable Tyr and Met residues in Cc^{3+} , only 20 μM Cc^{3+} is required. The stoichiometry of this protective effect suggests that the VA cation radical rapidly oxidizes Cc^{3+} , implying close proximity of the LiP and Cc^{3+} , rather than losing a proton to form the benzylic radical which would lead to the formation of veratraldehyde. The results in Table 4.2 confirm that, in the presence of Cc^{3+} , very little VA is converted to veratraldehyde. Inactivation of LiP is due to the oxidation of LiP compound II by H_2O_2 to form LiP compound III and III* with subsequent bleaching (Wariishi & Gold, 1990). VA protects LiP from inactivation by reducing LiP compound II to native LiP, preventing the formation of LiPIII and LiPIII*. If the VA cation radical is reduced by Cc^{3+} while still in its binding site, then the VA produced by this recycling reaction could immediately reduce LiP compound II. In contrast, if the VA cation radical were to diffuse away, another VA molecule would be required to reduce compound II. This latter situation would be essentially identical to having VA as the lone substrate. However, the results in Fig. 4.6 show that 20 μM VA alone does not protect the enzyme from inactivation, while 20 μM VA and 20 μM Cc^{3+} do afford complete protection.

The results described here lead us to propose a role for VA in these reactions. We propose that VA binds to LiP between the heme and the surface of the enzyme as predicted by molecular modeling (Poulos et al., 1993). This location for VA would facilitate the oxidation of a polymer located at the surface of LiP. Thus, LiP oxidizes VA to the cation radical which is reduced back to VA during the oxidation of Cc^{3+} .

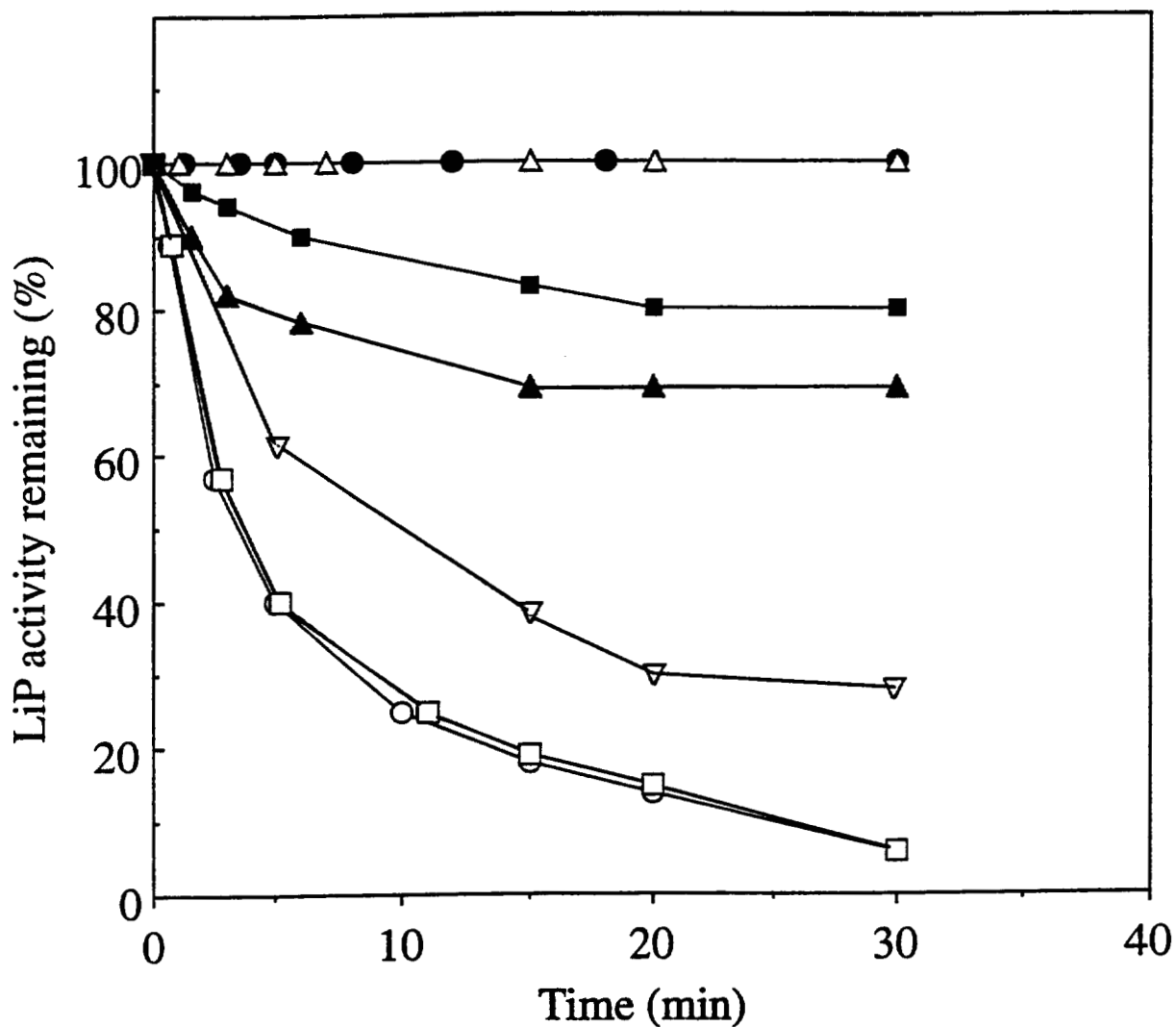


Fig. 4.5 Effects of VA and Cc^{3+} on LiP inactivation by H_2O_2 . LiP (100 μ g/ml, 2.4 μ M) was incubated with H_2O_2 (100 μ M) in 20 mM sodium succinate, pH 3.0, alone (\square), with 20 μ M VA (\circ), with 500 μ M VA (\bullet), with 20 μ M Cc^{3+} (∇), with 5 μ M VA and 20 μ M Cc^{3+} (\blacktriangle), with 10 μ M VA and 20 μ M Cc^{3+} (\blacksquare), and with 20 μ M VA and 20 μ M Cc^{3+} (\triangle). At intervals, aliquots (20 μ l) were removed and assayed for LiP activity, as described in the text.



Fig. 4.6 SDS-PAGE of Cc^{3+} oxidation products. Reactions and SDS-PAGE were as described in the text. Lane 1, untreated Cc^{3+} ; lane 2, reaction products of Cc^{3+} and H_2O_2 ; lane 3, reaction products of Cc^{3+} , H_2O_2 , and LiP; lane 4, reaction products of Cc^{3+} , H_2O_2 , LiP, and VA. The molecular weight markers at left are: lactate dehydrogenase (36.5 kD), carbonic anhydrase (31 kD), trypsin inhibitor (21.5 kD), lysozyme (14.4 kD), and aprotinin (6.0 kD).

In this sense, VA functions as an electron transfer cofactor between the LiP heme and the surface of the enzyme. VA may act analogously to Trp191 in CcP reactions (Hahm et al., 1994; Liu et al., 1994; Miller et al., 1994a,b). This accomplishes two things: it ensures the rapid oxidation of the terminal substrate and it ensures that the enzyme completes its catalytic cycle without being shunted into compounds III and III*.

4.4.3 Polymerization of Cc^{3+} and formation of dityrosine

In addition to heme bleaching, some of the Cc^{3+} molecules are polymerized by LiP in the presence of VA and H_2O_2 (Fig. 4.6). It has been reported that both free tyrosine and Tyr residues in a variety of proteins can be oxidized to Tyr radicals by peroxidases (Amado et al., 1984), and two Tyr radicals can undergo phenolic coupling to form dityrosine. The coupling of Tyr radicals in proteins can be intramolecular, intermolecular, or both. Intermolecular coupling can lead to dimerization of proteins (Amado et al., 1984). For example, the reaction of sperm whale myoglobin with H_2O_2 decreases the Tyr content of the protein and results in the formation of dimeric myoglobin (Rice et al., 1983).

The formation of dityrosine within proteins has been confirmed by amino acid analysis (Amado et al., 1984). Amino acid analyses of the monomeric and dimeric products of LiP-catalyzed Cc^{3+} oxidation demonstrate that the Tyr content of the dimer decreases during the reaction, suggesting the formation of dityrosine. The crystal structure of Cc^{3+} (Bushnell et al., 1990) suggests that the Tyr residues on the surface of the protein (Tyr48, Tyr74, and Tyr97) might be susceptible to oxidation resulting in dimerization of the protein.

In vitro studies with pure LiP have demonstrated the partial polymerization of synthetic lignin containing free phenolic groups. This polymerization does not occur when exhaustively methylated synthetic lignin is used (Hammel et al., 1993), indicating that LiP oxidizes phenols in synthetic lignin to form phenoxy radicals which can couple to form polymerized products. A similar LiP mechanism may result in the coupling of phenoxy radicals in synthetic lignin and in lignin model compounds, as apparently occurs in the coupling of Tyr radicals in Cc^{3+} . The ability

of LiP to oxidize Tyr residues in proteins may explain the complete absence of Tyr residues in both LiP and MnP (Tien & Tu, 1987; Smith et al., 1988; Ritch et al., 1991; Gold & Alic, 1993).

4.4.4 Conclusions

LiP catalyzes a novel VA-dependent irreversible oxidation of Cc^{3+} , leading to complete bleaching of the Cc^{3+} heme and polymerization of some of the Cc^{3+} molecules. Our results suggest that VA acts as an enzyme-bound radical mediator in this reaction. Cc^{3+} heme oxidative cleavage may contribute to bleaching of the heme with subsequent loss of heme iron. The polymerization reaction appears to result from coupling of Tyr radicals formed by LiP oxidation. Cc^{3+} has a higher redox potential than Cc^{2+} and, therefore, is a better model polymer for studying the LiP-catalyzed oxidation of lignin. In addition, the LiP-catalyzed oxidation of Cc^{3+} is easily measured via the decreasing Soret band intensity. We are planning additional studies to further probe the role of VA in these reactions.

CHAPTER 5
OXIDATIVE POLYMERIZATION OF RIBONUCLEASE A BY LIGNIN
PEROXIDASE FROM *PHANEROCHAETE CHRYSOSPORIUM*:
ROLE OF VERATRYL ALCOHOL IN POLYMER OXIDATION

5.1 Introduction

Lignin is a heterogeneous, phenylpropanoid polymer that constitutes 20–30% of woody plant cell walls (Sarkanen & Ludwig, 1971). White-rot basidiomycete fungi are primarily responsible for initiating the depolymerization of lignin, which is a key step in the earth's carbon cycle (Buswell & Odier, 1987; Kirk & Farrell, 1987; Gold et al., 1989). The best-studied lignin-degrading fungus, *Phanerochaete chrysosporium*, secretes two types of extracellular heme peroxidases, manganese peroxidase and lignin peroxidase (LiP), which, along with an H₂O₂-generating system, are the major extracellular components of its lignin degradative system (Buswell & Odier, 1987; Kersten & Kirk, 1987; Kirk & Farrell, 1987; Gold et al., 1989; Hammel et al., 1993). Nucleotide sequences of a number of *lip* cDNA and genomic clones (Tien & Tu, 1987; Ritch et al., 1991; Gold & Alic, 1993; Cullen, 1987), as well as X-ray crystal structures (Edwards et al., 1993; Piontek et al., 1993; Poulos et al., 1993), demonstrate that important catalytic residues, including the proximal and distal His, the distal Arg, and an H-bonded Asp, are all conserved within the heme pocket of LiP. Although the catalytic cycle of LiP is similar to that of other plant and fungal peroxidases (Renganathan et al., 1986; Marquez et al., 1988; Tien et al., 1986; Gold et al., 1989), LiP has several unique features, including an apparently high redox potential (Kirk & Farrell, 1987; Gold et al., 1989; Schoemaker, 1990) and a low pH optimum of ~3.0 (Tien et al., 1986; Renganathan et al., 1987).

In the presence of veratryl (3,4-dimethoxybenzyl) alcohol (VA), a secondary metabolite that is secreted by *P. chrysosporium*, LiP slowly depolymerizes synthetic

lignin *in vitro* (Hammel et al., 1993). Likewise, in the presence of VA, LiP oxidizes nonphenolic lignin model compounds and aromatic pollutants with redox potentials beyond the reach of other peroxidases (Buswell & Odier, 1987; Kirk & Farrell, 1987; Gold et al., 1989; Schoemaker, 1990; Valli & Gold, 1990; Joshi & Gold, 1994). X-ray crystallographic studies demonstrate that the heme in LiP is buried, ruling out a direct interaction between the heme and polymeric substrates (Poulos et al., 1993). Therefore, we have examined the LiP oxidation of model protein polymeric substrates, including ferrocyanochrome *c* (Cc^{2+}) (Wariishi et al., 1994) and ferricyanochrome *c* (Cc^{3+}) (Sheng & Gold, 1998), and the role of VA in these oxidations, in order to better understand the mechanism of LiP in the depolymerization of lignin. However, transient-state kinetic studies using these model compounds are difficult, since the strong Soret absorptions of Cc^{2+} and Cc^{3+} overlap with that of LiP. Therefore, in the current study, the oxidation of the nonheme protein, bovine pancreatic ribonuclease A (RNase), is examined. In addition to other biochemical and kinetic assays, we investigate the oxidation of RNase by LiP compound I (LiPI) and LiP compound II (LiPII) using stopped-flow techniques. To our knowledge, this is the first study of the LiP oxidation of a polymeric substrate using transient-state kinetics.

5.2 Experimental Procedures

5.2.1 Protein preparation

LiP isoenzyme 2 (H8) was purified from acetate-buffered cultures of *P. chrysosporium* strain OGC101 as previously described (Gold et al., 1984; Wariishi & Gold, 1990). The purified enzyme was electrophoretically homogeneous and had an R_z value (A_{408}/A_{280}) of 5.0. Enzyme concentration was determined at 408 nm using an extinction coefficient of $133 \text{ mM}^{-1}\text{cm}^{-1}$ (Gold et al., 1984). Bovine pancreatic RNase A and horseradish peroxidase (HRP) were obtained from Sigma and used without further purification.

5.2.2 Chemicals

H₂O₂ (30% solution) was obtained from Sigma and the concentration of the stock solution was determined as described (Cotton & Dunford, 1973). VA was obtained from Aldrich and purified by silica gel column chromatography (ethyl acetate:hexane=1:1,v:v) before use. S-Sepharose cation exchanger was obtained from Sigma. Other chemicals were reagent grade. All solutions were prepared using deionized water from a MilliQ 50 system (Millipore).

5.2.3 Fluorescence spectrophotometry

All reactions were run at 25°C. For RNase and tyrosine oxidations, reaction mixtures (3 ml) contained LiP (1 µg/ml, 0.024 µM), RNase (10 µM) or tyrosine (400 µM), with or without VA (500 µM), in 20 mM sodium succinate, pH 3.0. The reactions were initiated by the addition of H₂O₂ (100 µM). Fluorescence data were collected using a Perkin-Elmer MPF-66 fluorescence spectrophotometer with an excitation wavelength of 315 nm. The emission spectra owing to the formation of dityrosine were recorded between 325 nm and 500 nm (Amado et al., 1984). For RNase oxidations with varying amounts of VA, reaction mixtures (3 ml) contained LiP (1 µg/ml), RNase (100 µM), and VA (0–1 mM) in 20 mM sodium succinate, pH 3.0. The reactions were initiated by the addition of H₂O₂ (100 µM). The relative emission due to RNase oxidation was measured as above at 410 nm, with an excitation wavelength of 315 nm. The emission due to veratraldehyde formation from VA was measured at 410 nm under the same conditions in the absence of RNase.

5.2.4 UV-visible spectrophotometry

All reactions were carried out at 25°C. Reaction mixtures (1 ml) contained LiP (1 µg/ml), VA (500 µM), and RNase (0–20 µM) in 20 mM sodium succinate, pH 3.0. The reactions were initiated by the addition of H₂O₂ (100 µM). The effect of RNase concentration on VA oxidation was measured by following the increase in absorbance at 310 nm due to veratraldehyde formation (Kirk & Farrell, 1987; Gold et al., 1989), using a Shimadzu UV-260 spectrophotometer.

5.2.5 HPLC analysis of VA oxidation

The effect of RNase concentration on VA oxidation also was examined using high performance liquid chromatography (HPLC). Reaction mixtures were as described above for UV-visible spectrophotometry. HPLC was carried out with a Hewlett-Packard LiChrospher 100 RP-18 column. Veratraldehyde formation was analyzed over 22 min at 280 nm using a linear gradient of 10–50% acetonitrile in 0.05% phosphoric acid. Veratraldehyde was quantitated using a standard curve.

5.2.6 LiP inactivation studies

Reaction mixtures contained LiP (50 $\mu\text{g/ml}$, 1.2 μM), with or without RNase (50 μM) and/or VA (5–500 μM), in 20 mM sodium succinate, pH 3.0. Aliquots (15 μl) were removed periodically during the reaction, and LiP activity was assayed by measuring the formation of veratraldehyde at 310 nm. For LiP spectral studies, reaction mixtures contained LiP (1.2 μM), with or without VA (100 μM) or RNase (100 μM), or with VA and RNase (50 μM each). Spectra (375–700 nm) were recorded at 1.5-min intervals following the addition of H_2O_2 (100 μM). The final spectra (450–700 nm) were recorded after 6 min.

5.2.7 Identification of dityrosine

Reaction mixtures (10 ml) contained LiP (1 $\mu\text{g/ml}$) or HRP (10 $\mu\text{g/ml}$), Tyr (400 μM), and H_2O_2 (100 μM) in 20 mM sodium succinate, pH 3.0. The reactions were monitored by HPLC with an HP LiChrospher 100 RP-18 column. The major product peak from the LiP reaction was collected and lyophilized. Product identification was performed using a VG Analytical 7070E mass spectrometer with fast atom bombardment (FAB) as the ionization source and thioglycerol as the supporting matrix.

5.2.8 SDS-PAGE and amino acid analysis

Reaction mixtures contained RNase (10 μM) and H_2O_2 (100 μM), with or without LiP (0.02 μM) and VA (500 μM). The protein products were concentrated by ultrafiltration using an Amicon-10 membrane and subjected to 12% sodium

dodecyl sulfate–polyacrylamide gel electrophoresis (SDS–PAGE) (Mini-PROTEAN, BioRad) (Laemmli, 1970). Dimeric and trimeric RNases were separated from the monomer by cation exchange chromatography with S-Sepharose. The column was equilibrated with 10 mM sodium acetate, pH 6.0 (buffer A), the sample was added, and the column was washed with buffer A (5 ml). The column was eluted with a linear gradient of sodium acetate, pH 6.0 (10 mM to 1 M over 30 min), at a flow rate of 1 ml/min, with detection at 280 nm. The oxidized monomer and dimer peaks were desalted, concentrated, and sent for amino acid analysis (Debra McMillen, Biotechnology Laboratory, University of Oregon).

5.2.9 Transient-state kinetic studies

Kinetic measurements were made at $25 \pm 0.5^\circ\text{C}$ using an Applied Photophysics stopped-flow reaction analyzer (SX.18MV) with sequential mixing. For LiPI reduction, one syringe contained enzyme ($2 \mu\text{M}$ final concentration) in 20 mM sodium succinate, pH 3.0, and the other syringe contained 1 equiv of H_2O_2 in the same buffer. The two components were premixed and incubated for 4 sec to assure the formation of LiPI, which was confirmed by rapid scanning using a diode array photometer. Substrate(s) was added with a third syringe and the rate of LiPI reduction was followed at 416.7 nm, the isosbestic point between native LiP and LiPII. Similarly, LiPII was formed by mixing LiP ($2 \mu\text{M}$ final concentration) with 1 equiv of H_2O_2 and 1 equiv of potassium ferrocyanide. Subsequently, substrate was added and the rate of LiPII reduction was monitored at 397 nm, the isosbestic point between LiPI and LiPII. The concentration of substrate(s) in the final solution was at least 10-fold in excess, assuring pseudo first-order kinetic conditions. All of the kinetic traces exhibited single exponential character from which pseudo first-order rate constants were calculated.

5.3 Results

5.3.1 LiP oxidation of RNase and tyrosine

The fluorescence emission spectrum obtained from the oxidation of RNase by LiP and H₂O₂ in the presence of VA (Fig. 5.1A) was essentially identical to that reported for the HRP-catalyzed polymerization of insulin (Amado et al., 1984) with a peak at 410 nm, suggesting the formation of dityrosine. In the presence of 100 μ M H₂O₂ but in the absence of VA, essentially no emission spectrum was observed (Fig. 5.1A), suggesting that under these conditions RNase oxidation was dependent on VA. All spectra exhibited an emission at 354 nm due to the Raman shift of water (Fig. 5.1) (Hirschfeld et al., 1973).

The fluorescence spectrum obtained from the oxidation of free tyrosine by LiP and H₂O₂ (Fig. 5.1B) was characteristic of dityrosine and was essentially identical to that obtained with the HRP-catalyzed oxidation of free tyrosine (Amado et al., 1984; data not shown). Identical spectra were obtained in the presence and absence of VA. The FAB mass spectrum of the major product from the LiP oxidation of tyrosine showed a peak at 361 (M+1), corresponding to dityrosine (Ushijima et al., 1984).

5.3.2 SDS-PAGE and amino acid analysis of oxidized RNase

Fig. 5.2 shows the SDS-PAGE of the products of the LiP-catalyzed oxidation of RNase in the presence and absence of VA. When the reaction was run in the presence of H₂O₂, with or without LiP, no polymerized products were observed (Fig. 5.2, lanes 2 and 3). In the presence of H₂O₂, LiP, and VA, the RNase dimer (27.1 kD) was the major product, and a smaller amount of the RNase trimer (40.0 kD) also was detected (Fig. 5.2, lane 4). The existence of a double band at the RNase dimer position suggested that a variety of intermolecular Tyr couples led to RNase polymerization. The monomeric and polymeric products of the RNase oxidation reaction were separated by cation exchange chromatography, and the polymeric products also were analyzed by SDS-PAGE. The polymeric product peak from the cation exchange column contained both the RNase dimer and trimer (Fig. 5.2, lane 5). The fluorescence spectrum of the cation exchange-separated polymeric product

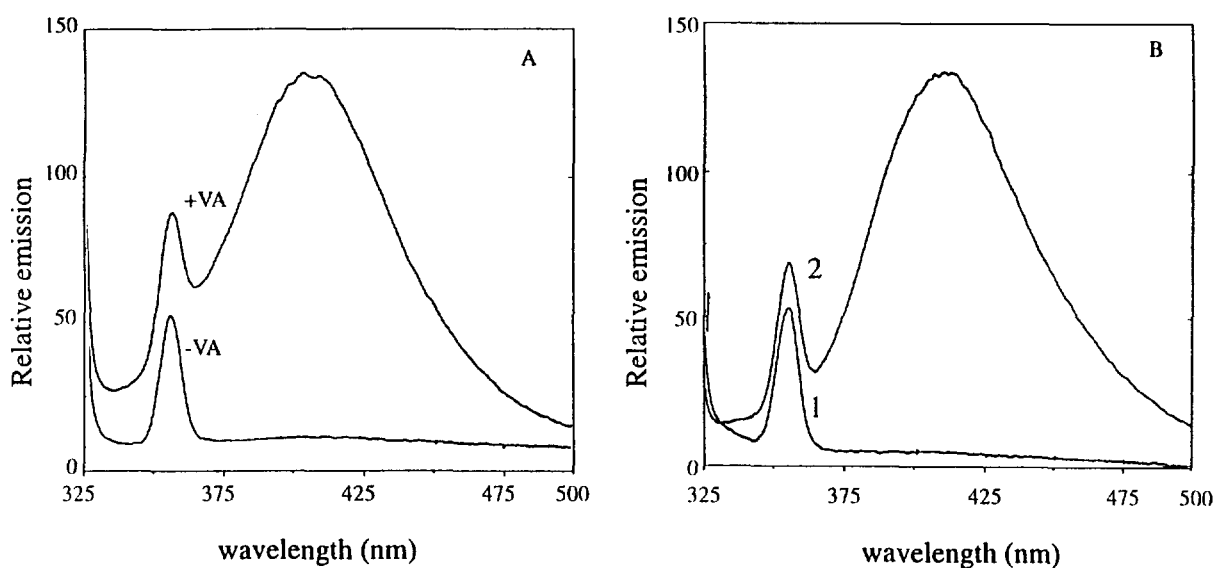


Figure 5.1 Fluorescence spectra of RNase and tyrosine oxidation by LiP. The emission spectra were recorded between 325 nm and 500 nm. *A*, The reaction mixtures contained LiP (1 $\mu\text{g}/\text{ml}$) and RNase (10 μM), with or without VA (500 μM), in 20 mM sodium succinate, pH 3.0. The spectra were recorded following a 5-min incubation with H_2O_2 (100 μM). *B*, The reaction mixture contained LiP (1 $\mu\text{g}/\text{ml}$) and Tyr (400 μM) in 20 mM sodium succinate, pH 3.0. The spectra were recorded immediately before (1) and following (2) the addition of H_2O_2 (100 μM).

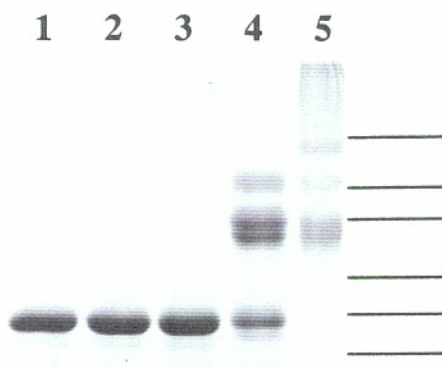


Figure 5.2 SDS-PAGE of RNase oxidation products. Reactions were as described in the text. Molecular weight markers, indicated on the right, were, from the bottom: aprotinin (6 kD), lysozyme (14.4 kD), trypsin inhibitor (21.5 kD), carbonic anhydrase (31 kD), lactate dehydrogenase (36.5 kD), and glutamate dehydrogenase (55.4 kD). *Lane 1*, untreated RNase; *lane 2*, reaction products of RNase and H_2O_2 ; *lane 3*, same as lane 2, with the addition of LiP; *lane 4*, same as lane 3, with the addition of VA; *lane 5*, major product of the reaction in lane 4, following cation exchange chromatography.

(data not shown) was identical to that obtained for the LiP-catalyzed RNase oxidation reaction (Fig. 5.1A).

Amino acid analyses of native RNase and of the monomeric and dimeric products of the LiP-catalyzed oxidation of RNase, purified by cation exchange chromatography, demonstrated that the Tyr and Met contents of the oxidized proteins were decreased compared with native RNase, but that the amino acid compositions of the proteins were otherwise very similar (Table 5.1). The Tyr content decreased by 33% in the oxidized monomer and by 50% in the oxidized dimer, compared with native RNase and the theoretical value based on the amino acid sequence (Smyth et al., 1963). This suggested that Tyr residues were oxidized, resulting in the formation of dityrosine. The Met content decreased by 23% and 40% in the oxidized monomer and dimer, respectively, as compared with native RNase and the theoretical value (Table 5.1). These results suggested that LiP oxidized Met and Tyr residues in the protein, resulting in intramolecular and intermolecular dityrosine formation, and that the latter resulted in the dimerization of RNase.

5.3.3 RNase oxidation and veratraldehyde formation

In the presence of 100 μM H_2O_2 , the LiP-catalyzed oxidation of RNase was strictly dependent on the presence of VA, reaching a maximum at a VA concentration of 500 μM . Importantly, VA concentrations as high as 1 mM did not inhibit RNase oxidation (Fig. 5.3). Veratraldehyde formed from the LiP-catalyzed oxidation of VA also exhibited a weak fluorescence emission at 410 nm (data not shown). However, as demonstrated below, RNase strongly inhibited VA oxidation, indicating that any emission at 410 nm due to veratraldehyde formation was negligible.

In the presence of RNase, the LiP-catalyzed oxidation of VA exhibited biphasic kinetics with a significant lag phase (Fig. 5.4, inset). Furthermore, the lag phase for veratraldehyde formation increased with increasing RNase concentrations (Fig. 5.4). Thus, RNase inhibited the oxidation of VA to veratraldehyde, but even very high concentrations of VA did not inhibit RNase oxidation (Fig. 5.3).

The LiP oxidation of VA to veratraldehyde in the presence of various concentrations of RNase also was determined by HPLC (Table 5.2). As little as 20

Table 5.1

Amino Acid Analyses of Native and Oxidized RNase Proteins

Amino acids	Theoretical ^a	Native ^b	Monomer ^c	Dimer ^d
Asx	15	15.2	15.0	14.2
Thr	10	9.2	9.6	9.3
Ser	15	14.1	13.5	13.4
Glx	12	12.0	12.0	12.1
Pro	4	4.0	4.0	4
Gly	3	3.1	3.1	3.2
Ala	12	12.7	12.2	11.9
Val	9	8.4	8.8	8.5
Met	4	4.0	3.1	2.4
Ile	3	2.2	2.2	2.2
Leu	2	2.0	2.2	2.1
Tyr	6	6.0	4.0	3.0
Phe	3	3.0	3.0	3.0
Lys	19	14.0	12.0	10.5
His	4	4.2	4.4	3.9
Arg	4	4.0	4.3	3.9
Cys	8	nd ^e	nd	nd

^a Content based on the sequence of bovine pancreatic RNase A (Smyth et al., 1963).

^b Untreated RNase.

^c LiP-oxidized RNase monomer purified by cation exchange chromatography.

^d LiP-oxidized RNase dimer purified by cation exchange chromatography. The values represent 50% of the yield for each amino acid.

^e Not determined.

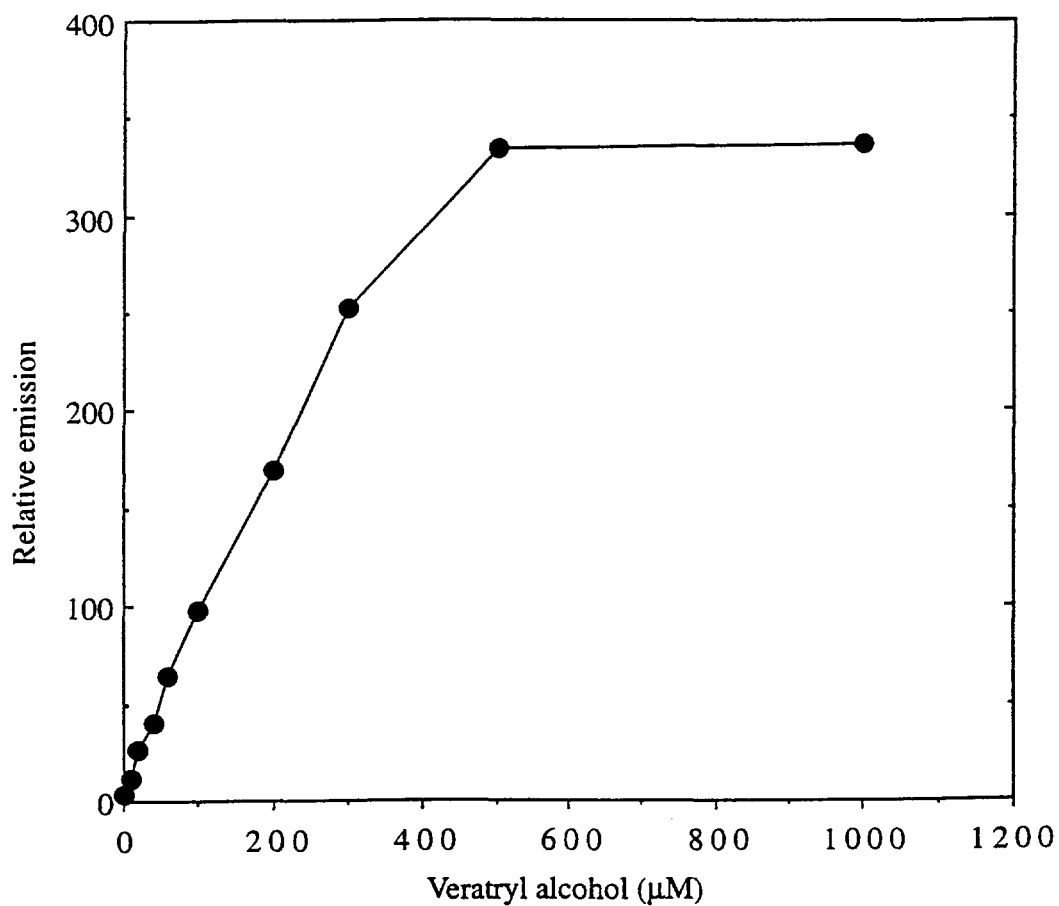


Figure 5.3 Effect of VA on the oxidation of RNase. The relative emission was recorded at 410 nm with an excitation wavelength of 315 nm. Reaction mixtures consisted of LiP (1 $\mu\text{g}/\text{ml}$) and RNase (100 μM), at the indicated concentrations of VA, in 20 mM sodium succinate, pH 3.0. Reactions were initiated by the addition of H_2O_2 (100 μM).

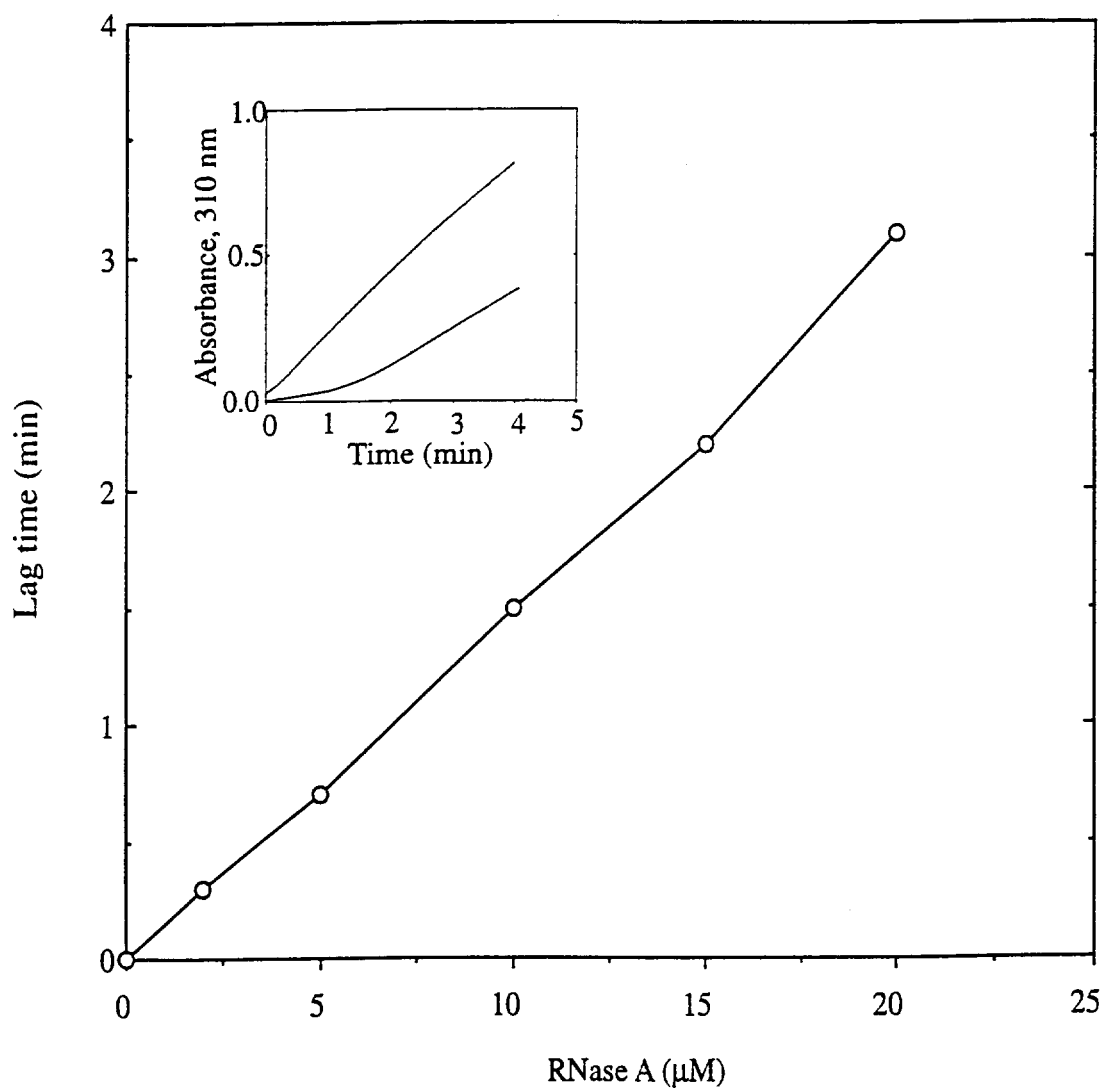


Figure 5.4 Effect of RNase concentration on the lag time for VA oxidation by LiP. Reaction mixtures consisted of LiP ($1 \mu\text{g/ml}$), VA ($500 \mu\text{M}$), and RNase, as indicated, in 20 mM sodium succinate, pH 3.0. Reactions were initiated by the addition of H_2O_2 ($100 \mu\text{M}$). The lag time (in min) for the formation of veratraldehyde, as measured by the increase in absorbance in 310 nm , is plotted against the RNase concentration. *Inset*, The oxidation of VA, as measured at 310 nm , in the absence (upper line) and presence (lower line) of RNase ($10 \mu\text{M}$).

Table 5.2Veratraldehyde Formation in the Presence and Absence of RNase^a

RNase (μM)	Veratraldehyde (μM)
0	24
10	6.1
15	1.6
20	0.2

^a Reaction mixtures (1 ml) contained LiP (1 $\mu\text{g}/\text{ml}$), VA (500 μM), and the indicated amounts of RNase in 20 mM sodium succinate, pH 3.0. Reactions were started by the addition of H_2O_2 (100 μM), incubated at 25°C for 1 min, and stopped by the addition of HCl. Veratraldehyde formation was measured by HPLC as described in the text.

μM RNase almost completely inhibited the formation of veratraldehyde from 500 μM VA, demonstrating that RNase is a strong inhibitor of veratraldehyde formation.

5.3.4 Effects of RNase and VA on the H_2O_2 -induced inactivation of LiP

As shown in Fig. 5.5, when LiP (1.2 μM) was incubated with 100 μM H_2O_2 at 25°C and pH 3.0, almost all LiP activity was lost within 30 min. Although the presence of 50 μM VA did not prevent this inactivation, essentially all LiP activity was retained after 30 min in the presence of 500 μM VA. Likewise, in the presence of 50 μM RNase, 70% of LiP activity was lost within 30 min. However in the presence of 20 μM VA and 50 μM RNase, 90% of the LiP activity was retained after 30 min. Indeed, in the presence of 50 μM RNase, as little as 5 μM VA significantly protected LiP from H_2O_2 -induced inactivation (Fig. 5.5).

As shown in Fig. 5.6A, the incubation of LiP with 100 μM H_2O_2 resulted in a red shift of the LiP Soret band from 408 nm to 419 nm and the appearance of peaks at 543 nm and 578 nm, suggesting the formation of LiP compound III (LiPIII) and LiPIII*, which are inactive forms of the enzyme (Wariishi & Gold, 1990). When the reaction included VA (100 μM), the initial spectrum suggested a mixture of LiPII and LiPIII (Wariishi et al., 1990). Subsequently, there was a decrease in the absorbances at 500 nm and 632 nm and partial recovery of the Soret absorbance, as well as the appearance of shoulders at 543 nm and 578 nm (Fig. 5.6B), suggesting a mixture of native LiP, LiPIII and LiPIII*. In contrast, when the reaction mixture included RNase (100 μM) instead of VA, the peaks at 419, 543, and 578 nm were more clearly defined (Fig. 5.6C), indicating the formation of LiPIII*. Finally, when LiP was incubated with 100 μM H_2O_2 in the presence of both VA and RNase (50 μM each), a native LiP spectrum was observed (Fig. 5.6D), suggesting that, in the presence of both VA and RNase, LiP was protected completely against H_2O_2 -induced inactivation.

5.3.5 Transient-state kinetic studies

The rates of LiPI reduction by various substrates were followed at 416.7 nm, the isosbestic point between LiPII and native LiP. All of the kinetic traces were of a

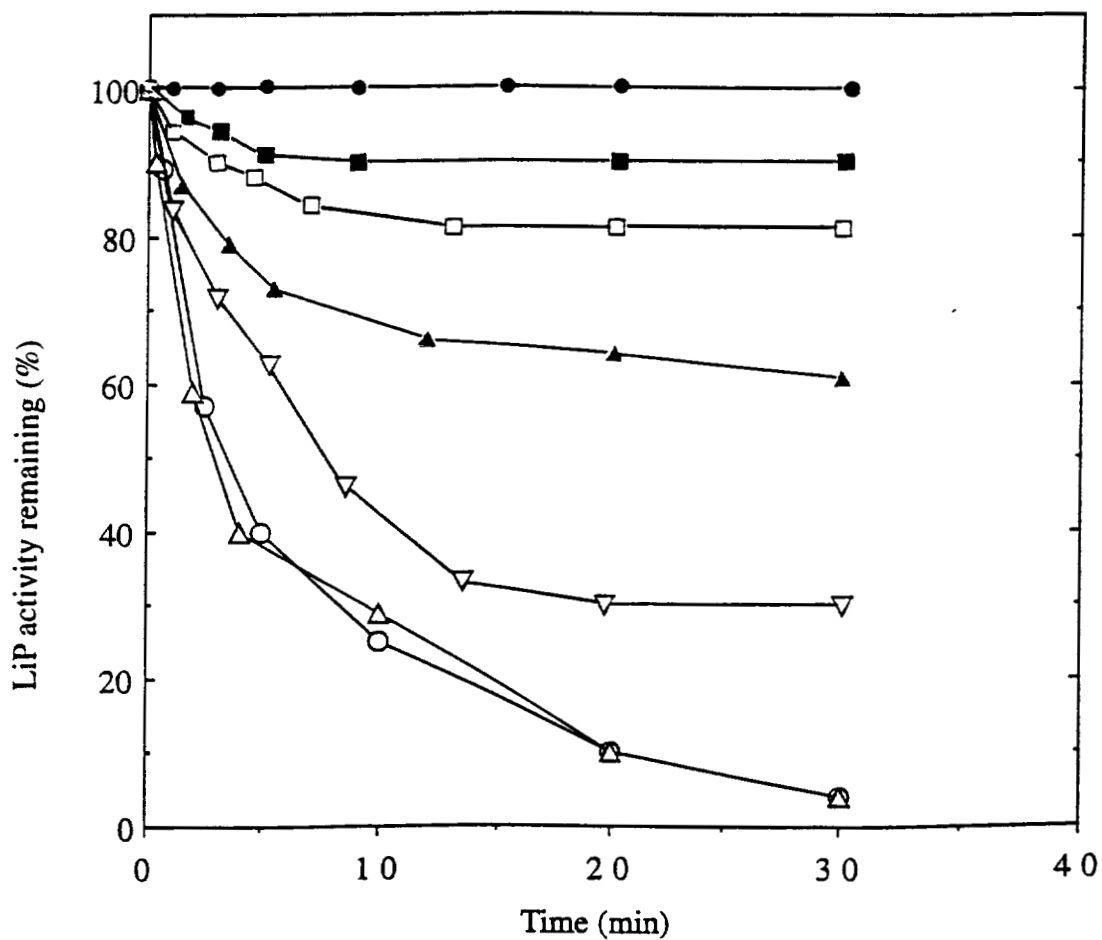


Figure 5.5 Effects of RNase and VA on LiP inactivation. Reaction mixtures contained LiP (50 $\mu\text{g/ml}$) and H_2O_2 (100 μM) in 20 mM sodium succinate, pH 3.0, alone (○); with VA (50 μM) (Δ) or VA (500 μM) (●); with RNase (50 μM) (∇); or with RNase (50 μM) and VA (5 μM) (\blacktriangle), VA (10 μM) (\square) or VA (20 μM) (\blacksquare). Aliquots (15 μl) were assayed for LiP activity at the indicated intervals, as described in the text.

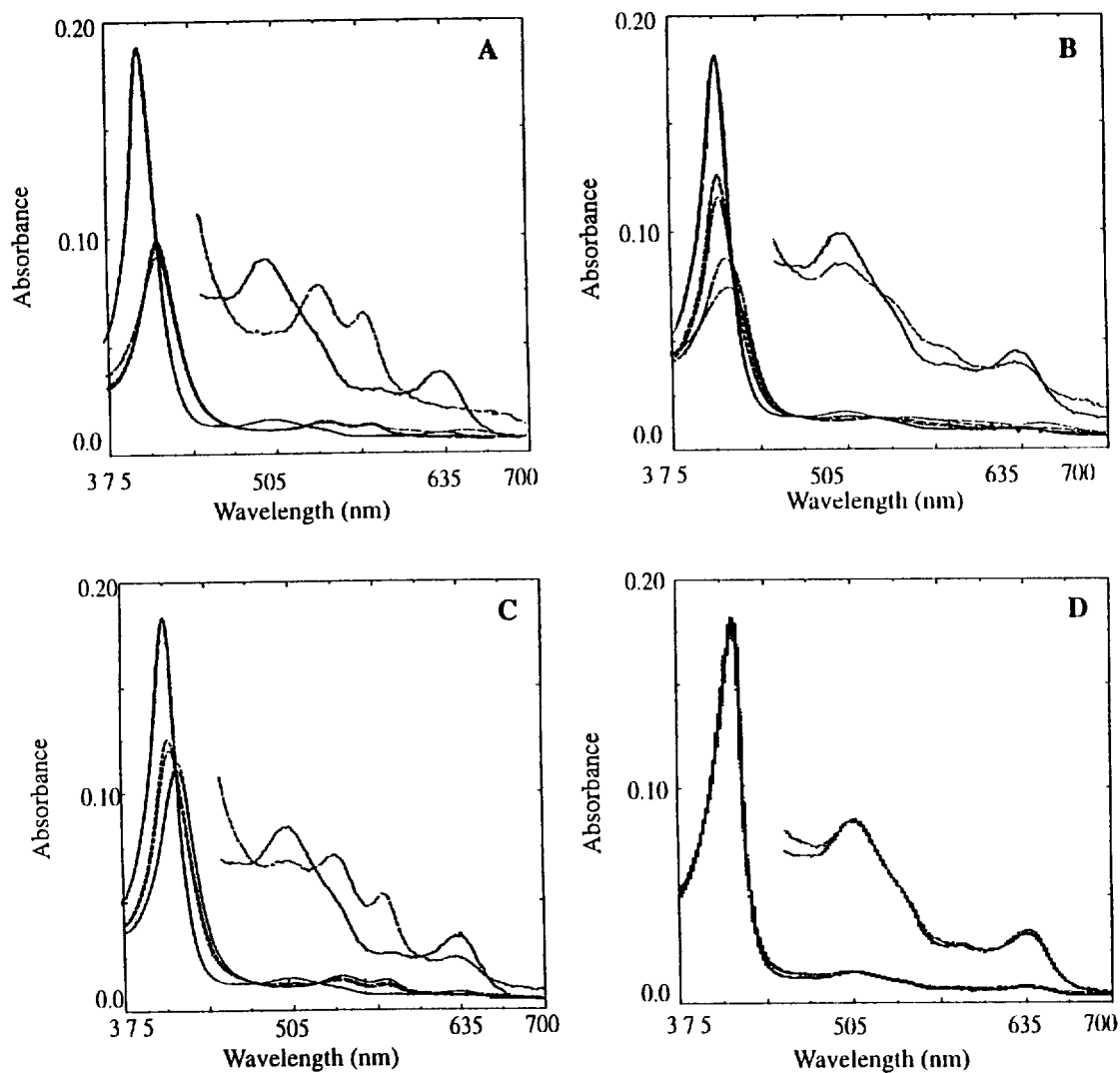
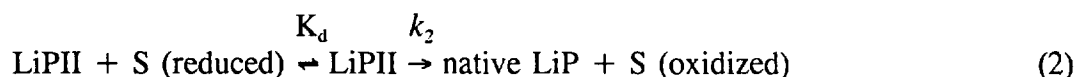


Figure 5.6 Effects of RNase and VA on the LiP visible spectra. Reactions were as described in the text. Spectra were recorded at 1.5-min intervals following the addition of H_2O_2 ($100 \mu\text{M}$). The final spectra from 450–700 nm were recorded after 6 min (dotted line). *A*, Reaction mixture contained LiP ($1.2 \mu\text{M}$); *B*, same as in *A*, with the addition of VA ($100 \mu\text{M}$); *C*, same as in *A*, with the addition of RNase ($100 \mu\text{M}$); *D*, same as in *A*, with the addition of VA and RNase ($50 \mu\text{M}$ each).

single exponential character, and the observed rate constants were linearly proportional to the substrate concentrations. The plots of k_{obs} versus substrate concentration passed through the origin within experimental error (Fig. 5.7A), indicating that the reactions between LiPI and the substrates obeyed second-order kinetics and that the reactions were irreversible, as shown in equation 1:



where S = VA, RNase, or equal amounts of VA and RNase, and k_1 is the second-order rate constant ($\text{M}^{-1}\text{s}^{-1}$). LiPII reduction by various substrates was monitored at 397 nm, the isosbestic point between LiPI and LiPII. Again, all of the kinetic traces were of a single exponential character from which the k_{obs} values were calculated. At pH 3.0, the plots of k_{obs} versus VA concentrations were hyperbolic, suggesting that an equilibrium reaction preceded the electron transfer reaction, as formulated in equation 2:



where S = VA, k_2 is the first-order rate constant (s^{-1}) (Table 5.3), and K_d is the dissociation constant (μM). Given a rapid equilibrium for the binding of substrate to compound II, the rate of LiPII reduction can be described by equation 3:

$$k_{\text{obs}} = k_2[\text{S}]/(K_d + [\text{S}]) \quad (3)$$

Interestingly, when RNase was used as a substrate for LiPII, the plot of k_{obs} versus substrate concentration was linear (Fig. 5.7B) and a second-order rate constant was determined (Table 5.3). However, when equal concentrations of VA and RNase were present, the plot of k_{obs} versus substrate concentration again was hyperbolic, suggesting a first-order reaction as shown in equation 2.

5.4 Discussion

LiP is a well-characterized heme peroxidase that is secreted by *P. chrysosporium* under ligninolytic conditions (Buswell & Odier, 1987; Kersten & Kirk, 1987; Kirk & Farrell, 1987; Gold et al., 1989; Higuchi, 1990; Schoemaker, 1990).

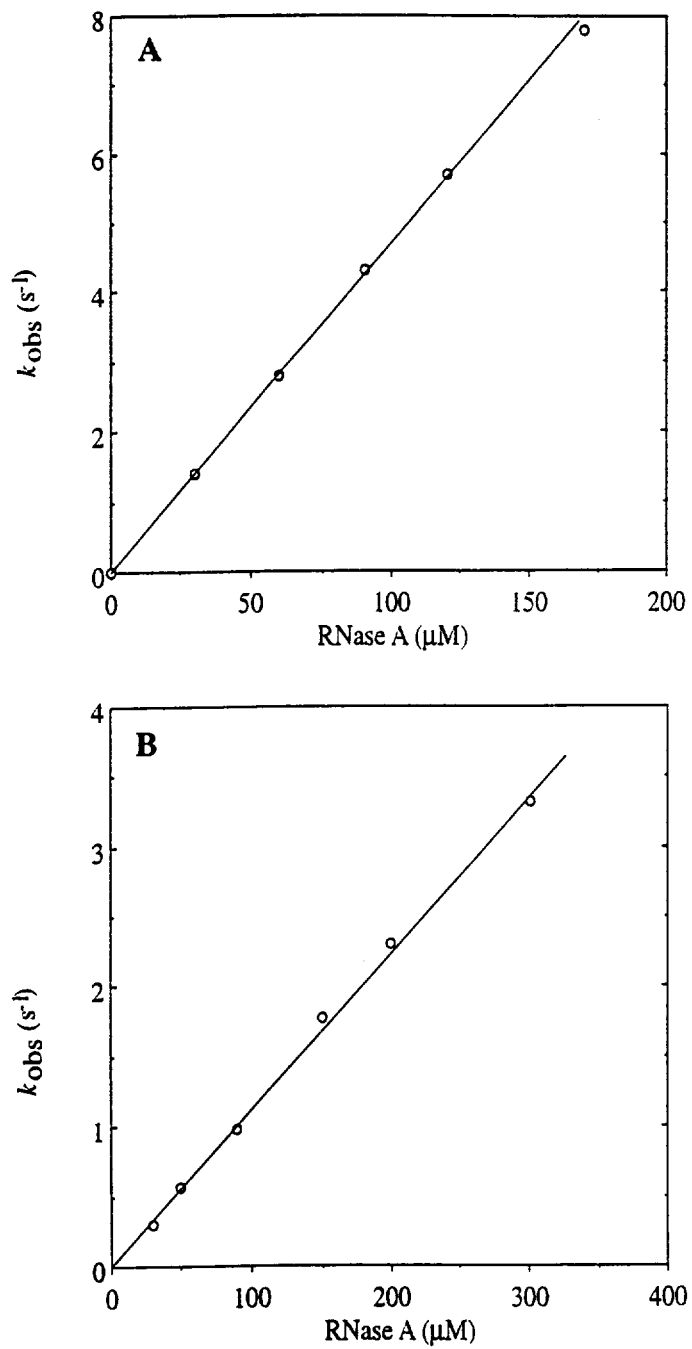


Figure 5.7 Order plots of the reductions of LiPI (A) and LiPII (B) by RNase. Reactions were as described in the text.

Table 5.3

Transient-State Kinetic Values for the Reductions
of LiP Compounds I and II by VA and RNase^a

Substrates	LiPI	LiPII	
	Second-order rate constant ($M^{-1}s^{-1}$)	First-order rate constant	
		k (s^{-1})	kD (μM)
VA	3.7×10^5	34	198
RNase and VA ^b	3.4×10^5	37	240
		Second-order rate constant ($M^{-1}s^{-1}$)	
RNase alone	6.0×10^4	1.1×10^4	

^a Reactions were conducted and kinetic values were obtained as described in the text.

^b Equal amounts of VA and RNase were present.

Considerable work has been reported on the structure and mechanism of LiP (Harvey et al., 1986; Valli & Gold, 1990; Valli et al., 1990; Wariishi et al., 1990; Gold & Alic, 1993; Koduri & Tien, 1994, 1995; Harvey & Candeias, 1995; Khindaria et al., 1996; Tien & Ma, 1997). However the precise mechanism by which LiP degrades polymeric lignin remains unresolved. In particular, the crystal structure reveals that the heme in LiP is buried (Edwards et al., 1993; Piontek et al., 1993; Poulos et al., 1993) and therefore unavailable for direct interaction with polymeric substrates such as lignin and proteins. It has been suggested that long-range electron transfer between the heme and the substrate at the surface of LiP may be involved in polymer degradation (Wariishi et al., 1994).

P. chrysosporium and other LiP-producing fungi secrete VA (Kirk & Farrell, 1987; de Jong et al., 1994; Hatakka, 1994). In addition to being a preferred substrate for LiP, VA stimulates the LiP-catalyzed depolymerization of synthetic lignin (Hammel et al., 1993) and the oxidation of a variety of recalcitrant substrates (Haemmerli et al., 1986; Harvey et al., 1986; Valli et al., 1992a,b; Joshi & Gold, 1993, 1994); however, the exact mechanism(s) by which VA stimulates the oxidation of polymeric and recalcitrant substrates remains to be clarified. Several mechanisms have been proposed to account for the stimulation of LiP reactions by VA. VA appears to protect the enzyme from H₂O₂-induced irreversible inactivation by preventing LiPII from reacting with H₂O₂ to form LiPIII (Valli et al., 1990) and by converting LiPIII*, an inactive form of the enzyme, back to the native enzyme (Wariishi & Gold, 1990). It also has been reported that VA is an obligatory substrate for reducing LiPII (Paszczyński & Crawford, 1991; Koduri & Tien, 1994), thus enabling recalcitrant substrates to be oxidized by LiPI alone. Finally, it has been proposed that VA functions as a diffusible mediator, wherein the VA cation radical, produced via the one-electron oxidation of VA, diffuses away from the enzyme surface and oxidizes terminal substrates, including lignin (Harvey et al., 1986; Akamatsu et al., 1990). However, recent chemical and biophysical studies demonstrate that the free VA cation radical is too short-lived to act as a diffusible mediator (Joshi & Gold, 1996; Khindaria et al., 1995, 1996). Another possibility is

that VA acts as a weakly-bound electron transfer cofactor analogous to Trp191 in the cytochrome *c* peroxidase catalytic cycle (Liu et al., 1995).

Previously, we used Cc^{2+} and Cc^{3+} as polymeric lignin model substrates in order to explore further the role(s) of VA in the LiP catalytic mechanism (Wariishi et al., 1994; Sheng & Gold, 1998). In the present study, we have used RNase as a lignin model polymer for several reasons: (1) The molecular mass of bovine pancreatic RNase A (13,688) is considerably greater than that of chemically synthesized lignins (3–7 kD). (2) RNase is a well-characterized protein biopolymer in comparison to either synthetic lignin or lignin extracted from wood. (3) The LiP-catalyzed oxidation of RNase can be monitored readily by fluorescence spectroscopy. (4) In contrast to *Cc*, RNase does not absorb in the Soret region, thereby simplifying transient-state kinetic studies on the reductions of LiP compounds I and II by this substrate.

5.4.1 LiP-catalyzed polymerization of RNase

Fluorescence spectra demonstrate that RNase is oxidized by LiP in the presence of H_2O_2 and VA (Fig. 5.1A). The spectrum obtained from the LiP-catalyzed oxidation of RNase (Fig. 5.1A) is essentially identical to that reported for peroxidase-catalyzed dityrosine formation in proteins (Amado et al., 1984). Furthermore, at pH 3.0, free tyrosine is converted to dityrosine by LiP as confirmed by its fluorescence spectra (Fig. 5.1B) and by mass spectrometry (data not shown). These results strongly suggest that dityrosine is formed during the oxidation of RNase by LiP.

SDS-PAGE (Fig. 5.2) and amino acid analysis results (Table 5.1) indicate that oxidation of RNase by LiP in the presence of H_2O_2 and VA yields the RNase dimer (~27.1 kD) as the major product, as well as small amounts of the RNase trimer (~40.0 kD). The dimer and trimer, after separation by cation exchange chromatography (Fig. 5.2, lane 5), exhibit a characteristic dityrosine fluorescence spectrum (data not shown). Furthermore, amino acid analysis demonstrates that the Tyr content of the RNase dimer is decreased by 50%, compared with native RNase (Table 5.1). This suggests that the LiP oxidation of Tyr residue(s), leading to intermolecular coupling of Tyr radicals to form dityrosine, is responsible for the LiP-

catalyzed polymerization of RNase. The peroxidase-catalyzed oxidation of both free tyrosine and Tyr residues in proteins has been reported, and the Tyr radicals couple to form covalently linked dityrosine, as shown in Fig. 5.8 (Amado et al., 1984). Tyr radicals in proteins can couple intramolecularly and/or intermolecularly.

Intermolecular coupling of Tyr radicals in proteins results in dimeric and more highly polymerized proteins (Amado et al., 1984). Tyrosine coupling in proteins is involved in several biological processes, including egg fertilization (Kay & Shapiro, 1987; Battaglia & Shapiro, 1988) and aging (Wells-Knecht et al., 1993).

Since RNase A does not contain free cysteines, the formation of intermolecular disulfide linkages between LiP-oxidized Cys residues would not occur. The reduction in the Met content of the oxidized monomers and dimers (Table 5.1) probably is due to the LiP-catalyzed oxidation of Met residues to methionine sulfoxide and methionine sulfone, as is observed with the LiP-catalyzed oxidation of Cc^{3+} (Sheng & Gold, 1998). The oxidation of Met would not lead to the polymerization of RNase. Therefore, the LiP-catalyzed polymerization of RNase appears to result from intermolecular dityrosine formation. Physicochemical experiments indicate that only three of the six Tyr in RNase (Tyr73, Tyr76, Tyr115) are at the protein surface (Eberhardt et al., 1996). These surface Tyr residues are probably the most susceptible to oxidation.

It has been reported that synthetic lignin containing free phenolic groups is partially polymerized, as well as depolymerized, by pure LiP *in vitro* (Hammel et al., 1993). This suggests that LiP oxidizes phenolic substituents in synthetic lignin to phenoxy radicals, which then couple to form polymerized products. This coupling reaction between phenoxy radicals in lignin probably occurs by a mechanism that is similar to the LiP-catalyzed coupling of Tyr radicals in RNase.

5.4.2 RNase oxidation and veratraldehyde formation

In the presence of 100 μ M H_2O_2 , the LiP oxidation of RNase is strictly dependent on VA (Fig. 5.1A). Furthermore, even high concentrations of VA do not inhibit RNase oxidation (Fig. 5.3). In contrast, the results in Fig. 5.4 demonstrate that the presence of RNase results in a lag in the LiP oxidation of VA. This is

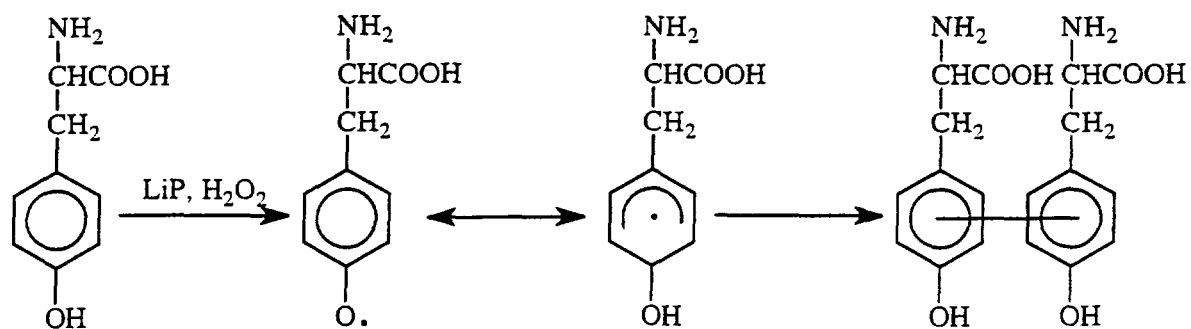


Figure 5.8 Proposed mechanism for the dimerization of tyrosine by peroxidases (Amado et al., 1984).

similar to the lag observed in the LiP oxidation of VA in the presence of guaiacol (Harvey & Palmer, 1990). As seen in Fig. 5.4, this lag time increases with increasing RNase concentrations. Only after all of the RNase is oxidized does the net oxidation of VA proceed (Fig. 5.4). The results in Table 5.2 confirm that VA oxidation is inhibited by RNase. In the presence of 500 μM VA, strong inhibition of VA oxidation to veratraldehyde is observed in the presence of as little as 20 μM RNase. Thus, VA stimulates RNase oxidation, but RNase inhibits VA oxidation. This strongly suggests that LiP preferentially oxidizes VA to the cation radical which, in turn, oxidizes RNase and thus is reduced back to VA without further oxidation to veratraldehyde.

5.4.3 LiP inactivation

The results of the LiP inactivation studies support the conclusion that VA mediates the oxidation of RNase. In the presence of 100 μM H_2O_2 , 500 μM VA prevents LiP inactivation but 50 μM VA does not. However, in the presence of 50 μM RNase and 20 μM VA together, 90% of the LiP activity is retained after 30 min (Fig. 5.5). Indeed, in the presence of 50 μM RNase, as little as 5 μM VA significantly protects LiP from inactivation. The spectral studies in Fig. 5.6 demonstrate that neither 100 μM VA nor 100 μM RNase alone can prevent the H_2O_2 -induced formation of LiPIII and LiPIII*, which are indicative of enzyme inactivation (Fig. 5.6, B and C). In contrast, 50 μM each of VA and RNase completely protect LiP from conversion to LiPIII and LiPIII* (Fig. 5.6D). The simplest explanation for these results is that LiP oxidizes VA to the cation radical, which rapidly turns over via the oxidation of Tyr and Met residues in RNase, thus enabling LiP to complete its catalytic cycle. These results further suggest the VA cation radical remains in its protein binding site, turning over by rapidly oxidizing RNase. Thus, the regenerated VA is available immediately to reduce LiPII, thereby preventing the formation of LiPIII*. The transient-state kinetics studies support this hypothesis.

5.4.4 Transient-state kinetics

At pH 3.0, RNase reduces both LiPI and LiPII, but the rates of LiPI and LiPII reduction are comparatively slow. The second-order rate constants for LiPI and LiPII reduction are $6.0 \times 10^4 \text{ M}^{-1}\text{s}^{-1}$ and $1.1 \times 10^4 \text{ M}^{-1}\text{s}^{-1}$, respectively (Table 5.3). In particular, the second-order rate constant for LiPII reduction by RNase is the same as that for the reaction between LiPII and H_2O_2 ($1.0 \times 10^4 \text{ M}^{-1}\text{s}^{-1}$) which results in the formation of LiPIII (Wariishi & Gold, 1990). Thus, in the presence of RNase, the reaction between LiPII and H_2O_2 would proceed, resulting in the formation of LiPIII and LiPIII* (Fig. 5.6, A and C). At equal concentrations of H_2O_2 and RNase, 50% of the LiPII would react with H_2O_2 to form LiPIII during each catalytic cycle, resulting in enzyme inactivation. However, conversion of the first-order rate constant for VA reduction of LiPII to a second-order rate constant (k/K_d) suggests that the reduction of LiPII by VA is 10–15 times faster than the reactions between LiPII and either H_2O_2 (Wariishi & Gold, 1990) or RNase (Table 5.3). Thus, high concentrations of VA alone can compete effectively with H_2O_2 , preventing the formation of LiPIII or LiPIII* (Fig. 5.5) (Wariishi & Gold, 1990). Most importantly, in the presence of equal concentrations of VA and RNase, LiPII reduction to the native enzyme proceeds by a first-order rather than a second-order reaction with no formation of LiPIII (Table 5.3). The values for the apparent binding constant (K_d) and for the electron transfer rate constant (k) are similar to those obtained with VA alone (Table 5.3). It is noteworthy that the reduction of LiPII by VA occurs via first-order kinetics, suggesting a binding equilibrium between VA and the enzyme, whereas the reduction of LiPII by RNase occurs via second-order kinetics. Finally, the reduction of LiPII in the presence of both RNase and VA occurs via first-order kinetics, suggesting that VA is the preferred substrate for LiPII and that RNase is oxidized by the VA cation radical. These results also indicate that the most efficient use of VA is as a mediator in which the VA cation radical formed by the reduction of LiPI is, in turn, reduced back to VA without leaving the binding site, enabling the regenerated VA to reduce LiPII. In the absence of a terminal substrate such as RNase or lignin, the VA cation radical would lose a proton to form the benzylic

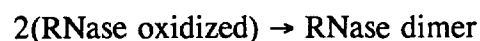
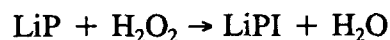
radical which might diffuse from the active site. This probably would be a slower process than electron transfer from a second substrate at the surface of the protein.

5.4.5 VA as a radical mediator

The results discussed above suggest that the most efficient mechanism would be for VA to turn over while still occupying its binding site, i.e., VA would act as a redox cofactor. If the VA cation radical were to leave its binding site to act as a diffusible mediator as has been suggested (Harvey & Palmer, 1990), another VA would have to bind before LiPII could be reduced. Under those conditions, H₂O₂ could react with LiPII to form LiPIII. In contrast, if, in the presence of a terminal substrate, VA were to turn over while still docked in its binding site, the formation of LiPIII would be prevented. This would explain the results in Figs. 5.5 and 5.6, which show that VA plus RNase protects LiP from inactivation, whereas the same concentration of VA alone does not prevent the formation of LiPIII.

Although no strong evidence for the diffusible mediator hypothesis has been reported, recent chemical and spectroscopic evidence also argues against this hypothesis. These studies indicate that the VA cation radical is too short-lived to diffuse away from the enzyme active site and oxidize a terminal substrate such as lignin or RNase (Khindaria et al., 1995, 1996; Joshi & Gold, 1996). For example, the LiP oxidation of dimethoxytoluene leads to dimer formation via the coupling of a cation radical with a neutral species. In contrast, the LiP oxidation of VA does not lead to dimer formation, strongly suggesting that the VA cation radical loses a benzylic proton to form the benzylic radical prior to diffusing away from the enzyme (Joshi & Gold, 1996). In addition, fast-flow electron spin resonance studies indicate that the free VA cation radical is very unstable ($t_{1/2} \sim 0.6$ ms), whereas the enzyme-bound cation radical is much more stable ($t_{1/2} \sim 370$ ms) (Khindaria et al., 1995, 1996). Taken together, the evidence strongly suggests that if VA is a radical mediator, it needs to act as an enzyme-bound redox cofactor rather than as a diffusible species.

All of the results described suggest the mechanism in Scheme 1 for the VA-mediated oxidation of RNase by LiP.

Scheme I

In the presence of H_2O_2 , LiP is oxidized to form compound I. The latter is reduced to compound II with the production of the VA cation radical. The latter, while still bound to LiP, oxidizes RNase with the generation of a LiPII-VA complex. The same VA molecule is then oxidized to a cation radical, preventing the formation of compound III. The LiP-VA[†] complex then oxidizes RNase, completing the catalytic cycle. Finally, two molecules of oxidized RNase couple to form a dimer.

In conclusion, LiP oxidizes RNase to form an RNase dimer, apparently by oxidizing Tyr residues in the protein to Tyr radicals, which subsequently undergo intermolecular coupling. In the presence of H_2O_2 , this reaction is dependent on VA. Although VA is not an inhibitor of RNase oxidation, RNase is a strong inhibitor of VA oxidation. These results, in addition to the kinetic studies presented here and previous studies (Khindaria et al., 1995, 1996; Joshi & Gold, 1996), suggest that VA is acting as an enzyme-bound mediator in the oxidation of RNase and, by extension, in the LiP-catalyzed oxidation of lignin.

CHAPTER 6
HALOPEROXIDASE ACTIVITY OF MANGANESE PEROXIDASE
FROM *PHANEROCHAETE CHRYSOSPORIUM*

6.1 Introduction

White-rot basidiomycete fungi are capable of degrading the plant cell wall polymer lignin (Buswell et al., 1987; Kirk & Farrell, 1987; Gold et al., 1989) and a variety of aromatic pollutants (Bumpus & Aust, 1987; Hammel, 1989; Gold et al., 1994). When cultured under ligninolytic conditions, *P. chrysosporium* secretes two types of extracellular heme peroxidases, lignin peroxidase (LiP)** and manganese peroxidase (MnP), which, along with a H₂O₂-generating system, comprise the major components of its extracellular lignin-degrading system (Kuwahara et al., 1984; Buswell et al., 1987; Kersten & Kirk, 1987; Kirk & Farrell, 1987; Gold et al., 1989; Wariishi et al., 1991b; Gold & Alic, 1993). Both LiP and MnP are able to depolymerize lignin *in vitro* (Wariishi et al., 1991b; Hammel et al., 1993; Bao et al., 1994), and MnP activity has been found in all lignin-degrading fungi that have been examined (Périé & Gold, 1991; Orth et al., 1993; Hatakka, 1994).

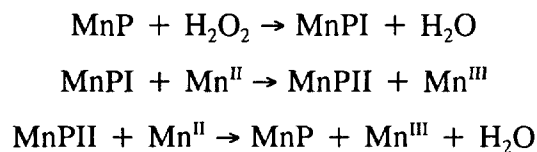
MnP has been purified from *P. chrysosporium* cultures and characterized biochemically and kinetically (Glenn & Gold, 1985; Glenn et al., 1986; Gold et al., 1989; Wariishi et al., 1992b; Gold & Alic, 1993; Kishi et al., 1994). The sequences

* Reprinted with permission from: Sheng, D. and Gold, M. H. (1997) Haloperoxidase activity of manganese peroxidase from *Phanerochaete chrysosporium*. *Arch. Biochem. Biophys.* **345**, 126-134. Copyright 1997 Academic Press.

** Abbreviations used: BSTFA, *N,O*-bis(trimethylsilyl) trifluoroacetamide; CPO, chloroperoxidase; MCD, monochlorodimedone, HPLC, high-performance liquid chromatography; HRP, horseradish peroxidase; LiP, lignin peroxidase; MnP, manganese peroxidase; MnPI and MnPII, manganese peroxidase compounds I and II; MPO, myeloperoxidase; TLC, thin-layer chromatography; VA, veratryl (3,4-dimethoxy)benzyl alcohol.

of cDNA and genomic clones encoding three *P. chrysosporium* MnP isozymes have been determined (Pease et al., 1989; Pribnow et al., 1989; Goldfrey et al., 1990; Gold & Alic, 1993; Mayfield et al., 1994a; Orth et al., 1994; Alic et al., 1997). Spectroscopic studies (Dunford & Stillman, 1976; Glen & Gold, 1985; Mino et al., 1988; Wariishi et al., 1988, 1992b; Harris et al., 1991; Banci et al., 1992), and DNA sequences demonstrate that the heme environment of MnP is similar to that of other plant and fungal peroxidases. Kinetic and spectral characterizations of the oxidized intermediates, MnP compounds I and II (MnPI and II), indicate that the catalytic cycle of MnP is similar to that of LiP and horseradish peroxidase (HRP) (Dunford & Stillman, 1976; Glenn et al., 1986; Renganathan & Gold, 1986; Wariishi et al., 1988; Gold et al., 1989). The crystal structure of MnP (Sundaramoorthy et al., 1994) confirms that the heme environment of MnP is similar to that of other heme peroxidases. However, MnP is unique in its ability to oxidize Mn^{II} to Mn^{III} (Glen & Gold, 1985; Glenn et al., 1986; Wariishi et al., 1992b), as shown in Scheme I.

Scheme I



The enzyme-generated Mn^{III} is stabilized by organic acid chelators such as oxalate which is secreted by the fungus (Wariishi et al., 1992b; Kuan et al., 1993; Kishi et al., 1994). The Mn^{III}-organic acid complex oxidizes the terminal substrate, including lignin substructures (Tuor et al., 1992) and aromatic pollutants (Joshi & Gold, 1993; Gold et al., 1994).

Halide ions are oxidized by a unique peroxidase mechanism, as compared with other electron donors. Most electron donors are oxidized by compound I via a single-electron mechanism with the intermediate formation of compound II (Scheme I); whereas, halides are oxidized by compound I via a two-electron mechanism, yielding the native enzyme directly (Morison & Schonbaum, 1976; Griffin, 1991). Heme peroxidases from a variety of sources exhibit various haloperoxidase activities.

Chloroperoxidase (CPO) and myeloperoxidase (MPO) oxidize chloride, bromide, and iodide (Neidleman & Geigert, 1986); whereas, HRP and LiP catalyze only the oxidation of bromide and iodide (Neidleman & Geigert, 1986; Renganathan et al., 1987). In this study, we demonstrate that MnP from *P. chrysosporium* oxidizes bromide and iodide in the absence of Mn at low pH. We also show that, in the absence of an organic substrate, MnP is inactivated during the oxidation of bromide.

6.2 Experimental Procedures

6.2.1 Enzyme preparation

Wild-type MnP isozyme 1 and MnP variants D179N and E35Q-D179N were expressed and isolated as previously described (Glenn & Gold, 1985; Wariishi et al., 1992b; Kusters-van Someren et al., 1995; Kishi et al., 1996). The purified MnPs were free of LiP activity, as determined by the veratryl alcohol assay (Kirk & Farrell, 1987; Gold et al., 1989). The purified enzymes were electrophoretically homogeneous and had *RZ* ($A_{406/280}$) values of ~ 5.0 . An extinction coefficient of $129 \text{ mM}^{-1} \text{ cm}^{-1}$ at 406 nm was used to determine MnP enzyme concentration.

6.2.2 Chemicals

Veratryl (3,4-dimethoxybenzyl) alcohol (VA), cinnamic acid, and 3,4-dimethoxycinnamic acid were obtained from Aldrich. VA was purified by silica gel column chromatography (ethyl acetate:hexane 1:1). Cinnamic acid and 3,4-dimethoxycinnamic acid were recrystallized from ethanol before use. H_2O_2 and monochlorodimedone (MCD) were obtained from Sigma. The concentration of H_2O_2 in stock solutions was determined as described (Cotton & Dunford, 1973). Sodium halides were analytical grade.

6.2.3 Enzyme assays

The enzymatic oxidation of halides was measured by following the formation of their tribromide and triiodide complexes. Oxidation rates were calculated using an extinction coefficient of $3.6 \times 10^4 \text{ M}^{-1} \text{ cm}^{-1}$ at 266 nm for the tribromide complex

(Libby et al., 1982) and $2.5 \times 10^4 \text{ M}^{-1} \text{ cm}^{-1}$ at 353 nm for the triiodide complex (Cotton & Dunford, 1973). Reactions were initiated by the addition of enzyme and were monitored at room temperature.

For iodide oxidation, reaction mixtures contained MnP (0.1 $\mu\text{g}/\text{ml}$) and iodide (0.5–40 mM) in 20 mM sodium succinate, pH 3.0. The reaction was initiated by addition of H_2O_2 (0.1 mM). $1/V$ versus $1/[\text{iodide}]$ was plotted at a fixed concentration of H_2O_2 . Since MnP inactivation was observed during bromide oxidation in the absence of an organic substrate, steady-state kinetic studies were not carried out with bromide.

6.2.4 Transient-state kinetics

Kinetic measurements were conducted at $25 \pm 0.5^\circ\text{C}$ using an Applied Photophysics stopped-flow reaction analyzer (SX.18MV) with sequential mixing. One syringe contained enzyme in 20 mM sodium succinate, pH 3.0, and the other syringe contained 1 equiv of H_2O_2 in the same buffer. These two components were mixed and incubated for 4 s, and compound I formation was confirmed by rapid-scanning spectroscopy, using the diode array detector accessory for the Applied Photophysics instrument. Four seconds after the reaction was started, halides were added with the third syringe. The final halide concentration was at least 10-fold in excess of the enzyme. Rapid-scan spectra indicated that the reduction of MnP compound I by halides was a single two-electron process with the direct formation of native enzyme. Therefore, the rate of MnP compound I reduction by halide was followed at 406 nm, the Soret band of the native enzyme. All kinetic traces exhibited single-exponential character from which pseudo-first-order rate constants were calculated.

6.2.5 Inactivation of MnP

MnP inactivation during bromide oxidation was monitored by following the decrease in the Soret band at 406 nm. Reaction mixtures consisted of MnP (1 μM), sodium bromide (20 mM), and H_2O_2 (40 μM) in the presence or absence of VA (0.5 mM). Reactions were initiated by the addition of H_2O_2 , and spectra were recorded periodically. Inactivation also was monitored by the Selwyn test (Sellwyn, 1965;

Wariishi et al., 1994). In this case, the rates of tribromide and triiodide formation at pH 3.0 were plotted against (MnP concentration \times time) at three MnP concentrations. MnP concentrations of 0.5, 1, and 2 $\mu\text{g}/\text{ml}$ were used for bromide oxidation, and MnP concentrations of 0.025, 0.05, and 0.1 $\mu\text{g}/\text{ml}$ were used for iodide oxidation. To compensate for the differences in enzyme concentration, the recorder chart speed was varied accordingly.

6.2.6 Halide binding

Both the reference and sample cuvettes contained MnP (1 μM) in 20 mM sodium succinate, pH 3.0, or as indicated. Halides in the same buffer were added to the sample cuvette, the same volume of buffer was added to the reference cuvette and difference spectra were determined from 500–300 nm. The apparent dissociation constants (K_D) were calculated from plots of $1/\Delta A$ versus $1/[\text{halide}]$, where ΔA was the difference between the maximum and minimum absorptions.

6.2.7 Bromination of organic substrates

Reaction mixtures contained 20 mM sodium succinate, pH 3.0, NaBr (20 mM), H_2O_2 (0.1 mM), MnP (1 $\mu\text{g}/\text{ml}$), and aromatic substrates (VA, 3,4-dimethoxycinnamic acid, or cinnamic acid) (0.5 mM) or non-aromatic substrates (malonic acid or MCD) (4 mM). Reactions were incubated at room temperature for 30 min and stopped by acidification with HCl. Mixtures were extracted with ethyl acetate, dried over anhydrous Na_2SO_4 , and evaporated under nitrogen. Products were derivatized by silylation (BSTFA/pyridine, 2:1 v/v) or by methylation (freshly prepared diazomethane) and identified by GC-MS. GC-MS was performed at 70 eV with a VG Analytical 7070E mass spectrometer fitted with an HP 5790A GC and a 15-m fused silica column (DB-5, J & W Scientific).

6.3 Results

6.3.1 Haloperoxidase activity

The MnP-catalyzed oxidation of bromide to bromine was monitored by measuring the formation of the tribromide complex which has a characteristic spectrum with a maximum at 266 nm (Fig. 6.1A) (Libby et al., 1982; Renganathan et al., 1987). MnP also catalyzed the oxidation of iodide as measured by the formation of the triiodide complex. The spectrum of the latter, exhibiting maxima at 285 and 353 nm, is shown in Fig. 6.1B (Brown & Haer, 1967). Identical spectra for the tribromide and triiodide complexes were observed when either LiP or HRP was used to oxidize bromide or iodide.

The pH dependence of the MnP-catalyzed oxidation of bromide and iodide is shown in Fig. 6.2. The rates of bromide oxidation by MnP increased with decreasing pH in the range 5.0–2.5. Owing to enzyme inactivation during bromide oxidation, the rates of tribromide formation probably were underestimated. The rates of iodide oxidation also increased with decreasing pH, reaching a maximum at pH 3.0.

6.3.2 Steady-state kinetics studies

Under steady-state conditions, linear Lineweaver-Burk plots were obtained over a range of iodide concentrations in 20 mM succinate, pH 3.0 (data not shown). The kinetic parameters for iodide oxidation by the wild-type MnP and MnP variants are summarized in Table 6.1. The apparent K_m values for the wild-type MnP and the MnP variants were ~ 4.0 mM. The apparent k_{cat} values for the wild-type MnP, the D179N variant, and the E35Q-D179N double variant were 270, 210, and 220 s^{-1} , respectively. Thus, the kinetic parameters for iodide oxidation were not affected significantly by mutations of the Mn binding ligands. In contrast, for Mn^{II} oxidation by MnP, a significant difference in the kinetic parameters was observed between wild-type MnP and the MnP variants (Table 6.1). The apparent K_m values for Mn^{II} oxidation by the D179N variant and the E35Q-D179N double variant were 50 and 110-fold higher, respectively, than that of wild-type MnP. The apparent k_{cat} values for Mn^{II} oxidation by the D179N and E35Q-D179N variants were 300 and 1000-fold lower than that for wild-type MnP.

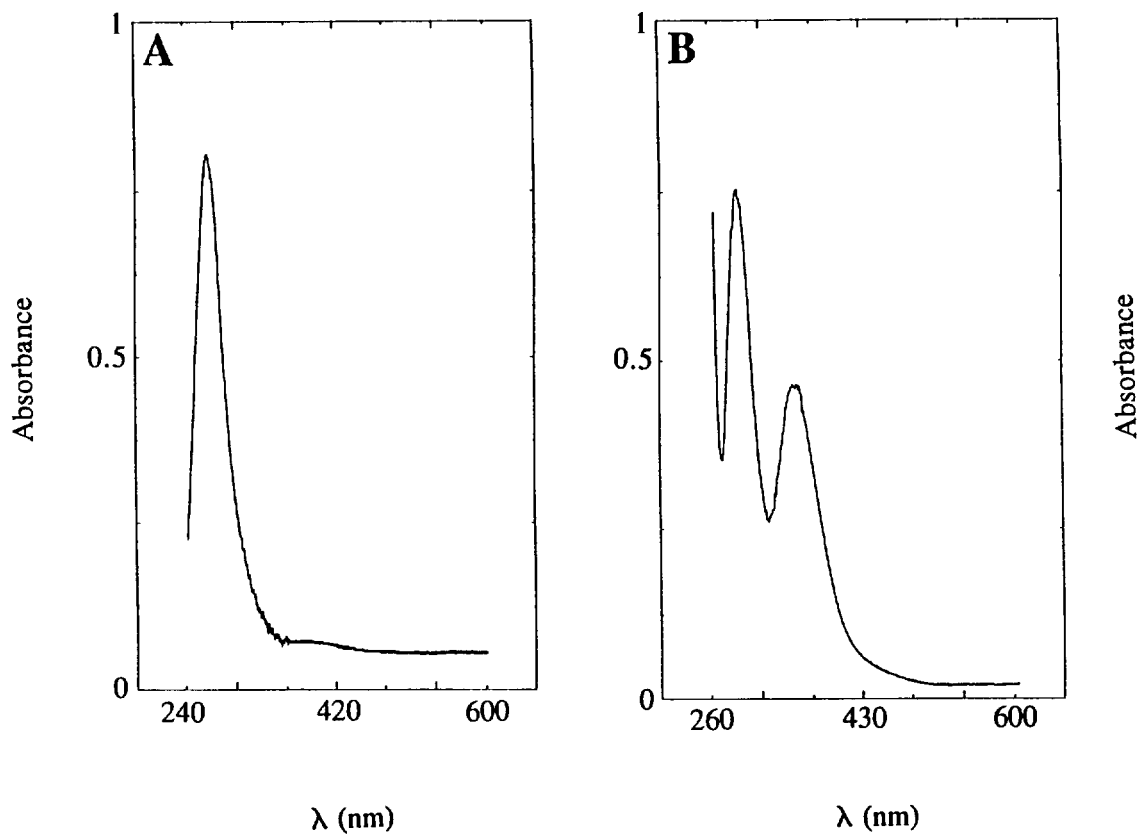


Fig. 6.1 MnP-catalyzed formation of triiodide and tribromide complexes. **(A)** Reaction mixture (1 mL) consisted of MnP (1 μg), bromide (20 mM), and H_2O_2 (0.1 mM). **(B)** Reaction mixture (1 mL) consisted of MnP (0.1 μg), iodide (20 mM), and H_2O_2 (0.1 mM). Reactions were carried out in 20 mM sodium succinate, pH 3.0.

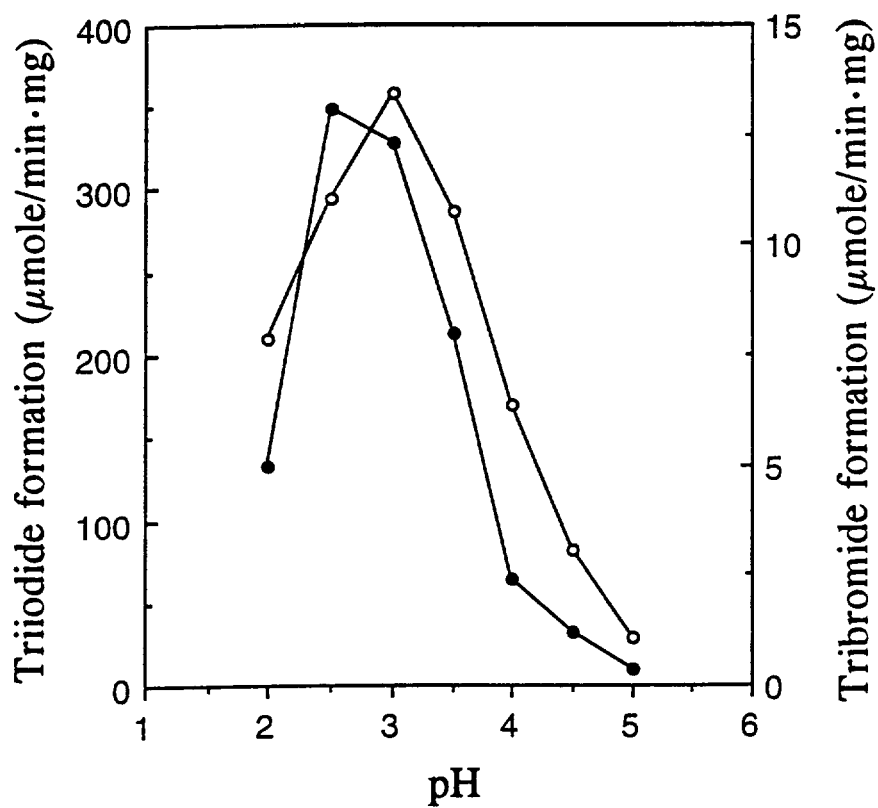


Fig. 6.2 pH dependence of MnP-catalyzed iodide and bromide oxidations. Triiodide (\circ) and tribromide (\bullet) formations were followed by measuring the increase in absorbance at 353 nm and 266 nm, respectively. The reaction conditions were similar to those described in the legend to Fig. 6.1, except 20 mM sodium succinate of various pHs was used.

Table 6.1

Steady-State Kinetic Parameters of Mn^{II}
and I⁻ Oxidations by Wild-Type MnP, MnP D179N, and MnP E25Q-179N

	Mn ^{II} ^a		I ⁻	
	K_m app (μ M)	k_{cat} app (s ⁻¹)	K_m app (μ M)	k_{cat} app (s ⁻¹)
Wild-type MnP	73	3.0×10^2	4.0×10^3	2.7×10^2
MnP D179N	3.7×10^3	1.1	3.7×10^3	2.1×10^2
MnP E35Q-D179N	8.1×10^3	0.29	4.2×10^3	2.2×10^2

^a Kishi et al., 1996.

6.3.3 Reduction of peroxidase compound I by halides

During the reaction of MnPI with either bromide or iodide, the rapid-scan spectra revealed an isosbestic point between compound I and the native enzyme at 426 nm, indicating that this was a single two-electron reaction (data not shown). Therefore, reduction of compound I to the native enzyme was followed at 406 nm, the Soret peak of the native enzyme. Each trace displayed single-exponential character. For the reduction of MnPI with either bromide or iodide, the plots of k_{obs} versus halide ion concentration were linear and passed through the origin within experimental error, suggesting that the reaction obeyed second-order kinetics and was irreversible (Fig. 6.3). The rate constants for the reaction of MnPI with bromide and iodide were determined to be $(4.1 \pm 0.2) \times 10^3$ and $(1.1 \pm 0.1) \times 10^5 \text{ M}^{-1} \text{ s}^{-1}$, respectively.

6.3.4 Identification of bromination products

In the presence of H_2O_2 and bromide, MnP brominated MCD. The MnP- and CPO-catalyzed MCD bromination products migrated identically ($R_f = 0.86$) on TLC (hexane:ethyl acetate:acidic acid 15:50:1), demonstrating that MnP produced 1-bromo-1-chloro-dimedone (Fig. 6.4). MnP also brominated malonic acid to form 2-bromo-malonic acid, which was identified as its dimethyl ester by comparison of its GC retention time and MS fragmentation pattern with the standard. MS: m/z (dimethyl ester) 210, 212 (M^+), 179, 181 ($\text{M}^+ - \text{OCH}_3$). Brominated aromatic products were identified by comparison of their retention times on HPLC and comparison of their fragmentation patterns on GC-MS with the same products produced by LiP. The LiP-generated products were unambiguously identified previously by NMR (Renganathan, 1987). The major product produced by the MnP bromination of VA was identified as 2-bromo-4,5-dimethoxybenzyl alcohol (II). MS: m/z (trimethylsilyl (TMS) ether) 320, 318 (M^+), 231, 229 ($\text{M}^+ - \text{OTMS}$). Two brominated products were formed when 3,4-dimethoxycinnamic acid (III) was used as a substrate. The first was identified as *trans*-2-bromo-1-(3,4-dimethoxyphenyl) ethylene (IV). MS: m/z 244, 242 (M^+), 229, 227 ($\text{M}^+ - \text{CH}_3$). The second was identified as 2-bromo-3-(3,4-dimethoxyphenyl)-3-hydroxypropionic acid (V). MS:

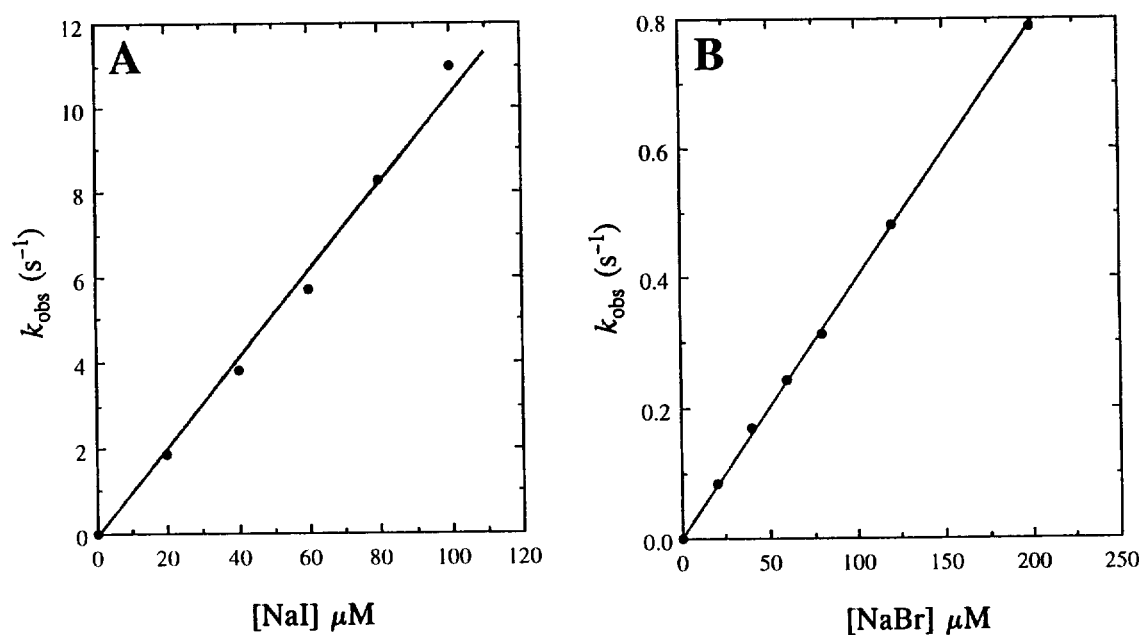


Fig. 6.3 Transient-state kinetics for the reduction of MnP compound I by bromide (A) and iodide (B). Reactions were conducted in 20 mM sodium succinate, pH 3.0. Each trace exhibited single-exponential character. k_{obs} were plotted against halide concentrations.

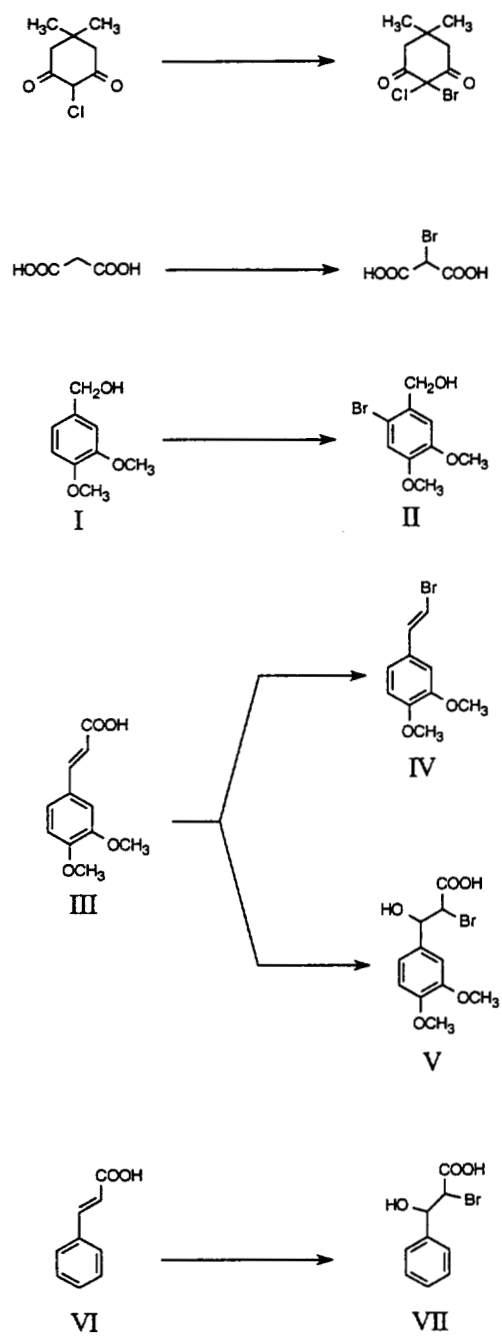


Fig. 6.4 Products obtained from the bromination of various substrates by MnP.

m/z (di-TMS) 450, 448 (M^+), 369 ($M^+ - Br$). With cinnamic acid (VI) as the substrate, 2-bromo-3-hydroxy-3-phenylpropionic acid (VII) was identified as the major product. MS: m/z (di-TMS) 375, 373 ($M^+ - CH_3$), 309 ($M^+ - Br$) (Fig. 6.4).

6.3.5 Halide binding

MnP bound halides to produce characteristic difference spectra. At pH 3.0, the bromide-MnP difference spectrum exhibited a maximum of 401 nm and a minimum of 360 nm (Fig. 6.5). The binding of bromide at pH 3.0 and 4.5 gave K_D of 45 and 700 mM, respectively. K_D of 13 and 20 mM were determined for fluoride and chloride, respectively, at pH 3.0 (data not shown). The binding of iodide to MnP was not observed under these experimental conditions, suggesting that iodide binding to MnP was weak.

6.3.6 Enzyme inactivation

At pH 3.0, the addition of H_2O_2 to MnP resulted in enzyme inactivation. The red shift in the Soret band from 406 to 419 nm suggested the formation of MnP compound III (Fig. 6.6A). In contrast, in the presence of bromide, the addition of H_2O_2 to MnP resulted in the bleaching of the Soret band, but no band shift was observed (Fig. 6.6B). Finally, in the presence of a substrate such as VA (0.5 mM), the addition of bromide and H_2O_2 resulted in neither a shift nor a decrease in the Soret band (Fig. 6.6C).

The effect of MnP inactivation on the rates of bromide and iodide oxidation at pH 3.0 is shown in Fig. 6.7. In these experiments, the formation of tribromide and triiodide was plotted against (MnP concentration \times time) at three different MnP concentrations (Selwyn, 1965; Wariishi et al., 1994). The results demonstrated that the enzyme was inactivated during bromide oxidation. However, during MnP-catalyzed iodide oxidation, little MnP inactivation was observed.

In the presence of Mn, the MnP oxidation of bromide, but not of iodide, was strongly inhibited. At pH 3.0, the concentrations of $MnSO_4$ which resulted in half maximal and total inhibition were 3.5 and 24 μM , respectively.

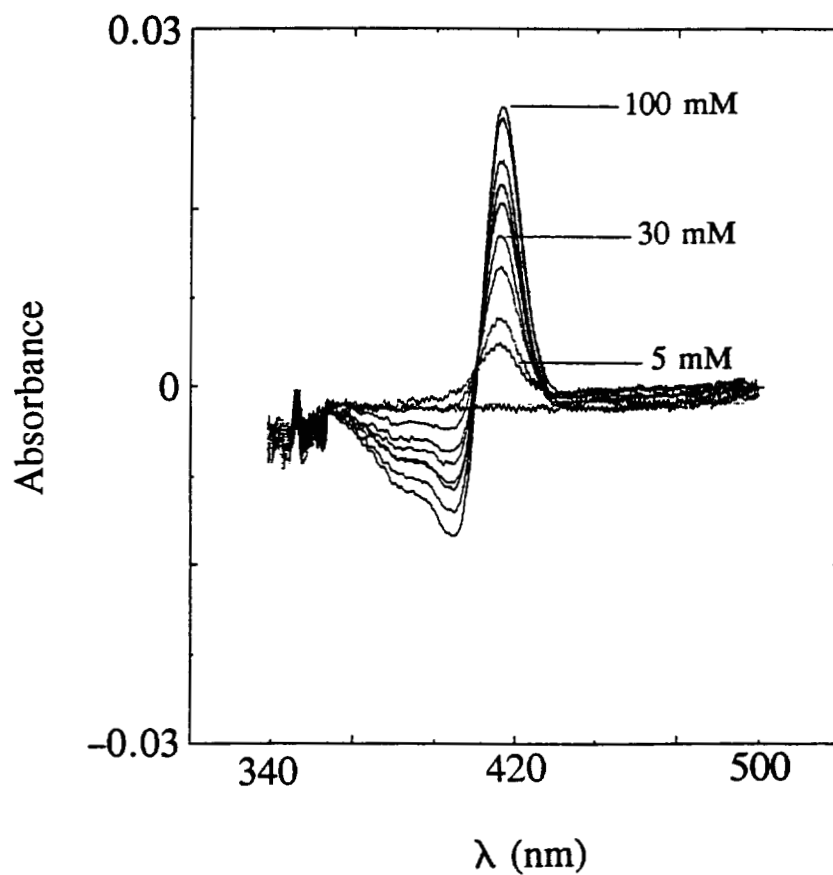


Fig. 6.5 Bromide binding to MnP. Both the reference and sample cuvettes contained MnP ($1 \mu\text{M}$) in 20 mM sodium succinate, pH 3.0. Spectra were recorded after each addition of bromide to the sample cuvette.

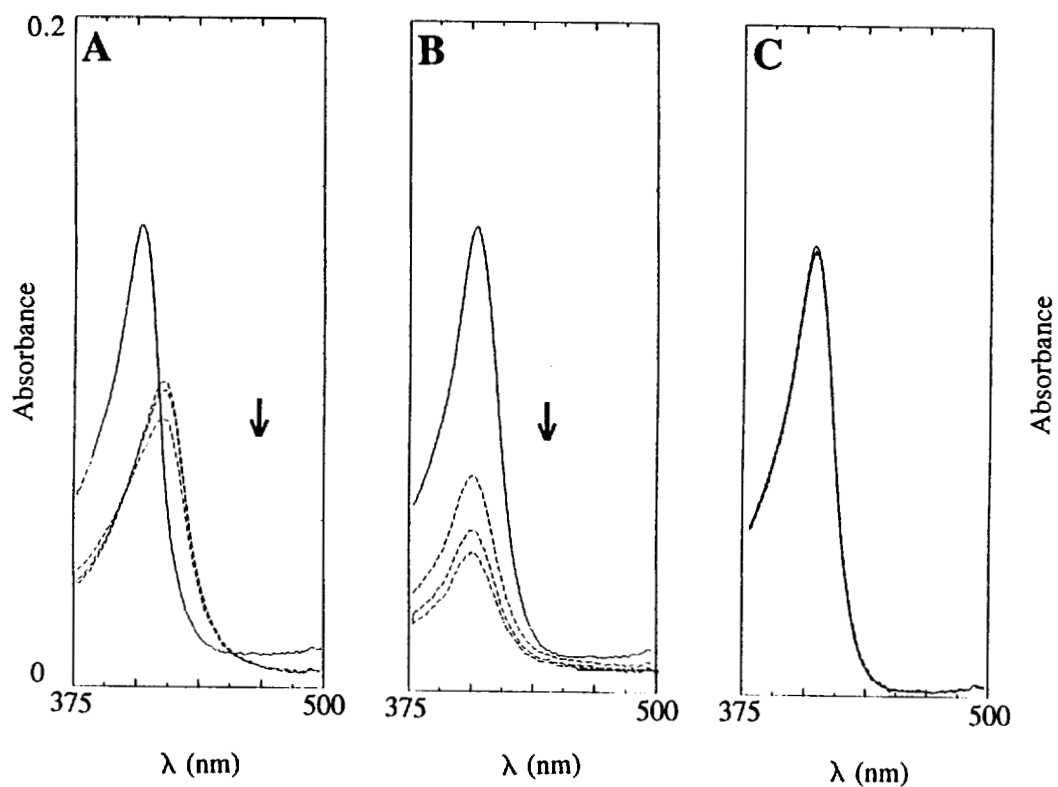


Fig. 6.6 Bleaching of the heme prosthetic group of MnP. Visible spectra of MnP were recorded at 2-min intervals after addition of substrate. Reactions were conducted in 20mM sodium succinate, pH 3.0. (A) MnP ($1.2 \mu\text{M}$), H_2O_2 ($50 \mu\text{M}$). (B) Same as A but with the addition of bromide (20 mM). (C) Same as B but with the addition of VA (0.5 mM). Arrows indicate increasing time.

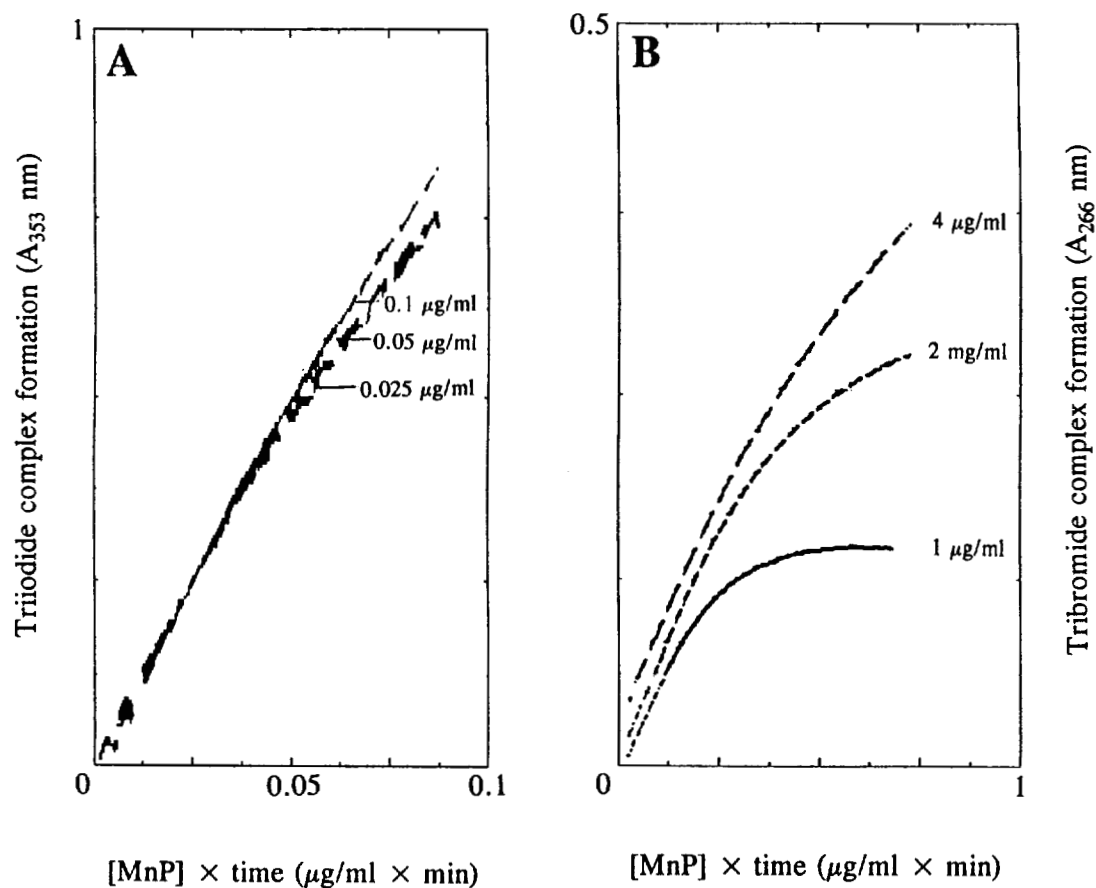


Fig. 6.7 MnP inactivation assay (Selwyn test). The amounts of triiodide (A) and tribromide (B) produced were plotted against (enzyme concentration \times time) as described (44, 45). Assays were carried out in 1 mL of 20 mM sodium succinate, pH 3.0. (A) Reaction mixtures contained 20 mM potassium iodide, 0.1 mM H_2O_2 , and either 0.025, 0.05, or 0.1 μg of MnP. (B) Reaction mixtures contained 20 mM potassium bromide, 0.1 mM H_2O_2 , and either 1, 2, or 4 μg of MnP. The recorder chart speed was adjusted to compensate for the enzyme concentrations used.

6.4 Discussion

Although the catalytic cycle of MnP is similar to that of other plant and fungal peroxidases (Dunford & Stillman, 1976; Renganathan & Gold, 1986; Gold et al., 1989; Wariishi et al., 1989, 1992b), this enzyme is unique in that it oxidizes Mn^{II} to Mn^{III} (Glenn et al., 1986; Wariishi et al., 1989, 1992b). The latter, complexed with an organic acid chelator, in turn oxidizes the terminal phenolic substrate. In the present study, we demonstrate that, like several other heme peroxidases (Morrison & Schonbaum, 1976; Renganathan et al., 1987; Farhangrazi et al., 1992), MnP also catalyzes the oxidation of halides in the absence of Mn.

Haloperoxidase-mediated halogenation reactions are the major source of natural organohalogen compounds (Neidleman & Geigert, 1986). The haloperoxidase reaction pathways of heme-containing peroxidases involve the initial oxidation of the native ferric peroxidase by H₂O₂ to produce the two-electron oxidized state, compound I. It has been suggested that for the best-studied haloperoxidase, CPO, compound I in turn oxidizes the halide by two electrons to generate an Fe^{III}-hypohalite intermediate (Roman & Dunford, 1972; Libby et al., 1982). The latter rapidly transfers the halonium ion to the substrate to regenerate the ferric enzyme (Morrison & Schonbaum, 1976; Libby et al., 1982). However, whether CPO-catalyzed halogenation involves an enzyme-bound halogenating intermediate, EOX, or a diffusible agent, such as HOX/X₂ (Neidleman & Geigert, 1986; Marquez & Dunford, 1994; Libby et al., 1996), had not been clarified. However, a recent paper presents strong evidence that the chlorinating intermediate in MPO reactions is Cl₂ (Hazen et al., 1996). CPO and MPO oxidize chloride, bromide, and iodide (Neidleman & Geigert, 1986), whereas HRP, LPO, and LiP catalyze only the oxidation of bromide and iodide (Morrison & Schonbaum, 1976; Ashley & Griffin, 1981; Renganathan et al., 1987).

Under our experimental conditions, MnP oxidizes bromide and iodide, but not chloride. Since there is little steric hindrance in the binding of either chloride, bromide or iodide to peroxidase compound I (Libby et al., 1982; Farhangrazi et al., 1992), this suggests that the rate-limiting step in trihalide formation is probably the

reaction of compound I with the halide. At pH 3.0, the redox potentials of the redox couples of HOCl/Cl⁻, HOBr/Br⁻ and HOI/I⁻ are 1.36, 1.24 and 0.9 V, respectively. Therefore, the redox potential of the redox couple MnPI/ferric MnP should be between 1.24 and 1.36 V. Given this assumption, it is possible that the difference in redox potentials between the redox couples of compound I/ferric enzyme and HOX/X⁻ is the major factor determining the rate of trihalide complex formation. The rate of bromide and iodide oxidation increases with decreasing pH to reach a maximum around 3.0. In contrast, the pH optimum for Mn oxidation by MnP is ~4.5 (Glenn et al., 1986). The higher pH of Mn oxidation may reflect the effect of pH on the binding of Mn to binding site ligands as well as chelators.

The steady-state kinetic parameters for iodide oxidation by MnP and the MnP variants are shown in Table 6.1. The apparent K_m and k_{cat} values for iodide oxidation by wild-type MnP and the two MnP variants are similar. The two MnP variants contain mutations in the Mn binding site of MnP. These mutations in the Mn^{II} binding site dramatically change the catalytic properties of MnP towards Mn (Kusters-van Someren et al., 1995; Kishi et al., 1996) (Table 6.1). The k_{cat} for Mn^{II} oxidation by MnP (D179N) and MnP (E35Q-D179N) decrease 300- and 1000-fold with respect to that of wild-type MnP. The K_m values for MnP (D179N) and MnP (E35Q-D179N) are 60 and 110 times higher, respectively, than that of wild-type MnP (Table 6.1). These results suggest that Mn and halides bind at different sites in the MnP protein. Whereas Mn binds at the Mn binding site (Sundaaaramoorthy et al., 1994; Kishi et al., 1996), halides probably bind close to the Δ -meso edge of the heme (Sakurada et al., 1987). The steady-state kinetic parameters also suggest that these mutations in the Mn^{II} binding site do not alter the redox potential of the redox couple of MnPI and the ferric enzyme.

The transient-state kinetic results for the reduction of compound I by iodide and bromide are shown in Fig. 6.3. Plots of k_{obs} versus halide concentration are linear and pass through the origin, suggesting a second-order reaction as previously shown for iodide oxidation by HRP (Roman & Dunford, 1972). The second order rate constants for iodide and bromide oxidation are $(1.1 \pm 0.1) \times 10^5$ and $(4.1 \pm 0.2) \times 10^3 \text{ M}^{-1} \text{ s}^{-1}$, respectively. The second order rate constant for the HRP

oxidation of iodide was determined to be $1.5 \times 10^6 \text{ M}^{-1} \text{ s}^{-1}$ (Roman & Dunford, 1972). Since the binding of bromide to native MnP is stronger than the binding of iodide, this 29-fold increase in the second-order rate constant for iodide over bromide probably reflects the difference in the redox potentials of the two X^-/HOX couples. The second-order rate constant for compound I reduction by iodide, $(1.1 \pm 0.1) \times 10^5 \text{ M}^{-1} \text{ s}^{-1}$, agrees reasonably well with our steady-state value ($k_{\text{cat}}/K_{\text{m}}$) for iodide oxidation ($6.7 \times 10^4 \text{ M}^{-1} \text{ s}^{-1}$).

6.4.1 Bromination of organic substrates

MCD, a common haloperoxidase substrate, is brominated by MnP to produce 1-bromo-1-chloro-dimedone. The two carbonyl groups in this substrate make the α -carbon more acidic, facilitating the bromination reaction. Similarly, malonic acid is readily brominated to form bromomalonic acid (Fig. 6.4).

Aromatic rings in the lignin polymer contain from one to three alkoxy substitutions which increase their electron density. In addition, on the periphery of the polymer, double bonds from the precursor *p*-hydroxycinnamyl alcohol derivatives are conjugated to aromatic rings (Sarkanen, 1971). Since these functional groups are susceptible to halogenation, we chose to study the halogenation of lignin-related aromatic compounds, as well as VA, a secondary metabolite of *P. chrysosporium* (Buswell & Odier, 1987; Kirk & Farrell, 1987; Gold & Alic, 1993). The choice of these substrates simplifies the product profile, since MnP cannot directly oxidize non-phenolic aromatic substrates. MnP quantitatively brominates the 6-position of the aromatic ring of VA to produce 2-bromo-4,5-dimethoxybenzyl alcohol (Fig. 6.4). The olefin, 3,4-dimethoxycinnamic acid (III), is brominated and decarboxylated to form 2-bromo-1-(3,4-dimethoxyphenyl) ethylene (IV) and is hydrobrominated to form 2-bromo-3-(3,4-dimethoxyphenyl)-3-hydroxypropionic acid (V). In an analogous reaction, MnP catalyzes the addition of HOBr across the double bond of cinnamic acid (VI) to generate 2-bromo-3-hydroxy-3-phenylpropionic acid (VII). These results suggest that MnP might brominate lignin itself under appropriate conditions.

There is still discussion as to whether CPO-catalyzed halogenation involves an enzyme-bound halogenating intermediate, EOX, or a diffusible agent such as HOX/X₂

(Libby et al., 1982; Neidleman & Geigert, 1986; Hazen et al., 1996). MnP forms molecular bromine and iodine under the assay conditions and its bromoperoxidase reactions can be accounted for qualitatively by the reaction of HOBr/Br₂ with the substrates examined. At low pH, the equilibrium



favors the formation of Br₂, which is relatively stable (Cotton & Wilkinson, 1972). Thus, the increased halogenating activity of the enzyme as the pH decreases may reflect an increased concentration of Br₂.

6.4.2 Enzyme inactivation

Incubation of MnP with bromide and H₂O₂, in the absence of an organic substrate, leads to the bleaching of the heme prosthetic group. MnP forms tribromide and triiodide complexes under our experimental conditions, and, perhaps, the enzyme-produced Br₂/HOBr reacts with the heme prosthetic group, resulting in heme bleaching. Similar oxidative inactivation of LiP has been reported (Neidleman & Geigert, 1986). In the presence of an organic substrate, Br₂/HOBr will brominate/hydrobrominate the substrate, and this may protect the porphyrin from bromination. In contrast, during iodide oxidation in the absence of an organic substrate, no enzyme inactivation is observed. However, the redox potential of the redox couple HOI/I⁻ (0.9 V at pH 3.0) is lower than that of HOBr/Br⁻ (1.2 V at pH 3.0). In addition, compared to HOBr, HOI is unstable under acidic conditions (Cotton & Wilkinson, 1972). Perhaps for these reasons, the heme moiety is not as susceptible to iodination.

6.4.3 Halide binding to MnP

The peroxidases bind halide ions irrespective of their ability to oxidize halides (Morrison & Schonbaum, 1976). Fluoride and chloride, which are not substrates for MnP, form strong complexes with *K*_Ds of 0.13 and 20 mM, respectively. It has been suggested that an anion binding site near the heme is usually occupied by a dissociable carboxylate ion. At low pH values, the carboxyl group is protonated, releasing the site for halide binding (Thomas et al., 1970b). The binding of halide

ions to MnP increases with decreasing pH. The K_D for bromide increases dramatically from 40 mM at pH 3.0 to 700 mM at pH 4.5. The binding of halide ions to LiP, HRP, and CPO also increases with decreasing pH (Libby et al., 1982, 1996; Renganathan et al., 1987). $^1\text{H-NMR}$ experiments suggest that iodide binds to HRP at a distal site, equidistant from the 1- and 8-heme methyl groups and 6–10 Å from the heme iron (Sakurada et al., 1987). The location of the halide ion binding site in MnP is not known.

Free Mn^{II} inhibits the formation of MnP-catalyzed tribromide, but not triiodide. The concentrations of Mn leading to half-maximal and total inhibition are 3.5 and 24 μM , respectively. It is likely that the binding sites for bromide and iodide are identical, given the similar chemical properties of halides. Therefore, the inhibition of bromide, but not iodide, oxidation cannot be explained by a simple competitive or non-competitive mechanism. Enzymatic or chemically ($\text{Br}_2 + \text{NaBr}$) generated tribromide reacts with H_2O_2 at a considerable rate under our experimental conditions (pH 3.0), and free Mn^{II} can accelerate this reaction. Thus, the cosubstrate H_2O_2 may be depleted in these reactions. These observations may partially explain the inhibition of tribromide formation by Mn^{II} , although the exact mechanism is not understood.

In conclusion, we have demonstrated that MnP oxidizes bromide and iodide. As with LiP and CPO, MnP catalyzes the bromination of aromatic rings, 1,3-diketones, and α,β -olefins. We also have shown that, in the absence of an organic substrate, the oxidation of bromide results in the inactivation of the enzyme. It has been reported that white-rot fungi are important natural sources of halomethane (Harper, 1985). The possible physiological significance of halogenation reactions catalyzed by MnP and LiP will require the identification of other halogenated compounds produced by white-rot fungi.

CHAPTER 7

FINAL COMMENTS AND FUTURE DIRECTIONS

Although lignin peroxidase (LiP) shares common structural and mechanistic features with other peroxidases, it is unique in its ability to oxidize non-phenolic compounds with redox potentials beyond the reach of other plant and fungal peroxidases (Kirk & Farrell, 1987, Gold et al., 1989; Valli et al., 1990). Veratryl alcohol (VA), a secondary metabolite of *Phanerochaete chrysosporium*, stimulates the LiP-catalyzed oxidations of recalcitrant substrates, such as anisyl alcohol (AA) and 4-methoxymandelic acid (4-MMA) (Harvey et al., 1986). VA also stimulates the LiP-catalyzed oxidation of polymeric substrates, including ferrocyanochrome *c*, ferricytochrome *c*, and synthetic lignin, which are precluded from the LiP active site (Hammel et al., 1993; Wariishi et al., 1994; Sheng & Gold, 1998). Therefore, the involvement of VA in long-range electron transfer must be considered. It has been proposed that the VA cation radical, derived from the one-electron oxidation of VA by LiP, can function as a diffusible mediator to oxidize terminal substrates (Harvey et al., 1986). However, this proposal was strongly questioned by recent fast-flow electron spin resonance and chemical studies which suggest that the VA cation radical is too unstable to function as a diffusible mediator (Khindaria et al., 1995, 1996; Joshi & Gold, 1996). It also has been proposed that VA either converts LiPIII*, an inactive form of the enzyme, to the native enzyme or competes with H₂O₂ effectively to react with LiPII, preventing H₂O₂-derived inactivation of LiP (Valli et al., 1990; Wariishi & Gold, 1990; Koduri & Tien, 1994). However, these possibilities do not fully explain certain experimental phenomena, such as the stimulation of 4-methoxymandelic acid and ferrocyanochrome *c* oxidation by VA (Wariishi et al., 1994; Candeias & Harvey, 1995).

For my thesis research, I studied the oxidation of VA by LiP and the role of VA in the LiP-catalyzed oxidation of proteins. Chemical evidence for the formation of a VA cation radical and a benzylic radical during VA oxidation by LiP was obtained (Chapter 2). By using protein substrates as lignin model compounds, the role of VA in the LiP-catalyzed oxidation of polymeric compounds was studied (Chapters 3, 4 and 5). The results support a mechanism by which VA serves as an enzyme-bound cofactor in the LiP-catalyzed reaction. In addition, the haloperoxidase activity of Mn peroxidase (MnP) was studied (Chapter 6).

To further understand the role of VA in the LiP-catalyzed reaction and explore the applications of the LiP system in bioremediation, it would be useful to (i) elucidate the binding site of VA in LiP, (ii) identify other possible redox mediators besides VA, and (iii) select additional polymeric lignin model compounds which are more similar to natural lignins.

7.1 VA Binding Site of LiP

To date, direct observation of the LiP-VA complex from crystallographic studies has not been successful, probably owing to the weak binding of VA to the LiP protein and/or the conditions used to grow the crystal. However, molecular modeling studies suggest that VA binds in a pocket approximately 6–7 Å from the heme (Fig. 1.5). Fast-flow EPR studies demonstrate that the enzyme-bound VA cation radical exhibits a much longer half life than that of the free VA cation radical (Khindaria et al., 1996); however, the factors affecting the stability of this very reactive species have not been defined. It has been postulated that the carbohydrate at Ser334 on the protein surface at the entrance to the substrate channel stabilizes the VA cation radical (Schoemaker et al., 1994); however, there is no experimental evidence to support this proposal. Future studies on amino acids involved in VA binding and on stabilizing the VA cation radical would aid our understanding of the oxidation of VA by LiP and the role of VA in polymeric substrate oxidation. Site-directed mutagenesis will be a powerful tool in this study. A good expression system must be developed which allows separation of recombinant from endogenous LiP. A homogeneous expression

system has been successfully developed for recombinant MnP in *P. chrysosporium* (Mayfield et al., 1994b). In this expression system, the promoter region of the glyceraldehyde-3-phosphate dehydrogenase gene was used to drive expression of *mnp1*, the gene encoding MnP isozyme 1, in primary metabolic cultures of *P. chrysosporium*. Recombinant MnP was expressed and secreted by transformed cultures *P. chrysosporium* under primary metabolic growth conditions (high carbon and high nitrogen), whereas endogenous wild-type *mnp* genes are not expressed under these conditions. This system appears to be capable of expressing recombinant LiP (preliminary finding, our laboratory). Alternatively, protein engineering studies may provide another tool to express and isolate recombinant LiP. In this experiment, 18 nucleotides which encode 6 His residues could be attached to the 3' end of the *lip* gene. If the protein product of this gene is successfully produced and secreted, the mature LiP protein will have six additional His residues at the C-terminal compared to that of endogenous LiP. LiP protein with six adjacent His residues can be readily separated from endogenous LiP by a commercially available affinity column with Ni²⁺ as the affinity ligand.

Using either expression system, amino acid residues which are proposed to be involved in VA binding and/or in stabilizing the VA cation radical—in particular, His82, Gln222 and Ser334 (see Section 1.5.2.3, Fig. 1.5)—could be mutated by site-directed mutagenesis as was done for the binding site of MnP (Kusters-van Someren et al., 1995; Kishi et al., 1996). By examining the kinetic parameters of these LiP variants, we can obtain crucial information regarding the binding of VA, the electron transfer pathways between the buried heme in LiP and polymeric substrates, and factors involved in stabilizing the VA cation radical.

7.2 Other Aromatic Compounds as Redox Mediators of VA

One role of VA in protecting LiP from inactivation has been proposed. VA can convert LiPIII*, an inactive form of the enzyme, to native enzyme, and can also compete with H₂O₂ to react with LiPII to prevent LiP from undergoing H₂O₂-derived inactivation (Valli et al., 1990; Wariishi & Gold, 1990; Koduri & Tien, 1994).

However the efficiency of these reactions has been questioned. It also has been proposed that VA serves as a mediator in the stimulation of the oxidation of other substrates via formation of VA cation radicals (Joshi & Gold, 1994, 1996; Goodwin et al., 1995; Khindaria et al., 1995a,b; Koduri et al., 1996; Tien & Ma, 1997). The ideal mediator should be able to stimulate the enzyme-catalyzed reaction without being quickly consumed itself. In this context, VA may not be the best mediator because it is often oxidized to veratraldehyde during the oxidation of recalcitrant substrates (Harvey et al., 1986; Valli et al., 1990). Future experiments designed to identify other mediators besides VA would be useful. Indeed, certain wood-degrading fungi also secrete other aromatic compounds in addition to VA, such as anisyl alcohol and chloroanisyl alcohol (see Section 1.3). By examining the effect of these and other compounds on the LiP-catalyzed oxidation of polymeric protein substrates, such as ferricytochrome *c* and RNase A, we should be able to screen for better mediators. Furthermore, screening other methoxy-substituted benzyl alcohols may lead to the identification of additional compounds which can mediate LiP reactions. Indeed, preliminary results show that 3,5- and 2,5-dimethoxybenzyl alcohol, which are not readily converted to their aldehydes by LiP, successfully stimulate the oxidation of anisyl alcohol by LiP. Studies on the details of these reactions should provide insights into the mechanism of VA mediation in LiP reactions.

7.3 Studies of Lignin Oxidation by LiP

Detailed kinetic studies of lignin oxidation by LiP are made difficult by the heterogeneity and low solubility of both synthetic lignin and lignin extracted from wood.

There are several ways to increase the solubility of lignin. (i) Selection of a miscible organic-water solvent system to solubilize synthetic lignin and lignin extracted from wood. The organic solvent should be carefully selected, because LiP is inactivated/denatured by organic solvents. (ii) Modification of lignin by the introduction of hydrophilic groups, such as OH⁻ and SO³⁻, to the aromatic rings in

lignin. However, these groups will dramatically change the redox potentials of lignin and complicate the resultant analysis.

To date, obtaining homogeneous preparations of synthetic lignin and lignin extracted from wood has not been possible. Therefore, studies with suitable model protein substrates are important. The advantage of using protein substrates for LiP is that many commercial proteins are homogeneous and have a high solubility in water, simplifying kinetic analyses. In addition, many proteins have a high molecular mass, which is comparable to that of lignin. In our current studies, we used ferricytochrome *c* and RNase A as polymeric model compounds to explore the mechanism of the LiP reaction. We showed that these proteins are dimerized owing to intermolecular coupling between tyrosine residues. These results also suggest that the native proteins may not be the most ideal lignin model compounds, because the redox potential of tyrosine is lower than that of the blocked aromatic nuclei in lignin. Therefore, it might be useful to change the redox potential of Tyr residues by suitable modification. First, we can block the phenoxy group in Tyr by alkylation. The alkyl groups could be methyl or ethyl groups. Secondly, we can modify Tyr residues by hydroxylation/methylation. By this method, we might introduce another phenoxy group to the Tyr residue by tyrosine hydroxylase; subsequently the phenol could be methylated. Alternatively, we could oxidize Tyr residues by tyrosinase to an ortho-quinone, followed by reduction and methylation. Provided these enzymes catalyze reactions with Tyr residues in protein, these modifications may increase the redox potential of Tyr residues in the protein substrates. With these modified proteins, which may be more comparable to natural lignin in terms of molecular weight and redox potential, we may be able to obtain more useful information about the LiP-catalyzed oxidations of polymeric compounds, including lignins.

LITERATURE CITED

- Adediran, S. A., and Lambeir, A. M. (1989) Kinetics of the reaction of compound II of horseradish peroxidase with hydrogen peroxide to form compound III. *Eur. J. Biochem.* **186**:571-576.
- Adhi, T. P., Korus, R. A., and Crawford, D. L. (1989) Production of major extracellular enzyme during lignocellulose degradation by two streptomycetes in agitated submerged culture. *Appl. Environ. Microbiol.* **55**:1165-1168.
- Adler, E. (1977) Lignin chemistry. Past, present and future. *Wood Sci. Technol.* **11**:169-218.
- Akamatsu, Y., Ma, D. B., Higuchi, T., and Shimada, M. (1990) A novel enzymatic decarboxylation of oxalic acid by the lignin peroxidase system of white-rot fungus *Phanerochaete chrysosporium*. *FEBS Lett.* **269**:261-263.
- Alic, M., Akileswaran, L., and Gold, M. H. (1997) Characterization of the gene encoding manganese peroxidase isozyme 3 from *Phanerochaete chrysosporium*. *Biochim. Biophys. Acta* **1338**:1-7.
- Amado, R., Aeschbach, R., and Neukom, H. (1984) Dityrosine: *in vitro* production and characterization. *Methods Enzymol.* **107**:377-388.
- Ander, P., and Eriksson, K.-E. (1976) The importance of phenol oxidase activity in lignin degradation by the white-rot fungus *Sporotrichum pulverulentum*. *Arch. Microbiol.* **109**:1-8.
- Ander, P., Eriksson, K.-E., and Yu, H.-S. (1984) Metabolism of lignin-derived aromatic acids by wood-rotting fungi. *J. Gen. Microbiol.* **130**:63-68.
- Ander, P., Stoytshev, I., and Eriksson, K.-E. (1988) Cleavage and metabolism of methoxyl groups from vanillic and ferulic acids by brown-rot and soft-rot fungi. *Cellulose Chem. Technol.* **22**:255-266.
- Andersson, L. A., Renganathan, V., Loehr, T. M., and Gold, M. H. (1987) Lignin peroxidase: resonance Raman spectral evidence for compound II and for a temperature-dependent coordination-state equilibrium in the ferric enzyme. *Biochemistry* **26**:2258-2263.

- Araiso, T., Ronnberg, M., Dunford, H. B., and Ellfolk, N. (1980) The formation of the primary compound from hydrogen peroxide and *Pseudomonas* cytochrome *c* peroxidase. *FEBS Lett.* **118**:99-102.
- Aramayo, R., and Timberlake, W. E. (1990) Sequence and molecular structure of the *Aspergillus nidulans* *yA* (laccase I) gene. *Nucleic Acids Res.* **18**:3415.
- Archibald, F. S. (1992) The role of fungus-fibers contact in the biobleaching of kraft brownstock by *Trametes (Coriolus) versicolor*. *Holzforschung* **46**:305-310.
- Archibald, F., and Roy, B. (1992) Production of manganic chelates by laccase from the lignin-degrading fungus *Trametes (Coriolus) versicolor*. *Appl. Environ. Microbiol.* **58**:1496-1499.
- Ashley, P. L., and Griffin, B. W. (1981) Chloroperoxidase-catalyzed halogenation of antipyrine, a drug substrate of liver microsomal cytochrome P-450. *Arch. Biochem. Biophys.* **210**:167-178.
- Ator, M. A., and Ortiz de Montellano, P. R. (1987) Protein control of prosthetic heme reactivity. Reaction of substrates with the heme edge of horseradish peroxidase. *J. Biol. Chem.* **262**:1542-1551.
- Ator, M. A., David, S. K., and Ortiz de Montellano, P. R. (1987) Structure and catalytic mechanism of horseradish peroxidase. Regiospecific meso alkylation of the prosthetic heme group by alkylhydrazines. *J. Biol. Chem.* **262**:14954-14960.
- Balny, C., Anni, H., and Yonetani, T. (1987) A stopped-flow study of the reaction of cytochrome *c* peroxidase with hydroperoxides. *FEBS Lett.* **221**:349-354.
- Banci, L., Bertini, I., Pease, E. A., Tien, M., and Turano, P. (1992) ¹H NMR investigation of manganese peroxidase from *Phanerochaete chrysosporium*. A comparison with other peroxidases. *Biochemistry* **31**:10009-10017.
- Banci, L., Bertini, I., Bini, T., Tien, M., and Turano, P. (1993) Binding of horseradish, lignin, and manganese peroxidases to their respective substrates. *Biochemistry* **32**:5825-5831.
- Bao, W., Fukushima, Y., Jensen, K. A., Jr., Moen, M. A., and Hammel, K. E. (1994) Oxidative degradation of non-phenolic lignin during lipid peroxidation by fungal manganese peroxidase. *FEBS Lett.* **354**:297-300.
- Battaglia, D. E., and Shapiro, B. M. (1988) Hierarchies of protein cross-linking in the extracellular matrix: involvement of an egg surface transglutaminase in early stages of fertilization envelope assembly. *J. Cell Biol.* **107**:2447-2454.

- Bavendamm, W. (1928) Über das Vorkommen und den Nachweis von Oxydasen bei holzzerstorenden Pilzen. *Z. Pflanzenkr. Pflanzenschutz* **38**:257-276.
- Blanchette, R. A. (1991) Delignification by wood-decay fungi. *Annu. Rev. Phytopathol.* **29**:381-398.
- Bollag, J. M., Shuttleworth, K. L., and Anderson, D. H. (1988) Laccase-mediated detoxification of phenolic compounds. *Appl. Environ. Microbiol.* **54**:3086-3091.
- Bonnarme, P., and Jeffries, T. W. (1990) Mn(II) regulation of lignin peroxidases and manganese-dependent peroxidases from lignin-degrading white-rot fungi. *Appl. Environ. Microbiol.* **56**:210-217.
- Boominathan, K., and Reddy, C. A. (1992) cAMP-mediated differential regulation of lignin peroxidase and manganese-dependent peroxidase production in the white-rot basidiomycete *Phanerochaete chrysosporium*. *Proc. Natl. Acad. Sci. U.S.A.* **89**:5586-5590.
- Bourbonnais, R., and Paice, M. G. (1988) Veratryl alcohol oxidases from the lignin-degrading basidiomycete *Pleurotus sajor-caju*. *Biochem. J.* **255**:445-450.
- Bourbonnais, R., and Paice, M. G. (1990) Oxidation of non-phenolic substrates. An expanded role for laccase in lignin biodegradation. *FEBS Lett.* **267**:99-102.
- Brown, F. S., and Hager, L. P. (1967) Chloroperoxidase. IV. Evidence for an ionic electrophilic substitution mechanism. *J. Am. Chem. Soc.* **89**:719-720.
- Brown, J. A., Glenn, J. K., and Gold, M. H. (1990) Manganese regulates expression of manganese peroxidase by *Phanerochaete chrysosporium*. *J. Bacteriol.* **172**:3125-3130.
- Brown, J. A., Alic, M., and Gold, M. H. (1991) Manganese peroxidase gene transcription in *Phanerochaete chrysosporium*: activation by manganese. *J. Bacteriol.* **173**:4101-4106.
- Buffard, D., Breda, C., van Huystee, R. B., Asemota, O., Pierre, M., Ha, D. B., and Esnault, R. (1990) Molecular cloning of complementary DNAs encoding two cationic peroxidases from cultivated peanut cells. *Proc. Natl. Acad. Sci. U.S.A.* **87**:8874-8878.
- Bull, H. B., and Breese, K. (1966) Ionization of cytochrome. *Biochem. Biophys. Res. Commun.* **24**:74-78.

Bumpus, J. A., and Aust, S. D. (1987) Biodegradation of environmental pollutants by the white rot fungus *Phanerochaete chrysosporium*: involvement of the lignin-degrading system. *BioEssays* **6**:166-170.

Burdsall, H. H., and Eslyn, W. E. (1974) A new *Phanerochaete* with a *chrysosporium* imperfect state. *Mycotaxon* **1**:123-133.

Bushnell, G. W., Louie, G. V., and Brayer, G. D. (1990) High-resolution three-dimensional structure of horse heart cytochrome *c*. *J. Mol. Biol.* **214**:585-595.

Buswell, J. A., and Odier, E. (1987) Lignin degradation. *CRC Crit. Rev. Biotechnol.* **6**:1-60.

Candeias, L. P., and Harvey, P. J. (1995) Lifetime and reactivity of the veratryl alcohol radical cation. Implications for lignin peroxidase catalysis. *J. Biol. Chem.* **270**:16745-16748.

Catalano, C. E., Choe, Y. S., and Ortiz de Montellano, P. R. (1989) Reactions of the protein radical in peroxide-treated myoglobin. Formation of a heme-protein cross-link. *J. Biol. Chem.* **264**:10534-10541.

Chance, B., Powers, L., Ching, Y., Poulos, T., Schonbaum, G. R., Yamazaki, I., and Paul, K. G. (1984) X-ray absorption studies of intermediates in peroxidase activity. *Arch. Biochem. Biophys.* **235**:596-611.

Chivukula, M., Spadaro, J. T., and Renganathan, V. (1995) Lignin peroxidase-catalyzed oxidation of sulfonated azo dyes generates novel sulfophenyl hydroperoxides. *Biochemistry* **34**:7765-7772.

Choudhury, K., Sundaramoorthy, M., Mauro, J. M., and Poulos, T. L. (1992) Conversion of the proximal histidine ligand to glutamine restores activity to an inactive mutant of cytochrome *c* peroxidase. *J. Biol. Chem.* **267**:25656-25659.

Choudhury, K., Sundaramoorthy, M., Hickman, A., Yonetani, T., Woehl, E., Dunn, M. F., and Poulos, T. L. (1994) Role of the proximal ligand in peroxidase catalysis. Crystallographic, kinetic, and spectral studies of cytochrome *c* peroxidase proximal ligand mutants. *J. Biol. Chem.* **269**:20239-20249.

Chung, N., and Aust, S. D. (1995) Inactivation of lignin peroxidase by hydrogen peroxide during the oxidation of phenols. *Arch. Biochem. Biophys.* **316**:851-855.

Cotton, F. A., and Wilkinson, G. (1972) *Advanced Inorganic Chemistry*, 3rd ed., Interscience Publishers, New York.

Cotton, M. L., and Dunford, H. B. (1973) Studies on horseradish peroxidase. XI. On the nature of compounds I and II as determined from the kinetics of the oxidation of ferrocyanide. *Can. J. Chem.* **51**:582-587.

Crawford, R. L. (1981) *Lignin Biodegradation and Transformation*, Wiley-Interscience, New York.

Critchlow, J. E., and Dunford, H. B. (1972a) Studies on horseradish peroxidase. IX. Kinetics of the oxidation of *p*-cresol by compound II. *J. Biol. Chem.* **247**:3703-3713.

Critchlow, J. E., and Dunford, H. B. (1972b) Studies on horseradish peroxidase. X. The mechanism of the oxidation of *p*-cresol, ferrocyanide, and iodide by compound II. *J. Biol. Chem.* **247**:3714-3725.

Cui, F., and Dolphin, D. (1990) The role of manganese in model systems related to lignin biodegradation. *Holzforschung* **44**:279-283.

Cullen, D. (1997) Recent advances on the molecular genetics of ligninolytic fungi. *J. Biotechnol.* **53**:273-289.

Dawson, J. H. (1988) Probing structure-function relations in heme-containing oxygenases and peroxidases. *Science* **240**:433-439.

de Jong, E., Field, J. A., de Bont J. A. M. 1994. Aryl alcohols in the physiology of ligninolytic fungi. *FEMS Microbiol. Rev.* **13**:153-188.

DePillis, G. D., Wariishi, H., Gold, M. H., and Ortiz de Montellano, P. R. (1990) Inactivation of lignin peroxidase by phenylhydrazine and sodium azide. *Arch. Biochem. Biophys.* **280**:217-223.

DePillis, G. D., Sishta, B. P., Mauk, A. G., and Ortiz de Montellano, P. R. (1991) Small substrates and cytochrome *c* are oxidized at different sites of cytochrome *c* peroxidase. *J. Biol. Chem.* **266**:19334-19341.

Dolphin, D., Forman, A., Borg, D. C., Fajer, J., and Felton, R. H. (1971) Compounds I of catalase and horse radish peroxidase: π -cation radicals. *Proc. Natl. Acad. Sci. U.S.A.* **68**:614-618.

Dunford, H. B. (1982) Peroxidases. *Adv. Inorg. Biochem.* **4**:41-68.

Dunford, H. B. (1991) Horseradish peroxidase: structure and kinetic properties. In *Peroxidases in Chemistry and Biology*, Vol. 2, pp. 1-24 (J. Everse, K. E. Everse, and M. B. Grisham, Eds.), CRC Press, Boca Raton, FL.

- Dunford, H. B., and Cotton, M. L. (1975) Kinetics of the oxidation of *p*-aminobenzoic acid catalyzed by horseradish peroxidase compounds I and II. *J. Biol. Chem.* **250**:2920-2932.
- Dunford, H. B., and Stillman, J. S. (1976) On the function and mechanism of action of peroxidase. *Coord. Chem. Rev.* **19**:187-251.
- Eberhardt, E. S., Wittmayer, P. K., Templer, B. M., and Raines, R. T. (1996) Contribution of a tyrosine side chain to ribonuclease A catalysis and stability. *Protein Sci.* **5**:1697-1703.
- Ebersson, L., and Radner, F. (1991) Light-initiated and thermal nitration reactions during photolysis of naphthalene/tetranitromethane or 1-methoxynaphthalene/tetranitromethane in dichloromethane. *J. Am. Chem. Soc.* **113**:5825-5834.
- Ebersson, L., Hartshorn, M. P., Radner, F., and Robinson, W. T. (1992) The addition-elimination mechanism in the photonitration of naphthalene by tetranitromethane. *J. Chem. Soc. Commun.* 566-567.
- Edwards, S. L., Nguyen, H. X., Hamlin, R. C., and Kraut, J. (1987) Crystal structure of cytochrome *c* peroxidase compound I. *Biochemistry* **26**:1503-1511.
- Edwards, S. L., Raag, R., Wariishi, H., Gold, M. H., and Poulos, T. L. (1993) Crystal structure of lignin peroxidase. *Proc. Natl. Acad. Sci. U.S.A.* **90**:750-754.
- Eggert, C., Temp, U., Dean, J. F., and Eriksson, K.-E. (1996) A fungal metabolite mediates degradation of non-phenolic lignin structures and synthetic lignin by laccase. *FEBS Lett.* **391**:144-148.
- Erecínska, M., Oshino, N., Loh, P., and Brocklehurst, E. (1973) *In vitro* studies on yeast cytochrome *c* peroxidase and its possible function in the electron transfer and energy coupling reactions. *Biochim. Biophys. Acta* **292**:1-12.
- Eriksson, K.-E. L. (1990) Biotechnology in the pulp and paper industry. *Wood Sci. Technol.* **24**:79-101.
- Eriksson, K.-E., Pettersson, B., Volc, J., and Musilek, V. (1986) Formation and partial characterization of glucose-2 oxidase, a H₂O₂ producing enzyme in *Phanerochaete chrysosporium*. *Appl. Microbiol. Biotechnol.* **23**:257-262.
- Erman, J. E., and Vitello, L. B. (1980) The binding of cytochrome *c* peroxidase and ferricytochrome *c*. A spectrophotometric determination of the equilibrium association constant as a function of ionic strength. *J. Biol. Chem.* **255**:6224-6227.

Erman, J. E., Vitello, L. B., Miller, M. A., Shaw, A., Brown, K. A., and Kraut, J. (1993) Histidine 52 is a critical residue for rapid formation of cytochrome *c* peroxidase compound I. *Biochemistry* **32**:9798-9806.

Fahraeus, G., and Reinhammar, B. (1967) Large scale production and purification of laccase from cultures of the fungus *Polyporus versicolor* and some properties of laccase A. *Acta Chem. Scand.* **21**:2367-2378.

Farhangrazi, Z. S., Sinclair, R., Yamazaki, I., and Powers, L. S. (1992) Haloperoxidase activity of *Phanerochaete chrysosporium* lignin peroxidases H2 and H8. *Biochemistry* **31**:10763-10768.

Farhangrazi, Z. S., Copeland, B. R., Nakayama, T., Amachi, T., Yamazaki, I., and Powers, L. S. (1994) Oxidation-reduction properties of compounds I and II of *Arthromyces ramosus* peroxidase. *Biochemistry* **33**:5647-5652.

Farmer, V. C., Henderson, M. E. K., and Russell, J. D. (1960) Aromatic-alcohol-oxidase activity in the growth medium of *Polystictus versicolor*. *Biochem. J.* **74**:257-262.

Fawer, M. S., Stierli, J., Cliffe, S., and Fiechter, A. (1991) The characterisation of immobilised lignin peroxidase by flow injection analysis. *Biochim. Biophys. Acta* **1076**:15-22.

Felton, R. H., Romans, A. Y., Yu, N. T., and Schonbaum, G. R. (1976) Laser Raman spectra of oxidized hydroperoxidases. *Biochim. Biophys. Acta* **434**:82-89.

Fenn, P., and Kirk, T. K. (1981) Relationship of nitrogen to the onset and suppression of ligninolytic activity and secondary metabolism in *Phanerochaete chrysosporium*. *Arch. Microbiol.* **130**:59-65.

Ferguson-Miller, S., Brautigan, D. L., and Margoliash, E. (1979) The electron transfer function of cytochrome *c*. In *The Porphyrins*, Vol. 7, pp. 149-240 (D. Dolphin, Ed.), Academic Press, New York.

Ferrer, J. C., Ring, M., and Mauk, A. G. (1991) Recombinant cytochrome *c* peroxidase folds properly without conformational "annealing". *Biochem. Biophys. Res. Commun.* **176**:1469-1472.

Finzel, B. C., Poulos, T. L., and Kraut, J. (1984) Crystal structure of yeast cytochrome *c* peroxidase refined at 1.7-Å resolution. *J. Biol. Chem.* **259**:13027-13036.

Fishel, L. A., Villafranca, J. E., Mauro, J. M., and Kraut, J. (1987) Yeast cytochrome *c* peroxidase: mutagenesis and expression in *Escherichia coli* show tryptophan-51 is not the radical site in compound I. *Biochemistry* **26**:351-360.

- Fitzgerald, M. M., Trester, M. L., Jensen, G. M., McRee, D. E., and Goodin, D. B. (1995) The role of aspartate-235 in the binding of cations to an artificial cavity at the radical site of cytochrome *c* peroxidase. *Protein Sci.* **4**:1844–1850.
- Florence, T. M. (1985) The degradation of cytochrome *c* by hydrogen peroxide. *J. Inorg. Biochem.* **23**:131–141.
- Germann, U. A., and Lerch, K. (1986) Isolation and partial nucleotide sequence of the laccase gene from *Neurospora crassa*: amino acid sequence homology of the protein to human ceruloplasmin. *Proc. Natl. Acad. Sci. U.S.A.* **83**:8854–8858.
- Gilbertson, R. L. (1980) Wood-rotting fungi of North America. *Mycologia* **72**:1–49.
- Glenn, J. K., and Gold, M. H. (1985) Purification and characterization of an extracellular Mn(II)-dependent peroxidase from the lignin-degrading basidiomycete, *Phanerochaete chrysosporium*. *Arch. Biochem. Biophys.* **242**:329–341.
- Glenn, J. K., Morgan, M. A., Mayfield, M. B., Kuwahara, M., and Gold, M. H. (1983) An extracellular H₂O₂-requiring enzyme preparation involved in lignin biodegradation by the white rot basidiomycete *Phanerochaete chrysosporium*. *Biochem. Biophys. Res. Commun.* **114**:1077–1083.
- Glenn, J. K., Akileswaran, L., and Gold, M. H. (1986) Mn(II) oxidation is the principal function of the extracellular Mn-peroxidase from *Phanerochaete chrysosporium*. *Arch. Biochem. Biophys.* **251**:688–696.
- Godfrey, B. J., Mayfield, M. B., Brown, J. A., and Gold, M. H. (1990) Characterization of a gene encoding a manganese peroxidase from *Phanerochaete chrysosporium*. *Gene* **93**:119–124.
- Gold, M. H., and Alic, M. (1993) Molecular biology of the lignin-degrading basidiomycete *Phanerochaete chrysosporium*. *Microbiol. Rev.* **57**:605–622.
- Gold, M. H., and Cheng, T. M. (1978) Induction of colonial growth and replica plating of the white rot basidiomycete *Phanaerochaete chrysosporium*. *Appl. Environ. Microbiol.* **35**:1223–1225.
- Gold, M. H., Kuwahara, M., Chiu, A. A., and Glenn, J. K. (1984) Purification and characterization of an extracellular H₂O₂-requiring diarylpropane oxygenase from the white rot basidiomycete, *Phanerochaete chrysosporium*. *Arch. Biochem. Biophys.* **234**:353–362.
- Gold, M. H., Wariishi, H., and Valli, K. (1989) Extracellular peroxidases involved in lignin degradation by the white rot basidiomycete *Phanerochaete chrysosporium*. In *Biocatalysis in Agricultural Biotechnology*, Vol. 389, pp. 127–140 (J. R. Whitaker, P.

E. Sonnet, Eds.), ACS Symposium Series. American Chemical Society, Washington, DC.

Gold, M. H., Joshi, D. K., Valli, K., and Wariishi, H. (1994) Degradation of chlorinated phenols and chlorinated dibenzo-*p*-dioxins by *Phanerochaete chrysosporium*. In *Bioremediation of Chlorinated and Polycyclic Aromatic Hydrocarbon Compounds*, pp. 231-238 (Hinchee, R. E., Leeson, A., Semprini, L., and Ong, S. K., Eds.), Lewis Publishers, Boca Raton, FL.

Goodin, D. B., and McRee, D. E. (1993) The Asp-His-Fe triad of cytochrome *c* peroxidase controls the reduction potential, electronic structure, and coupling of the tryptophan free radical to the heme. *Biochemistry* **32**:3313-3324.

Goodin, D. B., Mauk, A. G., and Smith, M. (1986) Studies of the radical species in compound ES of cytochrome *c* peroxidase altered by site-directed mutagenesis. *Proc. Natl. Acad. Sci. U.S.A.* **83**:1295-1299.

Goodin, D. B., Mauk, A. G., and Smith, M. (1987) The peroxide complex of yeast cytochrome *c* peroxidase contains two distinct radical species, neither of which resides at methionine 172 or tryptophan 51. *J. Biol. Chem.* **262**:7719-7724.

Goodin, D. B., Davidson, M. G., Roe, J. A., Mauk, A. G., and Smith, M. (1991) Amino acid substitutions at tryptophan-51 of cytochrome *c* peroxidase: effects on coordination, species preference for cytochrome *c*, and electron transfer. *Biochemistry* **30**:4953-4962.

Goodwin, D. C., Aust, S. D., and Grover, T. A. (1995) Evidence for veratryl alcohol as a redox mediator in lignin peroxidase-catalyzed oxidation. *Biochemistry* **34**:5060-5065.

Griffin, B. W. (1991) Chloroperoxidase: A review. In *Peroxidase in Chemistry and Biology*, Vol. II, pp. 85-137 (J. Everse, K. E. Everse, and M. B. Grisham, Eds.), CRC Press, Boca Raton, FL.

Grisebach, H. (1981) *The Biochemistry of Plants*, Academic Press, New York.

Haemmerli, S. D., Leisola, M. S. A., Sanglard, D., and Fiechter, A. (1986) Oxidation of benzo(a)pyrene by extracellular ligninases of *Phanerochaete chrysosporium*. Veratryl alcohol and stability of ligninase. *J. Biol. Chem.* **261**:6900-6903.

Hahm, S., Miller, M. A., Geren, L., Kraut, J., Durham, B., and Millett, F. (1994) Reaction of horse cytochrome *c* with the radical and the oxyferryl heme in cytochrome *c* peroxidase compound I. *Biochemistry* **33**, 1473-1480.

Hammel, K. E. (1989) Organopollutant degradation by ligninolytic fungi. *Enzyme Microb. Technol.* **11**:776-777.

Hammel, K. E., Kalyanaraman, B., and Kirk, T. K. (1986) Oxidation of polycyclic aromatic hydrocarbons and dibenzo[*p*]-dioxins by *Phanerochaete chrysosporium* ligninase. *J. Biol. Chem.* **261**:16948-16952.

Hammel, K. E., Jensen, K. A., Jr., Mozuch, M. D., Landucci, L. L., Tien, M., and Pease, E. A. (1993) Ligninolysis by a purified lignin peroxidase. *J. Biol. Chem.* **268**:12274-12281.

Harkin, J. M., and Obst, J. R. (1973) Demethylation of 2,4,6-trimethoxyphenol by phenol oxidase. *Science* **180**:296-298.

Harper, D. B. (1985) Halomethane from halide ion—a highly efficient fungal conversion of environmental significance. *Nature (London)* **315**:55-57.

Harris, R. Z., Wariishi, H., Gold, M. H., and Ortiz de Montellano, P. R. (1991) The catalytic site of manganese peroxidase. Regiospecific addition of sodium azide and alkyldiazines to the heme group. *J. Biol. Chem.* **266**:8751-8758.

Harvey, P. J., and Candeias, L. P. (1995) Radical cation cofactors in lignin peroxidase catalysis. *Biochem. Soc. Trans.* **23**:262-267.

Harvey, P. J., and Palmer, J. M. (1990) Oxidation of phenolic compounds by ligninase. *J. Biotechnol.* **13**:169-179.

Harvey, P. J., Schoemaker, H. E., and Palmer, J. M. (1986) Veratryl alcohol as a mediator and the role of radical cations in lignin biodegradation by *Phanerochaete chrysosporium*. *FEBS Lett.* **195**:242-246.

Harvey, P. J., Schoemaker, H. E., and Palmer, J. M. (1987) Mechanisms of ligninase catalysis. In *Lignin Enzymic and Microbial Degradation*, pp. 145-150 (E. Odier, Ed.), Institut National de la Recherche Agronomique, Paris.

Haschke, R. H., and Friedhoff, J. M. (1978) Calcium-related properties of horseradish peroxidase. *Biochem. Biophys. Res. Commun.* **80**:1039-1042.

Hashimoto, S., Nakajima, R., Yamazaki, I., Tatsuno, Y., and Kitagawa, T. (1986a) Oxygen exchange between the Fe(IV)=O heme and bulk water for the A2 isozyme of horseradish peroxidase. *FEBS Lett.* **208**:305-307.

Hashimoto, S., Tatsuno, Y., and Kitagawa, T. (1986b) Resonance Raman evidence for oxygen exchange between the Fe(IV)=O heme and bulk water during enzymic

catalysis of horseradish peroxidase and its relation with the heme-linked ionization. *Proc. Natl. Acad. Sci. U.S.A.* **83**:2417-2421.

Hashimoto, S., Teraoka, J., Inubushi, T., Yonetani, T., and Kitagawa, T. (1986c) Resonance Raman study on cytochrome *c* peroxidase and its intermediate. Presence of the Fe(IV)=O bond in compound ES and heme-linked ionization. *J. Biol. Chem.* **261**:11110-11118.

Hatakka, A. (1994) Lignin-modified enzymes from selected white-rot fungi: production and role in lignin degradation. *FEMS Microbiol. Rev.* **13**:125-136.

Hayashi, Y., and Yamazaki, I. (1979) The oxidation reduction potential of compound I/compound II and compound II/ferric couples of horseradish peroxidase A2 and C. *J. Biol. Chem.* **254**:9101-9106.

Hazen, S. L., Hsu, F. F., Mueller, D. M., Crowley, J. R., and Heinecke, J. W. (1996) Human neutrophils employ chlorine gas as an oxidant during phagocytosis. *J. Clin. Invest.* **98**:1283-1289.

Hewson, W. D., and Dunford, H. B. (1976) Oxidation of *p*-cresol by horseradish peroxidase compound I. *J. Biol. Chem.* **251**:6036-6042.

Higuchi, T. (1989) Mechanisms of lignin degradation by lignin peroxidase and laccase of white-rot fungi. In *Plant Cell Wall Polymers*, pp. 482-502, ACS Symp. Ser. 399 (N. G. Lewis and M. G. Paice, Eds.), American Chemical Society, Washington, DC.

Higuchi, T. (1990) Lignin biochemistry: biosynthesis and biodegradation. *Wood Sci. Technol.* **24**:23-63.

Hirschfeld, T., Schildkraut, E. R., Tannenbaum, H., and Tannenbaum, D. (1973) Remote spectroscopic analysis of PPM-level air pollutants by Raman spectroscopy. *Appl. Phys. Lett.* **22**:38-40.

Hori, H., and Yonetani, T. (1985) Powder and single-crystal electron paramagnetic resonance studies of yeast cytochrome *c* peroxidase and its peroxide and its peroxide compound, Compound ES. *J. Biol. Chem.* **260**:349-355.

Huggins, T. G., Wells-Knecht, M. C., Detorie, N. A., Baynes, J. W., and Thorpe, S. R. (1993) Formation of *o*-tyrosine and dityrosine in proteins during radiolytic and metal-catalyzed oxidation. *J. Biol. Chem.* **268**:12341-12347.

Huyett, J. E., Doan, P. E., Gurbiel, R., Houseman, A. L. P., Sivaraja, M., Goodin, D. B., and Hoffman, B. M. (1995) Compound ES of cytochrome *c* peroxidase contains a Trp π -cation radical: characterization by CW and pulsed Q-band ENDOR spectroscopy. *J. Am. Chem. Soc.* **117**:9033-9041.

Ivanetich, K. M., Bradshaw, J. J., and Kaminsky, L. S. (1976) Methionine sulfoxide cytochrome *c*. *Biochemistry* **15**:1144–1153.

Jeffries, T. W., Choi, S., and Kirk, T. K. (1981) Nutritional regulation of lignin degradation by *Phanerochaete chrysosporium*. *Appl. Environ. Microbiol.* **42**:290–296.

Jensen, J. K. A., Evans, K. M. C., Kirk, T. K., and Hammel, K. E. (1994) Biosynthetic pathways for veratryl alcohol in the ligninolytic fungus *Phanerochaete chrysosporium*. *Appl. Environ. Microbiol.* **60**:709–714.

Jin, L., Schultz, T. P., and Nicholas, D. D. (1990) Structural characterization of brown rotted lignin. *Horzforschung* **44**:133–138.

Johansson, T., and Nyman, P. O. (1993) Isozymes of lignin peroxidase and manganese(II) peroxidase from the white-rot basidiomycete *Trametes versicolor*. I. Isolation of enzyme forms and characterization of physical and catalytic properties. *Arch. Biochem. Biophys.* **300**:49–56.

Johansson, T., Welinder, K. G., and Nyman, P. O. (1993) Isozymes of lignin peroxidase and manganese(II) peroxidase from the white-rot basidiomycete *Trametes versicolor*. II. Partial sequences, peptide maps, and amino acid and carbohydrate compositions. *Arch. Biochem. Biophys.* **300**:57–62.

Joshi, D. K., and Gold, M. H. (1993) Degradation of 2,4,5-trichlorophenol by the lignin-degrading basidiomycete *Phanerochaete chrysosporium*. *Appl. Environ. Microbiol.* **59**:1779–1785.

Joshi, D. K., and Gold, M. H. (1994) Oxidation of dibenzo-*p*-dioxin by lignin peroxidase from the basidiomycete *Phanerochaete chrysosporium*. *Biochemistry* **33**:10969–10976.

Joshi, D. K., and Gold, M. H. (1996) Oxidation of dimethoxylated aromatic compounds by lignin peroxidase from *Phanerochaete chrysosporium*. *Eur. J. Biochem.* **237**:45–57.

Kang, C. H., Ferguson-Miller, S., and Margoliash, E. (1977) Steady state kinetics and binding of eukaryotic cytochromes *c* with yeast cytochrome *c* peroxidase. *J. Biol. Chem.* **252**:919–926.

Kang, D. S., and Erman, J. E. (1982) The cytochrome *c* peroxidase-catalyzed oxidation of ferrocycytochrome *c* by hydrogen peroxide. Steady state kinetic mechanism. *J. Biol. Chem.* **257**:12775–12779.

Karhunen, E., Niku-Paavola, M. L., Viikari, L., Haltia, T., van der Meer, R. A., and Duine, J. A. (1990) A novel combination of prosthetic groups in a fungal laccase; PQQ and two copper atoms. *FEBS Lett.* **267**:6-8.

Kawai, S., Umezawa, T., and Higuchi, T. (1988) Degradation mechanisms of phenolic β 1 lignin substructure model compounds by laccase of *Coriolus versicolor*. *Arch. Biochem. Biophys.* **262**:99-110.

Kawai, S., Umezawa, T., and Higuchi, T. (1989) Oxidation of methoxylated benzyl alcohols by laccase of *Coriolus versicolor* in the presence of syringaldehyde. *Wood Res.* **76**:10-16.

Kay, E. S., and Shapiro, B. M. (1987) Ovoperoxidase assembly into the sea urchin fertilization envelope and dityrosine crosslinking. *Dev. Biol.* **121**:325-334.

Kay, E., Eddy, E. M., and Shapiro, B. M. (1982) Assembly of the fertilization membrane of the sea urchin: isolation of a divalent cation-dependent intermediate and its crosslinking *in vitro*. *Cell* **29**:867-875.

Kelley, R. L., and Reddy, C. A. (1986) Purification and characterization of glucose oxidase from ligninolytic cultures of *Phanerochaete chrysosporium*. *J. Bacteriol.* **166**:269-274.

Kersten, P. J., and Cullen, D. (1993) Cloning and characterization of cDNA encoding glyoxal oxidase, a H₂O₂-producing enzyme from the lignin-degrading basidiomycete *Phanerochaete chrysosporium*. *Proc. Natl. Acad. Sci. U.S.A.* **90**:7411-7413.

Kersten, P. J., and Kirk, T. K. (1987) Involvement of a new enzyme, glyoxal oxidase, in extracellular H₂O₂ production by *Phanerochaete chrysosporium*. *J. Bacteriol.* **169**:2195-2201.

Kersten, P. J., Tien, M., Kalyanaraman, B., and Kirk, T. K. (1985) The ligninase of *Phanerochaete chrysosporium* generates cation radicals from methoxybenzenes. *J. Biol. Chem.* **260**:2609-2612.

Kersten, P. J., Kalyanaraman, B., Hammel, K. E., Reinhammar, B., and Kirk, T. K. (1990) Comparison of lignin peroxidase, horseradish peroxidase and laccase in the oxidation of methoxybenzenes. *Biochem. J.* **268**:475-480.

Kersten, P. J., Witek, C., vanden Wymelenberg, A., and Cullen, D. (1995) *Phanerochaete chrysosporium* glyoxal oxidase is encoded by two allelic variants: structure, genomic organization, and heterologous expression of glx1 and glx2. *J. Bacteriol.* **177**:6106-6110.

- Khindaria, A., Grover, T. A., and Aust, S. D. (1995) Evidence for formation of the veratryl alcohol cation radical by lignin peroxidase. *Biochemistry* **34**:6020–6025.
- Khindaria, A., Yamazaki, I., and Aust, S. D. (1996) Stabilization of the veratryl alcohol cation radical by lignin peroxidase. *Biochemistry* **35**:6418–6424.
- Kim, K. L., Kang, D. S., Vitello, L. B., and Erman, J. E. (1990) Cytochrome *c* peroxidase catalyzed oxidation of ferrocyclochrome *c* by hydrogen peroxide: ionic strength dependence of the steady-state rate parameters. *Biochemistry* **29**:9150–9159.
- Kirk, T. K. (1975) Effects of a brown-rot fungus, *Lenzites trabea*, on lignin in spruce wood. *Holzforshung* **29**:99–107.
- Kirk, T. K., and Adler, E. (1970) Methoxyl-deficient structural elements in lignin of sweetbum decayed by a brown-rot fungus. *Acta Chem. Scand.* **24**:3379–3390.
- Kirk, T. K., and Chang, H.-M. (1974) Decomposition of lignin by white-rot fungi. I. Isolation of heavily degraded lignins from decayed spruce. *Holzforshung* **28**:217–222.
- Kirk, T. K., and Chang, H.-M. (1975) Decomposition of lignin by white-rot fungi. II. Characterization of heavily degraded lignins from decayed spruce. *Holzforshung* **29**:56–64.
- Kirk, T. K., and Cowling, E. B. (1984) The chemistry of solid wood. In *Advances in Chemistry*, Vol. 207, pp. 435–487 (R. M. Rowell, Ed.), American Chemical Society, Washington, DC.
- Kirk, T. K., and Farrell, R. L. (1987) Enzymatic "combustion": the microbial degradation of lignin. *Annu. Rev. Microbiol.* **41**:465–505.
- Kirk, T. K., and Kelman, A. (1965) Lignin degradation as related to the phenoloxidases of selected wood-decaying basidiomycetes. *Phytopathology* **55**:739–745.
- Kirk, T. K., Harkin, J. M., and Cowling, E. B. (1968a) Oxidation of guaiacyl- and veratryl-glycerol- β -gualacyl ether by *Polyporus versicolor* and *Stereum frustulatum*. *Biochim. Biophys. Acta* **165**:134–144.
- Kirk, T. K., Harkin, J. M., and Cowling, E. B. (1968b) Degradation of the lignin model compound syringylglycol- β -guaiacyl ether by *Polyporus versicolor* and *Stereum frustalatum*. *Biochim. Biophys. Acta* **165**:145–163.

- Kishi, K., Wariishi, H., Marquez, L., Dunford, H. B., and Gold, M. H. (1994) Mechanism of manganese peroxidase compound II reduction. Effect of organic acid chelators and pH. *Biochemistry* **33**:8694–8701.
- Kishi, K., Kusters-van Someren, M., Mayfield, M. B., Sun, J., Loehr, T. M., and Gold, M. H. (1996) Characterization of manganese(II) binding site mutants of manganese peroxidase. *Biochemistry* **35**:8986–8994.
- Koduri, R. S., and Tien, M. (1994) Kinetic analysis of lignin peroxidase: explanation for the mediation phenomenon by veratryl alcohol. *Biochemistry* **33**:4225–4230.
- Koduri, R. S., and Tien, M. (1995) Oxidation of guaiacol by lignin peroxidase. Role of veratryl alcohol. *J. Biol. Chem.* **270**:22254–22258.
- Koduri, R. S., Whitwam, R. E., Barr, D., Aust, S. D., and Tien, M. (1996) Oxidation of 1,2,4,5-tetramethoxybenzene by lignin peroxidase of *Phanerochaete chrysosporium*. *Arch. Biochem. Biophys.* **326**:261–265.
- Kojima, Y., Tsukuda, Y., Kawai, Y., Tsukamoto, A., Sugiura, J., Sakaino, M., and Kita, Y. (1990) Cloning, sequence analysis, and expression of ligninolytic phenoloxidase genes of the white-rot basidiomycete *Coriolus hirsutus*. *J. Biol. Chem.* **265**:15224–15230.
- Koppenol, W. H., and Margoliash, E. (1982) The asymmetric distribution of charges on the surface of horse cytochrome *c*. Functional implications. *J. Biol. Chem.* **257**:4426–4437.
- Kuan, I. C., and Tien, M. (1993a) Glyoxylate-supported reactions catalyzed by Mn peroxidase of *Phanerochaete chrysosporium*: activity in the absence of added hydrogen peroxide. *Arch. Biochem. Biophys.* **302**:447–454.
- Kuan, I. C., and Tien, M. (1993b) Stimulation of Mn peroxidase activity: a possible role for oxalate in lignin biodegradation. *Proc. Natl. Acad. Sci. U.S.A.* **90**:1242–1246.
- Kuan, I. C., Johnson, K. A., and Tien, M. (1993) Kinetic analysis of manganese peroxidase. The reaction with manganese complexes. *J. Biol. Chem.* **268**:20064–20070.
- Kurek, B., and Kersten, J. (1995) Physiological regulation of glyoxal oxidase from *Phanerochaete chrysosporium* by peroxidase systems. *Enzyme Microb. Technol.* **17**:751–756.

- Kusters-van Someren, M., Kishi, K., Lundell, T., and Gold, M. H. (1995) The manganese binding site of manganese peroxidase: characterization of an Asp179Asn site-directed mutant protein. *Biochemistry* **34**:10620–10627.
- Kuwahara, M., Glenn, J. K., Morgan, M. A., and Gold, M. H. (1984) Separation and characterization of two extracellular H₂O₂-dependent oxidase from ligninolytic cultures of *Phanerochaete chrysosporium*. *FEBS Lett.* **169**:247–250.
- Lackner, R., Srebotnik, E., and Messner, K. (1991) Oxidative degradation of high molecular weight chlorolignin by manganese peroxidase of *Phanerochaete chrysosporium*. *Biochem. Biophys. Res. Commun.* **178**:1092–1098.
- Laemmli, U. K. (1970) Cleavage of structural proteins during the assembly of the head of bacteriophage T4. *Nature (London)* **227**:680–695.
- La Mar, G. N., de Ropp, J. S., Smith, K. M., and Langry, K. C. (1981) Proton nuclear magnetic resonance investigation of the electronic structure of compound I of horseradish peroxidase. *J. Biol. Chem.* **256**:237–243.
- La Mar, G. N., de Ropp, J. S., Latos Grazynski, L., Balch, A. L., Johnson, R. B., Smith, K. M., Parish, D. W., and Chang, R. (1983) Proton NMR characterization of the ferryl group in model heme complexes and hemoproteins: Evidence for the Fe(IV)=O group in ferryl myoglobin and compound II of horseradish peroxidase. *J. Am. Chem. Soc.* **105**:782–787.
- Lambeir, A. M., and Dunford, H. B. (1983) A kinetic and spectral study of the alkaline transitions of chloroperoxidase. *Arch. Biochem. Biophys.* **220**:549–556.
- Leisola, M. S., Schmidt, B., and Fiechter, A. (1986) Enzymatic determination of veratryl alcohol. *Anal. Biochem.* **155**:108–111.
- Leisola, M. S., Kozulic, B., Meussdoerffer, F., and Fiechter, A. (1987) Homology among multiple extracellular peroxidases from *Phanerochaete chrysosporium*. *J. Biol. Chem.* **262**:419–424.
- Leonowicz, A., Edgehill, R. U., and Bollag, J.-M. (1984) The effect of pH on the transformation of syringic and vanillic acids by the laccases of *Rhizoctonia praticola* and *Trametes versicolor*. *Arch. Microbiol.* **137**:89–96.
- Lerch, K., Deinum, J., and Reinhammar, B. (1978) The state of copper in *Neurospora laccase*. *Biochim. Biophys. Acta* **534**:7–14.
- Li, D., Alic, M., Brown, J. A., and Gold, M. H. (1995) Regulation of manganese peroxidase gene transcription by hydrogen peroxide, chemical stress, and molecular oxygen. *Appl. Environ. Microbiol.* **61**:341–345.

- Libby, R. D., Thomas, J. A., Kaiser, L. W., and Hager, L. P. (1982) Chloroperoxidase halogenation reactions. Chemical versus enzymic halogenating intermediates. *J. Biol. Chem.* **257**:5030–5037.
- Libby, R. D., Beachy, T. M., and Phipps, A. K. (1996) Quantitating direct chlorine transfer from enzyme to substrate in chloroperoxidase-catalyzed reactions. *J. Biol. Chem.* **271**:21820–21827.
- Lin, S. Y., and Dence, C. W., Eds. (1992) *Methods in Lignin Chemistry*. Springer-Verlag, Berlin, Heidelberg.
- Liu, R. Q., Miller, M. A., Han, G. W., Hahm, S., Geren, L., Hibdon, S., Kraut, J., Durham, B., and Millett, F. (1994) Role of methionine 230 in intramolecular electron transfer between the oxyferryl heme and tryptophan 191 in cytochrome *c* peroxidase compound II. *Biochemistry* **33**:8678–8685.
- Liu, R. Q., Hahm, S., Miller, M., Durham, B., and Millet, F. (1995) Photooxidation of Trp-191 in cytochrome *c* peroxidase by ruthenium-cytochrome *c* derivatives. *Biochemistry* **34**:973–983.
- Loo, S., and Erman, J. E. (1977) The rate of reaction between cytochrome *c* peroxidase and hydrogen peroxide is not diffusion limited. *Biochim. Biophys. Acta* **481**:279–282.
- Maccacchini, M. L. (1981) Import of proteins into mitochondria. *Methods Cell Biol.* **23**:39–50.
- Maccacchini, M. L., Rudin, Y., and Schatz, G. (1979) Transport of proteins across the mitochondrial outer membrane. A precursor form of the cytoplasmically made intermembrane enzyme cytochrome *c* peroxidase. *J. Biol. Chem.* **254**:7468–7471.
- MacDonald, M. J., Paterson, A., and Broda, P. (1984) Possible relationship between cyclic AMP and idiophasic metabolism in the white rot fungus *Phanerochaete chrysosporium*. *J. Bacteriol.* **160**:470–472.
- Manthey, J. A., and Hager, L. P. (1981) Purification and properties of bromoperoxidase from *Penicillium capitatus*. *J. Biol. Chem.* **256**:11232–11238.
- Marcus, R. A., and Sutin, N. (1985) Electron transfers in chemistry and biology. *Biochim. Biophys. Acta* **811**:265–322.
- Margoliash, E., and Frohwirt, N. (1959) Spectrum of horse-heart cytochrome *c*. *Biochem. J.* **71**:570–572.

- Margoliash, E., Ferguson-Miller, S., Kang, C. H., and Brautigan, D. L. (1976) Do evolutionary changes in cytochrome *c* structure reflect functional adaptations? *Fed. Proc.* **35**:2124-2130.
- Marquez, L. A., and Dunford, H. B. (1990) Reaction of compound III of myeloperoxidase with ascorbic acid. *J. Biol. Chem.* **265**:6074-6078.
- Marquez, L., and Dunford, H. B. (1994) Chlorination of taurine by myeloperoxidase. Kinetic evidence for an enzyme-bound intermediate. *J. Biol. Chem.* **269**:7950-7956.
- Marquez, L., Wariishi, H., Dunford, H. B., and Gold, M. H. (1988) Spectroscopic and kinetic properties of the oxidized intermediates of lignin peroxidase from *Phanerochaete chrysosporium*. *J. Biol. Chem.* **263**:10549-10552.
- Marquez, L. A., Quitariano, M., Zilinskas, B. A., and Dunford, H. B. (1996) Kinetic and spectral properties of pea cytosolic ascorbate peroxidase. *FEBS Lett.* **389**:153-156.
- Mauro, J. M., Fishel, L. A., Hazzard, J. T., Meyer, T. E., Tollin, G., Cusanovich, M. A., and Kraut, J. (1988) Tryptophan-191—phenylalanine, a proximal-side mutation in yeast cytochrome *c* peroxidase that strongly affects the kinetics of ferrocytochrome *c* oxidation. *Biochemistry* **27**:6243-6256.
- Mayfield, M. B., Godfrey, B. J., and Gold, M. H. (1994a) Characterization of the *mnp2* gene encoding manganese peroxidase isozyme 2 from the basidiomycete *Phanerochaete chrysosporium*. *Gene* **142**:231-235.
- Mayfield, M. B., Kishi, K., Alic, M., and Gold, M. H. (1994b) Homologous expression of recombinant manganese peroxidase in *Phanerochaete chrysosporium*. *Appl. Environ. Microbiol.* **60**:4303-4309.
- McCarthy, A. J. (1987) Lignocellulose-degrading actinomycetes. *FEMS Microbiol. Rev.* **46**:145-163.
- McCord, J. M., and Fridovich, I. (1969) Superoxide dismutase. An enzymic function for erythrocyte (heme)cuprein. *J. Biol. Chem.* **244**:6049-6055.
- Messerschmidt, A., and Huber, R. (1990) The blue oxidases, ascorbate oxidase, laccase and ceruloplasmin. Modelling and structural relationships. *Eur. J. Biochem.* **187**:341-352.
- Michel, F. C., Jr., Dass, S. B., Grulke, E. A., and Reddy, C. A. (1991) Role of manganese peroxidases and lignin peroxidases of *Phanerochaete chrysosporium* in the decolorization of kraft bleach plant effluent. *Appl. Environ. Microbiol.* **57**:2368-2375.

Miki, K., Renganathan, V., and Gold, M. H. (1986) Mechanism of β -aryl ether dimeric lignin model compound oxidation by lignin peroxidase of *Phanerochaete chrysosporium*. *Biochemistry* **25**:4790–4796.

Miller, M. A., Han, G. W., and Kraut, J. (1994a) A cation binding motif stabilizes the compound I radical of cytochrome *c* peroxidase. *Proc. Natl. Acad. Sci. U.S.A.* **91**:11118–11122.

Miller, M. A., Liu, R. Q., Hahm, S., Geren, L., Hibdon, S., Kraut, J., Durham, B., and Millett, F. (1994b) Interaction domain for the reaction of cytochrome *c* with the radical and the oxyferryl heme in cytochrome *c* peroxidase compound I. *Biochemistry* **33**:8686–8693.

Millis, C. D., Cai, D. Y., Stankovich, M. T., and Tien, M. (1989) Oxidation-reduction potentials and ionization states of extracellular peroxidases from the lignin-degrading fungus *Phanerochaete chrysosporium*. *Biochemistry* **28**:8484–8489.

Mino, Y., Wariishi, H., Blackburn, N. J., Loehr, T. M., and Gold, M. H. (1988) Spectral characterization of manganese peroxidase, an extracellular heme enzyme from the lignin-degrading basidiomycete, *Phanerochaete chrysosporium*. *J. Biol. Chem.* **263**:7029–7036.

Mliki, A., and Zimmermann, W. (1992) Purification and characterization of an intracellular peroxidase from *Streptomyces cyaneus*. *Appl. Environ. Microbiol.* **58**:916–919.

Monties, B. (1994) Chemical assessment of lignin biodegradation some qualitative and quantitative aspects. *FEMS Microbiol. Rev.* **13**:277–283.

Morohoshi, N., and Haraguchi, T. (1987) Degradation of lignin by the extracellular enzymes of *Coriolus versicolor*. VI. Degradation of syringylglycerol- β -syringyl ether by laccase III-c purified from laccase III by isoelectric focusing. *Mokuzai Gakkaishi* **33**:495–502.

Morris, D. R., and Hager, L. P. (1966) Chloroperoxidase. I. Isolation and properties of the crystalline glycoprotein. *J. Biol. Chem.* **241**:1763–1768.

Morrison, M., and Schonbaum, G. R. (1976) Peroxidase-catalyzed halogenation. *Annu. Rev. Biochem.* **45**:861–888.

Muheim, A., Waldner, R., Leisola, M. S. A., and Fiechter, A. (1990) An extracellular aryl alcohol oxidase from the white-rot fungus *Bjerkandera adusta*. *Enzyme Microb. Technol.* **12**:204–209.

- Muheim, A., Fiechter, A., Harvey, P. J., and Schoemaker, H. E. (1992) On the mechanism of oxidation of non-phenolic lignin model compounds by laccase-ABTS couple. *Holzforschung* **46**:121-126.
- Neidleman, S. L., and Geigert, J. (1986) *Biohalogenation Principles, Basic Roles and Applications*, Ellis Horwood, Chichester, U.K.
- Newmyer, S. L., and Ortiz de Montellano, P. R. (1995) Horseradish peroxidase His-42 → Ala, His-42 → Val, and Phe-41 → Ala mutants. Histidine catalysis and control of substrate access to the heme iron. *J. Biol. Chem.* **270**:19430-19438.
- Nie, G., and Aust, S. D. (1997) Effect of calcium on the reversible thermal inactivation of lignin peroxidase. *Arch. Biochem. Biophys.* **337**:225-231.
- Nishida, A., and Eriksson, K.-E. (1987) Formation, purification and partial characterization of methanol oxidase, a H₂O₂-producing enzyme in *Phanerochaete chrysosporium*. *Biotechnol. Appl. Biochem.* **9**:325-338.
- Orth, A. B., Royse, D. J., and Tien, M. (1993) Ubiquity of lignin-degrading peroxidases among various wood-degrading fungi. *Appl. Environ. Microbiol.* **59**:4017-4023.
- Orth, A. B., Rzhetskaya, M., Cullen, D., and Tien, M. (1994) Characterization of a cDNA encoding a manganese peroxidase from *Phanerochaete chrysosporium*: genomic organization of lignin and manganese peroxidase-encoding genes. *Gene* **148**:161-165.
- Ortiz de Montellano, P. R., David, S. K., Ator, M. A., and Tew, D. (1988) Mechanism-based inactivation of horseradish peroxidase by sodium azide. Formation of meso-azidoporphyrin IX. *Biochemistry* **27**:5470-5476.
- Paice, M. G., Reid, I. D., Boubonnais, R., Archibald, F. S., and Jurasek, L. (1993) Manganese peroxidase, produced by *Trametes versicolor* during pulp bleaching, demethylation and delignifies kraft pulp. *Appl. Environ. Microbiol.* **59**:260-265.
- Pall, M. S. (1981) Adenosine 3', 5'-phosphate in fungi. *Microbiology* **57**:462-480.
- Paszczyński, A., and Crawford, R. L. (1991) Degradation of azo compounds by ligninase from *Phanerochaete chrysosporium*: involvement of veratryl alcohol. *Biochem. Biophys. Res. Commun.* **178**:1056-1063.
- Paszczyński, A., Pasti-Grigsby, M. B., Goszczynski, S., Crawford, R. L., and Crawford, D. L. (1992) Mineralization of sulfonated azo dyes and sulfanilic acid by *Phanerochaete chrysosporium* and *Streptomyces chromofuscus*. *Appl. Environ. Microbiol.* **58**:3598-3604.

- Patterson, W. R., and Poulos, T. L. (1995) Crystal structure of recombinant pea cytosolic ascorbate peroxidase. *Biochemistry* **34**:4331–4341.
- Patterson, W. R., Poulos, T. L., and Goodin, D. B. (1995) Identification of a porphyrin π cation radical in ascorbate peroxidase compound I. *Biochemistry* **34**:4342–4345.
- Pease, E. A., Andrawis, A., and Tien, M. (1989) Manganese-dependent peroxidase from *Phanerochaete chrysosporium*. Primary structure deduced from cDNA sequence. *J. Biol. Chem.* **264**:13531–13535.
- Pedler, A., Pollard, F. H., Gibson, G., and Kalnin, I. (1957) Nitrogen (IV) oxide (dinitrogen tetroxide). In *Inorganic Syntheses*, Vol. V, pp. 87–91 (T. Moeller, Ed.), McGraw-Hill, New York.
- Pelletier, H., and Kraut, J. (1992) Crystal structure of a complex between electron transfer partners, cytochrome *c* peroxidase and cytochrome *c*. *Science* **258**:1748–1755.
- Penner-Hahn, J. E., Eble, K. S., McMurry, T. J., Renner, M., Balch, A. L., Groves, J. T., Dawson, J. H., and Hodgson, K. O. (1986) Structural characterization of horseradish peroxidase using EXAF spectroscopy. Evidence for Fe(IV)=O ligation in compounds I and II. *J. Am. Chem. Soc.* **108**:7819–7825.
- Périé, F. H., and Gold, M. H. (1991) Manganese regulation of manganese peroxidase expression and lignin degradation by the white rot fungus *Dichomitus squalens*. *Appl. Environ. Microbiol.* **57**:2240–2245.
- Périé, F. H., Sheng, D., and Gold, M. H. (1996) Purification and characterization of two manganese peroxidase isozymes from the white-rot basidiomycete *Dichomitus squalens*. *Biochim. Biophys. Acta* **1297**:139–148.
- Perry, C. R., Matcham, S. E., Wood, D. A., and Thurston, C. F. (1993a) The structure of laccase protein and its synthesis by the commercial mushroom *Agaricus bisporus*. *J. Gen. Microbiol.* **139**:171–178.
- Perry, C. R., Smith, M., Britnell, C. H., Wood, D. A., and Thurston, C. F. (1993b) Identification of two laccase genes in the cultivated mushroom *Agaricus bisporus*. *J. Gen. Microbiol.* **139**:1209–1218.
- Piontek, K., Glumoff, T., and Winterhalter, K. (1993) Low pH crystal structure of glycosylated lignin peroxidase from *Phanerochaete chrysosporium* at 2.5 Å resolution. *FEBS Lett.* **315**:119–124.

- Popp, J. L., Kalyanaraman, B., and Kirk, T. K. (1990) Lignin peroxidase oxidation of Mn^{2+} in the presence of veratryl alcohol, malonic or oxalic acid, and oxygen. *Biochemistry* **29**:10475-10480.
- Poulos, T. L., and Kraut, J. (1980) The stereochemistry of peroxidase catalysis. *J. Biol. Chem.* **255**:8199-8205.
- Poulos, T. L., Edwards, S. L., Wariishi, H., and Gold, M. H. (1993) Crystallographic refinement of lignin peroxidase at 2 Å. *J. Biol. Chem.* **268**:4429-4440.
- Pribnow, D., Mayfield, M. B., Nipper, V. J., Brown, J. A., and Gold, M. H. (1989) Characterization of a cDNA encoding a manganese peroxidase, from the lignin-degrading basidiomycete *Phanerochaete chrysosporium*. *J. Biol. Chem.* **264**:5036-5040.
- Prutz, W. A., Monig, H., Butler, J., and Land, E. J. (1985) Reactions of nitrogen dioxide in aqueous model systems: oxidation of tyrosine units in peptides and proteins. *Arch. Biochem. Biophys.* **243**:125-134.
- Ramachandra, M., Crawford, D. L., and Hertel, G. (1988) Characterization of an extracellular lignin peroxidase of the lignocellulolytic actinomycete *Streptomyces viridosporus*. *Appl. Environ. Microbiol.* **54**:3057-3063.
- Reddy, C. A. (1993) An overview of the recent advances on the physiology and molecular biology of lignin peroxidases of *Phanerochaete chrysosporium*. *J. Biotechnol.* **30**:91-107.
- Reddy, C. A., and D'Souza, T. M. (1994) Physiology and molecular biology of the lignin peroxidases of *Phanerochaete chrysosporium*. *FEMS Microbiol. Rev.* **13**:137-152.
- Reinhammar, B. (1984) Laccase. In *Copper Proteins and Copper Enzymes*, Vol. 3, pp. 1-36 (R. Lontie, Ed.), CRC Press, Boca Raton, FL.
- Renganathan, V., and Gold, M. H. (1986) Spectral characterization of the oxidized states of lignin peroxidase, an extracellular heme enzyme from the white rot basidiomycete *Phanerochaete chrysosporium*. *Biochemistry* **25**:1626-1631.
- Renganathan, V., Miki, K., and Gold, M. H. (1985) Multiple molecular forms of diarylpropane oxygenase, an H_2O_2 -requiring, lignin-degrading enzyme from *Phanerochaete chrysosporium*. *Arch. Biochem. Biophys.* **241**:304-314.
- Renganathan, V., Miki, K., and Gold, M. H. (1986) Role of molecular oxygen in lignin peroxidase reactions. *Arch. Biochem. Biophys.* **246**:155-161.

- Renganathan, V., Miki, K., and Gold, M. H. (1987) Haloperoxidase reactions catalyzed by lignin peroxidase, an extracellular enzyme from the basidiomycete *Phanerochaete chrysosporium*. *Biochemistry* **26**:5127-5132.
- Rice, R. H., Lee, Y. M., and Brown, W. D. (1983) Interaction of heme proteins with hydrogen peroxide: protein crosslinking and covalent binding of benzo[a]pyrene and 17- β -estradiol. *Arch. Biochem. Biophys.* **221**:417-427.
- Riordan, J. F., and Vallee, B. L. (1972) Nitration with tetranitromethane. *Methods Enzymol.* **25**:515-521.
- Ritch, T. G., Jr., and Gold, M. H. (1992) Characterization of a highly expressed lignin peroxidase-encoding gene from the basidiomycete *Phanerochaete chrysosporium*. *Gene* **118**:73-80.
- Ritch, T. G., Jr., Nipper, V. J., Akileswaran, L., Smith, A., Pribnow, D., and Gold, M. H. (1991) Lignin peroxidase from the basidiomycete *Phanerochaete chrysosporium* is synthesized as a preproenzyme. *Gene* **107**:119-126.
- Roberts, J. E., Hoffman, B. M., Rutter, R., and Hager, L. P. (1981a) 17O ENDOR of horseradish peroxidase compound I. *J. Am. Chem. Soc.* **103**:7654-7656.
- Roberts, J. E., Hoffman, B. M., Rutter, R., and Hager, L. P. (1981b) Electron-nuclear double resonance of horseradish peroxidase compound I. Detection of the porphyrin π -cation radical. *J. Biol. Chem.* **256**:2118-2121.
- Roman, R., and Dunford, H. B. (1972) pH dependence of the oxidation of iodide by compound I of horseradish peroxidase. *Biochemistry* **11**:2076-2082.
- Sakurada, J., Takahashi, S., and Hosoya, T. (1987) Proton nuclear magnetic resonance studies on the iodide binding by horseradish peroxidase. *J. Biol. Chem.* **262**:4007-4010.
- Saloheimo, M., Niku-Paavola, M. L., and Knowles, J. K. (1991) Isolation and structural analysis of the laccase gene from the lignin-degrading fungus *Phlebia radiata*. *J. Gen. Microbiol.* **137**:1537-1544.
- Salowe, S. P., Ator, M. A., and Stubbe, J. (1987) Products of the inactivation of ribonucleoside diphosphate reductase from *Escherichia coli* with 2'-azido-2'-deoxyuridine 5'-diphosphate. *Biochemistry* **26**:3408-3416.
- Sannia, G., Limongi, P., Cocca, E., Buonocore, F., Nitti, G., Giardina, P. (1991) Purification and characterization of a veratryl alcohol oxidase enzyme from the lignin degrading basidiomycete *Pleurotus ostreatus*. *Biochim. Biophys. Acta* **1073**:114-119.

- Sarkanen, K. V. (1971) *Lignins. Occurrence, Formation, Structure, and Reactions*, pp. 93–163 (K. V. Sarkanen and C. H. Ludwig, Eds.), Wiley-Interscience, New York.
- Sasaki, Y., and Takao, S. (1967) Organic acid production by basidiomycetes. III. Cultural conditions for L-malic acid production. *Appl. Microbiol.* **15**:373–377.
- Schmidt, H. W. H., Haemmerli, S. D., Schoemaker, H. E., and Leisola, M. S. A. (1989) Oxidative degradation of 3,4-dimethoxybenzyl alcohol and its methyl ether by the lignin peroxidase of *Phanerochaete chrysosporium*. *Biochemistry* **28**:1776–1783.
- Schoemaker, H. E. (1990) On the chemistry of lignin biodegradation. *Recl. Trav. Chim. Pays-Bas* **109**:255–272.
- Schoemaker, H. E., Lundell, T. K., Floris, R., Glumoff, T., Winterhalter, K. H., and Piontek, K. (1994) Do carbohydrates play a role in the lignin peroxidase cycle? Redox catalysis in the endergonic region of the driving force. *Bioorg. Med. Chem.* **2**:509–519.
- Schuller, D. J., Ban, N., Huystee, R. B., McPherson, A., and Poulos, T. L. (1996) The crystal structure of peanut peroxidase. *Structure* **4**:311–321.
- Schulz, C. E., Rutter, R., Sage, J. T., Debrunner, P. G., and Hager, L. P. (1984) Mossbauer and electron paramagnetic resonance studies of horseradish peroxidase and its catalytic intermediates. *Biochemistry* **23**:4743–4754.
- Selwyn, M. J. (1965) Simple test for inactivation of an enzyme during assay. *Biochim. Biophys. Acta* **105**:193–195.
- Sheng, D., and Gold, M. H. (1997) Haloperoxidase activity of manganese peroxidase from *Phanerochaete chrysosporium*. *Arch. Biochem. Biophys.* **345**:126–134.
- Sheng, D., and M. H. Gold (1998) Irreversible oxidation of ferricytochrome *c* by lignin peroxidase. *Biochemistry*, in press.
- Shimada, M., Ma, D., Akamatsu, Y., and Hattori, T. (1994) A proposed role of oxalic acid in wood decay systems of wood-rotting basidiomycetes. *FEMS Microbiol. Rev.* **13**:285–296.
- Sitter, A. J., Reczek, C. M., and Terner, J. (1985) Observation of the Fe(IV)=O stretching vibration of ferryl myoglobin by resonance Raman spectroscopy. *Biochim. Biophys. Acta* **828**:229–235.

- Sivaraja, M., Goodin, D. B., Smith, M., and Hoffman, B. M. (1989) Identification by ENDOR of Trp191 as the free-radical site in cytochrome *c* peroxidase compound ES. *Science* **245**:738–740.
- Smith, T. L., Schalch, H., Gaskell, J., Covert, S., and Cullen, D. (1988) Nucleotide sequence of a ligninase gene from *Phanerochaete chrysosporium*. *Nucleic Acids Res.* **16**:1219.
- Smulevich, G., Paoli, M., Burke, J. F., Sanders, S. A., Thorneley, R. N., and Smith, A. T. (1994) Characterization of recombinant horseradish peroxidase *c* and three site-directed mutants, F41V, F41W, and R38K, by resonance Raman spectroscopy. *Biochemistry* **33**:7398–7407.
- Smyth, D. G., Stein, W. H., and Moore, S. (1963) The sequence of amino acid residues in bovine pancreatic ribonuclease: revisions and confirmations. *J. Biol. Chem.* **238**:227–234.
- Spadaro, J. T., and Renganathan, V. (1994) Peroxidase-catalyzed oxidation of azo dyes: mechanism of disperse Yellow 3 degradation. *Arch. Biochem. Biophys.* **312**:301–307.
- Spadaro, J. T., Gold, M. H., and Renganathan, V. (1992) Degradation of azo dyes by the lignin-degrading fungus *Phanerochaete chrysosporium*. *Appl. Environ. Microbiol.* **58**:2397–2401.
- Stewart, P., Kersten, P., Vanden Wymelenberg, A., Gaskell, J., and Cullen, D. (1992) Lignin peroxidase gene family of *Phanerochaete chrysosporium*: complex regulation by carbon and nitrogen limitation and identification of a second dimorphic chromosome. *J. Bacteriol.* **174**:5036–5042.
- Sun, W., Kadima, T. A., Pickard, M. A., and Dunford, H. B. (1994) Catalase activity of chloroperoxidase and its interaction with peroxidase activity. *Biochem. Cell Biol.* **72**:321–331.
- Sundaramoorthy, M., Kishi, K., Gold, M. H., and Poulos, T. L. (1994) The crystal structure of manganese peroxidase from *Phanerochaete chrysosporium* at 2.06-Å resolution. *J. Biol. Chem.* **269**:32759–32767.
- Sutherland, G. R., Khindaria, A., and Aust, S. D. (1996) The effect of veratryl alcohol on manganese oxidation by lignin peroxidase. *Arch. Biochem. Biophys.* **327**:20–26.
- Thomas, J. A., Morris, D. R., and Hager, L. P. (1970a) Chloroperoxidase. VII. Classical peroxidatic, catalatic, and halogenating forms of the enzyme. *J. Biol. Chem.* **245**:3129–3134.

- Thomas, J. A., Morris, D. R., and Hager, L. P. (1970b) Chloroperoxidase. 8. Formation of peroxide and halide complexes and their relation to the mechanism of the halogenation reaction. *J. Biol. Chem.* **245**:3135-3142.
- Tien, M., and Kirk, T. K. (1983) Lignin-degrading enzyme from the hymenomycete *Phanerochaete chrysosporium* burds. *Science* **221**:661-663.
- Tien, M., and Kirk, T. K. (1984) Lignin-degrading enzyme from *Phanerochaete chrysosporium*. Purification, characterization, and catalytic properties of a unique H₂O₂ requiring oxygenase. *Proc. Natl. Acad. Sci. U.S.A.* **81**:2280-2284.
- Tien, M., and Ma, D. (1997) Oxidation of 4-methoxymandelic acid by lignin peroxidase. Mediation by veratryl alcohol. *J. Biol. Chem.* **272**:8912-8917.
- Tien, M., and Tu, C. P. (1987) Cloning and sequencing of a cDNA for a ligninase from *Phanerochaete chrysosporium*. *Nature* **326**:520-523.
- Tien, M., Kirk, T. K., Bull, C., and Fee, J. A. (1986) Steady-state and transient-state kinetic studies on the oxidation of 3,4-dimethoxybenzyl alcohol catalyzed by the ligninase of *Phanerochaete chrysosporium* Burds. *J. Biol. Chem.* **261**:1687-1693.
- Tuisel, H., Sinclair, R., Bumpus, J. A., Ashbaugh, W., Brock, B. J., and Aust, S. D. (1990) Lignin peroxidase H₂ from *Phanerochaete chrysosporium*: purification, characterization and stability to temperature and pH. *Arch. Biochem. Biophys.* **279**:158-166.
- Tuor, U., Wariishi, H., Schoemaker, H. E., and Gold, M. H. (1992) Oxidation of phenolic arylglycerol β -aryl ether lignin model compounds by manganese peroxidase from *Phanerochaete chrysosporium*: oxidative cleavage of an α -carbonyl model compound. *Biochemistry* **31**:4986-4995.
- Umezawa, T., and Higuchi, T. (1989) Cleavages of aromatic ring and β -O-4 bond of synthetic lignin (DHP) by lignin peroxidase. *FEBS Lett.* **242**:325-359.
- Ushijima, Y., Nakano, M., and Goto, T. (1984) Production and identification of bityrosine in horseradish peroxidase-H₂O₂-tyrosine system. *Biochem. Biophys. Res. Commun.* **125**:916-918.
- Valli, K., Wariishi, H., and Gold, M. H. (1990) Oxidation of monomethoxylated aromatic compounds by lignin peroxidase: role of veratryl alcohol in lignin biodegradation. *Biochemistry* **29**:8535-8539.
- Valli, K., Brock, B. J., Joshi, D. K., and Gold, M. H. (1992a) Degradation of 2,4-dinitrotoluene by the lignin-degrading fungus *Phanerochaete chrysosporium*. *Appl. Environ. Microbiol.* **58**:221-228.

- Valli, K., Wariishi, H., and Gold, M. H. (1992b) Degradation of 2,7-dichlorodibenzo-*p*-dioxin by the lignin-degrading basidiomycete *Phanerochaete chrysosporium*. *J. Bacteriol.* **174**:2131-2137.
- Vicuna, R. (1988) Bacterial degradation of lignin. *Enzyme Microb. Technol.* **10**:645-655.
- Vitello, L. B., Erman, J. E., Mauro, J. M., and Kraut, J. (1990a) Characterization of the hydrogen peroxide-enzyme reaction for two cytochrome *c* peroxidase mutants. *Biochim. Biophys. Acta* **1038**:90-97.
- Vitello, L. B., Huang, M., and Erman, J. E. (1990b) pH-Dependent spectral and kinetic properties of cytochrome *c* peroxidase: comparison of freshly isolated and stored enzyme. *Biochemistry* **29**:4283-4288.
- Vitello, L. B., Erman, J. E., Miller, M. A., Wang, J., and Kraut, J. (1993) Effect of arginine-48 replacement on the reaction between cytochrome *c* peroxidase and hydrogen peroxide. *Biochemistry* **32**:9807-9818.
- Wang, J. M., Mauro, M., Edwards, S. L., Oatley, S. J., Fishel, L. A., Ashford, V. A., Xuong, N. H., and Kraut, J. (1990) X-ray structures of recombinant yeast cytochrome *c* peroxidase and three heme-cleft mutants prepared by site-directed mutagenesis. *Biochemistry* **29**:7160-7173.
- Wang, Z. M., Bleakley, B. H., Crawford, D. L., Hertel, G., and Rafii, F. (1990) Cloning and expression of a lignin peroxidase gene from *Streptomyces viridosporus* in *Streptomyces lividans*. *J. Biotechnol.* **13**:131-144.
- Wariishi, H., and Gold, M. H. (1989) Lignin peroxidase compound III: Formation, inactivation, and conversion to the native enzyme. *FEBS Lett.* **243**:165-168.
- Wariishi, H., and Gold, M. H. (1990) Lignin peroxidase compound III. Mechanism of formation and decomposition. *J. Biol. Chem.* **265**:2070-2077.
- Wariishi, H., Morohoshi, N. B., and Haraguchi, T. (1987) Degradation of lignin by the extracellular enzymes of *Coriolus versicolor* VII. Effective degradation of syringyl type β aryl ether lignin model compound by laccase III. *Mokuzai Gakkaishi* **33**:892-898.
- Wariishi, H., Akileswaran, L., and Gold, M. H. (1988) Manganese peroxidase from the basidiomycete *Phanerochaete chrysosporium*: spectral characterization of the oxidized states and the catalytic cycle. *Biochemistry* **27**:5365-5370.
- Wariishi, H., Dunford, H. B., MacDonald, I. D., and Gold, M. H. (1989) Manganese peroxidase from the lignin-degrading basidiomycete *Phanerochaete*

chryso sporium. Transient state kinetics and reaction mechanism. *J. Biol. Chem.* **264**:3335–3340.

Wariishi, H., Marquez, L., Dunford, H. B., and Gold, M. H. (1990) Lignin peroxidase compounds II and III. Spectral and kinetic characterization of reactions with peroxides. *J. Biol. Chem.* **265**:11137–11142.

Wariishi, H., Huang, J., Dunford, H. B., and Gold, M. H. (1991a) Reactions of lignin peroxidase compounds I and II with veratryl alcohol. Transient-state kinetic characterization. *J. Biol. Chem.* **266**:20694–20699.

Wariishi, H., Valli, K., and Gold, M. H. (1991b) *In vitro* depolymerization of lignin by manganese peroxidase of *Phanerochaete chryso sporium*. *Biochem. Biophys. Res. Commun.* **176**:269–275.

Wariishi, H., Huang, J., Dunford, H. B., and Gold, M. H. (1992a) Mechanism of lignin peroxidase from *Phanerochaete chryso sporium*. The role of veratryl alcohol in the catalytic mechanism. In *Biotechnology in the Pulp and Paper Industry*, pp. 333–338 (M. Kuwahara, M. and M. Shimada, Eds.), Uni Publishing Co., Ltd., Tokyo.

Wariishi, H., Valli, K., and Gold, M. H. (1992b) Manganese(II) oxidation by manganese peroxidase from the basidiomycete *Phanerochaete chryso sporium*. Kinetic mechanism and role of chelators. *J. Biol. Chem.* **267**:23688–23695.

Wariishi, H., Sheng, D., and Gold, M. H. (1994) Oxidation of ferrocyanide by lignin peroxidase. *Biochemistry* **33**:5545–5552.

Welinder, K. G., Bjornholm, B., and Dunford, H. B. (1995) Functions of electrostatic potentials and conserved distal and proximal His-Asp H-bonding networks in haem peroxidases. *Biochem. Soc. Trans.* **23**:257–262.

Wells-Knecht, M. C., Huggins, T. G., Dyer, D. G., Thorpe, S. R., and Baynes, J. W. (1993) Oxidized amino acids in lens protein with age. Measurement of o-tyrosine and dityrosine in the aging human lens. *J. Biol. Chem.* **268**:12348–12352.

Whittaker, M. M., Kersten, P. J., Nakamura, N., Sanders-Loehr, J., Schweizer, E. S., and Whittaker, J. W. (1996) Glyoxal oxidase from *Phanerochaete chryso sporium* is a new radical-copper oxidase. *J. Biol. Chem.* **271**:681–687.

Williams, P. G., and Stewart, P. R. (1976) The intramitochondrial location of cytochrome *c* peroxidase in wild-type and petite *Saccharomyces cerevisiae*. *Arch. Microbiol.* **107**:63–70.

Wood, D. A. (1980) Production, purification and properties of extracellular laccase of *Agaricus bisporus*. *J. Gen. Microbiol.* **117**:327-338.

Yonetani, T. (1967) Studies on cytochrome *c* peroxidase. X. Crystalline apo- and reconstituted haloenzymes. *J. Biol. Chem.* **242**:5008-5013.

Yonetani, T. (1976) Cytochrome *c* peroxidase. In *The Enzymes*, Vol. 13, pp. 345-361 (P. D. Boyer, Ed.), Academic Press, Orlando, FL.

Yonetani, T., and Ray, G. (1966) Studies on cytochrome *c* peroxidase. 3. Kinetics of the peroxidatic oxidation of ferrocytochrome *c* catalyzed by cytochrome *c* peroxidase. *J. Biol. Chem.* **241**:700-706.

Zimmermann, W. (1990) Degradation of lignin by bacteria. *J. Biotechnol.* **13**:119-130.

BIOGRAPHICAL SKETCH

Dawei Sheng was born in Jilin, P.R. China, on April 23, 1965. He received his Bachelor of Science degree from Peking University, China, in July, 1987, and his Master of Science degree from Peking University in July, 1990. He worked as a research assistant in the same institution from 1990 to 1992.

In September, 1992, the author began his studies at the Oregon Graduate Institute of Science and Technology where he completed the requirements for the degree of Doctor of Philosophy in February, 1998.

List of Publications

Wariishi, H., Sheng, D., and Gold, M. H. (1994) Oxidation of cytochrome *c* by lignin peroxidase. *Biochemistry* **33**, 5545–5552.

Périé, F. H., Sheng, D., and Gold, M. H. (1996) Purification and characterization of two manganese peroxidase isozymes from the white-rot basidiomycete *Dichomitus squalens*. *Biochim. Biophys. Acta* **1297**, 139–148.

Sheng, D. and Gold, M. H. (1997) Haloperoxidase activity of manganese peroxidase from *Phanerochaete chrysosporium*. *Arch. Biochem. Biophys.* **345**, 126–134.

Sheng, D. and Gold, M. H. (1998) Irreversible oxidation of ferricytochrome *c* by lignin peroxidase. *Biochemistry* **37**, 2029–2036.

Sheng, D., Joshi, D. K., and Gold, M. H. (1998) Nitration of veratryl alcohol by lignin peroxidase and tetranitromethane. *Arch. Biochem. Biophys.* in press.